VIBRATIONS AND STABILITY OF FLUID CONVEYING PIPES RESTING ON ELASTIC MEDIA

THESIS SUBMITTED TO THE OSMANIA UNIVERSITY
FOR THE AWARD OF THE DEGREE OF

Doctor of Philosophy

IN
MECHANICAL ENGINEERING

BY

HARI S. SIMHA

DEPARTMENT OF MECHANICAL ENGINEERING
UNIVERSITY COLLEGE OF ENGINEERING (A)
OSMANIA UNIVERSITY
HYDERABAD, A. P. - 500 007

2012

DEPARTMENT OF MECHANICAL ENGINEERING
UNIVERSITY COLLEGE OF ENGINEERING (A)
OSMANIA UNIVERSITY
HYDERABAD, A. P. - 500 007

CERTIFICATE

This is to certify that the thesis entitled **"VIBRATIONS AND STABILITY OF FLUID CONVEYING PIPES RESTING ON ELASTIC MEDIA",** submitted by **Mr. Hari S. Simha,** for the award of the degree of **DOCTOR OF PHILOSOPHY** in **MECHANICAL ENGINEERING** to **OSMANIA UNIVERSITY, Hyderabad,** is a record of bonafide research work carried out by him. The contents of this thesis have not been submitted to any other Institute or University for the award of any degree.

Dr. Chellapilla Kameswara Rao
SUPERVISOR
Dean (Research and Development)
TKR College of Engineering and Technology
Meerpet, Hyderabad – 500 079

Head
Department of Mechanical Engineering
University College of Engineering (A)
Osmania University
Hyderabad – 500 007

Date:……

DECLARATION

This is to declare that the thesis entitled **"VIBRATIONS AND STABILITY OF FLUID CONVEYING PIPES RESTING ON ELASTIC MEDIA",** does not constitute any part of thesis/dissertation/monograph, submitted by me to this or any other University/Institute.

Date:……

Hari S. Simha
Research Scholar

हरिः ॐ

श्री गुरुभ्योनमः

श्री परमगुरुभ्योनमः

श्रीमद् आनन्दतीर्थ भगवत्पादाचार्यगुरुभ्योनमः

हरिः ॐ

हरि सर्वोत्तम वायु जीवोत्तम

Dedicated to

my father, Late Prof. Shyam Sunder Simha,

my mother, Dr. Rathna Simha,

my wife, Sarita

and my sons, Saurabh and Sumedh

ACKNOWLEDGEMENTS

It is with a deep sense of respect and gratitude that I thank my supervisor Dr. Chellapilla Kameswara Rao, Dean (R&D), TKR College of Engineering and Technology, Hyderabad, for his valuable guidance, encouragement and support in carrying out this research work successfully.

I also sincerely thank Dr. P. Laxminarayana, Professor & Head, and Dr. A. Krishnaiah, Chairman, Board of Studies, Department of Mechanical Engineering, University College of Engineering, Osmania University, Hyderabad, for their valuable suggestions in completing the thesis.

I wish to record my heartfelt thanks to Prof. Dr-Ing. Hubert Willi Klein, Professor, Fachbereich Ingenieur- und Wirtschaftswissenschaften, Fachhochschule Südwestfalen, Meschede, Germany, for his unstinted support and suggestions during the course of my research work.

My sincere thanks is also due to Late Mr. R. N. Parlikar, former Scientist H and Head, Design & Engineering Division, IICT, Hyderabad, for encouraging me to take up research work.

I wish to convey my heartfelt thanks to Prof. J. V. Subrahmanyam, Professor, Vasavi College of Engineering, Hyderabad, who always encouraged me to complete my work quickly and diligently.

I am extremely grateful to Dr. J. S. Yadav, Director, Indian Institute of Chemical Technology, Hyderabad, for permitting me to register for Ph. D. at the Osmania University. I also wish to thank Dr. Radhakrishna, Sr. Principal Scientist and Head, Design & Engineering Division, IICT, Hyderabad, with whom I work now, for constant encouragement and support during the entire course of this work. I take this opportunity to also thank Dr. Y. Bhaskar Rao, former Head, for permitting me to register for Ph. D. I appreciate the support and encouragement given to me by all the colleagues of my Division here in IICT. Special thanks are due to Dr. U. Ashutosh and Mr. M. Sridhar Kumar for helping me in completing my thesis.

I wish to record my deepest gratitude to my late father, Prof. Shyam Sunder Simha, for his constant encouragement and support and my mother, Dr. Rathna Simha, whose motivation and encouragement were always there for me. I thank my wife, Sarita, and my two sons, Saurabh and Sumedh, for their unlimited patience and who all have sacrificed the rightful time I should have spent with them, to enable me to complete my work. I dedicate this work to my family.

Abstract

In this Thesis, the dynamic behaviour of fluid conveying pipes and carbon nanotubes resting on or embedded in elastic media is investigated. It is a well-known fact that the natural frequencies of fluid conveying pipes are affected by the velocity of the fluid flowing within. Consequently, a certain velocity of the fluid, called the *critical velocity*, can be calculated, at which, the natural frequency of the system becomes zero, theoretically.

The frequencies depend on various other factors like, the boundary conditions, the kind of continuous support the pipeline is resting on and, to some extent, the operating conditions of the fluid flowing within the pipeline. In this work, standard boundary conditions corresponding to pinned-pinned, clamped-pinned and clamped-clamped have been investigated. All the cases investigated for a fluid conveying pipe are for the pipe resting on an elastic medium, such as soil.

A thorough literature survey has indicated that lot of work has been reported on the dynamic behaviour of fluid conveying pipelines either without considering the elastic medium or resting on an elastic medium modeled as a simple Winkler foundation. In this work, the soil medium has not only been modeled as the popular single-parameter Winkler model but also as the two-parameter Pasternak model for the first time. By a similar analogy, the carbon nanotubes conveying fluid are considered to be embedded in

an elastic polymer or tissue matrix, which is modeled conforming to a Pasternak model, again for the first time. Nanotubes conveying fluid resting on a Winkler model are also considered for comparison purposes. A brief introduction to carbon nanotubes has been included, since this subject is relatively new to mechanical engineers. Also, the non-local continuum mechanics model of Eringen is briefly discussed and it is shown how this theory can be applied to carbon nanotubes conveying fluid.

Analytical expressions are derived to calculate the natural frequencies and critical velocities of the pipeline. The fluid conveying pipe/nanotube has been modeled in the entire work as an Euler-Bernoulli beam, thus disregarding the effects of shear deformation and rotary inertia. Furthermore, the governing equations of motion for the nanotube conveying fluid have been derived considering the non-local continuum mechanics model, to include the nano-scale effects in the dynamic behaviour of the nanotube. The effect of internal pressure and fluid viscosity effects have not been considered, and the flow is considered to be a steady plug type of flow with constant fluid velocity.

The solution methods used in this work are also slightly different from that reported in the literature. For the case of pinned-pinned boundary conditions, a Fourier series approach has been adopted, while, for the pinned-clamped and the clamped-clamped boundary conditions, a Galerkin solution method utilizing assumed beam modes has been used.

Detailed numerical results have been obtained for different values of boundary condition parameters, the stiffness parameters of the elastic media, mass ratio parameters and flow

velocity parameters. Wherever possible, comparisons have been made with the reported results in the literature, to validate the approach adopted in this work. The results have been usefully tabulated and graphs showing the trends have been plotted. The intention is to give the piping designers enough data to be able to analyze the dynamic behaviour of the system. Interesting conclusions have been drawn from the results of the numerical analyses.

Some recommendations for future research have been included to conclude the thesis.

LIST OF PUBLICATIONS THAT HAVE RESULTED FROM THIS RESEARCH WORK

International Journals

1. **Kameswara Rao, C. & Simha, H. S.**, "Vibrations of Fluid-Conveying Pipes Resting on Two-parameter Foundation", *The Open Acoustics Journal,* **1**, 24-33, 2008.

2. **Kameswara Rao, C. & Simha, H. S.,** "Critical Velocity of Fluid Conveying Pipes Resting on Two-parameter Foundation", *Journal of Sound and Vibration* **302**, 387–397, 2006.

International Conferences

3. **Simha, H. S. & Kameswara Rao, C.**, "Free Vibrations of Fluid Conveying Single-Walled Carbon Nanotubes", *International Conference on Nanotechnology & Functional Materials, SNIST, Hyderabad,* January, 2012.

4. **Simha, H. S. & Kameswara Rao, C.,** "Thermal Buckling of Fluid Conveying Single-Walled Carbon Nanotubes Embedded in an Elastic Medium", *International Conference on Nanotechnology & Functional Materials, SNIST, Hyderabad,* January, 2012.

5. **Kameswara Rao, C. & Simha, H. S.**, "Critical Flow Velocities of Elastically Restrained Multi-span Fluid Conveying Pipes Resting on Continuous Elastic Foundation", *Proceedings of the 13th International Conference on Nuclear Engineering, Beijing, China, May 2005, Paper No.50473*, 2005.

6. **Simha, H. & Kameswara Rao, C.**, "Finite Element Analysis of Vibrations Fluid Conveying Pipes Resting on Soil Medium", *Proceedings of the Technical Conference on Pressure Vessels and Piping, pp 173-182, Hyderabad*, October 1997.

National Conferences

7. **Simha, H. & Kameswara Rao, C.**, "Finite Element Analysis of Vibrations of Rotationally Restrained Fluid Conveying Pipes Resting on Soil Medium", *Proceedings of the National Symposium on Advances in Structural Analysis and Design, pp 569-578, Allied Publishers, Chennai*, January 2001.

LIST OF FIGURES

LIST OF TABLES

NOMENCLATURE

a	Internal characteristic length of a carbon nanotube
a_{cz}	Acceleration of the carbon nanotube element in the vertical direction
a_{fz}	Acceleration of the fluid element in the vertical direction
a_n	Constant
a_{pz}	Acceleration of the pipe element in the vertical direction
a_r	Constant
A	Area of pipe/carbon nanotube
C_{ij}	Integration constants
e_0	Nano material constant
e_n	Nanoscale parameter
E	Modulus of elasticity
F	Normal force
I	Moment of inertia
k_P	Pasternak or shear elastic stiffness constant/ unit length
k_W	Winkler elastic stiffness constant/ unit length
l	Integer
L	Length of the pipe
m	Integer
m_c	Mass of carbon nanotube/ unit length
m_f	Mass of fluid/ unit length
m_p	Mass of pipe/ unit length

M	Total mass of pipe/carbon nanotube plus fluid/unit length
M_b	Transverse bending moment
n	Integer
p	Pressure of the fluid
q	Wall shear stress of the pipe/nanotube
Q	Shear force
r	Integer
R_P	Reaction force of the Pasternak medium
R_W	Reaction force of the Winkler medium
s	Integer
S	Internal perimeter of the pipe/nanotube
t	time
T	Longitudinal tension in the pipe/carbon nanotube wall
u	Axial displacement of the pipe
U,v	Steady flow velocity of fluid
U_x	x-component of the steady flow velocity of fluid
V	Non-dimensional flow velocity parameter
V_{cr}	Critical velocity parameter
w	Lateral displacement of the pipe
x	Dimension along the length of pipe
z	Dimension along the direction perpendicular to the pipe

Greek symbols

ξ	Non-dimensional length parameter
β	Non-dimensional mass-ratio parameter
γ_W	Non-dimensional Winkler elastic stiffness parameter
γ_P	Non-dimensional Pasternak elastic stiffness parameter
γ_{xz}	Shear strain of the Pasternak medium
θ	Shear angle of the Pasternak medium
λ_r	Beam frequency parameter
ρ	Density of fluid per unit length
σ_r	Frequency function
τ_{xz}	Shear stress of the Pasternak medium
ψ_r	Beam eigen-functions
ω_j	j^{th} mode of vibration
Ω	Non-dimensional frequency parameter

CONTENTS

Chapter 1

Introduction

1.1 Background

A mechanical engineer's role in Chemical Process Plant (CPI) design involves, among other things, mechanical design and detailing of different process systems such as process equipment, piping, utilities, plant layout and so on. Detailed designers of process plants, traditionally develop their designs to conform to various design codes. For example, the process equipment are designed to the requirements of codes such as ASME Section VIII, Division 1 and piping is designed as per ANSI codes.

In developing such designs, the designer is more focused on satisfying the requirements of the specific code, because there is inherent safety built-in in these procedures. Any unknown or unforeseen aspect is normally taken into account by the safety factors employed. In piping design, for example, attention is given more to the ability of the pipeline to withstand pressure and thermal expansion forces than other aspects like vibration and fatigue. These aspects would have to be considered by other

means not specified by the codes, such as finite element analysis, analytical or experimental methods.

The focus in this thesis is on a part of one of the important components of mechanical design and detailed engineering of CPIs, namely, piping design. Although comprehensive piping design comprises of various activities starting from pipe material selection followed by pipeline sizing, design for strength, design for flexibility, calculation of support reactions, selection of suitable supports, calculation of loads on connected equipment and so on, the work in this thesis concentrates on the dynamic behaviour of pipelines conveying a fluid. As will be seen in the following pages, some grey areas in this field have been identified and an attempt is made to throw more light on these areas. The final intention is to generate enough design data to enable the piping designer to take into account the vibrations for piping design, at the design stage itself.

1.1.1 Fluid conveying pipes

The present study can be considered a subset of a large, all-encompassing field of dynamics of slender cylindrical bodies in axial flow, as very comprehensively elucidated by Païdoussis **[41,42]**, in his monographs. In the above references, he has given an interesting insight into the origins of research work in this field. Before serious study was taken up in this field, most researchers were mainly concerned with the dynamical behaviour of cylindrical structures in cross-flow, i.e. transverse flow. This was understandable because flows of even moderate velocities in the transverse direction would cause severe and noticeable vibrations leading to related problems. The practical importance of such systems has been evidenced by the application of

results to a variety of problems like heat exchanger tube bundle vibrations, flutter of aircraft wing spans, and so on. The main characteristic of such problems is the large amplitude vibrations causing structural damage. Hence, all effort of the researchers went naturally in finding solutions to such practical problems.

On the other hand, the dynamic behaviour of cylindrical structures in axial flow is characterized by small amplitude vibrations, which often were inconsequential as far as practical engineering applications were concerned. Typically, the amplitudes are in the range $10^{-3} < A/D < 10^{-2}$, where, A is the root-mean-square amplitude of vibration and D is the diameter of the cylinder, Païdoussis **[42]**. However, there are many examples of slender cylindrical structures in axial flow, for instance, pipes conveying fluids, heat exchanger tubes immersed in an external axial flow region and also conveying fluid, nuclear reactor fuel elements, the fireman's water hose, and in physiological examples, the pulmonary and the urinary systems. In many such cases, vibrations of even small amplitude would be cause for damage in the long term, as a result of fretting, stress corrosion cracking and high cycle fatigue, which could ultimately lead to rupture of the tubes with severe consequences, Païdoussis **[42]**. This is mainly because of the inherent geometry of construction of such elements, where close spacing between the bodies would result in impact and wear.

In the course of study of literature pertaining to dynamics of pipelines, it was found that many researchers started working on the dynamics of Fluid Conveying Pipes (FCPs), from 1950 onwards. It was also discovered that the current commercial finite element packages were inadequate to handle this particular dynamical problem. In an excellent review published in 1993, Païdoussis **[40]**, extols this problem as *"A Model*

Dynamical Problem". Further, he has given an illuminating insight into the historical connection to this problem. Given in the next paragraph, is a gist of the history of this model problem, from his paper.

As far back as 1878, Aitken (cited from **[40]**), conducted experiments on traveling chains which is considered among the earliest work concerning the physics of a fluid conveying pipe. In 1939, Bourrièrs (cited from **[40]**) developed equations of motion of a fluid conveying cantilever pipe, for the first time and provided accurate conclusion regarding stability. This published work was however lost during the World War II, leading to a number of researchers re-deriving the governing equations in the 1950s and '60s (cited from **[40]**). Bourrièrs' work was rediscovered by Païdoussis **[40]**, in 1974 by chance. In this thesis, literature survey starts from 1950s, when Ashley and Haviland **[1]** published their paper leading to a flurry of activity on this topic. In fact, as indicated by Païdoussis **[41, 42]**, studies leading to a fundamental understanding of the problem of the dynamics of fluid conveying pipes, formulation of the governing differential equations of motion and methods of their solution have been very useful in the study of several other dynamical models, for instance, thin shells conveying fluid or immersed in axial flow, plates in axial flow and tubular beams axially towed in a quiescent fluid.

The knowledge gained by the study of this *"model dynamical problem"* has been successfully applied to the solution of practical problems like the dynamics of heat exchanger tube arrays and nuclear fuel rod arrays, solar thermal power plant chimney subjected to internal or annular flows, see for instance, Wang and Ni **[43]**. The similarity between the modal shapes of a fluttering cantilever and a slender fish, like

an eel, swimming in water, has even resulted in a patented novel method for aquatic propulsion of a water-craft, Païdoussis **[41]**. As mentioned by Wang and Ni **[43]**, all these unexpected applications came 10 – 40 years after the basic research in the field had already been done.

The motivation to contribute to research on the dynamics of fluid conveying pipes was hence born. Also, during the course of work on this thesis, it was observed that a number of researchers in the recent past were applying the fundamental knowledge of the dynamics of fluid conveying pipes to the exciting new area of carbon nanotubes conveying fluid. This is basically possible because the governing differential equations of fluid conveying carbon nanotubes have the same form as a fluid conveying pipe.

After a fairly exhaustive literature survey, it was decided to research on the dynamic behaviour of fluid conveying pipes resting on elastic media, like soil, since little work was done on this aspect. More so, it was observed that although some work was carried out by earlier researchers on the dynamics of fluid conveying pipes resting on a single parameter elastic support medium, the simplest of which is a Winkler model of the foundation, no work was reported on the dynamics and stability of a fluid conveying pipe resting on a two-parameter elastic medium. The two-parameter foundation model considered in this work is the popular Pasternak model, which takes into account an additional shear layer, and which can be considered a more realistic way to represent the elastic support medium. This is reflected in the initial chapters of this thesis.

For the physics of the problem to be clearly understood, we proceed in a systematic manner, introducing one extra term at a time, thus developing the relevant governing equation of motion.

We start our study by considering the basic equation for flexural vibrations of an Euler-Bernoulli beam:

$$EI\frac{\partial^4 w}{\partial x^4} + m_p \frac{\partial^2 w}{\partial t^2} = 0 \tag{1.1}$$

The symbols are defined in the notation, unless otherwise specified. The first term in the above equation is the elastic restoring force due to the elasticity of the pipe material and the second term is the inertia force due to the pipe. Here, the pipe is considered as an Euler-Bernoulli beam.

When the pipe conveys a fluid, the above equation is modified as follows:

$$EI\frac{\partial^4 w}{\partial x^4} + M\frac{\partial^2 w}{\partial t^2} + \rho A v^2 \frac{\partial^2 w}{\partial x^2} + 2\rho A v \frac{\partial^2 w}{\partial x \partial t} = 0 \tag{1.2}$$

Two extra terms are introduced due to the flowing fluid in the equation. The third term in the above equation is the centrifugal force due to the fluid flowing in the slightly curvilinear shape of the deformed pipe and the fourth term is the coriolis force of the flowing fluid.

Now, considering a pipe conveying fluid resting on an elastic medium like soil, a fifth term gets added to the equation of motion, which is due to the reaction force of the

constant stiffness elastic medium, modeled as a Winkler-type foundation. Equation (1.3) represents this condition:

$$EI\frac{\partial^4 w}{\partial x^4} + M\frac{\partial^2 w}{\partial t^2} + \rho A v^2\frac{\partial^2 w}{\partial x^2} + 2\rho A v\frac{\partial^2 w}{\partial x \partial t} + k_w w = 0 \qquad (1.3)$$

Many researchers have contributed to the development and analysis of the above equation, as can be seen in the next section. In this thesis, the equation of motion is further modified to include the effects of a more realistic model of the elastic media. The model chosen is the two-parameter Pasternak foundation model, utilizing which, the new equation becomes:

$$EI\frac{\partial^4 w}{\partial x^4} + M\frac{\partial^2 w}{\partial t^2} + \left(\rho A v^2 - k_P\right)\frac{\partial^2 w}{\partial x^2} + 2\rho A v\frac{\partial^2 w}{\partial x \partial t} + k_w w = 0 \qquad (1.4)$$

As can be observed from Equation (1.4) above, the third term has been modified due to the second foundation parameter. The effort in this thesis will be to derive and solve the above equation for pipes conveying fluid and analyze the results obtained.

1.2 Survey of Literature - Fluid conveying pipes

1.2.1 Fundamental analytical studies

Ashley and Haviland **[1]** were the first to analyze the transverse vibrations of fluid conveying pipes. The practical problem in question was the observed severe vibrations of the Trans-Arabian Oil Pipeline. They derived an equation considering the fluid velocity also. They also showed the fundamental frequency of the system decreases with increasing fluid velocity. An approximate power series solution was used to

estimate the fundamental frequencies. In 1952, Housner **[2]**, developed a more accurate governing equation which included the inertia forces due to fluid flowing in the slightly curved pipe (due to bending). He also observed that Ashley and Haviland had considered only one half of the inertia forces due to Coriolis acceleration. He used Fourier series to solve the equation. He also showed that there existed a critical velocity at which the fundamental frequency becomes zero, leading to the buckling of the pipe. Both the above studies considered the pipe to be simply supported. Movchan, in 1965 **[87]** (cited from **[84]**), studied the stability of fluid conveying pipes using the direct Lyapunov method and it was shown that free vibrations of the pipe appear in the form of waves traveling along the pipe, for sub-critical values of velocities. Thurman and Mote, in 1969 **[3]**, studied the non-linear oscillations of a pipe conveying fluid and concluded that the linear analysis is limited in its applicability in many cases of practical importance. In their paper, the fluid was assumed to flow with a constant velocity. Later, in 1971, Chen **[4]**, presented results of a study on the dynamics of simply supported pipelines conveying pulsatile flow. He used Galerkin's method for solving the equations. Païdoussis and Issid **[5]**, in 1974, analyzed the dynamic behaviour of fluid conveying pipes considering both steady and harmonically perturbed flow conditions. They showed for the first time that pipes with both ends supported, which is a conservative system, is not only subject to buckling (divergence) but also to coupled-mode flutter at high flow velocities. They also corrected an error in Chen's formulation **[4]**, which neglected the axial acceleration of the fluid due to the flow velocity perturbations. Lee et. al. **[6]**, in 1995, attempted to develop a more realistic equation of motion by considering fully coupled fluid-structure interaction mechanisms. They derived the equation and applied it to an example problem of a

straight pipeline with oscillatory flow. Païdoussis and Laithier **[7]**, 1976, extended their study to pipes modeled on the Timoshenko beam theory. They derived and solved the equations of motion by two methods – Finite Difference technique and a variational method and concluded that the variational method is more efficient. Also, it was shown that the frequencies and critical flow velocities decrease by considering the effect of transverse shear, which is neglected in the more popular Euler-Bernoulli model.

Very recently, Ibrahim **[84, 85]**, published an excellent two-part review paper on the mechanics of pipe conveying fluids. The first part addresses the fundamental studies and the second part looks into applications and fluid-elastic problems. Both the papers put together have over 920 references, which should be a single comprehensive source of information in this field.

The result of the above research was a reasonably accurate mathematical formulation of the problem and an insight into the different methods of solution, apart from a very good fundamental understanding of the physics of the problem. In the following paragraphs, studies concerned with some specific areas of the dynamics of fluid conveying pipes are surveyed.

1.2.2 Cantilevered pipes

Long **[8]**, in 1955, was the first to analyze the problem both analytically and experimentally. He also considered different boundary conditions like clamped-free, for the first time, apart from clamped-clamped and clamped-pinned, and solved the governing equations using an approximate power series solution. His experimental

results showed reasonable agreement with theory. He used a power series solution method, which restricted the applicability of his results to relatively small flow velocities. He concluded that the forced motions of cantilevered pipes are damped by internal flow of the fluid in the range of fluid velocities he investigated.

In all the above studies, the researchers concluded that at a certain critical flow velocity, the pipe instability is caused by the phenomenon of buckling, akin to a column under a compressive load. However, a cantilevered pipe is also subject to oscillatory instability (flutter) at very high internal flow velocities. This fact was predicted by Benjamin (cited from **[8]**) in 1961, who showed that a system of articulated cantilevered pipes could fail due to oscillatory instability. In 1966, Gregory and Païdoussis **[9]**, presented a very comprehensive study of cantilevered fluid conveying pipes, constrained to move in a horizontal plane, and confirmed Benjamin's hypothesis that the pipe could be subjected to oscillatory instability at sufficiently high flow velocities. The above authors have used exact as well as approximate methods to develop solutions, which have also been verified by experiments. In a later paper, Païdoussis **[10]**, 1970, found that a vertical cantilevered fluid conveying pipe, which also is subjected to gravity effects, is not subjected to buckling (divergence). Their conclusions were supported by experimental results as well. Another finding in this study was that standing cantilevers, buckling under their own weight in the absence of flow may regain stability in the presence of fluid flow in a certain range of velocities.

1.2.3 Internal pressure, axial tension and other effects

Many previous researchers neglected the effects of internal fluid pressure and axial tension in the pipe. Roth (cited from **[12]**) developed equations of motion considering the effects of axial deflections, damping forces, reactions from a foundation, compressibility of the fluid, transient pressure and flow and variable cross-section of the pipe. In 1968, Naguleswaran and Williams **[11]**, developed exact solutions for fluid conveying pipes with clamped-clamped, clamped-pinned and pinned-pinned ends. They also suggested that a two-term Fourier series approximation for a pinned-pinned pipe, and a two-term Galerkin approximation for other boundary conditions would estimate the fundamental frequency well. In their work, they have also considered the effect of internal fluid pressure as well as applied axial tension. They also verified their results with experimental work.

Stein and Tobriner **[12]**, in 1970, presented an excellent study taking into account the internal pressure of the fluid and also external damping. They developed the governing equation and its solution for an infinitely long fluid conveying pipe resting on an elastic foundation. They have also analyzed the wave propagation characteristics of the system and have concluded that the dynamic stability of an undamped pipe is dependent on the critical flow velocity, and also that higher values of the foundation modulus tend to stabilize the system. Further, they observed that internal pressure causes axial tension, tending to decrease the frequency, leading to instability.

Païdoussis and Issid **[5]**, in 1974, re-examined the dynamics of fluid conveying pipes with clamped-clamped, pinned-pinned and clamped-free boundary conditions. They

also considered the effects of internal pressure, axial tension in the pipe and harmonically perturbed fluid velocity in the pipe. The showed that even pipes with both ends supported are subject to not only buckling but also coupled-mode flutter instabilities. They also proposed some design criteria to help in industrial design of such pipelines. The effect of axial forces on the stability of a fluid conveying pipe was studied by Plaut and Huseyin, in 1975 **[88]**.

Recently, Olunloyo, et. al. **[86]** (cited from **[84]**), considered various effects like pressurization, temperature variations, cross-sectional area change, etc., in their formulation of the governing equations. It was shown that the cross-sectional change is the main reason for the phenomenon called 'pipe walking'.

1.2.4 Finite Element Methods

A number of different methods have been employed by various researchers to analyze the dynamics of fluid conveying pipes. The finite element method has been used by Kohli and Nakra **[13]**, in 1984, to study the dynamic behaviour fluid conveying pipes utilizing the Euler-Bernoulli theory, where they have used one-dimensional straight beam finite elements and derived the mass and stiffness matrices. They have also made use of the straight beam element to analyze curved tubes, considering both in-plane and out-of-plane vibrations. In 1991, Pramila et. al. **[14]**, used the so called heterosis elements to model a short fluid conveying pipe according to the Timoshenko beam theory. The numerical results of both the studies have been found to be in good agreement with the results reported in earlier literature.

1.2.5 Pipes supported on constant stiffness, variable stiffness, multi-parameter and partial elastic medium

All the above studies focused on the fundamental dynamics of the problem. All the researchers were mainly concerned with the effect of various parameters like internal pressure, fluid velocity, axial tension, transient phenomena and boundary conditions on the stability and vibration characteristics of the fluid conveying pipe. A useful conclusion, which can be considered important from the designers' point of view, is the recognition of critical flow velocity, beyond which, instability occurs. Only Stein and Tobriner **[12]** considered a fluid conveying pipe resting on an elastic foundation. The foundation considered there is a simple linear spring: the main focus of their study being the effect of internal pressure and the wave propagation characteristics of the system. Becker, et. al., in 1978 **[89]**, studied the stability of cantilevered pipes conveying fluid or gas and concluded that the critical flow velocity of a pipe on Winkler foundation is higher than that of a pipe without any foundation. This implies that the Winkler foundation has a stabilizing effect on the system **[84]**.

In 1986, Lottati and Kornecki **[15]**, published results of their study on the effect of elastic foundation on the stability of fluid conveying pipes. They considered two cases of clamped-clamped and cantilever boundary conditions. A Winkler foundation model was considered in their analysis. They concluded that the elastic foundation induces stabilization of the pipe for both the boundary conditions investigated. The focus in their study was to determine the effect of the mass ratio with varying foundation stiffness parameter. Dermendjian-Ivanova **[16]**, in 1992, studied the effect of a Winkler type foundation on the stability of a pinned-pinned fluid conveying pipe. It

was shown that the critical flow velocity increases with increasing foundation stiffness. Also, it was shown that the critical flow velocity increases with increasing length of the pipeline for higher values of foundation stiffness. However, the main concern was to determine the effect of long pipe spans, cross-sectional rigidity of the pipe material and value of the elastic constant of the foundation on the critical flow velocity.

In 1993, Chary **[17]** analyzed in detail the effect of a Winkler type foundation on the fundamental frequencies and critical flow velocities of a fluid conveying pipe with both ends supported. He also considered the effect of soil inertia on the vibration characteristics of the system and included response of such systems to seismic excitation. Chary, et. al. **[18]**, in 1993, presented approximate solutions for the natural frequencies and critical flow velocities of a fluid conveying pipe resting on a Winkler foundation. They used Fourier series solutions for the pinned-pinned boundary conditions and Galerkin method for the pinned-clamped and clamped-clamped pipe. They have presented results for various values of foundation stiffness parameter and also pipe-fluid mass ratio.

The problem of fluid conveying pipes resting on variable foundations has also been investigated by some researchers. Djondjorov et. al. **[19]**, in 2001, investigated the dynamic stability of fluid conveying pipes on variable stiffness foundations. In conclusion, they have shown that lower stiffness of the foundation at mid-span of the pipe compared to that at the ends of the pipe have lower stabilizing effect even in comparison to the standard Winkler foundation. Their work was restricted to cantilevers conveying fluid. In 2006, Vassilev and Djondjorov **[20]**, used Galerkin

method to compute the eigen frequencies and critical velocities for a cantilever supported be a variable modulus Winkler foundation. The stiffness of the foundation was assumed to vary as per a second order polynomial. Elishakoff and Impollonia **[21]**, in 2001, studied the effect of partial elastic foundation on the stability of fluid conveying cantilever pipes. They considered both a translational foundation like the Winkler foundation and a rotational foundation model in their study. They found that the critical velocity may either increase or decrease depending upon the "attachment ratio" of the foundation, i.e. the amount of foundation attached to the pipe compared to its length. In all the above studies, the researchers have concentrated mainly on the dynamics of cantilever, perhaps because these are subjected to flutter instability, which is more spectacular. Doaré and De Langre **[22]**, studied the stability aspects of fluid conveying pipes on a constant Winkler type foundation, in 2002, wherein they used a wave propagation approach to obtain results. They introduced the concepts of absolute and convective instability in their study to assess the effect of the length of the pipeline on stability.

The dynamics of fluid conveying pipes resting on elastic media other than Winkler foundation has not been studied in depth. Only two researchers have attempted to analyze this problem, to the best of the author's knowledge. The first was Dzhupanov **[23]**, who in 1998, modeled fluid conveying cantilever pipes resting on both Winkler and a two parameter foundation like a Pasternak foundation. The variability of the stiffness parameters was also considered. However, the study ends with only the derivation of the governing equations and the boundary conditions. Later, in 2004, Lilkova-Markova and Lolov **[24]**, presented numerical results for a cantilever

conveying fluid resting on Winkler and Pasternak foundations. The results were presented for some particular values of the foundation stiffness.

1.3 State-of-the-art

In the foregoing discussion, it is seen that all the above studies are concerned mainly with establishing the stability conditions of a pipe conveying fluid. The effect of a number of parameters has been considered and it has been shown that there exists a critical flow velocity, which determines the onset of instability. It is also seen that not many studies have been undertaken on the dynamics of fluid conveying pipes resting on elastic foundation. This is of great practical importance because soil can be suitably modeled as an elastic medium and the piping system analyzed for its dynamic behaviour.

The state-of-the-art is that the flow velocity, internal fluid pressure, ideal boundary conditions of pinned-pinned, pinned-clamped, clamped-clamped and clamped-free, harmonically perturbed internal flow, axial tension in the pipe, external damping and to some extent, elastic foundation modulus have been considered in deriving the equations of motion. These have been solved using various analytical methods. The results obtained from these studies have helped in understanding the problem better. However, there have not been many detailed inputs in the literature on the effect of different types of elastic foundation on the dynamics and stability characteristics of fluid conveying pipes. Even when some researchers have considered the elastic medium on which the pipe is resting, it has been modeled according to a simple Winkler model. Moreover, there appears to be not a single study to consider and compare the dynamic behaviour of fluid conveying pipes on elastic medium, with all

the three standard boundary conditions. The Pasternak foundation model for the elastic medium, which is more realistic, has been not studied at all for the three standard boundary conditions.

The above observations have been the motivating factor for the present work. It was found necessary to proceed in a systematic manner and address some of the issues not covered in the previous studies. The next section details the scope of the present research work.

1.4 Scope of the present work

As elaborated in the previous sections, some issues concerning fluid conveying pipes have yet to be addressed. Also, as will be discussed in detail in chapters 5 and 6, it is seen that the governing equations for a fluid conveying nanotube are very similar to that of a fluid conveying pipe. Hence it was decided to extend this study to analyze fluid conveying pipes embedded is an elastic medium. Thus the scope of the present work is accordingly detailed in the following sections.

1.4.1 Fluid conveying pipes

The present work attempts to analyze the vibrations and stability of fluid conveying pipes resting on elastic foundation. The types of foundation models considered are both the Winkler model and the Pasternak model. As has been elucidated in the literature survey, although information is available for pipes on Winkler foundations, they are widely scattered and not comprehensive. Here the effort will be consider all the three standard boundary conditions of pinned-pinned, pinned-clamped and

clamped-clamped, compare the results and consolidate the knowledge gained. A more realistic elastic medium, viz., the two-parameter Pasternak foundation, has been introduced for the first time in the formulation of the governing equations. The results for the Pasternak model will be a totally new contribution, since there is nothing reported in the literature.

The pipe is modeled as a long pipe according to the Euler-Bernoulli beam theory. The internal flow field is considered to be steady and of constant flow velocity. The effect of internal pressure, temperature, external damping and axial tension has not been considered in this analysis. Likewise, response to external excitations has also not been considered. This work mainly aims to provide new information on the effect of flow velocity and foundation modulus on the frequencies of the piping system and the critical flow velocity. The intention in pursuing this work is to provide piping designers with relevant data to be able to design cross-country pipelines.

1.4.2 Fluid conveying carbon nanotubes

It is very fortunate that similar equations can be used to model carbon nanotubes conveying fluid. In this thesis, the dynamic behaviour of single-walled carbon nanotubes (SWCNT) conveying fluid will be studied. The SWCNT is modeled according to the Euler-Bernoulli theory, and the effects of internal pressure, viscosity of the fluid, temperature and axial tension in the carbon nanotube are not considered in the analysis. The mathematical model will however, include the non-local parameter, giving more realistic results. The SWCNT will be considered to be embedded in an elastic medium of both the Winkler type and the Pasternak type. All

the three standard boundary conditions will be considered. The formulation of the problem and the results in this work will be the new contribution to this field.

The next section outlines the organization of this thesis, giving an overview of the contents in each chapter.

1.5 Organization of the thesis

Chapter 1 of the thesis, that is this chapter, *Introduction*, gives the background of this exciting field of dynamics of fluid conveying pipes. An attempt is made to enliven the information with some historical developments in this area. A fairly comprehensive literature survey is conducted in the topics relevant to the scope of this work in the fluid conveying pipes area. Finally, the scope of the present thesis is elucidated in the previous section.

In Chapter 2, *Fluid Conveying Pipes - Mathematical Formulation*, a detailed, step-by-step mathematical formulation of the fundamental governing equations of motion of a fluid conveying pipe is presented. Different models of elastic media are discussed and their mechanics explained. Two popular models of the elastic media are chosen for analysis. One is the simple Winkler model and the other is the more realistic Pasternak model. A pipe is considered resting on such media, which simulates an elastic foundation. The governing equations of motion are derived for pipes conveying fluid, including the effect of the two-parameter Pasternak type elastic medium for the first time. In this thesis, the terms “elastic medium” and “elastic foundation” are used synonymously. Although some of the matter presented in this chapter is well known,

it is strongly felt that a rigorous mathematical treatment must be a part of any research thesis, to enable future researchers to easily take forward the work done here.

In Chapter 3, *Stability of Fluid Conveying Pipes Resting on Elastic Media*, the expressions are derived for computing the critical flow velocities of pipes conveying fluid, considering the two different types of elastic media. The equations are solved to obtain closed-form solutions for the critical velocities for the three standard boundary conditions of pinned-pinned, pinned-clamped and clamped-clamped, and numerical results are presented in the form of graphs and tables. The three ideal boundary conditions are all considered such that comprehensive results are obtained and comparisons can be made. Many of these results are new contributions to the literature. The method of solution adopted is also different from those followed by most researchers. Some useful conclusions are drawn based on the results obtained.

In the previous chapter, solutions are obtained for the critical velocities of the fluid conveying carbon nanotubes and pipes. As a logical extension of the work done so far, the equations of motion derived in the second chapter have been solved analytically and expressions for the natural frequencies of the system have been obtained in Chapter 4, titled *Natural Frequencies of Fluid Conveying Pipes Resting on Elastic Media*. Again, three ideal boundary conditions are considered for analysis. The natural frequencies have been obtained for the cases of pipes conveying fluid resting on Winkler as well as Pasternak type elastic media. Comprehensive numerical results have been obtained and wherever possible, these have been compared with those available in existing literature. However, the results for pipes conveying fluid and

resting on Pasternak type of an elastic model are new and it is hoped that they will add to the existing knowledge.

As will be seen later, the governing equations for the analysis of a fluid conveying carbon nanotube are very similar to those of fluid conveying pipes. This fact has led to inclusion of the study of the dynamics of fluid conveying carbon nanotubes in this thesis. Since the carbon nanotube is a relatively new entity for mechanical engineering researchers, it was felt appropriate to include a brief introduction to the types of carbon nanotubes at the start of Chapter 5, *Fluid conveying Carbon Nanotubes – Mathematical formulation*. It was felt appropriate to include the literature survey on carbon nanotubes in this chapter. The literature survey starts with the discovery of carbon nanotubes by Iijima in 1991 and covers the more specific literature of fluid conveying carbon nanotubes. Moreover, in the analysis of carbon nanotubes, the effect of small length scales has to be taken into account, and this is carried out by using the non-local continuum mechanics model, which many researchers have agreed, is a more realistic method to model nanotubes. A brief introduction to the non-local continuum mechanics theory has also been included and the equations of motion for the fluid conveying carbon nanotubes have been derived. A carbon nanotube is appropriately considered to be embedded in the elastic media of both Winkler and the Pasternak type, the latter being a new contribution of this work.

In Chapter 6, *Natural Frequencies of Fluid Conveying Carbon Nanotubes Embedded in Elastic Media,* the equations derived in Chapter 5 are solved and extensive numerical results are obtained for the natural frequencies of fluid conveying carbon nanotubes. The method of solution followed is also different as compared to most

researches in this field. The results are compared with those available in the literature, wherever possible. The results for the natural frequencies of fluid conveying carbon nanotubes embedded in Pasternak type elastic medium have not been published so far and would be a contribution of this study. Also, the analysis considers the three ideal boundary conditions, many of which are new.

Finally, in Chapter 7, *Conclusions,* a summary of results is given highlighting the new contributions to this exciting and practically important field. The formulation of the equations, closed form solutions and results for pipes conveying fluid resting on Pasternak foundation are additions to the available literature. Similarly, the formulation of the governing equations for a carbon nanotube conveying fluid and embedded in a Pasternak type of elastic medium and the analytical results obtained are new additions to the literature. The effect of the various parameters used in the governing equations is clearly brought out and comparisons made wherever possible. Useful conclusions are drawn from the results and comparisons. Finally, the chapter ends with suggestions for further work in this area.

The thesis starts with the mandatory Certificates in the format prescribed by the Osmania University College of Engineering (A), followed by the usual section on Acknowledgements.

A brief Abstract of the work, giving a gist of the content in the thesis and what to expect in the following chapters is included in the beginning of the thesis.

The variables appearing in different equations are explained at appropriate points in the text the first time. In case of confusion, the reader can refer to the comprehensive

list of variables given in the Nomenclature at the beginning of the thesis. This list is given in alphabetical order to enable easy search for the desired variable notations.

The figures and tables have been labeled chapter-wise and appear at appropriate places in the text for ready comprehension. A list of Figures and Tables is included at the beginning of the thesis for easy reference.

A list of references is attached at the end of the thesis. This list is by no means comprehensive, considering the vast number of papers that have appeared on this topic, but nevertheless, publications most relevant to the present work are included in this list.

Chapter 2

Fluid Conveying Pipes - Mathematical Formulation

2.1 Introduction

In the study of vibrations in graduate courses in universities, the start is invariably made with the formulation of equations of motion for single degree of freedom systems, progressing to two degree of freedom systems and finally multi-degree of freedom cases. Then comes the more advanced topic of continuous systems in which there are infinite degrees of freedom. It is in this class of problems that the dynamics of fluid conveying pipes falls into.

Pipes of circular cross-section have been used for conveying fluids in a number of complex configurations. When a fluid flows in such a piping system, it will deflect the pipe and the energy due to the velocity of the flowing fluid is imparted to the piping system subjecting it to vibrations. The natural frequency of the pipe generally decreases with increase in the flow velocity. The severity with which the pipe vibrates

depends on a number of factors, some of which are: the flexural rigidity of the pipe, mass and velocity of the flowing fluid per unit length of the pipe, mass of the pipe itself per unit length of the pipe, the lateral deflection of the pipe due to the load imposed by the weight of the flowing fluid and the pipe material and the types of support on which the pipe is resting. In this chapter, the fundamental mathematical model is derived using the Newtonian mechanics approach. It is felt that this presentation is essential for a better understanding of the various terms that appear in the governing differential equation. To this end, an attempt is made to systematically derive the governing equations of motion for a fluid conveying pipe, starting with the fundamental equation for free transverse vibrations of a beam. Although, this equation is the most fundamental equation in the study of vibrations of continuous systems and its discussion seems to be out of place in a work like this, it was nevertheless felt that the derivation of this equation is useful at this stage, since it will a be basis for the subsequent derivations of the equations with fluid flow and would also serve to standardize the sign convention used in the derivations.

2.2 Transverse vibrations of a beam

For analysis purposes, the pipe, or for that matter, a nanotube is modeled as an elastic beam as shown in Fig. 2.1 (a). When such a pipe is given a small displacement in the z-direction and released, transverse or lateral oscillations occur. The assumptions in that analysis are as follows:

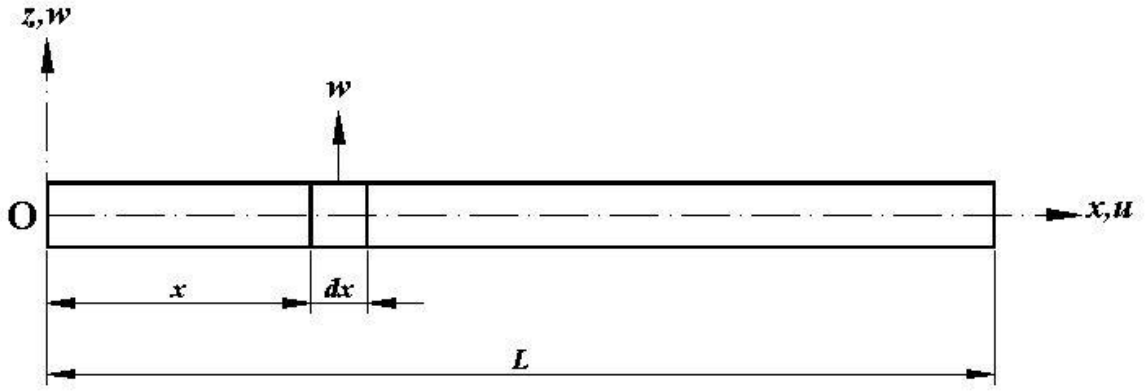

(a)

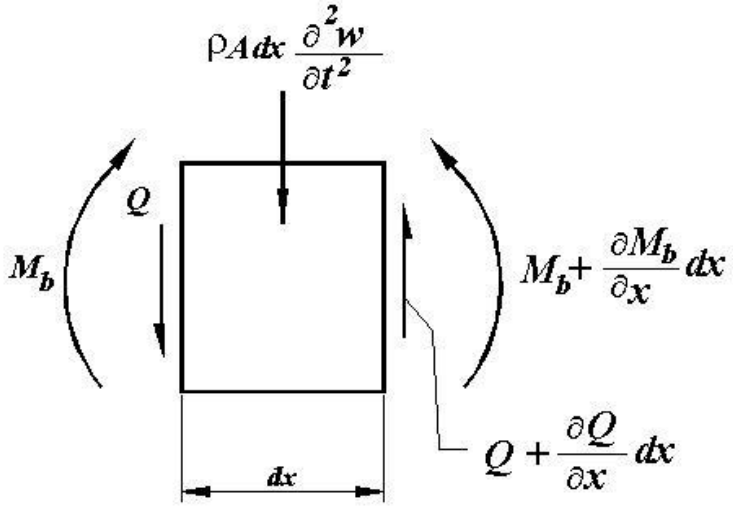

(b)

Figure 2.1 (a) A pipe in the x-z plane; (b) An element of the pipe cross-section **[39]**

Only elastic deflections occur

- Deflections at any point in the pipe are small
- Deflections occur only in a direction perpendicular to the pipe axis
- The effects of shear deformation and rotary inertia are absent, which is in conformity with the Euler-Bernoulli beam theory

The dynamic deflection of any point in the pipe is a function of both time and position and is represented by *w(x,t)*. Let us consider a small segment of the beam of length *dx*, located at a distance *x* from the left end. Such an element with inertial and internal forces and moments acting on it is shown in Fig. 2.1 (b). Referring to Fig. 2.1, M_b is the bending moment, *Q* is the shearing force, *A* is the area of the resisting section of the beam and ρ is the mass per unit length of the beam. The forces, moments and the deflection in Fig. 2.1 are all shown in the positive sense. This sign convention is mathematically rigorous and leaves no scope for confusion (see for instance, Kumar **[46]** and Ragab and Bayoumi **[47]**). This being the case, the differential equation for beam flexure becomes:

$$\frac{\partial^2 w}{\partial x^2} = \frac{M_b}{EI} \tag{2.1}$$

where *EI* is the flexural rigidity of the beam. When the beam undergoes transverse vibrations, one can write the force equilibrium equations in the z-direction as follows:

$$\frac{\partial V}{\partial x} dx - \rho A dx \frac{\partial^2 w}{\partial t^2} = 0 \tag{2.2}$$

and, the moment equilibrium equations can be written as

$$\frac{\partial M_b}{\partial x} dx + V dx = 0 \tag{2.3}$$

or,

$$V = -\frac{\partial M_b}{\partial x} \tag{2.4}$$

Substituting Equation (2.4) into Equation (2.2), we have

$$-\frac{\partial^2 M_b}{\partial x^2} = \rho A \frac{\partial^2 w}{\partial t^2} \tag{2.5}$$

Now, substituting for M_b from Equation (2.1), we obtain

$$EI \frac{\partial^4 w}{\partial x^4} + \rho A \frac{\partial^2 w}{\partial t^2} = 0 \tag{2.6}$$

In the above equation, the term on the left hand side of the equation $\left(EI\, \partial^4 w / \partial x^4 \right)$, represents the inertia force due to the elasticity of the pipe material and the term on the right hand side of the equation, $\left(\rho A \partial^2 w / \partial t^2 \right)$ represents the inertia force due to the acceleration of the pipe in the vertical direction. Equation (2.6) is the well known governing differential equation of motion for the analysis of free vibrations of a beam, as explained in standard texts on dynamics of continuous media, for example see Hutton **[48]** and Rao **[49]**.

2.3 Types of elastic media

Before we attempt to derive the governing equations, it would be interesting to review the various ways in which an elastic medium can be modeled. Fig. 2.2 schematically shows a typical pipeline resting on soil medium. The soil can be granular, soft, rocky, snow and the like. The researchers in the soil mechanics area have come up with many models which mathematically describe the behaviour of the soil. Kerr **[45]**, in 1964, described various foundation models of interest to engineers. Whether it is a pipe or a carbon nanotube, the mechanics of the interactions between the elastic medium and the pipe or nanotube is the same. The following sections reproduce the salient features of some of these models.

2.3.1 The Winkler model

Winkler, as far back as in 1867 (cited from **[45]**), produced the first mathematical model of the soil. He assumed that the soil consisted of a series of independent, very closely spaced linear springs. The reaction force provided by the foundation or the elastic medium is directly proportional to the deflection of the beam which it is supporting through a spring constant or, the *foundation modulus*. Thus, in this model there is only one foundation modulus parameter. In this Chapter, the reaction force of the Winkler foundation will be evaluated and this force will be included in the final governing differential equation of the pipe conveying fluid.

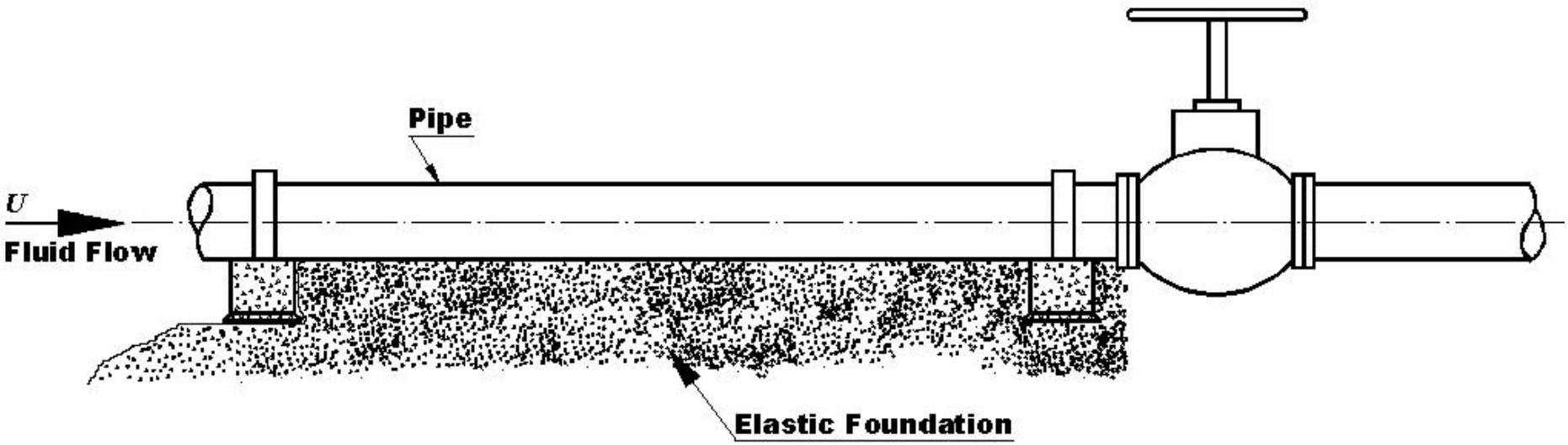

Figure 2.2 Schematic of a pipeline resting on a soil medium

2.3.2 The Filonenko-Borodich model

The Winkler model assumed that the springs are independent with no interactions amongst themselves, which was considered an inaccurate model of the real soil medium. Filonenko-Borodich, in 1940 (cited from **[45]**), considered the elastic medium to consist of a stretched membrane in tension connected to the top ends of the springs of the Winkler model, to account for some sort of interaction between the springs. This model has two foundation parameters, one of which is the Winkler parameter and the second is the parameter due to the tension of the attached membrane.

2.3.3 Hetényi model

Hetényi, in 1946 (cited from **[45]**), considered a beam or a plate in bending, instead of a stretched membrane to model the interactions between the Winkler springs. His model also introduced a second parameter to the foundation modulus. The second parameter is governed by the flexural rigidity of the beam of plate.

2.3.4 Pasternak model

The real soil medium, for which all these models have been developed, is more complex in its elastic behaviour than what is suggested by the simple Winkler model. The Winkler model assumes that the deformation is only in the loaded region, thus implying a deformation discontinuity between the loaded and the unloaded regions. To address such deficiencies, many researchers suggested an interaction between the

linear springs of the Winkler model, leading to the development of two-parameter models. The Pasternak model is one such model. This model of the elastic medium has found a lot of popularity among researchers because it is considered closer to the soil behaviour than other two-parameter models; see for example Dutta and Roy **[67]**. In this model the series of springs in the Winkler model are assumed to be connected at their top ends to a beam (in an two-dimensional case) or a plate (in a three-dimensional case) as in the Hetényi model; Pasternak, 1954 (cited from **[45]**). However, the beam or plate is considered to be an incompressible layer which does not deform by bending but only by shear. This model has found large popularity after the Winkler model among researchers. The second foundation parameter is the shear parameter here. The mathematical formulation of the model will be developed and it will be used to derive the governing equations of both fluid conveying pipes as well as fluid conveying carbon nanotubes for the first time in later sections of this chapter.

2.3.5 Vlasov model

Vlasov formulated the problem of the elastic foundation from the continuum point of view, by modeling it as a semi-infinite elastic medium, by using a variational approach in 1960 (cited from **[45]**). Although this model is mathematically rigorous and more accurate than all previous models, it is difficult to obtain an exact solution for the deformations and reactions. However, this model has been used after some simplifications and redefining of constants, leading to a relation which is identical to that of the Pasternak model.

2.4 The Winkler foundation model - analysis

As noted earlier, the Winkler model of the elastic media is over a century old and most popular because of its simplicity. In reality, the soil medium is very complex; the interest here is not to analyze the mechanics of the soil but to calculate the response of the medium to the load applied by the pipe. Fig. 2.3 schematically shows a pipe resting on a Winkler foundation. The foundation is represented mathematically be means of a series of closely spaced linear spring of equal and constant stiffness. If the pipe deflection is $w(x,t)$, and the reaction of the Winkler type elastic medium on the pipe is denoted by $R_W(x,t)$, the two are related by the equation

$$R_W(x,t) = -k_W w(x,t) \tag{2.7}$$

It is to be noted here that the reaction force due to the foundation $R_W(x,t)$ is always in the z-direction only, without any component in the x-direction. This assumption is consistent with the spring model that is considered. Here the constant k_W is the elastic foundation modulus or foundation stiffness per unit length of the pipe. This reaction force of the foundation shall be included in the governing differential equation of the carbon nanotube conveying fluid and resting on a Winkler foundation in the later sections of this chapter. As seen from Equation (2.7), there is only a single foundation parameter appearing in this model, popularly called the Winkler foundation modulus.

2.5 The Pasternak foundation model - analysis

Pasternak (cited from [45]), proposed a new model for the elastic foundation by introducing one more foundation parameter called the shear parameter. He assumed

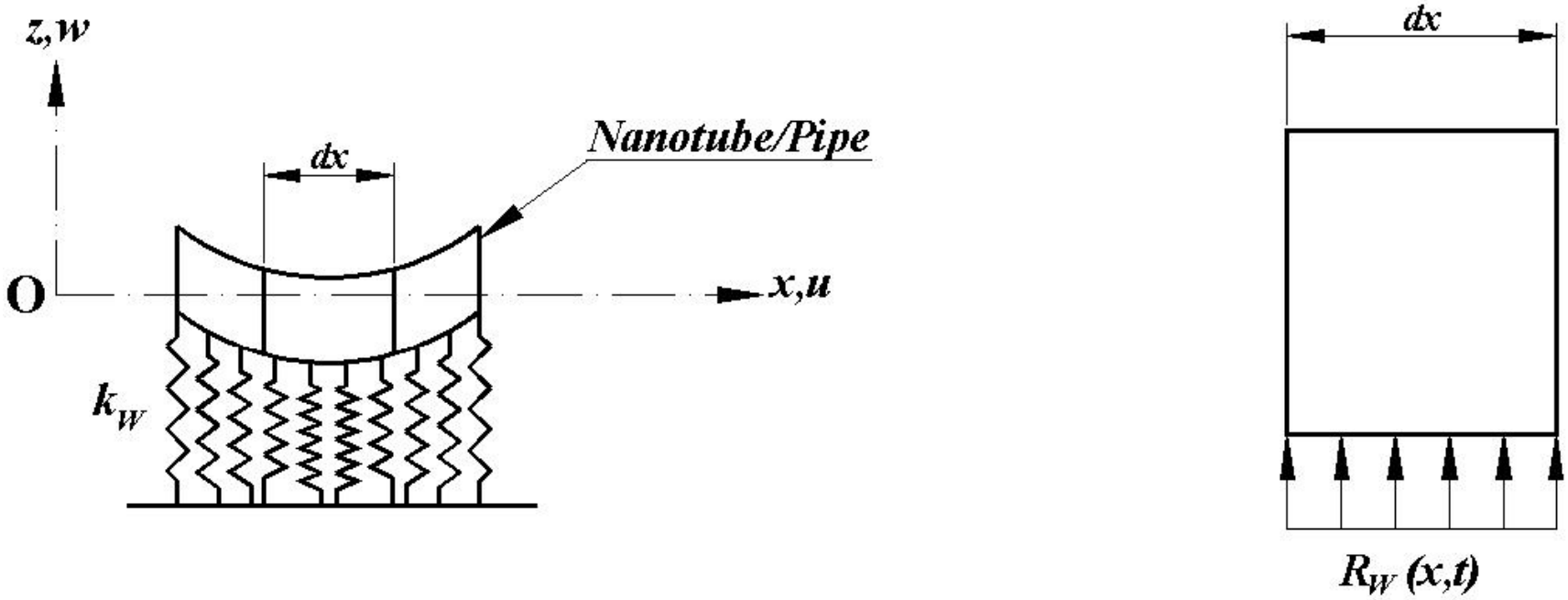

Figure 2.3 Model of a Winkler Foundation

that there existed shear interactions between the linear spring elements of the Winkler model, which can be realized by connecting the ends of the springs to an incompressible beam or plate, which can resist only transverse shear deformations. A model of the Pasternak foundation is shown in Fig. 2.4. In this model, the two foundation parameters are the Winkler modulus k_W and the Pasternak modulus k_P. The contribution due to the Winkler modulus remains the same, while the Pasternak modulus introduces an extra force term which has to be taken into account in the equation of motion. To derive this reaction force, we refer to the free-body diagram shown in Fig. 2.5.

The shear strain is given by

$$\gamma_{xz} = \theta = + \frac{\partial w}{\partial x} \tag{2.8}$$

Considering the force equilibrium for the element of the foundation shown in Fig. 2.6 (b), we have

$$\frac{\partial \tau_{xz}}{\partial x} - k_W w = 0 \tag{2.9}$$

where τ_{xz} is the shear stress acting on the resisting area per unit area. This quantity is given by

$$\tau_{xz} = k_P \gamma_{xz} = k_P \frac{\partial w}{\partial x} \tag{2.10}$$

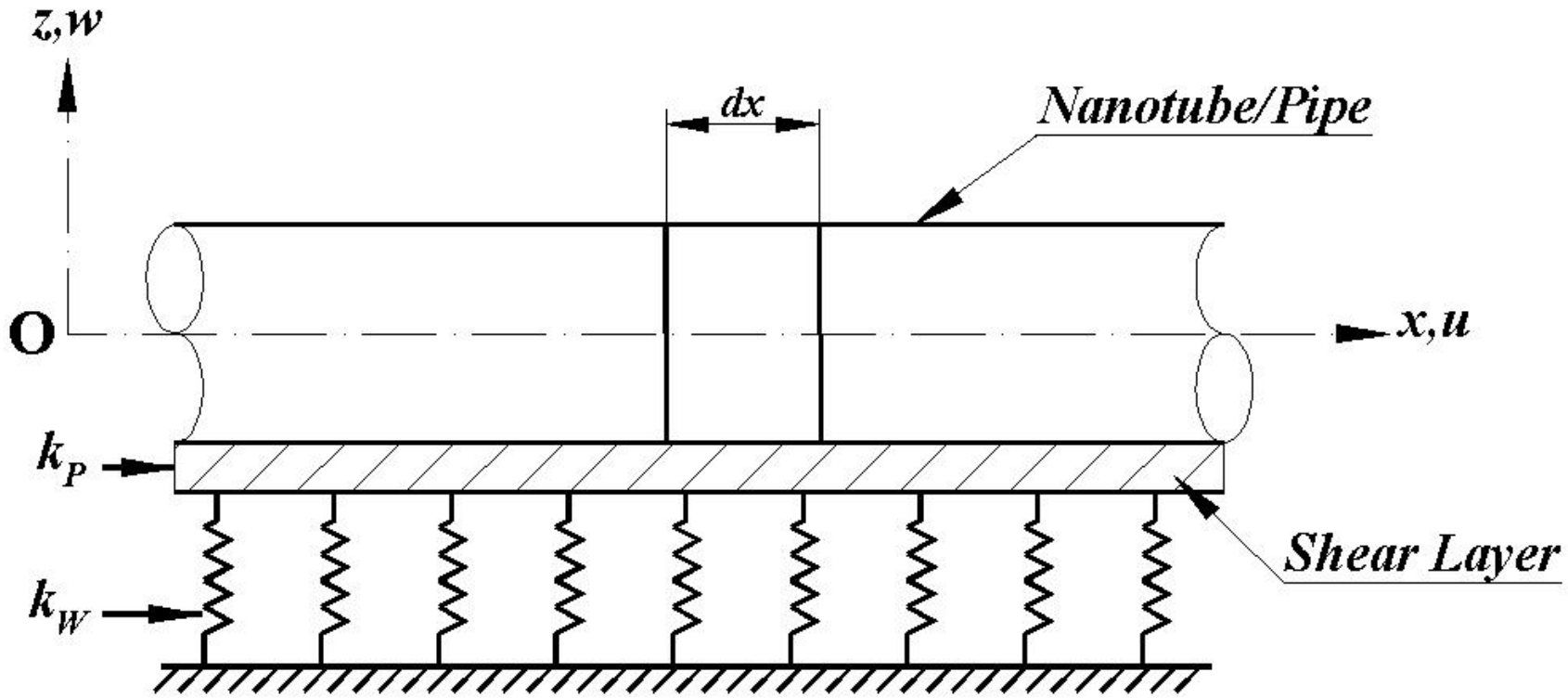

Figure 2.4 Model of a Pasternak Foundation

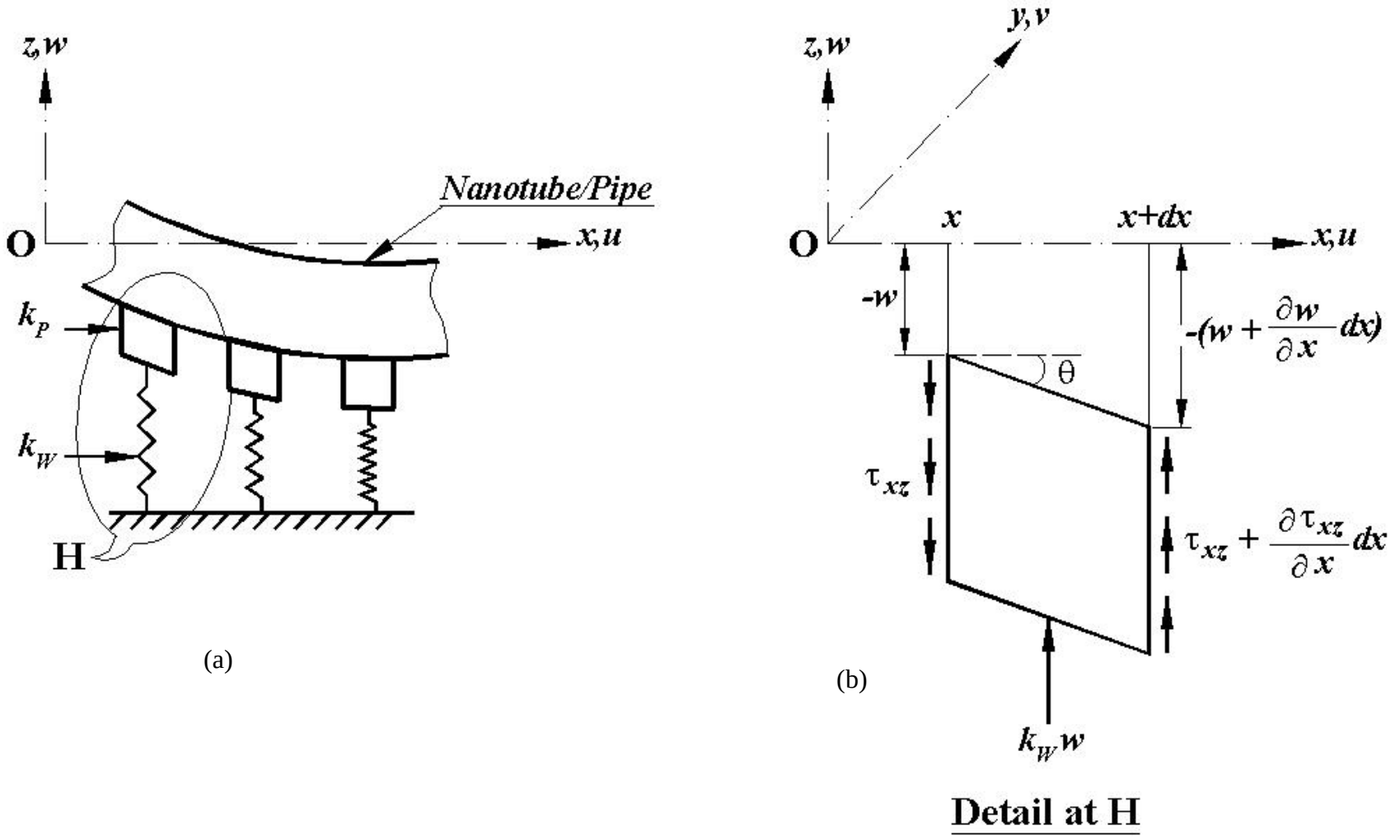

Figure 2.5 (a) Pasternak Model, (b) Forces acting on an element of the foundation

Substituting Equation (2.10) in Equation (2.9), we obtain the relation for the resisting force applied on the carbon nanotube by the Pasternak foundation per unit length as

$$k_P \frac{\partial^2 w}{\partial x^2} - k_W w = R_P(x,t) \tag{2.11}$$

This force has to appear in the governing differential equation of a carbon nanotube conveying fluid and embedded in a Pasternak type elastic medium.

2.6 Transverse vibrations of a fluid conveying pipe resting on a Pasternak type elastic medium

The study of vibrations of fluid conveying pipes was seriously pursued beginning with Ashley & Haviland **[1]**, in 1950 when they attempted to analyze the observed vibrations in the Trans-Arabian oil pipeline. It was observed that at some critical wind speeds, the above-ground oil pipeline, Fig. 2.6, vibrated with small amplitude but decayed quickly to rest. This observation led to the idea that there must be some agent which dampens the vibrations. It was shown in their analysis that this dampening agent was the fluid flow within the pipeline.

However, in their analysis there was a major error in the formulation of the governing equation of motion, as pointed out in 1952 by Housner **[2]**. He derived a more complete equation of motion and presented the results both for free vibrations of the pipeline as well as steady state forced vibrations. He also introduced the concept of critical velocity of the fluid, at which the frequency of the system becomes zero theoretically, leading to buckling (divergence). As will be seen later, Ashley &

Figure 2.6 Trans-Arabian Oil Pipeline (from the web sites)

Haviland omitted the all important term in the equation related to the effects of centrifugal forces. This term appears in the equation due to the fluid flowing along a pipe deflected into a curve. Both the fundamental papers above did not consider any kind of foundation and both authors restricted their analysis to pinned-pinned end conditions. In the next section, the equation of motion for a pipe resting on a Pasternak type foundation will be discussed.

2.6.1 The equations of motion

The pipe is a macro-structure and equations of motion are formulated using the classical continuum mechanics approach. In this section, a comprehensive equation of motion will be developed for a pipe conveying fluid, and resting on a Pasternak type elastic medium. The linear governing equation of motion will be derived according to the Newtonian approach. It can also be derived using the Hamiltonian approach, as clearly explained in Païdoussis **[40]**. Fig. 2.7 shows a pipe conveying fluid and resting on a Pasternak elastic medium. No supports are shown in the figure, all the three ideal types of supports being considered in the next Chapter. The system in the figure consists of a pipe of length L supported at both the ends in some way, flexural rigidity EI, mass per unit length m_p, conveying an incompressible fluid of mass m_f with a uniform flow velocity of U in the x-direction. The x-axis coincides with the horizontal axis of the pipe in its un-deformed state and the z-axis is vertically upwards, indicating that the deflection, w, of the pipe is measured in a positive sense in the upward vertical direction.

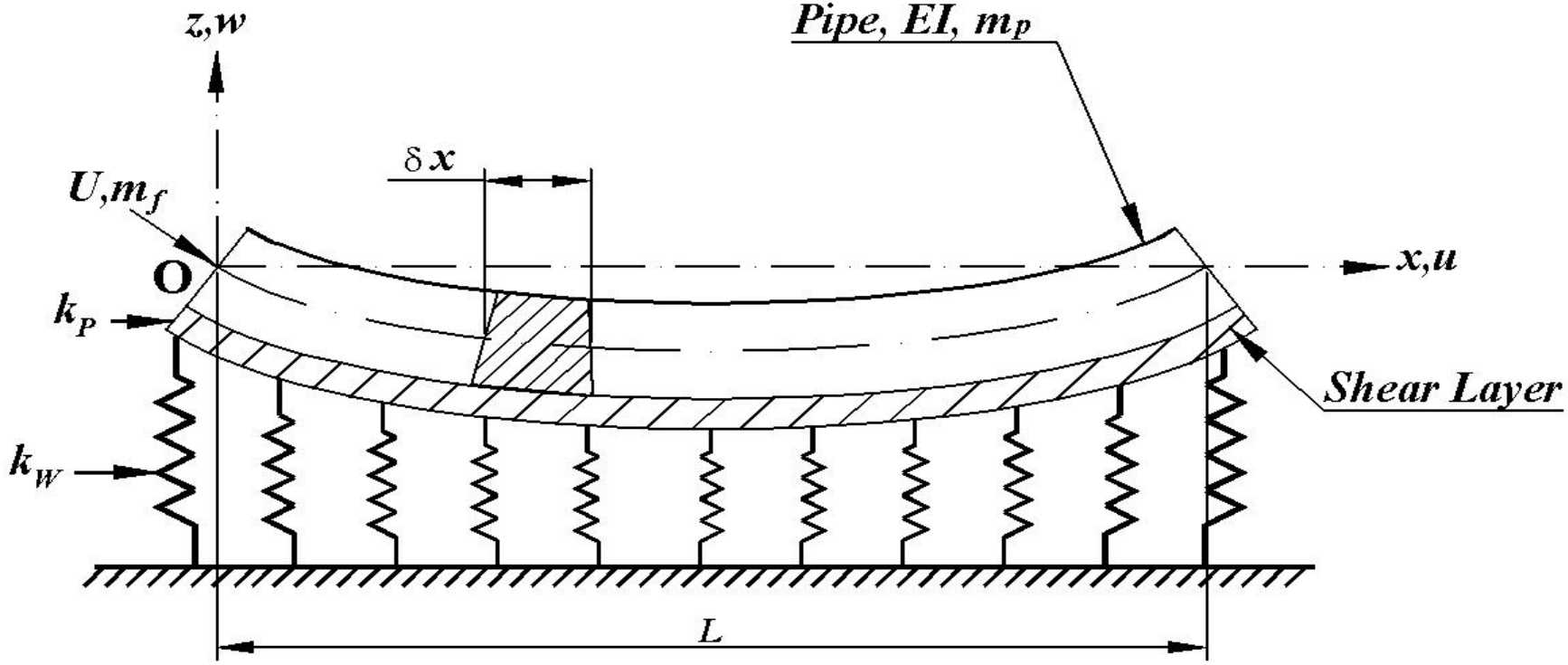

Figure 2.7 Model of a Pipe Conveying Fluid and Resting on a Pasternak Type Elastic Medium

The area of cross-section of the pipe through which the fluid flows is A. x and t are the axial space coordinate and time respectively.

We now consider for analysis purposes, a small element of the pipe and fluid of length δx as shown in Fig. 2.8 and Fig. 2.9, respectively. The forces acting on the fluid element shown in Fig. 2.8 are the pressure forces due to the guage pressure, p, reaction forces of the pipe wall on the fluid element which act normal to it, $F\delta x$, the tangential forces due to the friction between the nanotube wall and the fluid, $qS\delta x$, where S is the internal perimeter of the nanotube wall and q is the wall shear stress and the inertia forces due to the fluid acceleration in the z-direction, $m_f a_{fz}$. The fluid flow is considered to be a simple plug flow type.

Fig. 2.9 shows the corresponding pipe element. The forces acting on the pipe element are as follows: M_b is the bending moment induced in the pipe section and Q is the transverse shear force associated with it. The pipe is subjected to longitudinal tension due to the fluid pressure, represented by T. The normal reaction force on the pipe wall due to the fluid is denoted by $F\delta x$ and the tangential shear force on the pipe walls due to fluid flow is $qS\delta x$. The reaction forces of the Pasternak medium on the pipe are denoted by R_P. The inertial force due to the pipe element acceleration in the z-direction is given as $m_p a_{pz}$.

In the subsequent analysis, it is assumed that the pipe is a slender body, and its lateral motions $w(x,t)$ are small. Consequently, the pipe acceleration in the x-direction which is a term of the second order of magnitude has been neglected. Also these motions are assumed to be restricted to one plane only, the x-z plane.

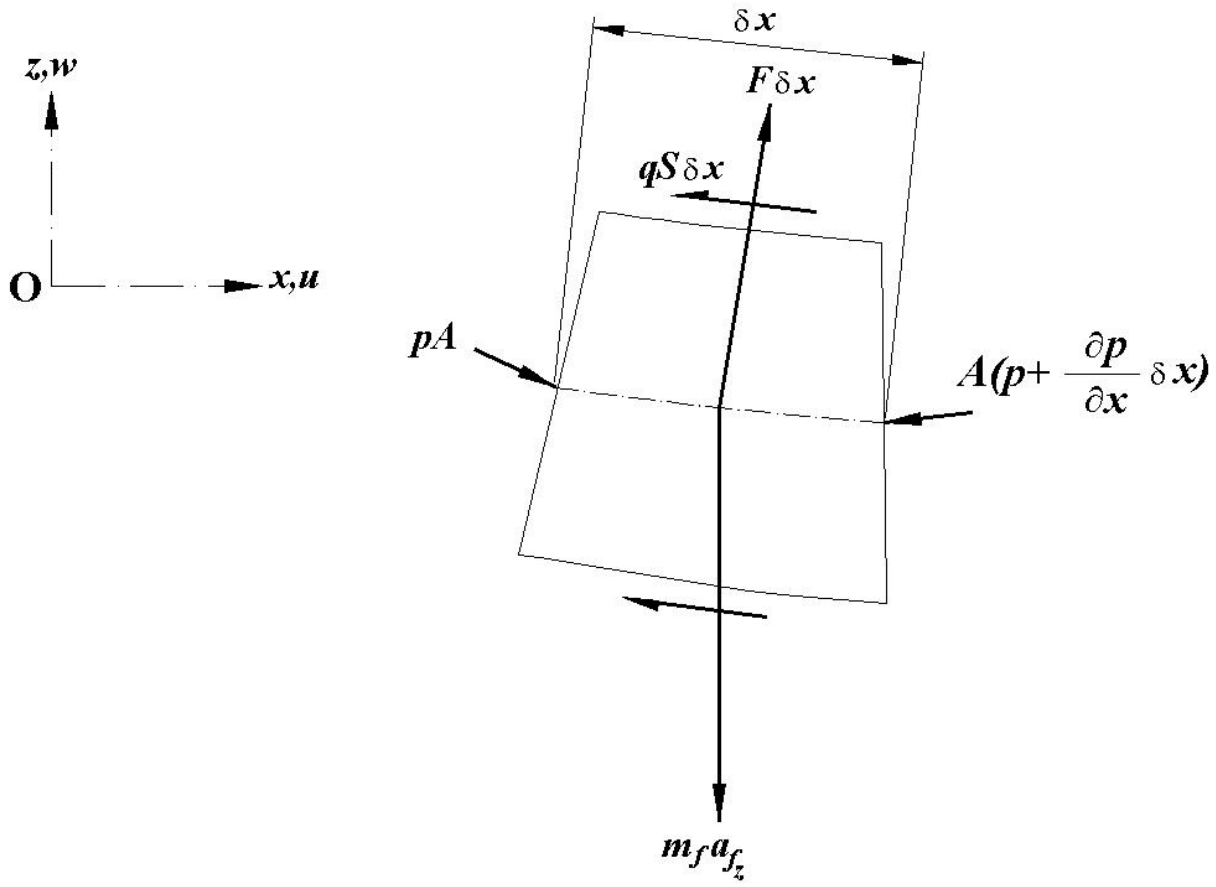

Figure 2.8 Forces acting on an element of the fluid flowing in the pipe

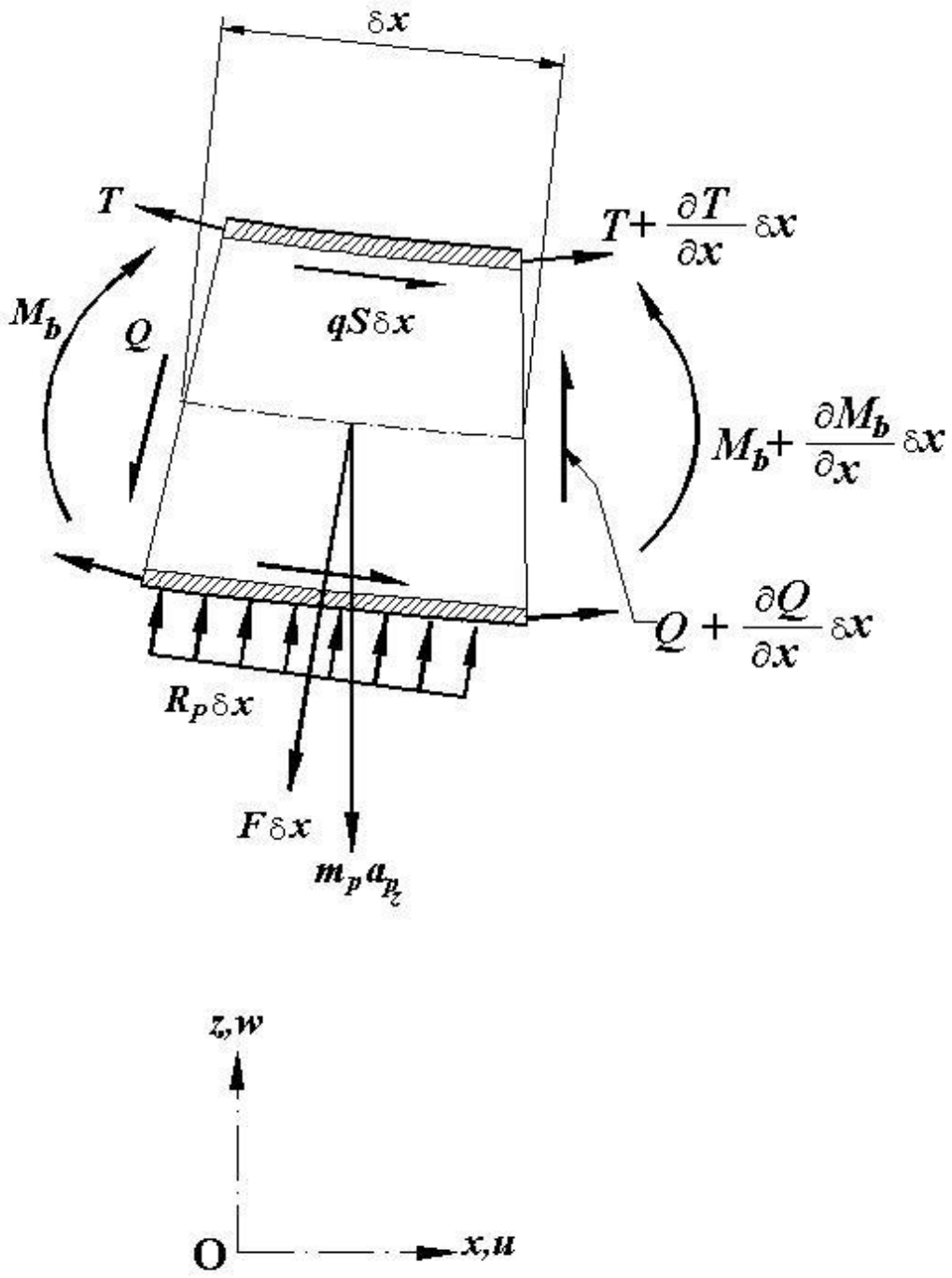

Figure 2.9 Forces acting on an element of the pipe

The transverse shear deformation and rotary inertia of the pipe have also been neglected, in accordance with the Euler-Bernoulli beam theory. These assumptions are in accordance with the theory developed by many researchers; see for example, Païdoussis **[40]**. All the forces shown in the Figs. 2.7 and 2.8 are to be taken in the positive sense.

Application of Newton's second law of motion to the fluid element in the x- and z-directions, we obtain the following equilibrium equations respectively:

$$-A\frac{\partial p}{\partial x} - qS - F\frac{\partial w}{\partial x} = 0 \tag{2.12}$$

and

$$-A\frac{\partial}{\partial x}\left[p\frac{\partial w}{\partial x}\right] - qS\frac{\partial w}{\partial x} + F = m_f a_{f_z} \tag{2.13}$$

Similarly, for the pipe element in the x- and z-directions, we obtain the following equilibrium equations respectively:

$$\frac{\partial T}{\partial x} + qS - \frac{\partial}{\partial x}\left(Q\frac{\partial w}{\partial x}\right) + F\frac{\partial w}{\partial x} = 0 \tag{2.14}$$

and

$$\frac{\partial}{\partial x}\left(T\frac{\partial w}{\partial x}\right) + qS\frac{\partial w}{\partial x} + \frac{\partial Q}{\partial x} - F + R_P = m_p a_{p_z} \tag{2.15}$$

Adding Equations (2.12) and (2.14), we have for the x-direction,

$$-A\frac{\partial p}{\partial x}+\frac{\partial T}{\partial x}-\frac{\partial}{\partial x}\left(Q\frac{\partial w}{\partial x}\right)=0 \tag{2.16}$$

And, adding equations (2.13) and (2.15), for the z-direction,

$$-A\frac{\partial}{\partial x}\left[p\frac{\partial w}{\partial x}\right]-\frac{\partial}{\partial x}\left(T\frac{\partial w}{\partial x}\right)+\frac{\partial Q}{\partial x}+R_P-m_p a_{p_z}-m_f a_{f_z}=0 \tag{2.17}$$

From elementary mechanics of materials, we have the following relations for bending moment, shear force and load:

$$M_b=EI\frac{\partial^2 w}{\partial x^2}$$

$$Q=-\frac{\partial M_b}{\partial x}=-EI\frac{\partial^3 w}{\partial x^3} \tag{2.18}$$

$$\frac{\partial Q}{\partial x}=-EI\frac{\partial^4 w}{\partial x^4}$$

It is to be noted that the above equations are consistent with the sign convention adopted in this thesis as explained in Section 2.2 and Fig. 2.1. Substituting for *Q* from second relation of Equation (2.18) into Equation (2.16), we obtain

$$-A\frac{\partial p}{\partial x}+\frac{\partial T}{\partial x}-\frac{\partial}{\partial x}\left(-EI\left\{\frac{\partial^3 w}{\partial x^3}\right\}\left\{\frac{\partial w}{\partial x}\right\}\right)=0 \tag{2.19}$$

In the above equation, the last term is a second order term in derivatives, and hence, in conformity with the small deflections theory of Euler-Bernoulli, it can be neglected. Thus Equation (2.19), after rearranging the terms suitably, simplifies to

$$\frac{\partial}{\partial x}\left(pA - T \right) = 0 \tag{2.20}$$

Now, substituting for ($\partial Q/\partial x$) from Equation (2.18) in Equation (2.17), we have,

$$-\frac{\partial}{\partial x}\left(pA - T \right)\frac{\partial w}{\partial x} - EI\frac{\partial^4 w}{\partial x^4} + R_P - m_p a_{p_z} - m_f a_{f_z} = 0 \tag{2.21}$$

The first term in the above equation is zero as per Equation (2.20), which leads to the following equation

$$EI\frac{\partial^4 w}{\partial x^4} - R_P + m_f a_{f_z} + m_p a_{p_z} = 0 \tag{2.22}$$

Now, we resolve the last two terms of inertial forces due to fluid acceleration and the pipe acceleration in the above equation. The force due to pipe acceleration is straight forward and leads to

$$m_p a_{p_z} = m_p \frac{\partial^2 w}{\partial t^2} \tag{2.23}$$

Substituting Equation (2.23) in Equation (2.22), we get

$$EI\frac{\partial^4 w}{\partial x^4} + m_p \frac{\partial^2 w}{\partial t^2} + m_f a_{f_z} - R_P = 0 \tag{2.24}$$

The fluid acceleration term, $m_f a_{f_z}$, needs further evaluation. The fluid velocity is denoted by *U*, whose x-component is U_x. The z-component of the fluid velocity,

which is induced due to the lateral motion of the pipe, is given by the total derivative as below:

$$\begin{aligned}\frac{Dw}{Dt} &= \frac{\partial w}{\partial t} + \frac{\partial w}{\partial x}\frac{\partial x}{\partial t} \\ &\equiv U_x \frac{\partial w}{\partial x} + \frac{\partial w}{\partial t}\end{aligned} \tag{2.25}$$

Therefore, the total fluid velocity vector with x- and z- components of flow becomes

$$\mathbf{U} = U_x \mathbf{i} + \left(U_x \frac{\partial w}{\partial x} + \frac{\partial w}{\partial t} \right) \mathbf{k} \tag{2.26}$$

The variables in **bold** are vectors in the above equation. The fluid acceleration is given by the material derivative of the fluid velocity, as is well explained in elementary texts on fluid mechanics; see for instance Allen & Ditsworth **[44]**, as below:

$$\mathbf{a_f} = \frac{D\mathbf{U}}{Dt} = \frac{\partial \mathbf{U}}{\partial x} U_x + \frac{\partial \mathbf{U}}{\partial y} U_y + \frac{\partial \mathbf{U}}{\partial z} U_z + \frac{\partial \mathbf{U}}{\partial t} \tag{2.27}$$

It is clear from the assumptions of steady axial flow conditions that the second and the third terms are non-existent.

Thus Equation (2.27) can be expanded into

$$\mathbf{a_f} = \frac{\partial}{\partial x}\left[U_x \mathbf{i} + \left(U_x \frac{\partial w}{\partial x} + \frac{\partial w}{\partial t} \right) \mathbf{k} \right] U_x + \frac{\partial}{\partial t}\left[U_x \mathbf{i} + \left(U_x \frac{\partial w}{\partial x} + \frac{\partial w}{\partial t} \right) \mathbf{k} \right] \tag{2.28}$$

The above equation, after some manipulations, and recognizing the fact that the flow is a steady axial flow, consequently leads to the z-component of the fluid acceleration to be

$$\mathbf{a}_{\mathbf{f}_z} = \left[\frac{\partial^2 w}{\partial t^2} + 2U_x \frac{\partial^2 w}{\partial x \partial t} + U_x{}^2 \frac{\partial^2 w}{\partial x^2} \right] \mathbf{k} \tag{2.29}$$

The terms in square brackets in the above equation can be written as

$$\mathbf{a}_{\mathbf{f}_z} = \left[\frac{\partial}{\partial t} + U_x \frac{\partial}{\partial x} \right]^2 w\mathbf{k} \tag{2.30}$$

Now, the inertia force die to fluid acceleration in the vertical z-direction can be evaluated as

$$m_f a_{f_z} = m_f \left[\frac{\partial}{\partial t} + U_x \frac{\partial}{\partial x} \right]^2 w \tag{2.31}$$

In the above equation the variable U_x can be replaced with U, consistent with the assumption that the flow field is steady axial flow. Substituting the expression for the inertial forces due to fluid acceleration from Equation (2.31) into Equation (2.24), we obtain

$$EI \frac{\partial^4 w}{\partial x^4} + m_p \frac{\partial^2 w}{\partial t^2} + m_f \left[\frac{\partial}{\partial t} + U \frac{\partial}{\partial x} \right]^2 w - R_P = 0 \tag{2.32}$$

Finally, we need to insert the expression for the reaction force due to the Pasternak elastic medium on the carbon nanotube into Equation (2.32) from Equation (2.11) as follows

$$EI\frac{\partial^4 w}{\partial x^4}+m_p\frac{\partial^2 w}{\partial t^2}+m_f\left[\frac{\partial}{\partial t}+U\frac{\partial}{\partial x}\right]^2 w-k_P\frac{\partial^2 w}{\partial x^2}+k_W w=0 \tag{2.33}$$

The above equation can be expanded as

$$EI\frac{\partial^4 w}{\partial x^4}+m_p\frac{\partial^2 w}{\partial t^2}+m_f\frac{\partial^2 w}{\partial t^2}+m_f U^2\frac{\partial^2 w}{\partial x^2}+2m_f U\frac{\partial^2 w}{\partial x\partial t}+k_W w-k_P\frac{\partial^2 w}{\partial x^2}=0 \tag{2.34}$$

In the above equation, the first term is due to the inertia of the pipe itself, represented by the elastic force term, the second and the third terms are because of the inertia force due to the vertical acceleration of the pipe and the fluid respectively, the fourth term is the inertia force associated with the fluid flowing along a curved path due to the enforced curvature of the deflecting pipe. This force may be considered as the centrifugal force experienced by the fluid. The fifth term in Equation (2.34) is the inertia force due to the fluid flowing with a velocity *U* relative to the pipe, while also experiencing an angular velocity $\partial^2 w/\partial x\partial t$ because the pipe itself has this angular velocity at any point along its length. This force is commonly referred to as the Coriolis force. The sixth and the seventh terms in the above equation represent the forces due to the elastic medium of the Pasternak type, with the former being the contribution of the Winkler modulus of the medium and the latter being the

contribution due to the Pasternak stiffness constant. Equation (2.34) can be put in a more familiar form as below

$$EI\frac{\partial^4 w}{\partial x^4} + M\frac{\partial^2 w}{\partial t^2} + \left(m_f U^2 - k_P\right)\frac{\partial^2 w}{\partial x^2} + 2m_f U\frac{\partial^2 w}{\partial x \partial t} + k_w w = 0 \qquad (2.35)$$

In the above equation, M is the total mass per unit length of pipe (m_p) plus fluid (m_f). Equation (2.35) is the final governing differential equation of motion for the analysis of transverse vibrations of a pipe conveying fluid and resting on a Pasternak type elastic medium. There is an interaction of the inertia, elastic, centrifugal and coriolis forces in the equation above. The inertia forces are due to both the pipe and the fluid inertias, **[84]**. The coriolis and the centrifugal forces arise due to the fluid flowing along a curved path and the elastic forces comprise of the pipe elasticity and the foundation stiffness.

This is the similar to Equation (1.4), where ρA there is denoted by m_f here and v there is represented by U here.

2.6.2 Transverse vibrations of a fluid conveying pipe resting on a Winkler foundation

It is observed from Equation (2.36) that the influence of the second foundation parameter k_p, due to the Pasternak modulus appears in the third term of the equation. Setting k_p equal to zero, the equation of motion of a fluid conveying pipe resting on a Winkler foundation may be obtained as

$$EI\frac{\partial^4 w}{\partial x^4} + M\frac{\partial^2 w}{\partial t^2} + m_f U^2\frac{\partial^2 w}{\partial x^2} + 2m_f U\frac{\partial^2 w}{\partial x \partial t} + k_w w = 0 \qquad (2.36)$$

This equation is the same as Equation (1.3). This foundation parameter was first considered by Stein and Tobriner **[12]**, followed by other researchers, **[15, 16, 17]**.

2.7 Summary

In this Chapter, a detailed formulation of the equation of motion of a fluid conveying carbon nanotube embedded in a Pasternak type elastic medium has been presented. To establish the rules for sign convention and for the sake of complete clarity, the derivation has started from the basic equation for the vibrations of a beam/pipe/nanotube, incrementally followed by the formulations for a bare fluid conveying pipe, and finally, a fluid conveying pipe resting on Pasternak elastic medium. The approach followed to formulate the governing equations of motion is the classical continuum mechanics model due to Euler-Bernoulli. Equation (2.35) shows this equation. It is for the first time that this equation has been formulated in the literature and it is hoped that it contributes to better understanding of the dynamics of such systems.

In an attempt to compare the results with those obtained by earlier researchers for fluid conveying pipes resting on Winkler type elastic foundation, the above equation was reduced to account for the same as Equation (2.36). The results from the analysis carried out using Equation (2.35) have been published in 2008, **[72]**.

In the next chapter, the above equations will be solved to obtain numerical results for the critical flow velocities of all such systems, for a number of cases of different parameters and conditions.

Chapter 3

Stability of Fluid Conveying Pipes Resting on Elastic Media

3.1 Introduction

The dynamic analysis of pipes conveying fluid requires one to compute the stability regions of the system. In 1952, Housner **[2]**, pointed out that there is a particular velocity of the fluid called the critical velocity where the natural frequencies become theoretically zero. At this velocity, the system becomes unstable and buckles. Therefore, a number of researchers have focused on computing the stability regions of the system; see for example **[5, 15, 16, 19, 20, 21, 22, 75, 82, 83]**. However, all the above researchers have analyzed mainly the vibrational behaviour of pipes conveying fluid. Computation of critical flow velocity is also essential for further study of the vibrations of the pipes.

Recalling from the theory of columns in elementary strength of materials texts, see for example, Timoshenko **[63]** and Popov **[64]**, the fourth order differential equation for elastic buckling of columns is

$$\frac{\partial^4 w}{\partial x^4} + \lambda^2 \frac{\partial^2 w}{\partial x^2} = 0 \tag{3.1}$$

where $\lambda^2 = P/EI$ and P is the axial load, which causes buckling of the column when it reaches a certain critical value P_{cr}. At this critical value, the natural frequency of the system becomes zero leading to buckling. The governing partial differential equation for a pipe conveying fluid, Equation (3.2), is reproduced below from Equation (2.35)

$$EI \frac{\partial^4 w}{\partial x^4} + M \frac{\partial^2 w}{\partial t^2} + \left(m_f U^2 - k_P \right) \frac{\partial^2 w}{\partial x^2} + 2 m_f U \frac{\partial^2 w}{\partial x \partial t} + k_W w = 0 \tag{3.2}$$

Recasting the above equation an a more convenient form, we have

$$\frac{\partial^4 w}{\partial x^4} + \frac{M}{EI} \frac{\partial^2 w}{\partial t^2} + \frac{\left(m_f U^2 - k_P \right)}{EI} \frac{\partial^2 w}{\partial x^2} + \frac{2 m_f U}{EI} \frac{\partial^2 w}{\partial x \partial t} + \frac{k_W}{EI} w = 0 \tag{3.3}$$

We observe that in the first and the third terms of Equation (3.3) are completely analogous to the terms in Equation (3.1).

Thus it follows that

$$\frac{\left(m_f U^2 - k_P \right)}{EI} = \lambda^2 \tag{3.4}$$

whence,

$$\left(m_f U^2 - k_P\right) = P \tag{3.5}$$

Hence, a critical value of the term in parentheses in Equation (3.5) is equivalent to the Eulerean critical buckling load. Thus, the term associated with the centrifugal force in Equation (3.2), which is influenced by the velocity of the fluid flowing within the pipe, is responsible for buckling or divergence of the pipe, as agreed by many previous researchers. When this conclusion was arrived at, the focus of the researchers was mainly on pipes conveying fluid. From Equation (3.5), it is seen that the Pasternak stiffness parameter of the elastic medium also contributes to this term, influencing instability. Moreover, the result is valid for both a pipe as well as a carbon nanotube conveying fluid. This result has not been reported so far in the literature. This important discovery enables us to study the stability of the fluid conveying pipes.

This chapter focuses on the stability of pipes conveying fluid resting on different elastic media. Solution of the governing differential equation of motion, Equation (3.2), is sought considering three ideal boundary conditions of pinned-pinned, pinned-clamped and clamped-clamped. A Fourier series solution approach is adopted for the case of the pinned-pinned carbon nanotube, as proposed by Housner **[2]**, while a Galerkin approximation is used to obtain a solution for the remaining two end conditions, as followed by Naguleswaran and Williams **[11]**. As both the approaches result in an infinite number of algebraic equations, the number of terms has been restricted to the first four only. The validity and justification for this approach is also shown in the later sections. The objective would be to compute critical flow velocities

of the pipe conveying fluid at which it loses stability. In this chapter, the equations for computing the critical flow velocities of the pipe conveying fluid are derived and the effect of elastic media on the critical flow velocities is also studied. Exhaustive numerical results are generated and analyzed in the course of discussion in this chapter.

3.2 Solution of the Equation for a fluid conveying pipe resting a Pasternak type elastic medium

The solutions for Equation (3.2) are now presented for the three ideal boundary conditions. These are considered ideal because the ends in real situations cannot be totally pinned or clamped. There is some small amount of resistance to the rotation of the pinned end, giving rise to a bending moment at that end. Likewise, a clamped end is not fully clamped in real situations, with the rotation at the end not being exactly equal to zero. These realities can be modeled by other means, for example by considering elastically restrained end conditions, in which the ends can be considered composed of a rotational and a linear spring whose stiffness can be varied to simulate any kind of end condition one desires. However these models are not within the purview of the present research work. Hence, for simplicity we consider the pipe or carbon nanotube to be supported by ideal boundary conditions.

3.2.1 Pinned-pinned pipe

The boundary conditions for a pinned-pinned pipe are

$$w(0,t) = 0$$

$$w(L,t) = 0$$

$$\frac{\partial^2 w(0,t)}{\partial x^2} = 0 \tag{3.6}$$

$$\frac{\partial^2 w(L,t)}{\partial x^2} = 0$$

The solution of Equation (3.2) is considered to be

$$w_j(x,t) = \sum_{n=1,3,5,\ldots} a_n \sin\left(\frac{n\pi x}{L}\right)\sin\omega_j t + \sum_{n=2,4,6,\ldots} a_n \sin\left(\frac{n\pi x}{L}\right)\cos\omega_j t; \quad j = 1,2,3,\ldots \tag{3.7}$$

where, ω_j is the natural frequency of the j[th] mode of vibration of the fluid conveying pipe of length L between the span. It must be noted that the fourth term of Equation (3.2) contains a mixed derivative ($\partial^2 w/\partial x \partial t$). This term is not the same as the viscous damping term which has a form ($\partial w/\partial t$), although it contains a first derivative with respect to time, as explained in a detailed manner by Housner **[2]**. It represents dynamic coupling between the coefficients of the modal solution. Differentiating Equation (3.7) according to the order of differentiation of the terms in Equation (3.2), with respect to the variables in the terms, and considering only n=1,2,3,4, for the sake of brevity, we obtain the following equations

$$\frac{\partial^2 w_j}{\partial x^2} = -\left[\begin{array}{l} a_1 \frac{\pi^2}{L^2} \sin\left(\frac{\pi x}{L}\right) \sin \omega_j t + a_2 \frac{4\pi^2}{L^2} \sin\left(\frac{2\pi x}{L}\right) \cos \omega_j t \\ \\ \quad + a_3 \frac{9\pi^2}{L^2} \sin\left(\frac{3\pi x}{L}\right) \sin \omega_j t + a_4 \frac{16\pi^2}{L^2} \sin\left(\frac{4\pi x}{L}\right) \cos \omega_j t \end{array} \right] \tag{3.8}$$

$$\frac{\partial^4 w_j}{\partial x^4} = \left[\begin{array}{l} a_1 \frac{\pi^4}{L^4} \sin\left(\frac{\pi x}{L}\right) \sin \omega_j t + a_2 \frac{16\pi^4}{L^4} \sin\left(\frac{2\pi x}{L}\right) \cos \omega_j t \\ \\ + a_3 \frac{81\pi^4}{L^4} \sin\left(\frac{3\pi x}{L}\right) \sin \omega_j t + a_4 \frac{256\pi^4}{L^4} \sin\left(\frac{4\pi x}{L}\right) \cos \omega_j t \end{array} \right] \tag{3.9}$$

$$\frac{\partial^2 w_j}{\partial x \partial t} = \left[\begin{array}{l} a_1 \frac{\pi}{L} \omega_j \cos\left(\frac{\pi x}{L}\right) \cos \omega_j t - a_2 \frac{2\pi}{L} \omega_j \cos\left(\frac{2\pi x}{L}\right) \sin \omega_j t \\ \\ + a_3 \frac{3\pi}{L} \omega_j \cos\left(\frac{3\pi x}{L}\right) \cos \omega_j t - a_4 \frac{4\pi}{L} \omega_j \cos\left(\frac{4\pi x}{L}\right) \sin \omega_j t \end{array} \right] \tag{3.10}$$

$$\frac{\partial^2 w_j}{\partial t^2} = -\left[\begin{array}{l} a_1 \omega_j^2 \sin\left(\frac{\pi x}{L}\right) \sin \omega_j t + a_2 \omega_j^2 \sin\left(\frac{2\pi x}{L}\right) \cos \omega_j t \\ \\ \quad + a_3 \omega_j^2 \sin\left(\frac{3\pi x}{L}\right) \sin \omega_j t + a_4 \omega_j^2 \sin\left(\frac{4\pi x}{L}\right) \cos \omega_j t \end{array} \right] \tag{3.11}$$

Substituting Equations (3.8) to (3.11) into the governing equation of motion, Equation (3.2), we obtain terms containing cosine functions of the spatial coordinate *x*, such as

$$\cos\left(\frac{i\pi x}{L}\right) \text{ and } \cos\left(\frac{k\pi x}{L}\right) \text{ ; } i\text{=1,3,5,... and } k\text{=2,4,6,...}$$

This is quite obviously due to the mixed derivative ($\partial^2 w/\partial x \partial t$), as seen from Equation (3.10). Since an equation in which both sine and cosine functions of the spatial coordinate appear is analytically difficult to solve, we seek a way to transform either of them to a single function. This is readily accomplished by utilizing Fourier series expansion of say, cosine functions into sine series. These terms may now be expanded in a Fourier series of sine functions over the length of the pipe, as explained in detail by Housner **[2]**, Naguleswaran and Williams **[11]**, and Chary **[17]**, as shown below

$$\cos\left(\frac{n\pi x}{L}\right) = \sum_{r=1}^{\infty} b_{nr} \sin\left(\frac{r\pi x}{L}\right) \; ; n=1,2,3,... \tag{3.12}$$

In the above equation, b_{nr} is given by

$$b_{nr} = \frac{2r}{\pi} \frac{\left[1-(-1)^{r+n}\right]}{\left[r^2-n^2\right]} \tag{3.13}$$

This leads to

$$b_{nr} = 0 \;\; ; \text{for } (r+n): \text{ even}$$

and (3.14)

$$b_{nr} = \frac{4r}{\pi\left[r^2-n^2\right]} \;\; ; \text{for } (r+n): \text{ odd}$$

Interchanging the subscripts in the above equation,

$$b_{rn} = 0 \ ; \text{for } (r+n): \text{ even}$$

and (3.15)

$$b_{rn} = -\frac{4n}{\pi\left[r^2 - n^2\right]} \ ; \text{for } (r+n): \text{ odd}$$

Using Equations (3.12), (3.14) and (3.15), the cosine functions of the spatial coordinate in the Equation (3.10) get transformed into a series of sine functions of the spatial coordinate.

This is illustrated below for $\cos\left(n\pi x/L\right)$, n = 1,2,3,4.

$$\cos\left(\frac{\pi x}{L}\right) = \frac{8}{3\pi}\sin\left(\frac{2\pi x}{L}\right) + \frac{16}{15\pi}\sin\left(\frac{4\pi x}{L}\right) + ... \quad (3.16)$$

$$\cos\left(\frac{2\pi x}{L}\right) = \frac{-4}{3\pi}\sin\left(\frac{\pi x}{L}\right) + \frac{12}{5\pi}\sin\left(\frac{3\pi x}{L}\right) + ... \quad (3.17)$$

$$\cos\left(\frac{3\pi x}{L}\right) = \frac{-8}{5\pi}\sin\left(\frac{2\pi x}{L}\right) + \frac{16}{7\pi}\sin\left(\frac{4\pi x}{L}\right) + ... \quad (3.18)$$

$$\cos\left(\frac{4\pi x}{L}\right) = \frac{-4}{15\pi}\sin\left(\frac{\pi x}{L}\right) - \frac{12}{7\pi}\sin\left(\frac{3\pi x}{L}\right) + ... \quad (3.19)$$

It is appropriate to mention at this stage that in the present analysis, only the first four terms have been considered in Equations (3.8) to (3.11). Also, in the Fourier expansion in Equations (3.16) to (3.19), only the first two terms have been considered. It should be noted that the solution will turn out to be more accurate if more number

of terms are considered while evaluating the above equations. This has been discussed elaborately by Elishakoff and Vittori **[65]**, for the case of a cantilever pipe conveying fluid. They have shown that by considering more and more number of terms the accuracy can be improved. In this work, only the first two terms of the Equations (3.16) to (3.19) will be used to substitute for the cosine terms in Equation (3.10). It will be shown later that considering only two terms of the above equations is sufficiently accurate for engineering purposes and the results compare well with those published earlier, using even different solution methods.

First, substituting for $\cos(n\pi x/L)$, n = 1,2,3,…, from Equations (3.16) to (3.19) into Equation (3.10), then substituting Equations (3.8) to (3.11) in Equation (3.2) and finally evaluating Equation (3.2), we obtain an equation containing coefficients of $\sin\omega_j t$ and $\cos\omega_j t$.

Collecting terms containing $\sin\omega_j t$ and $\cos\omega_j t$, and equating the coefficients of each to zero, we obtain the following two sets of equations:

$$\left\{\begin{array}{l} EI\dfrac{\pi^4}{L^4}\left[a_1\sin\dfrac{\pi x}{L}+81a_3\sin\dfrac{3\pi x}{L}\right]-\dfrac{\pi^2}{L^2}(m_fU^2-k_P)\left[a_1\sin\dfrac{\pi x}{L}+9a_3\sin\dfrac{3\pi x}{L}\right]+ \\ \\ \dfrac{\pi}{L}(2m_fU)\omega_j\left[\begin{array}{l} -2a_2\left(\dfrac{-4}{3\pi}\sin\dfrac{\pi x}{L}+\dfrac{12}{5\pi}\sin\dfrac{3\pi x}{L}\right) \\ \\ -4a_4\left(\dfrac{-4}{15\pi}\sin\dfrac{\pi x}{L}-\dfrac{12}{7\pi}\sin\dfrac{3\pi x}{L}\right) \end{array}\right]+k_W\left[a_1\sin\dfrac{\pi x}{L}+a_3\sin\dfrac{3\pi x}{L}\right]- \\ \\ M\omega_j^2\left[a_1\sin\dfrac{\pi x}{L}+a_3\sin\dfrac{3\pi x}{L}\right] \end{array}\right\}\sin\omega_j t=0 \qquad (3.20)$$

and,

$$\left\{ \begin{array}{l} EI\dfrac{\pi^4}{L^4}\left[16a_2\sin\dfrac{2\pi x}{L}+256a_4\sin\dfrac{4\pi x}{L}\right]-\dfrac{\pi^2}{L^2}(m_fU^2-k_P)\left[4a_2\sin\dfrac{2\pi x}{L}+16a_4\sin\dfrac{4\pi x}{L}\right]+ \\ \\ \dfrac{\pi}{L}(2m_fU)\omega_j\left[\begin{array}{l} a_1\left(\dfrac{8}{3\pi}\sin\dfrac{2\pi x}{L}+\dfrac{16}{15\pi}\sin\dfrac{4\pi x}{L}\right) \\ \\ +3a_3\left(\dfrac{-8}{5\pi}\sin\dfrac{2\pi x}{L}-\dfrac{16}{7\pi}\sin\dfrac{4\pi x}{L}\right) \end{array}\right]+k_W\left[a_2\sin\dfrac{2\pi x}{L}+a_4\sin\dfrac{4\pi x}{L}\right]- \\ \\ M\omega_j^2\left[a_2\sin\dfrac{2\pi x}{L}+a_4\sin\dfrac{4\pi x}{L}\right] \end{array}\right\}\cos\omega_j t=0 \qquad (3.21)$$

Equations (3.20) and (3.21) are evaluated for n = 1,2,3,4 only for illustration purposes.

For the above equations to hold, it is clear that $\sin\omega_j t$ and $\cos\omega_j t$ cannot be zero, as also $\sin(n\pi x/L)$. Thus it follows that the coefficients of $\sin(n\pi x/L)$ have to be equated to zero for the identity to hold. Consequently, these equations can respectively be further simplified and generalized to the following two systems of equation:

$$a_n\left\{EI\left(\frac{n\pi}{L}\right)^4-(m_fU^2-k_P)\left(\frac{n\pi}{L}\right)^2+k_W-M\omega_j^2\right\} = -\frac{8m_fU\omega_j}{L}\sum_{r=2,4,6,\ldots}a_r\frac{rn}{\left[r^2-n^2\right]}\ ;\ n=1,3,5,\ldots \tag{3.22}$$

and

$$a_n\left\{EI\left(\frac{n\pi}{L}\right)^4-(m_fU^2-k_P)\left(\frac{n\pi}{L}\right)^2+k_W-M\omega_j^2\right\} = +\frac{8m_fU\omega_j}{L}\sum_{r=1,3,5,\ldots}a_r\frac{rn}{\left[r^2-n^2\right]}\ ;\ n=2,4,6,\ldots \tag{3.23}$$

We can express the Equations (3.22) and (3.23) in a matrix form as below, bold face notation being used for representing matrices.

$$\left[\mathbf{K}-\omega_j^2\mathbf{MI}\right]\{\mathbf{a}\}=\mathbf{0} \tag{3.24}$$

where, **K** is the stiffness matrix, **M** is the mass matrix and **I** is the identity matrix, all of order *n X n*, and the vector

$$\{\mathbf{a}\}^{\mathbf{T}} = \{a_1, a_2, a_3, ..., a_n\}$$

The elements of the stiffness matrix **K** are given by

$$k_{lm} = \begin{cases} EIl^4\left(\frac{\pi}{L}\right)^4 - (m_f U^2 - k_P)l^2\left(\frac{\pi}{L}\right)^2 + k_W & ; \text{when } l = m \\ \frac{8m_f U\omega_j}{L}\left(\frac{lm}{l^2 - m^2}\right) & ; \text{when } l > m \text{ and } l+m : \text{ODD} \\ \frac{8m_f U\omega_j}{L}\left(\frac{lm}{m^2 - l^2}\right) & ; \text{when } l < m \text{ and } l+m : \text{ODD} \\ 0 & ; \text{when } l \neq m \text{ and } l+m : \text{EVEN} \end{cases} \quad (3.25)$$

To obtain non-trivial solutions of Equation (3.24), we have to set the determinant of the matrix to zero as shown below

$$\left|\mathbf{K} - \omega_j^2 \mathbf{MI}\right| = 0 \quad (3.26)$$

The system of equations represented by Equation (3.26) above is infinite in number, which cannot be numerically implemented. Hence we restrict the number of terms to a finite number to obtain an approximate solution. More specifically, here the number of terms is taken to be the first two. Naguleswaran and Williams **[11]**, have shown that a

two-term approximation of the Fourier series solution for the pinned-pinned boundary conditions is fairly accurate compared to the exact solution. Hence, retaining only the first two terms of Equation (3.26), we obtain the relation

$$\begin{vmatrix} \left\{ EI\left(\frac{\pi}{L}\right)^4 - (m_f U^2 - k_P)\left(\frac{\pi}{L}\right)^2 + k_W - M\omega_j^2 \right\} & \left\{ \frac{16 m_f U \omega_j}{3L} \right\} \\ \left\{ \frac{16 m_f U \omega_j}{3L} \right\} & \left\{ 16EI\left(\frac{\pi}{L}\right)^4 - 4(m_f U^2 - k_P)\left(\frac{\pi}{L}\right)^2 + k_W - M\omega_j^2 \right\} \end{vmatrix} = 0 \tag{3.27}$$

For the pipe to be stable, the fluid velocity should not equal a certain value called the critical flow velocity, at which the frequency of the system becomes zero. Thus, expanding the determinant in Equation (3.27) and setting the frequency ω_j to zero, we have

$$\left\{ 16\left(\frac{EI}{L^4}\right)^2 \pi^8 - 20EI(m_f U^2 - k_P)\left(\frac{\pi}{L}\right)^6 + 4(m_f U^2 - k_P)^2\left(\frac{\pi}{L}\right)^4 - 5k_W(m_f U^2 - k_P)^2\left(\frac{\pi}{L}\right)^2 + 17k_W EI\left(\frac{\pi}{L}\right)^4 + k_W^2 \right\} = 0 \tag{3.28}$$

It can be observed that the above equation contains our variable of interest, the flow velocity *U*. Thus, the solution of the above equation will enable us to compute the

critical flow velocity. However, before attempting to solve Equation (3.28), it will be convenient to non-dimensionalize the equation. The following non-dimensional parameters are defined for the purpose:

$$V = UL\sqrt{\frac{m_f}{EI}} \quad \text{; which is the flow velocity parameter}$$

$$\beta = \frac{m_f}{\left(m_c + m_f\right)} = \frac{m_f}{M} \quad \text{; where, } M = m_c + m_f$$

$$\text{; which is the mass ratio parameter} \tag{3.29}$$

$$\gamma_W = \frac{k_W L^4}{EI} \quad \text{; which is the Winkler elastic parameter}$$

$$\gamma_P = \frac{k_P L^2}{EI} \quad \text{; which is the Pasternak elastic parameter}$$

Using the parameters in Equation (3.29), Equation (3.28) can be written as

$$\left(V^2 - \gamma_P\right)^2 \left(4\pi^4\right) - \left(V^2 - \gamma_P\right)\left(5\pi^2\gamma_W + 20\pi^6\right) + \left(16\pi^8 + 17\pi^4\gamma_W + \gamma_W^2\right) = 0 \tag{3.30}$$

The above equation is a quadratic in V^2, and can be solved for V. The lowest root V would be the critical flow velocity parameter, V_{cr} , that we seek for pinned-pinned end conditions. The numerical results obtained on the solution of Equation (3.30) are presented in Section 3.3.

3.2.2 Pinned-clamped and clamped-clamped pipes

It has been shown by previous researchers that the Fourier series solution method adopted for the pinned-pinned boundary condition in the previous section requires the least effort. However, for other end conditions, the error in retaining only two terms has been shown to be considerable.

It has been shown by Naguleswaran and Williams **[11]** that even a two-term Galerkin approximation produces sufficiently accurate results. Hence, for the pinned-clamped and the clamped-clamped boundary conditions, the Galerkin approach is utilized.

The boundary conditions for a pinned-clamped pipe are

$$\begin{aligned} w(0,t) &= 0 \\ w(L,t) &= 0 \\ \frac{\partial w(0,t)}{\partial x} &= 0 \\ \frac{\partial^2 w(L,t)}{\partial x^2} &= 0 \end{aligned} \tag{3.31}$$

For a clamped-clamped carbon pipe, the boundary conditions are

$$w(0,t)=0$$

$$w(L,t)=0$$

$$\frac{\partial w(0,t)}{\partial x}=0 \tag{3.32}$$

$$\frac{\partial w(L,t)}{\partial x}=0$$

We seek a solution to the Equation (3.2) in the form

$$w(x,t)=\Re\left[\varphi(x)e^{i\omega t}\right] \tag{3.33}$$

where, "$\Re$" denotes the real part of the solution. Substituting Equation (3.33) into Equation (3.2), we get

$$EI\frac{\partial^4\varphi(x)}{\partial x^4}-M\omega^2\varphi(x)+\left(m_f U^2-k_P\right)\frac{\partial^2\varphi(x)}{\partial x^2}+ 2m_f Ui\omega\frac{\partial\varphi(x)}{\partial x}+k_W\varphi(x)=0 \tag{3.34}$$

In the Galerkin method, the function $\varphi(x)$ is taken as

$$\varphi(x)=\sum_{r=1}^{\infty}a_r\psi_r(x) \tag{3.35}$$

where, $\psi_r(x)$ are functions of the axial coordinate and a_r are constants.

After substituting the above equation in Equation (3.34), the result may be written as

$$\mathcal{L}\left(\varphi(x)\right) = 0 \tag{3.36}$$

where $\mathcal{L}$ is a differential operator, which in this case takes the form

$$\mathcal{L} = EI\frac{\partial^4}{\partial x^4} - M\omega^2 + \left(m_f U^2 - k_P\right)\frac{\partial^2}{\partial x^2} + 2m_f Ui\omega\frac{\partial}{\partial x} + k_W = 0 \tag{3.37}$$

The function $\varphi(x)$ in Equation (3.35) has infinite number of terms, which cannot be implemented in a solution in practice, leading to its replacement by

$$\varphi_N(x) = \sum_{r=1}^{N} a_r \psi_r(x) \tag{3.38}$$

where, *N* denotes the finite number of terms taken to be in the solution, see Elishakoff and Vittori **[65]**. If Equation (3.38) satisfies all the boundary conditions, Equations (3.31) and (3.32) as well as the differential equation, Equation (3.36), then it is an exact solution. However, in a majority of cases, substitution of Equation (3.38) into Equation (3.36) causes the expression not being identically zero and results in a residual error, which is

$$\mathcal{L}\left(\varphi(x)\right) = \mathcal{L}\left(\sum_{r=1}^{N} a_r \psi_r(x)\right) \equiv \in \tag{3.39}$$

According to the Galerkin procedure, each coordinate function $\psi_s(x)$ is multiplied by this error function and the inner product (projection) between the error function and

the coordinate function is set equal to zero. It is equivalent to the mean square of this error function being minimized over the interval $0 \le x \le L$ by setting (see Chary **[17]**)

$$\int_0^L \mathcal{L}\left(\sum_{r=1}^{N} a_r \psi_r(x)\right) \psi_s(x) dx = 0 \;\; ; \; s = 1, 2, 3, ..., N \tag{3.40}$$

Moreover, it is required that the coordinate functions satisfy the boundary conditions as well as orthogonality conditions. Non-dimensionalizing the axial coordinate, we have

$$\xi = \frac{x}{L} \;\; ; \; \xi : 0 - 1 \tag{3.41}$$

The eigen-functions of a beam for both these end conditions, which is equivalent to a carbon nanotube/pipe without fluid flow, are chosen as the functions $\psi_r(\xi)$, see for example Felgar **[66]**. Thus,

$$\psi_r(\xi) = \cosh\left(\lambda_r \xi\right) - \cos\left(\lambda_r \xi\right) - \sigma_r \left[\sinh\left(\lambda_r \xi\right) - \sin\left(\lambda_r \xi\right)\right] \tag{3.42}$$

where,

$$\sigma_r = \frac{\cosh\left(\lambda_r\right) - \cos\left(\lambda_r\right)}{\sinh\left(\lambda_r\right) - \sin\left(\lambda_r\right)} \tag{3.43}$$

In the above two equations, λ_r is the eigen-frequency of the carbon nanotube without fluid flow. Its values depend on the type of end conditions and are given below for *r* = 1,2.

- For pinned-clamped ends, $\lambda_1 = 3.92660231$ and $\lambda_2 = 7.06858275$
- For clamped -clamped ends, $\lambda_1 = 4.73004074$ and $\lambda_2 = 7.85320462$

Substitution of Equation (3.42) in Equation (3.40) results in

$$\int_0^1 \mathrm{L}\left(\sum_{r=1}^{N} a_r \psi_r(\xi)\right)\psi_s(\xi)d\xi =$$

$$\sum_{r=1}^{N} a_r \left(\begin{array}{l} \dfrac{EI}{L^4}\lambda_r^4 \displaystyle\sum_{s=1}^{N}\left\{\int_0^1 \psi_r\psi_s d\xi\right\} + \\ \dfrac{\left(m_f U^2 - k_P\right)}{L^2}\displaystyle\sum_{s=1}^{N}\left\{\int_0^1 \frac{\partial^2\psi_r}{\partial\xi^2}\psi_s d\xi\right\} + \\ \dfrac{2m_f U i\omega}{L}\displaystyle\sum_{s=1}^{N}\left\{\int_0^1 \frac{\partial\psi_r}{\partial\xi}\psi_s d\xi\right\} + \\ \left(k_W - M\omega^2\right)\displaystyle\sum_{s=1}^{N}\left\{\int_0^1 \psi_r\psi_s d\xi\right\} \end{array} \right) = 0 \qquad (3.44)$$

Since the coordinate functions are specified to be orthogonal, we use the following orthogonality relations, Equation (3.45) along with formulas for integrals containing mode shapes, Equation (3.46), taken from Felgar **[66]**, in the above equation,

$$\begin{aligned} &\int_0^1 \psi_r\psi_s d\xi = 0 \ \text{; for } r \neq s \text{ and} \\ &\int_0^1 \psi_r\psi_s d\xi = 1 \ \text{; for } r = s \end{aligned} \qquad (3.45)$$

$$\int_0^1 \frac{\partial \psi_r}{\partial \xi} \psi_s d\xi = b_{rs}$$

$$\int_0^1 \frac{\partial^2 \psi_r}{\partial \xi^2} \psi_s d\xi = c_{rs} \tag{3.46}$$

we obtain the following set of *N* linear algebraic equations:

$$a_r \left(\begin{array}{l} \dfrac{EI}{L^4}\lambda_r^4 + \dfrac{\left(m_f U^2 - k_P\right)}{L^2} \sum_{s=1}^{N} \{c_{rs}\} + \\ \\ \dfrac{2m_f U i\omega}{L} \sum_{s=1}^{N} \{b_{rs}\} + \left(k_W - M\omega^2\right) \end{array} \right) = 0 \;\; ; r = 1, 2, 3, ..., N \tag{3.47}$$

The values of the integrals b_{rs} and c_{rs} are given in Tables 3.1 and 3.2.

The system of equations in Equation (3.47) is infinite, which can be reduced to a finite number without loss of accuracy. In particular, for clamped-pinned and clamped-clamped cases, it is established that a two- term Galerkin solution is adequately accurate for engineering purposes, see Naguleswaran and Williams **[11]**.

For carrying out stability analysis of the carbon nanotube conveying fluid, making use of the condition that the natural frequency is zero at the critical flow velocity and using the non-dimensional parameters defined in Equation (3.29), and retaining only the first two terms, that is, for *r*, *s* = 1,2, we obtain the matrix-determinant form of the Equation (3.47) below:

Table 3.1 Values of integrals b_{rs} and c_{rs} for a clamped-pinned beam, Felgar **[66]**.

Parameter	**Clamped-hinged**
b_{rs}	$\frac{\lambda_r \lambda_s}{\lambda^4{}_s - \lambda^4{}_r}\left[\begin{array}{l} -(-1)^{r+s}\left(\lambda^2{}_s + \lambda^2{}_r\right)\sqrt{(\sigma^2{}_s+1)(\sigma^2{}_r+1)} + (-1)^s\left(\lambda^2{}_s - \lambda^2{}_r\right)\sqrt{(\sigma^2{}_s+1)(\sigma^2{}_r-1)} \\ -(-1)^r\left(\lambda^2{}_s - \lambda^2{}_r\right)\sqrt{(\sigma^2{}_s-1)(\sigma^2{}_r+1)} + \left(\lambda^2{}_s + \lambda^2{}_r\right)\sqrt{(\sigma^2{}_s-1)(\sigma^2{}_r-1)} + 4\lambda_r\lambda_s \end{array}\right]$
b_{rr}	0
c_{rs}	$\frac{4\lambda^2{}_r\lambda^2{}_s}{\lambda^4{}_s - \lambda^4{}_r}\left(\sigma_s\lambda_s - \sigma_r\lambda_r\right)$
c_{rr}	$\sigma_r\lambda_r\left(1-\sigma_r\lambda_r\right)$

Table 3.2 Values of integrals b_{rs} and c_{rs} for a clamped-clamped beam, Felgar **[66]**.

Parameter	**Clamped-clamped**
b_{rs}	$\frac{4\lambda^2{}_r\lambda^2{}_s}{\lambda^4{}_s-\lambda^4{}_r}\left[1-(-1)^{r+s}\right]$
b_{rr}	0
c_{rs}	$\frac{4\lambda^2{}_r\lambda^2{}_s}{\lambda^4{}_s-\lambda^4{}_r}\left(\sigma_s\lambda_s-\sigma_r\lambda_r\right)\left[1+(-1)^{r+s}\right]$
c_{rr}	$\sigma_r\lambda_r\left(2-\sigma_r\lambda_r\right)$

$$\begin{pmatrix} \left\{\lambda_1^4+\gamma_W+\left(V^2-\gamma_P\right)c_{11}\right\} & \left\{\left(V^2-\gamma_P\right)c_{12}\right\} \\ \left\{\left(V^2-\gamma_P\right)c_{21}\right\} & \left\{\lambda_2^4+\gamma_W+\left(V^2-\gamma_P\right)c_{22}\right\} \end{pmatrix} \begin{Bmatrix} a_1 \\ a_2 \end{Bmatrix} = 0 \qquad (3.48)$$

For a non-trivial solution of the above equation, we set the determinant of the coefficient matrix in the equation to zero, to obtain

For clamped-pinned condition,

$$\begin{aligned} &\left(V^2-\gamma_P\right)^2\left\{c_{11}c_{22}-c_{12}c_{21}\right\}- \\ &\left(V^2-\gamma_P\right)\left\{\left(\lambda_1^4+\gamma_W\right)c_{22}+\left(\lambda_2^4+\gamma_W\right)c_{11}\right\}+ \\ &\left\{\left(\lambda_1^4+\gamma_W\right)\left(\lambda_2^4+\gamma_W\right)\right\}=0 \end{aligned} \qquad (3.49)$$

For clamped-clamped condition, the constants c_{12} and c_{21} are zero, leading to the equation

$$\begin{aligned} &\left(V^2-\gamma_P\right)^2\left\{c_{11}c_{22}\right\}- \\ &\left(V^2-\gamma_P\right)\left\{\left(\lambda_1^4+\gamma_W\right)c_{22}+\left(\lambda_2^4+\gamma_W\right)c_{11}\right\}+ \\ &\left\{\left(\lambda_1^4+\gamma_W\right)\left(\lambda_2^4+\gamma_W\right)\right\}=0 \end{aligned} \qquad (3.50)$$

Both Equations (3.49) and (3.50) are quadratic in V^2, which can be solved to obtain the smallest root as the critical flow velocity of a pipe conveying fluid and resting on a Pasternak elastic medium, for the two boundary conditions specified above.

In the following sections, comprehensive numerical results are presented for all the three boundary conditions discussed in the preceding two sections.

3.3 Numerical Results and Discussion

Numerical results for each of the three boundary conditions will be presented in the form of tables and figures in this section. Wherever possible, a comparison will be made with published literature. The comparison is mainly possible for pipes conveying fluid resting on Winkler foundation or for pipes without any foundation. The results of the analysis with the Pasternak elastic medium are a new contribution in this thesis and hence comparisons are not possible. Likewise, the results for the pinned-clamped boundary condition are also a new contribution to the literature.

3.3.1 Pinned-pinned case

The lowest root of Equation (3.30) is the critical flow velocity parameter, which is denoted here by V_{cr}. Results are obtained by solving this quadratic equation in V^2 for different values of both the foundation parameters. Table 3.3 shows the numerical results for the pinned-pinned case. The Winkler foundation parameter γ_W is varied from a value of 0.1, which is equivalent to very low linear spring stiffness, to 1.0E+6, which is a very stiff foundation. Similarly, the Pasternak parameter is also varied to progressively higher values to bring out the effect of each parameter on the critical velocity parameter. In the table, only selected values of the parameters are indicated to save space.

Table 3.3 Values of critical flow velocity parameter, V_{cr}, for varying values of the Winkler, γ_W, and Pasternak, γ_P, stiffness parameters for a pinned-pinned pipe

γ_W	γ_P	V_{cr}
1.00E-01	1.00E-01	3.1591
1.00E-01	1.00E+00	3.2984
1.00E-01	1.00E+01	4.4587
1.00E-01	1.00E+02	10.4824
1.00E-01	1.00E+03	31.7786
1.00E-01	1.00E+04	100.0494
1.00E-01	1.00E+05	316.2434
1.00E-01	5.00E+05	707.1138
1.00E-01	1.00E+06	1000.005
1.00E+00	1.00E-01	3.1735
1.00E+00	1.00E+00	3.3122
1.00E+00	1.00E+01	4.4689
1.00E+00	1.00E+02	10.4867
1.00E+00	1.00E+03	31.78
1.00E+00	1.00E+04	100.0498
1.00E+00	1.00E+05	316.2435
1.00E+00	5.00E+05	707.1138
1.00E+00	1.00E+06	1000.005

Table 3.3 Continued

γ_W	γ_P	V_{cr}
1.00E+01	1.00E-01	3.314
1.00E+01	1.00E+00	3.4471
1.00E+01	1.00E+01	4.5698
1.00E+01	1.00E+02	10.5301
1.00E+01	1.00E+03	31.7944
1.00E+01	1.00E+04	100.0544
1.00E+01	1.00E+05	316.245
1.00E+01	5.00E+05	707.1145
1.00E+01	1.00E+06	1000.005
1.00E+02	1.00E-01	4.4835
1.00E+02	1.00E+00	4.5828
1.00E+02	1.00E+01	5.4774
1.00E+02	1.00E+02	10.9545
1.00E+02	1.00E+03	31.9375
1.00E+02	1.00E+04	100.1
1.00E+02	1.00E+05	316.2594
1.00E+02	5.00E+05	707.1209
1.00E+02	1.00E+06	1000.01

Table 3.3 Continued

γ_W	γ_P	V_{cr}
1.00E+03	1.00E-01	8.0566
1.00E+03	1.00E+00	8.1123
1.00E+03	1.00E+01	8.6492
1.00E+03	1.00E+02	12.8378
1.00E+03	1.00E+03	32.6314
1.00E+03	1.00E+04	100.3235
1.00E+03	1.00E+05	316.3302
1.00E+03	5.00E+05	707.1526
1.00E+03	1.00E+06	1000.032
1.00E+04	1.00E-01	17.1138
1.00E+04	1.00E+00	17.1401
1.00E+04	1.00E+01	17.4006
1.00E+04	1.00E+02	19.8187
1.00E+04	1.00E+03	35.9553
1.00E+04	1.00E+04	101.4533
1.00E+04	1.00E+05	316.6904
1.00E+04	5.00E+05	707.3138
1.00E+04	1.00E+06	1000.146

Table 3.3 Continued

γ_W	γ_P	V_{cr}
1.00E+05	1.00E-01	50.7209
1.00E+05	1.00E+00	50.7298
1.00E+05	1.00E+01	50.8184
1.00E+05	1.00E+02	51.6963
1.00E+05	1.00E+03	59.7705
1.00E+05	1.00E+04	112.1272
1.00E+05	1.00E+05	320.2694
1.00E+05	5.00E+05	708.9235
1.00E+05	1.00E+06	1001.285
1.00E+06	1.00E-01	159.2792
1.00E+06	1.00E+00	159.2821
1.00E+06	1.00E+01	159.3103
1.00E+06	1.00E+02	159.5925
1.00E+06	1.00E+03	162.3877
1.00E+06	1.00E+04	188.0685
1.00E+06	1.00E+05	354.0759
1.00E+06	5.00E+05	724.824
1.00E+06	1.00E+06	1012.605

Fig. 3.1 shows the variation of critical flow velocity parameter, V, with Pasternak stiffness parameter, γ_P for different values of the Winkler stiffness parameter, γ_W. It is seen from the curves that there is no significant effect on the critical velocity parameter for values of the Pasternak stiffness parameter up to a value of about 10.0. Thereafter, for increasing values of the Pasternak or shear parameter, there is a sharp increase in the critical flow velocity parameter. This trend is visible for the value of the Winkler stiffness parameter up to 10000.0. Above this value of the Winkler parameter, the rate of increase is not very high, and the curves tend to flatten out more and more, as shown in Fig. 3.2. The above tables and figures show the effect of the second stiffness parameter on the critical flow velocities for a comprehensive range of values of both the parameters.

In Table 3.4, two values of the Winkler stiffness parameter are chosen for illustration purposes and the effect of varying the Pasternak parameter for these two values is clearly shown in percentage change. It is seen from the data in the table that the critical flow velocity parameter, V_{cr}, increases exponentially when the values of the Pasternak stiffness parameter, γ_P, are gradually increased, although the percentage increase decreases for larger values of the Winkler stiffness parameter, γ_W, indicating that the second stiffness parameter has a significant influence on the critical flow velocities of a fluid conveying pipe.

3.3.2 Clamped - pinned case

The solution of the quadratic equation in V^2, Equation (3.49), gives the values of critical flow velocity parameters. Table 3.5 shows the numerical results obtained for

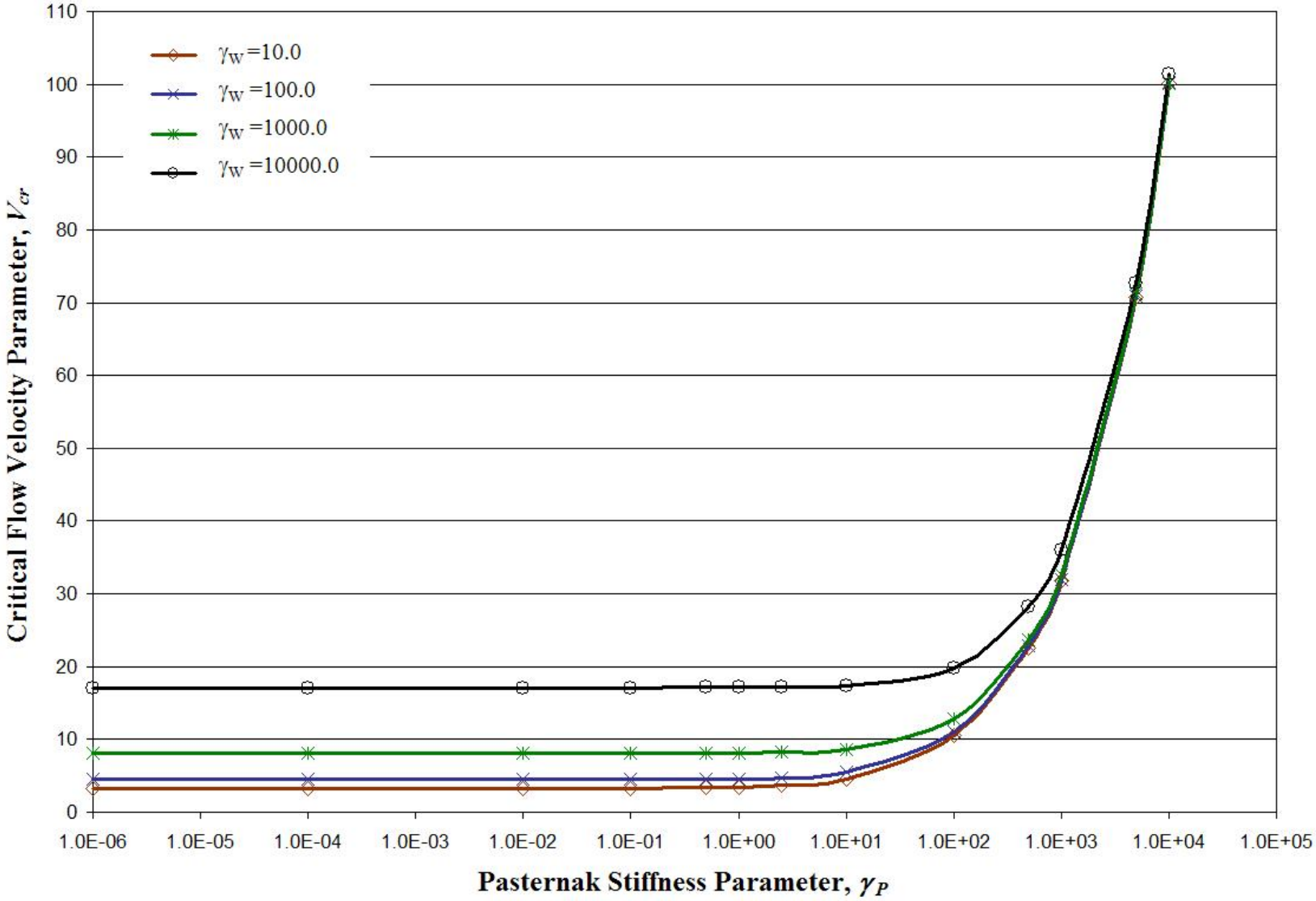

Figure 3.1 Variation of critical flow velocity parameter, V_{cr}, with Pasternak stiffness parameter, γ_P, for the values of Winkler stiffness parameter, γ_W, up to 10000.0, for a pinned-pinned pipe

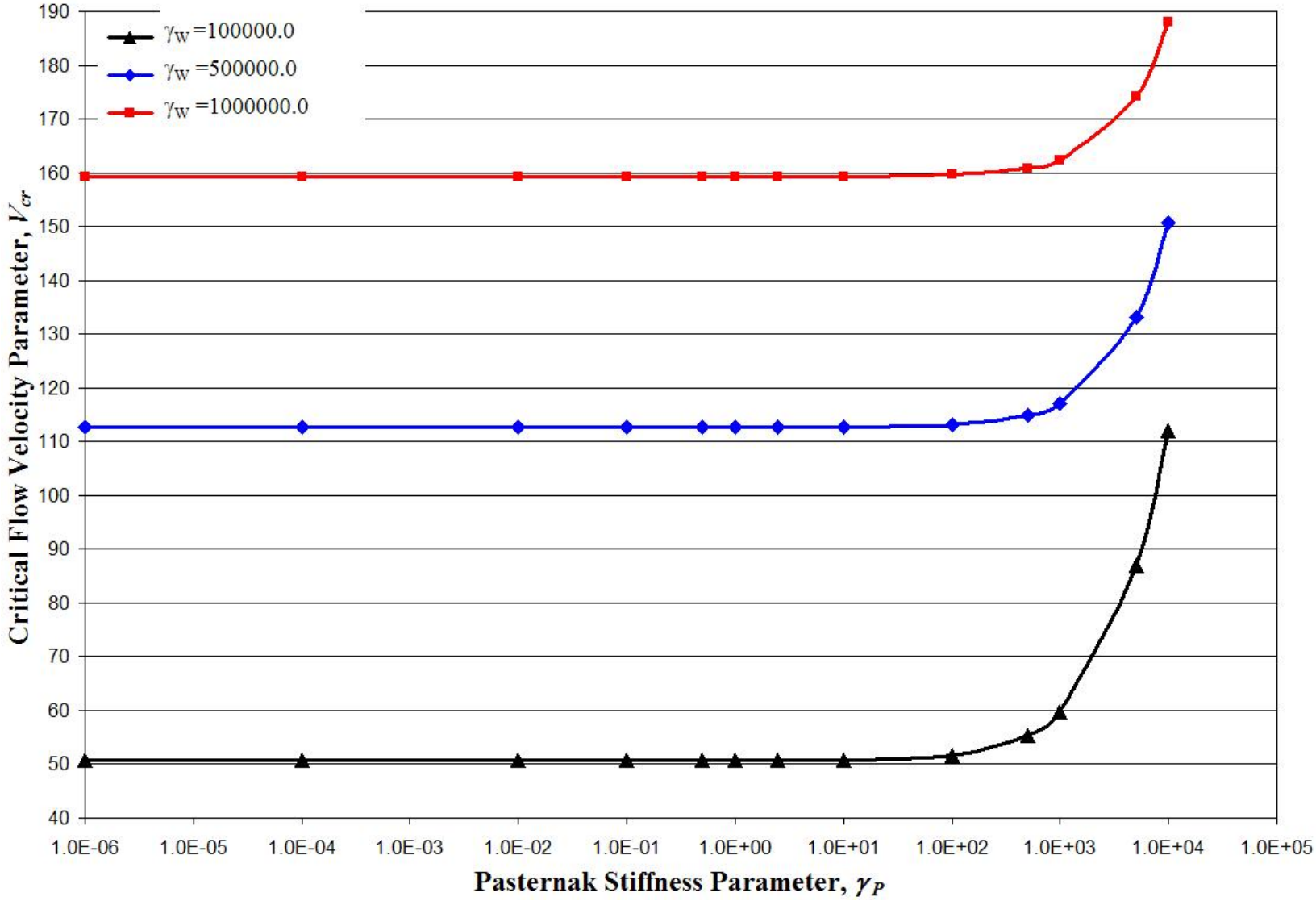

Figure 3.2 Variation of critical flow velocity parameter, V_{cr}, with Pasternak stiffness parameter, γ_P, for the values of Winkler stiffness parameter, γ_W, above 10000.0, for a pinned-pinned pipe

Table 3.4 Percentage variation of critical flow velocity parameter, V_{cr}, with increasing values of the Pasternak stiffness parameter, γ_P, for two particular values of the Winkler stiffness parameter, γ_W, for a pinned-pinned pipe.

γ_P	V_{cr}: γ_W=0.1	% Variation		V_{cr}: γ_W=10000.0	% Variation
1.00E-06	3.1432	0		17.1109	0
1.00E-04	3.1432	0		17.1109	0
1.00E-02	3.1448	0.1		17.1111	0
1.00E-01	3.1591	0.5		17.1138	0
5.00E-01	3.2218	2.5		17.1255	0.1
1.00E+00	3.2984	4.9		17.1401	0.2
2.50E+00	3.5185	11.9		17.1838	0.4
1.00E+01	4.4587	41.9		17.4006	1.7
1.00E+02	10.4824	233.5		19.8187	15.8
5.00E+02	22.5805	618.4		28.1564	64.6
1.00E+03	31.7786	911		35.9553	110.1
5.00E+03	70.7805	2151.9		72.7515	325.2
1.00E+04	100.0494	3083		101.4533	492.9
5.00E+04	223.6289	7014.7		224.2605	1210.6
1.00E+05	316.2434	9961.2		316.6904	1750.8
5.00E+05	707.1138	22396.6		707.3138	4033.7
1.00E+06	1000.005	31714.9		1000.146	5745.1

different values of both the stiffness parameters. The results are organized in the same pattern as for the pinned-pinned case for easy comparison. Fig. 3.3 shows the curves for the variation of critical flow velocity parameter, V_{cr}, with varying values of the Pasternak stiffness parameter, γ_P, for different values of the Winkler stiffness parameter, γ_W, for the clamped-pinned boundary condition. It can be observed that a similar trend is followed in comparison to the pinned-pinned end conditions, although the values are slightly different. The variation of the critical flow velocity parameter with the Pasternak stiffness parameter for values of Winkler stiffness parameter greater than 10000.0 is shown in Fig. 3.4. Here too, the flow velocity parameter does not vary much until the Pasternak parameter reaches a value of about 1000.0. For higher values of the Pasternak parameter, the variation in the critical flow velocity parameter is not as high as for lower values of the Winkler parameter.

Table 3.6 gives the percent variation of the critical flow velocity parameter, V_{cr}, for varying values of the Pasternak stiffness parameter, γ_P, for two illustrative values of the Winkler parameter, γ_W, of 0.1 and 10000.0. The percentage variation for lower values of the Winkler parameter is very high as the Pasternak parameter is increased from a very low value to a very high value. As was the case for the pinned-pinned boundary condition, this variation is not so appreciable for higher values of the Winkler stiffness parameter.

The trend seems to be that the critical flow velocity parameter curve flattens out for extremely stiff Winkler type elastic medium, indicating that the critical flow velocity attains an almost constant value whatever be the external conditions.

Table 3.5 Values of critical flow velocity parameter, V_{cr}, for varying values of the Winkler, γ_W, and Pasternak, γ_P, stiffness parameters for a clamped-pinned pipe

γ_W	γ_P	V_{cr}
1.00E-01	1.00E-01	4.5118
1.00E-01	1.00E+00	4.6104
1.00E-01	1.00E+01	5.5006
1.00E-01	1.00E+02	10.9661
1.00E-01	1.00E+03	31.9414
1.00E-01	1.00E+04	100.1012
1.00E-01	1.00E+05	316.2598
1.00E-01	5.00E+05	707.1211
1.00E-01	1.00E+06	1000.01
1.00E+00	1.00E-01	4.52
1.00E+00	1.00E+00	4.6185
1.00E+00	1.00E+01	5.5073
1.00E+00	1.00E+02	10.9695
1.00E+00	1.00E+03	31.9426
1.00E+00	1.00E+04	100.1016
1.00E+00	1.00E+05	316.2599
1.00E+00	5.00E+05	707.1212
1.00E+00	1.00E+06	1000.01

Table 3.5 Continued

γ_W	γ_P	V_{cr}
1.00E+01	1.00E-01	4.6017
1.00E+01	1.00E+00	4.6985
1.00E+01	1.00E+01	5.5746
1.00E+01	1.00E+02	11.0035
1.00E+01	1.00E+03	31.9543
1.00E+01	1.00E+04	100.1053
1.00E+01	1.00E+05	316.2611
1.00E+01	5.00E+05	707.1217
1.00E+01	1.00E+06	1000.011
1.00E+02	1.00E-01	5.3388
1.00E+02	1.00E+00	5.4224
1.00E+02	1.00E+01	6.197
1.00E+02	1.00E+02	11.3315
1.00E+02	1.00E+03	32.0687
1.00E+02	1.00E+04	100.1419
1.00E+02	1.00E+05	316.2727
1.00E+02	5.00E+05	707.1269
1.00E+02	1.00E+06	1000.014

Table 3.5 Continued

γ_W	γ_P	V_{cr}
1.00E+03	1.00E-01	8.6696
1.00E+03	1.00E+00	8.7214
1.00E+03	1.00E+01	9.2229
1.00E+03	1.00E+02	13.2311
1.00E+03	1.00E+03	32.7881
1.00E+03	1.00E+04	100.3746
1.00E+03	1.00E+05	316.3464
1.00E+03	5.00E+05	707.1599
1.00E+03	1.00E+06	1000.038
1.00E+04	1.00E-01	16.9225
1.00E+04	1.00E+00	16.9491
1.00E+04	1.00E+01	17.2125
1.00E+04	1.00E+02	19.6538
1.00E+04	1.00E+03	35.8646
1.00E+04	1.00E+04	101.4213
1.00E+04	1.00E+05	316.6801
1.00E+04	5.00E+05	707.3092
1.00E+04	1.00E+06	1000.143

Table 3.5 Continued

γ_W	γ_P	V_{cr}
1.00E+05	1.00E-01	48.5491
1.00E+05	1.00E+00	48.5583
1.00E+05	1.00E+01	48.6509
1.00E+05	1.00E+02	49.5672
1.00E+05	1.00E+03	57.9389
1.00E+05	1.00E+04	111.1616
1.00E+05	1.00E+05	319.9327
1.00E+05	5.00E+05	708.7714
1.00E+05	1.00E+06	1001.178
1.00E+06	1.00E-01	151.858
1.00E+06	1.00E+00	151.861
1.00E+06	1.00E+01	151.8906
1.00E+06	1.00E+02	152.1866
1.00E+06	1.00E+03	155.1153
1.00E+06	1.00E+04	181.8262
1.00E+06	1.00E+05	350.8002
1.00E+06	5.00E+05	723.2294
1.00E+06	1.00E+06	1011.465

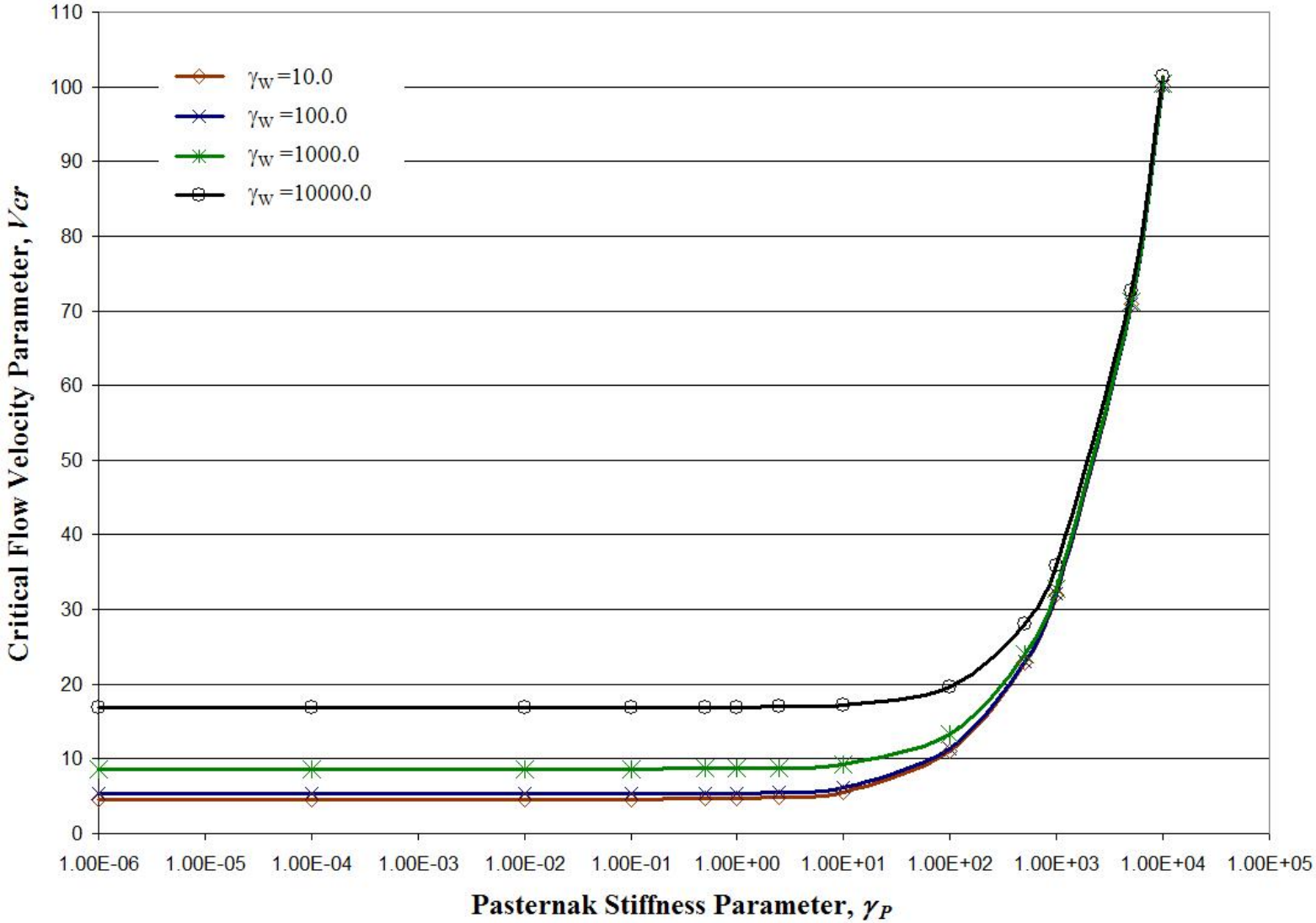

Figure 3.3 Variation of critical flow velocity parameter, V_{cr}, with Pasternak stiffness parameter, γ_P, for the values of Winkler stiffness parameter, γ_W, up to 10000.0, for a clamped-pinned pipe

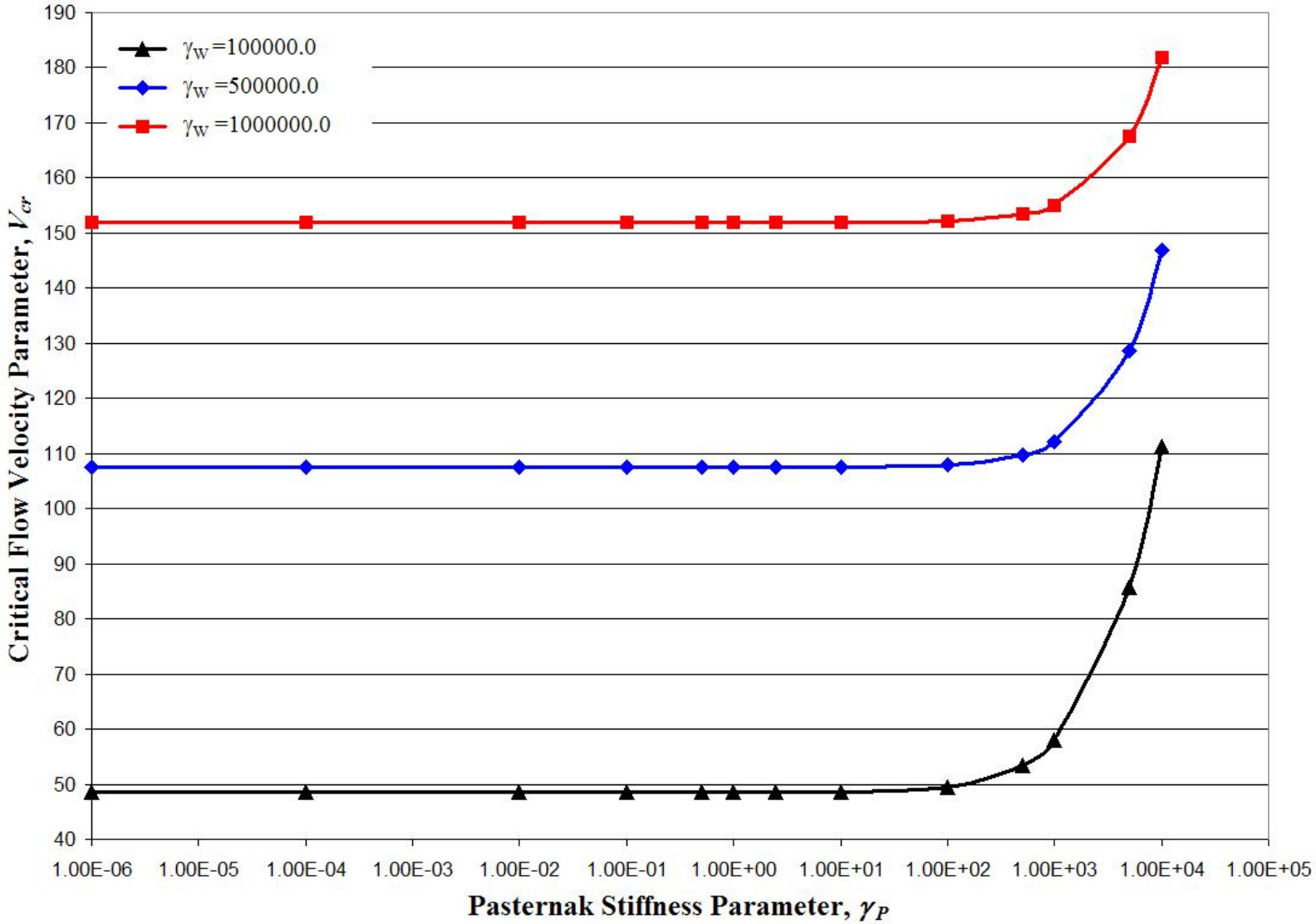

Figure 3.4 Variation of critical flow velocity parameter, V_{cr}, with Pasternak stiffness parameter, γ_P, for the values of Winkler stiffness parameter, γ_W, above 10000.0, for a clamped-pinned pipe

Table 3.6 Percentage variation of critical flow velocity parameter, V_{cr}, with increasing values of the Pasternak stiffness parameter, γ_P, for two particular values of the Winkler stiffness parameter, γ_W, for a clamped-pinned pipe.

γ_P	V_{cr}: γ_W=0.1	% Variation		V_{cr}: γ_W=10000.0	% Variation
1.00E-06	4.5007	0		16.9196	0
1.00E-04	4.5007	0		16.9196	0
1.00E-02	4.5018	0		16.9198	0
1.00E-01	4.5118	0.2		16.9225	0
5.00E-01	4.5559	1.2		16.9343	0.1
1.00E+00	4.6104	2.4		16.9491	0.2
2.50E+00	4.7703	6		16.9933	0.4
1.00E+01	5.5006	22.2		17.2125	1.7
1.00E+02	10.9661	143.7		19.6538	16.2
5.00E+02	22.8091	406.8		28.0405	65.7
1.00E+03	31.9414	609.7		35.8646	112
5.00E+03	70.8538	1474.3		72.7067	329.7
1.00E+04	100.1012	2124.1		101.4213	499.4
5.00E+04	223.6521	4869.3		224.246	1225.4
1.00E+05	316.2598	6926.9		316.6801	1771.7
5.00E+05	707.1211	15611.4		707.3092	4080.4
1.00E+06	1000.01	22119		1000.143	5811.2

3.3.3 Clamped - clamped case

For the clamped-clamped boundary conditions, the relevant equation to be solved is the Equation (3.50), which is also a quadratic in V^2. The numerical results from the solution of the equation are presented in Table 3.7. It is observed that for low values of the Winkler stiffness parameter, γ_W, the value of the critical flow velocity parameter, V_{cr}, is higher when compared to both the pinned-pinned and the clamped-pinned end conditions. For consistency in the presentation of results, similar curves have been obtained for the clamped-clamped case also, as shown in Figs. 3.5 and 3.6. A similar trend is observed for this case also as with the pinned-pinned and the clamped-pinned cases.

Table 3.8 shows the variation in percentage, clearly bringing out the influence the Pasternak stiffness parameter has on the stability of the pipe. The percentage variation is lower than for the other two end conditions. Some of these results have been published in 2007; see Chellapilla and Simha **[68]**.

3.3.4 Influence of end conditions

Since comprehensive numerical results have been obtained for all the three boundary conditions, it would be interesting to study the comparative influence of end conditions on the stability of the pipe.

Table 3.7 Values of critical flow velocity parameter, V_{cr}, for varying values of the Winkler, γ_W, and Pasternak, γ_P, stiffness parameters for a clamped-clamped pipe

γ_W	γ_P	V_{cr}
1.00E-01	1.00E-01	6.3872
1.00E-01	1.00E+00	6.4572
1.00E-01	1.00E+01	7.1201
1.00E-01	1.00E+02	11.8615
1.00E-01	1.00E+03	32.2598
1.00E-01	1.00E+04	100.2033
1.00E-01	1.00E+05	316.2921
1.00E-01	5.00E+05	707.1356
1.00E-01	1.00E+06	1000.02
1.00E+00	1.00E-01	6.3929
1.00E+00	1.00E+00	6.4629
1.00E+00	1.00E+01	7.1252
1.00E+00	1.00E+02	11.8646
1.00E+00	1.00E+03	32.2609
1.00E+00	1.00E+04	100.2036
1.00E+00	1.00E+05	316.2922
1.00E+00	5.00E+05	707.1356
1.00E+00	1.00E+06	1000.02

Table 3.7 Continued

γ_W	γ_P	V_{cr}
1.00E+01	1.00E-01	6.4498
1.00E+01	1.00E+00	6.5192
1.00E+01	1.00E+01	7.1764
1.00E+01	1.00E+02	11.8954
1.00E+01	1.00E+03	32.2723
1.00E+01	1.00E+04	100.2073
1.00E+01	1.00E+05	316.2934
1.00E+01	5.00E+05	707.1361
1.00E+01	1.00E+06	1000.021
1.00E+02	1.00E-01	6.994
1.00E+02	1.00E+00	7.058
1.00E+02	1.00E+01	7.6692
1.00E+02	1.00E+02	12.199
1.00E+02	1.00E+03	32.3854
1.00E+02	1.00E+04	100.2438
1.00E+02	1.00E+05	316.3049
1.00E+02	5.00E+05	707.1413
1.00E+02	1.00E+06	1000.024

Table 3.7 Continued

γ_W	γ_P	V_{cr}
1.00E+03	1.00E-01	10.2182
1.00E+03	1.00E+00	10.2621
1.00E+03	1.00E+01	10.6916
1.00E+03	1.00E+02	14.2937
1.00E+03	1.00E+03	33.2312
1.00E+03	1.00E+04	100.5202
1.00E+03	1.00E+05	316.3927
1.00E+03	5.00E+05	707.1805
1.00E+03	1.00E+06	1000.052
1.00E+04	1.00E-01	17.3162
1.00E+04	1.00E+00	17.3422
1.00E+04	1.00E+01	17.5997
1.00E+04	1.00E+02	19.9938
1.00E+04	1.00E+03	36.052
1.00E+04	1.00E+04	101.4877
1.00E+04	1.00E+05	316.7014
1.00E+04	5.00E+05	707.3187
1.00E+04	1.00E+06	1000.15

Table 3.7 Continued

γ_W	γ_P	V_{cr}
1.00E+05	1.00E-01	47.4789
1.00E+05	1.00E+00	47.4883
1.00E+05	1.00E+01	47.583
1.00E+05	1.00E+02	48.5195
1.00E+05	1.00E+03	57.0451
1.00E+05	1.00E+04	110.6984
1.00E+05	1.00E+05	319.772
1.00E+05	5.00E+05	708.6989
1.00E+05	1.00E+06	1001.126
1.00E+06	1.00E-01	147.642
1.00E+06	1.00E+00	147.6451
1.00E+06	1.00E+01	147.6755
1.00E+06	1.00E+02	147.9799
1.00E+06	1.00E+03	150.9903
1.00E+06	1.00E+04	178.3201
1.00E+06	1.00E+05	348.9958
1.00E+06	5.00E+05	722.3559
1.00E+06	1.00E+06	1010.84

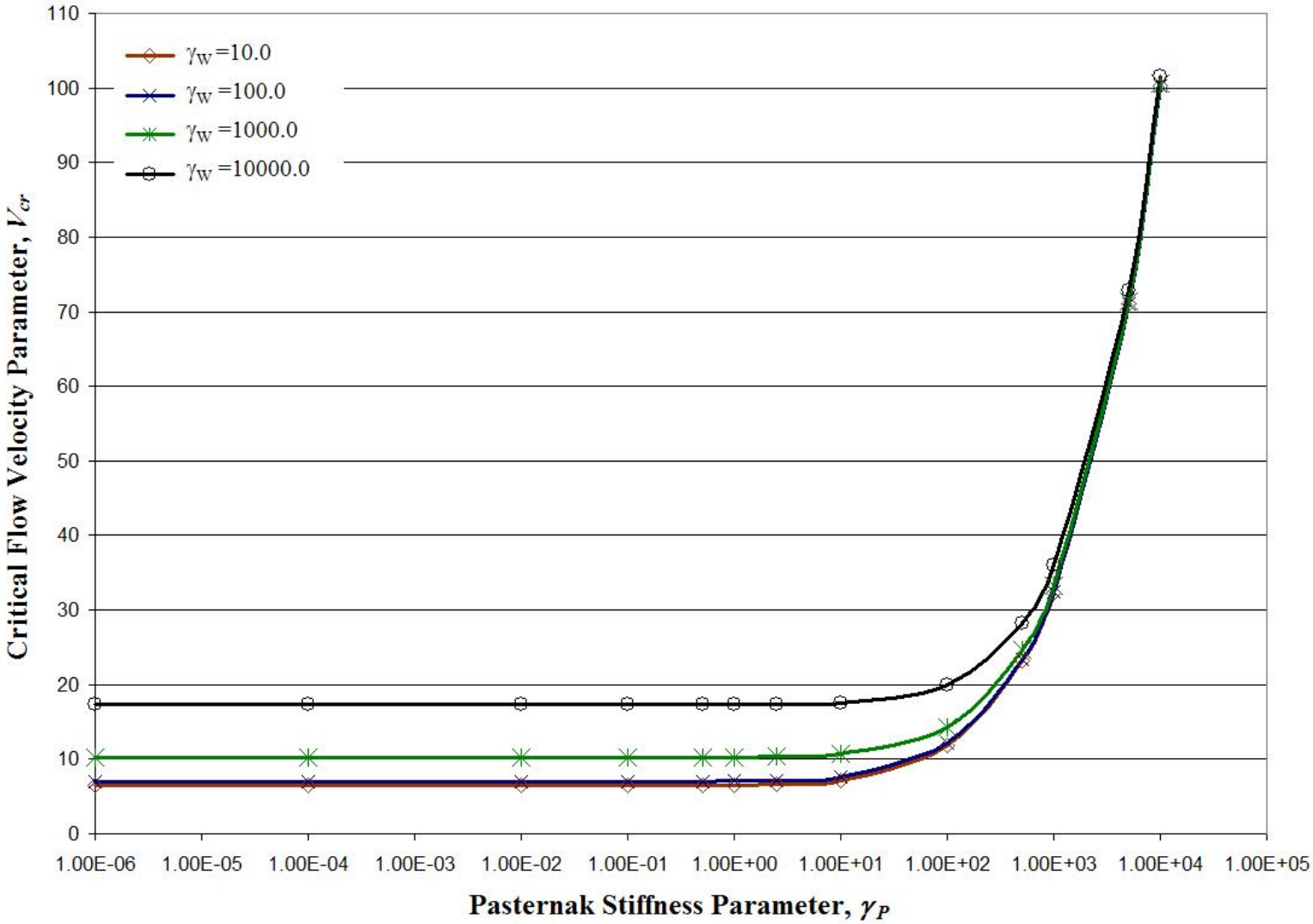

Figure 3.5 Variation of critical flow velocity parameter, V_{cr}, with Pasternak stiffness parameter, γ_P, for the values of Winkler stiffness parameter, γ_W, up to 10000.0, for a clamped-clamped pipe

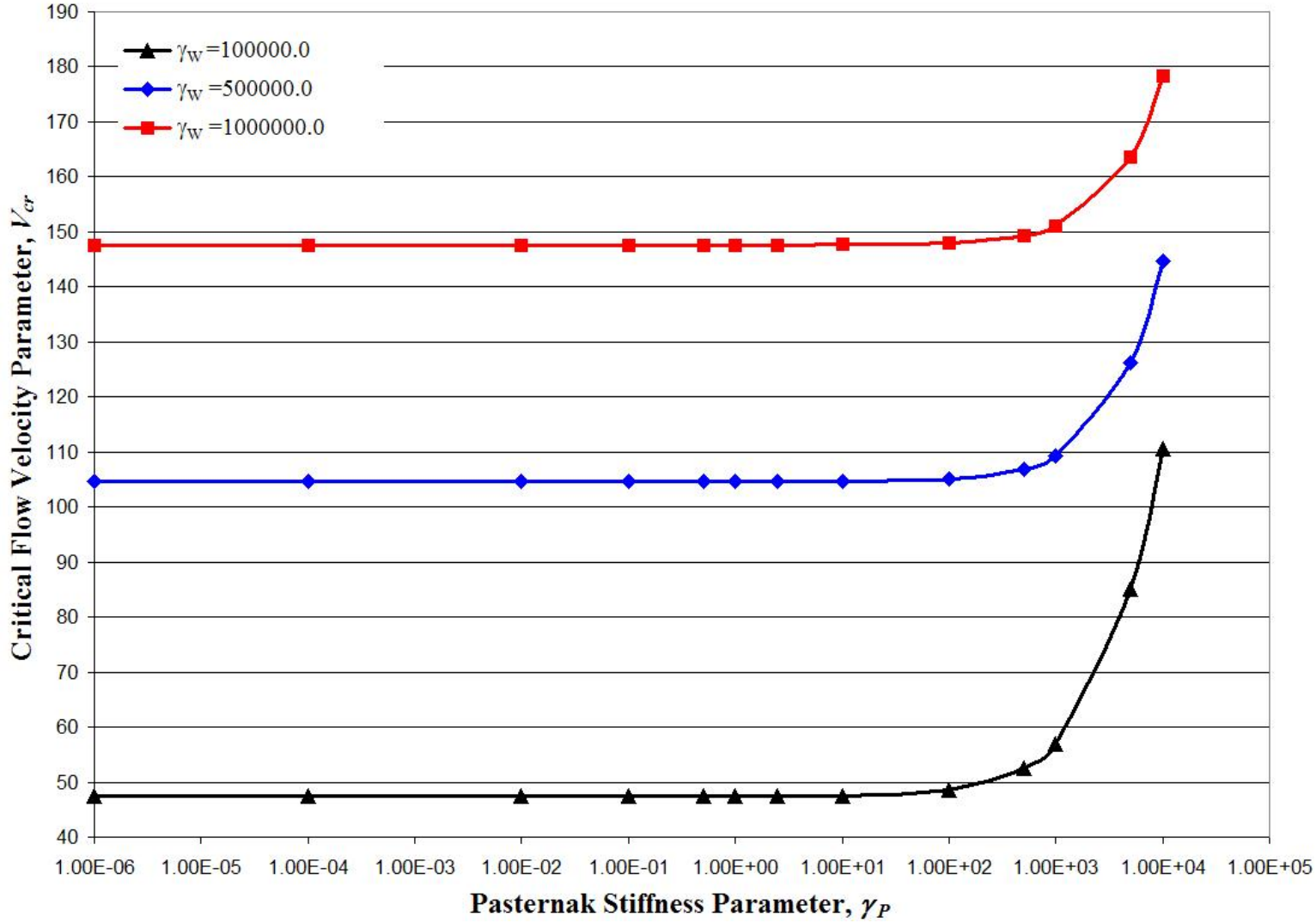

Figure 3.6 Variation of critical flow velocity parameter, V_{cr}, with Pasternak stiffness parameter, γ_P, for the values of Winkler stiffness parameter, γ_W, above 10000.0, for a clamped-clamped pipe

Table 3.8 Percentage variation of critical flow velocity parameter, V_{cr}, with increasing values of the Pasternak stiffness parameter, γ_P, for two particular values of the Winkler stiffness parameter, γ_W, for a clamped-clamped pipe.

γ_P	V_{cr}: γ_W=0.1	% Variation		V_{cr}: γ_W=10000.0	% Variation
1.00E-06	6.3793	0		17.3133	0
1.00E-04	6.3793	0		17.3133	0
1.00E-02	6.3801	0		17.3136	0
1.00E-01	6.3872	0.1		17.3162	0
5.00E-01	6.4184	0.6		17.3277	0.1
1.00E+00	6.4572	1.2		17.3422	0.2
2.50E+00	6.5723	3		17.3853	0.4
1.00E+01	7.1201	11.6		17.5997	1.7
1.00E+02	11.8615	85.9		19.9938	15.5
5.00E+02	23.2529	264.5		28.2799	63.3
1.00E+03	32.2598	405.7		36.052	108.2
5.00E+03	70.9979	1012.9		72.7994	320.5
1.00E+04	100.2033	1470.8		101.4877	486.2
5.00E+04	223.6978	3406.6		224.2761	1195.4
1.00E+05	316.2921	4858.1		316.7014	1729.2
5.00E+05	707.1356	10984.8		707.3187	3985.4
1.00E+06	1000.02	15576		1000.15	5676.8

This comparison is clearly shown in Fig. 3.7, for values of the Winkler stiffness parameter, γ_W, up to 10000.0. The values of the Pasternak stiffness parameter have been restricted to 1000.0 because, for higher values, the values of the critical flow velocity parameter, V_{cr}, tend to converge to almost the same value. It is seen from the figure that the critical flow velocity parameter is the smallest for the pinned-pinned end condition, followed by the clamped-pinned end condition and finally followed by the clamped-clamped end condition, for the same values of both the stiffness parameters. However, this gap is seen to be getting lesser as the Winkler stiffness parameter is increased to 10000.0, where all the three end conditions have more or less the same values of the critical flow velocity parameter. In Fig. 3.8, we observe that this trend has been reversed. For higher values of the Winkler stiffness parameter, for example, 500000.0 and 1000000.0, the clamped-clamped end condition gives values of flow velocity parameter lesser than those for pinned-pinned conditions.

3.4 Solution of the Equation for a pipe resting on a Winkler type elastic medium

The complete solution of the governing differential equation, Equation (3.2), of a pipe conveying fluid and resting on a Pasternak type elastic medium, has been obtained in Section 3.2, as Equations (3.30), (3.49) and (3.50), for the three boundary conditions. The solutions for a pipe resting on a Winkler type elastic medium can be very easily obtained by reducing the above equations by setting the Pasternak stiffness parameter, γ_P, to zero.

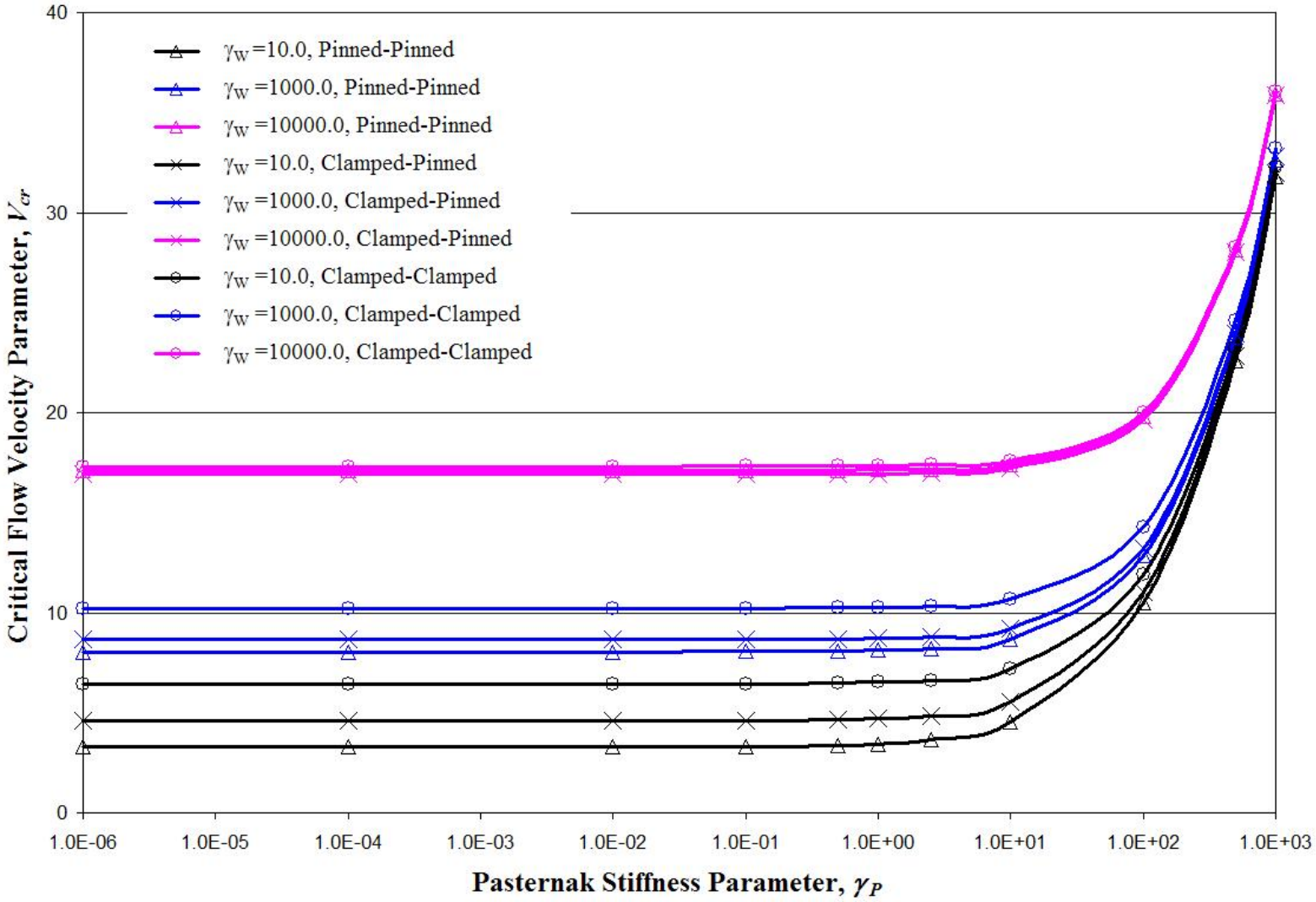

Figure 3.7 Comparison of the variation of critical flow velocity parameter, V_{cr}, with Pasternak stiffness parameter, γ_P, for the values of Winkler stiffness parameter, γ_W, up to 10000.0, for all the three boundary conditions

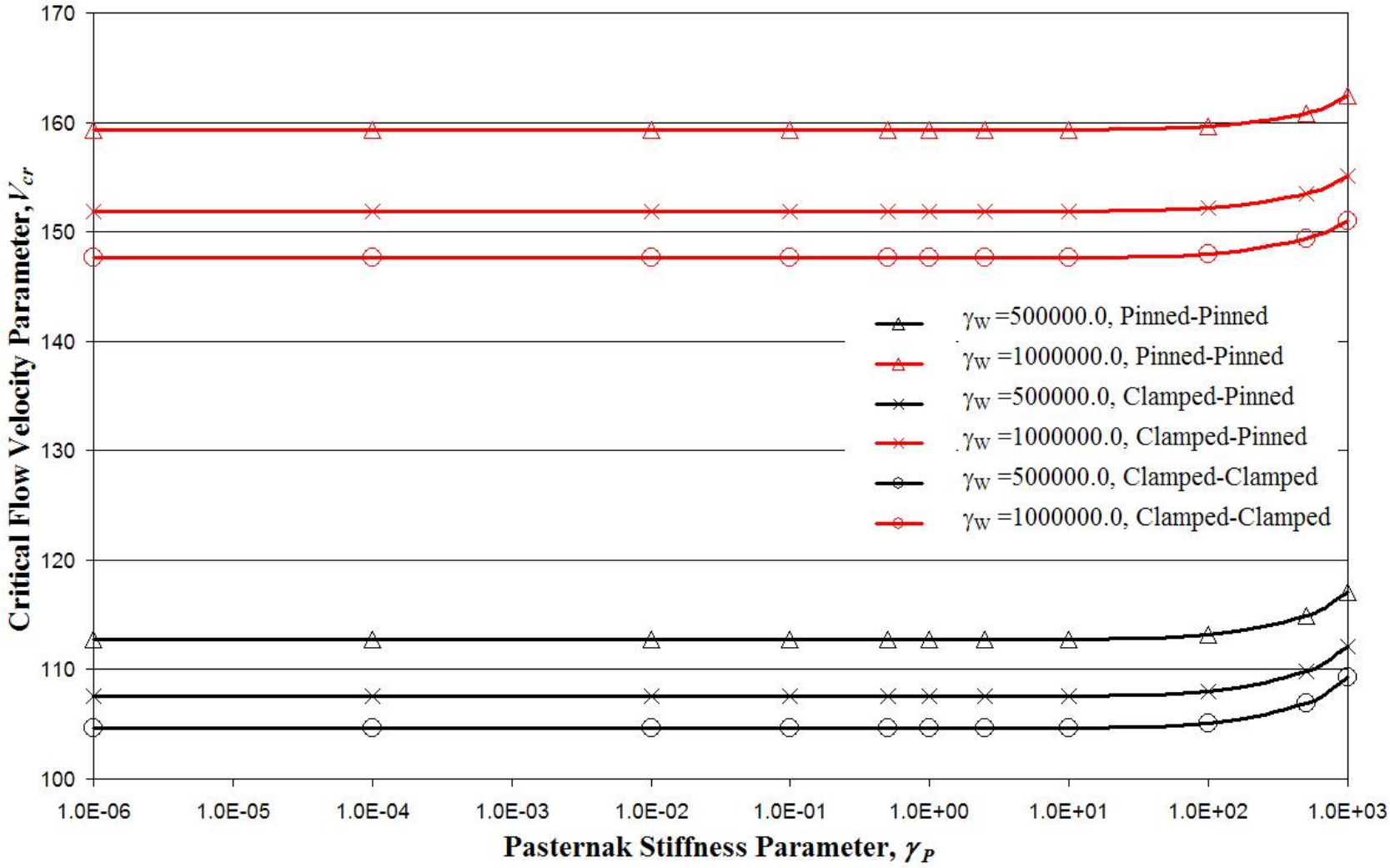

Figure 3.8 Comparison of the variation of critical flow velocity parameter, V_{cr}, with Pasternak stiffness parameter, γ_P, for the values of Winkler stiffness parameter, γ_W, above 10000.0, for all the three boundary conditions

The following sections discuss the details of the solutions for the three boundary conditions and comprehensive numerical results are presented. These results are similar to results published earlier by a number of authors, see for example, Chary **[17]** and Chary et. al. **[18]**. However, results are presented here for comparison purposes and to validate the solution method followed in this work.

3.4.1 Pinned - pinned case

Setting the Pasternak stiffness parameter, γ_P, to zero in Equation (3.30), we obtain the critical flow velocity equation for a pipe with Winkler elastic medium, as follows:

$$V^4\left(4\pi^4\right)-V^2\left(5\pi^2\gamma_W+20\pi^6\right)+\left(16\pi^8+17\pi^4\gamma_W+\gamma_W^2\right)=0 \qquad (3.51)$$

Equation (3.51) is a quadratic in V^2, which can be solved to obtain the values of the critical flow velocity parameter. Doaré and de Langre **[22]**, have used the Equation (3.52) below to obtain the critical flow velocities for a fluid conveying pipe on a Winkler foundation. This equation is based on the relations for a column under compressive load; see Timoshenko and Gere **[70]**.

$$V_{Cr}=N\pi\left(1+\frac{\gamma_W}{\left(N\pi\right)^4}\right)^{1/2} \qquad (3.52)$$

where, N is the smallest integer satisfying the condition

$$N^2\left(N+1\right)^2\geq\frac{\gamma_W}{\pi^4}$$

3.4.2 Clamped - pinned case

In Equation (3.49), putting γ_P equal to zero, we obtain the critical velocity equation for a clamped-pinned pipe on a Winkler foundation as

$$V^4\{c_{11}c_{22}-c_{12}c_{21}\}-V^2\left\{\left(\lambda_1^4+\gamma_W\right)c_{22}+\left(\lambda_2^4+\gamma_W\right)c_{11}\right\}+\left\{\left(\lambda_1^4+\gamma_W\right)\left(\lambda_2^4+\gamma_W\right)\right\}=0 \tag{3.53}$$

The solution of this quadratic equation in V^2 gives the values for the critical flow velocity parameter for this end condition.

3.4.3 Clamped - clamped case

Similarly, making γ_P equal to zero in Equation (3.50), we obtain the quadratic equation for the critical flow velocity parameter for a fluid conveying pipe on a Winkler elastic medium, Equation (3.54)

$$V^4\{c_{11}c_{22}\}-V^2\left\{\left(\lambda_1^4+\gamma_W\right)c_{22}+\left(\lambda_2^4+\gamma_W\right)c_{11}\right\}+\left\{\left(\lambda_1^4+\gamma_W\right)\left(\lambda_2^4+\gamma_W\right)\right\}=0 \tag{3.54}$$

For the clamped-clamped case, the following relations have been used by Doaré and de Langre **[22]**, to compute the critical velocities,

$$V_{cr}=2\pi\left(1+\frac{3\gamma_W}{(2\pi)^4}\right)^{\frac{1}{2}} \tag{3.55}$$

when $\gamma_W \le (84/11)\pi^4$, and

$$V_{cr} = \left(\frac{N^4 + 6N^2 + 1}{N^2 + 1} + \frac{\gamma_W}{\pi^4 \left(N^2 + 1 \right)} \right)^{\frac{1}{2}} \tag{3.56}$$

when $\gamma_W > (84/11)\pi^4$.

Here *N* is the smallest integer satisfying the inequality

$$N^4 + 2N^3 + 3N^2 + 2N + 6 \ge \frac{\gamma_W}{\pi^4}$$

3.5 Numerical Results and discussion

Table 3.9 shows the results obtained for the critical flow velocities, V_{cr}, for all the three boundary conditions, for varying values of the Winkler stiffness parameter, γ_W. Fig. 3.9 shows the plot of critical flow velocity parameter, V_{cr}, versus Winkler stiffness parameter, γ_W, for the three boundary conditions. These results compare very well with those obtained by Chary **[17]**, as expected.

Doaré and de Langre **[22]**, have shown results for a fluid conveying pipe resting on a Winkler type foundation. They have computed critical flow velocities for a pinned-pinned and a clamped-clamped pipe, using the Equation (3.52) for the pinned-pinned case and Equations (3.55) and (3.56), for the clamped-clamped case. It would be useful to compare the results obtained here with those obtained by Doaré and de Langre, because it will serve to validate the solution method adopted in this thesis.

Table 3.9 Values of critical flow velocity parameter, V_{cr}, for varying values of the Winkler stiffness parameter, γ_w, for all three boundary conditions of a pipe

Pinned – pinned case			Clamped – pinned case			Clamped – clamped case	
γ_w	V_{cr}		γ_w	V_{cr}		γ_w	V_{cr}
1.00E-01	3.14321		1.00E-01	4.50067		1.00E-01	6.37932
1.00E+00	3.15768		1.00E+00	4.50896		1.00E+00	6.38505
1.00E+01	3.29891		1.00E+01	4.59086		1.00E+01	6.44208
1.00E+02	4.47233		1.00E+02	5.32942		1.00E+02	6.98684
5.00E+02	7.22105		5.00E+02	7.47184		5.00E+02	9.01828
1.00E+03	8.05039		1.00E+03	8.66386		1.00E+03	10.21328
5.00E+03	12.88914		5.00E+03	13.07432		5.00E+03	13.82653
1.00E+04	17.11086		1.00E+04	16.91955		1.00E+04	17.3133
5.00E+04	36.13853		5.00E+04	34.73717		5.00E+04	34.18141
9.90E+04	50.46957		9.90E+04	48.31052		9.90E+04	47.24856

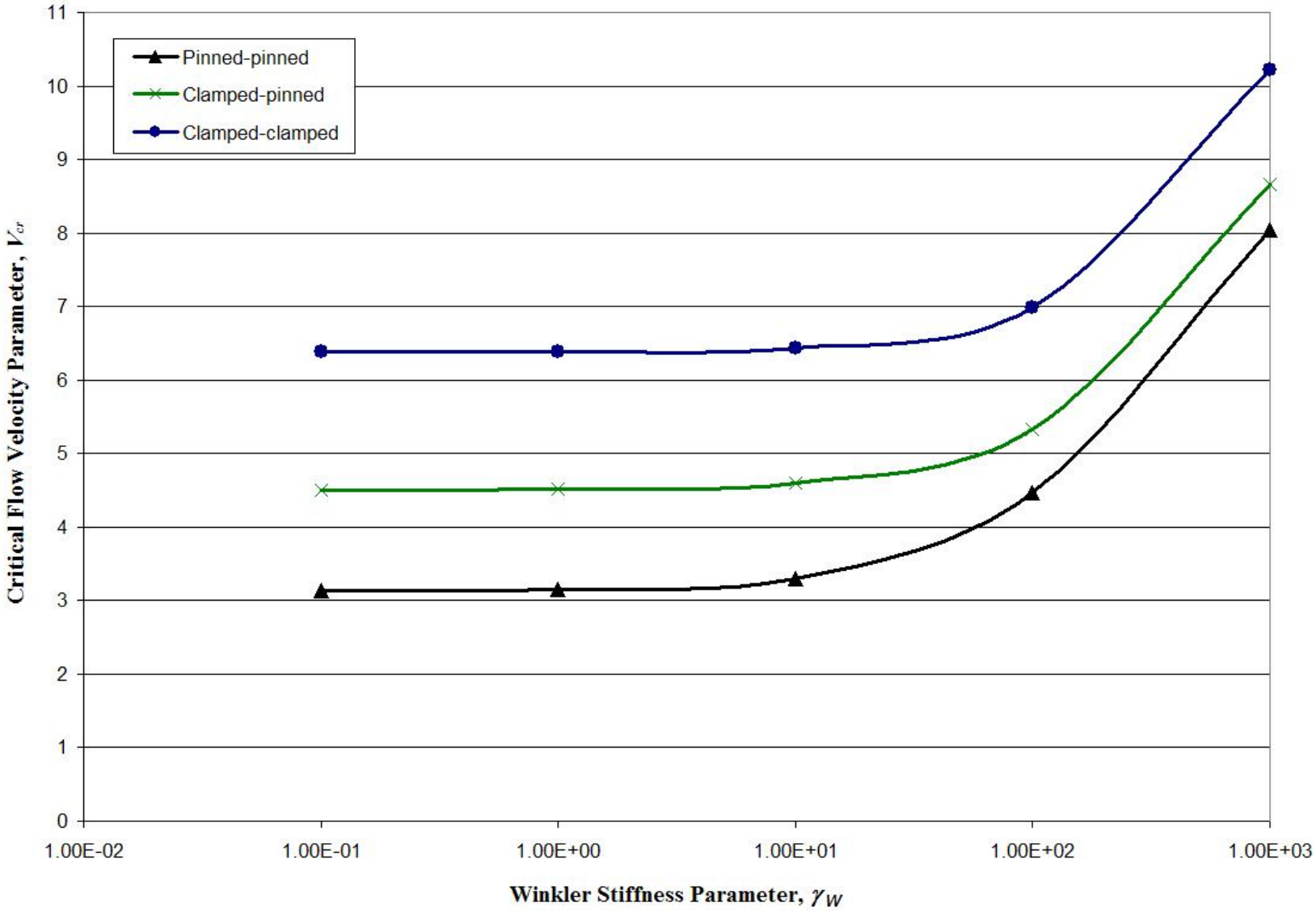

Figure 3.9 Variation of critical flow velocity parameter, V_{cr}, with Winkler stiffness parameter, γ_W, for all three boundary conditions of a pipe

Table 3.10 shows the percentage variation in results for the pinned-pinned and the clamped-clamped end conditions. It is seen that the variation is not significant, especially for lower values of the Winkler stiffness parameter.

The results have also been compared with the curves presented by Doaré and de Langre **[22]**. Figs. 3.10 and 3.11 show this comparison for the pinned-pinned and the clamped-clamped cases respectively. It can be seen that there is very good agreement with the curve given in Fig. 3 of reference **[22]** for a value of the Winkler stiffness parameter, γ_W = 4500.0 for the pinned-pinned end condition. Higher values of γ_W give higher values of the critical flow velocity as compared to the work of Doaré and de Langre. This deviation can be attributed to the use of only two terms in the Equation (3.25). A comparison of results for the clamped-clamped end conditions also shows a similar trend. Again the deviation for higher values of the stiffness parameter could be explained by the fact that only two terms have been considered in Equation (3.46). Thus, as the value of the Winkler stiffness parameter is increased, more modes should be considered in the solution, **[69]**.

Now that results for both the Pasternak stiffness parameter and the Winkler stiffness parameter are available, it would be interesting to analyze the influence of these parameters on the critical flow velocity of a pipe. Figs. 3.12, 3.13 and 3.14 show the effects of both the parameters for a pinned-pinned, a clamped-pinned and a clamped-clamped pipe, respectively. In these figures, the lower dashed curve is for critical velocity parameter, V_{cr}, versus Winkler stiffness parameter, γ_W, for the value of Pasternak stiffness parameter, γ_P = 0.0.

Table 3.10 Comparison of the values of critical flow velocity parameter, V_{cr}, for varying values of the Winkler stiffness parameter, γ_W, for the pinned-pinned and clamped-clamped boundary conditions of a pipe

γ_W	Pinned-pinned end condition			Clamped-clamped end condition		
	V_{cr} (ref. **[22]**)	V_{cr} (Present Work **[68]**)	% Variation	V_{cr} (ref. **[22]**)	V_{cr} (Present Work **[68]**)	% Variation
1.00E+00	3.1577	3.15768	0.0	6.2892	6.38505	1.5
1.00E+01	3.2989	3.29891	0.0	6.3434	6.44208	1.6
1.00E+02	4.4723	4.47233	0.0	6.8613	6.98684	1.8
2.00E+02	5.4894	5.48943	0.0	7.3944	7.54614	2.1
3.00E+02	6.3455	6.34555	0.0	7.8915	8.06676	2.2
4.00E+02	7.0435	7.04347	0.0	8.3591	8.55576	2.4
5.00E+02	7.2211	7.22105	0.0	8.8019	9.01828	2.5
6.00E+02	7.3944	7.39436	0.0	9.2235	9.45821	2.5
7.00E+02	7.5637	7.5637	0.0	9.6266	9.87856	2.6
8.00E+02	7.7293	7.72934	0.0	8.9447	9.9984	11.8
9.00E+02	7.8915	7.89149	0.0	9.2235	10.10641	9.6
1.00E+03	8.0504	8.05039	0.0	9.4942	10.21328	7.6
1.10E+03	8.2062	8.2062	0.0	9.7573	10.31904	5.8
1.30E+03	8.5093	8.50928	0.0	10.2634	10.52738	2.6
1.50E+03	8.8019	8.80192	0.0	10.5512	10.73167	1.7
1.70E+03	9.0851	9.08515	0.0	10.7415	10.93215	1.8
2.00E+03	9.4942	9.49416	0.0	11.0209	11.22615	1.9
2.50E+03	10.1392	10.13924	0.0	11.4713	11.69976	2.0
3.00E+03	10.7457	10.74566	0.0	11.9048	12.15492	2.1
3.50E+03	11.3196	11.31965	0.0	12.323	12.59364	2.2
4.00E+03	11.5697	11.8659	2.6	12.7274	13.01758	2.3
4.50E+03	11.8105	12.38809	4.9	13.1194	13.42815	2.4
5.00E+03	12.0464	12.88914	7.0	13.5001	13.82653	2.4

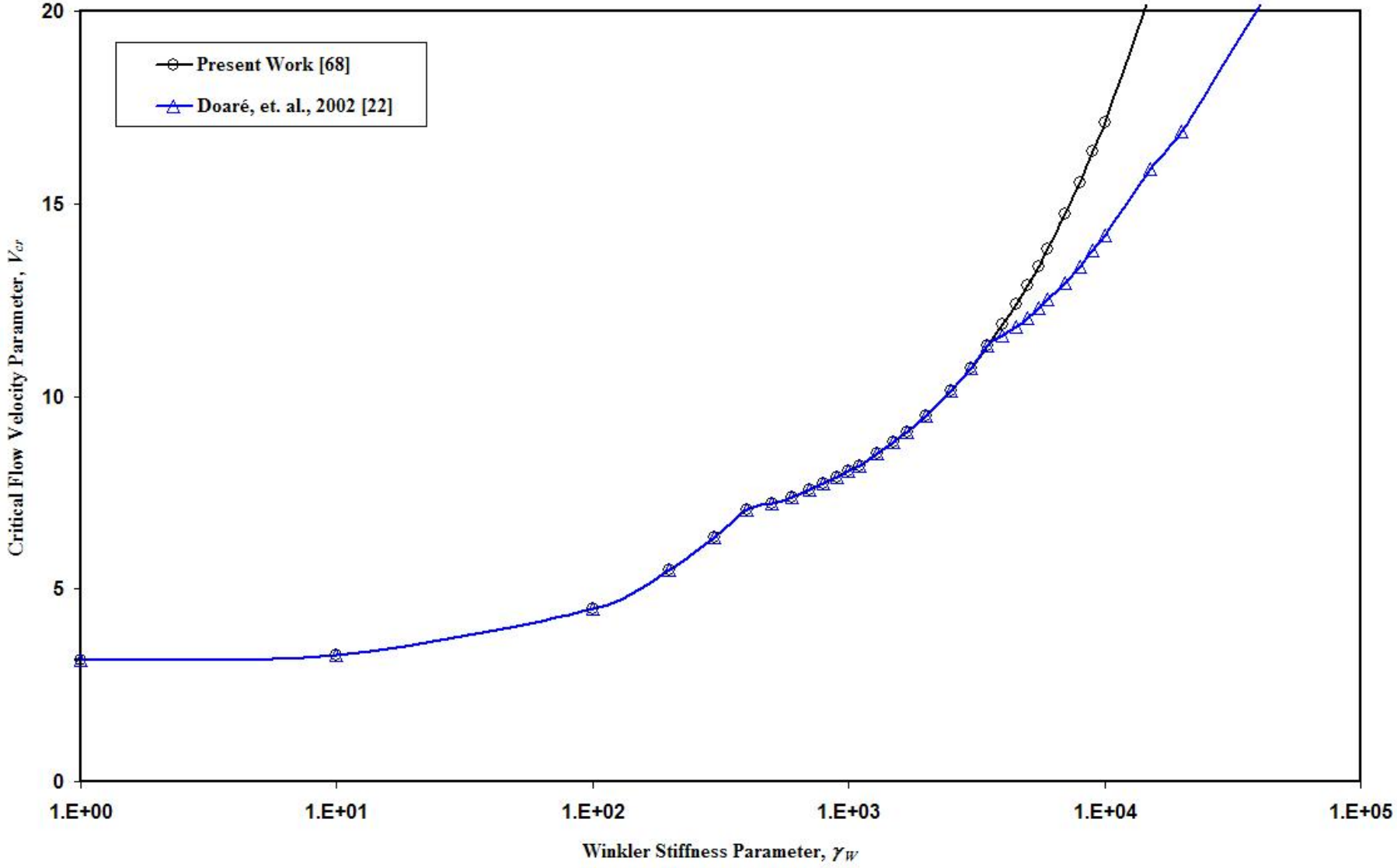

Figure 3.10 Comparison of results with Fig. 3 of Reference **[22]**, for a pinned-pinned pipe, **[68]**

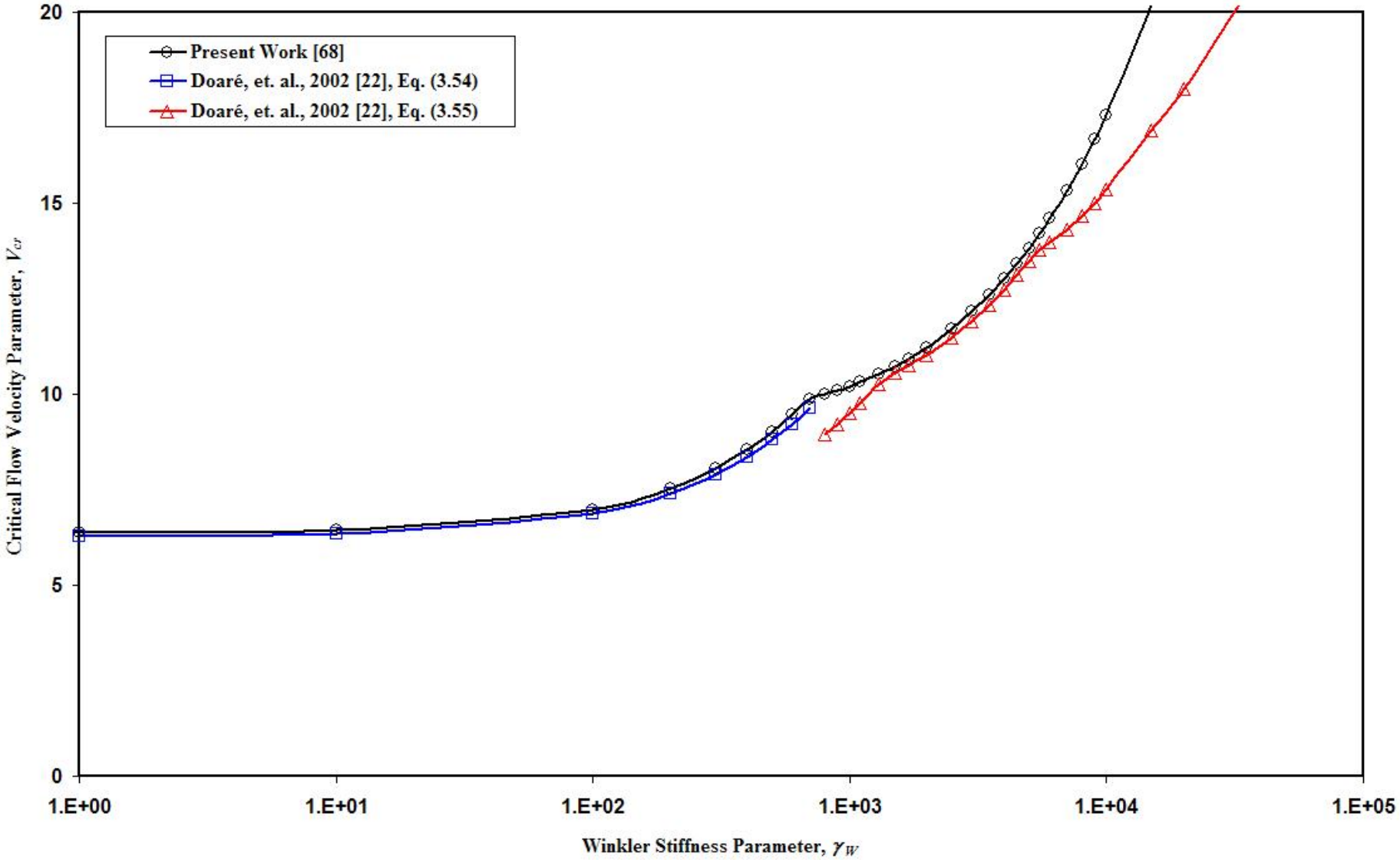

Figure 3.11 Comparison of results with Fig. 3 of Reference **[22]**, for a clamped-clamped pipe, **[68]**

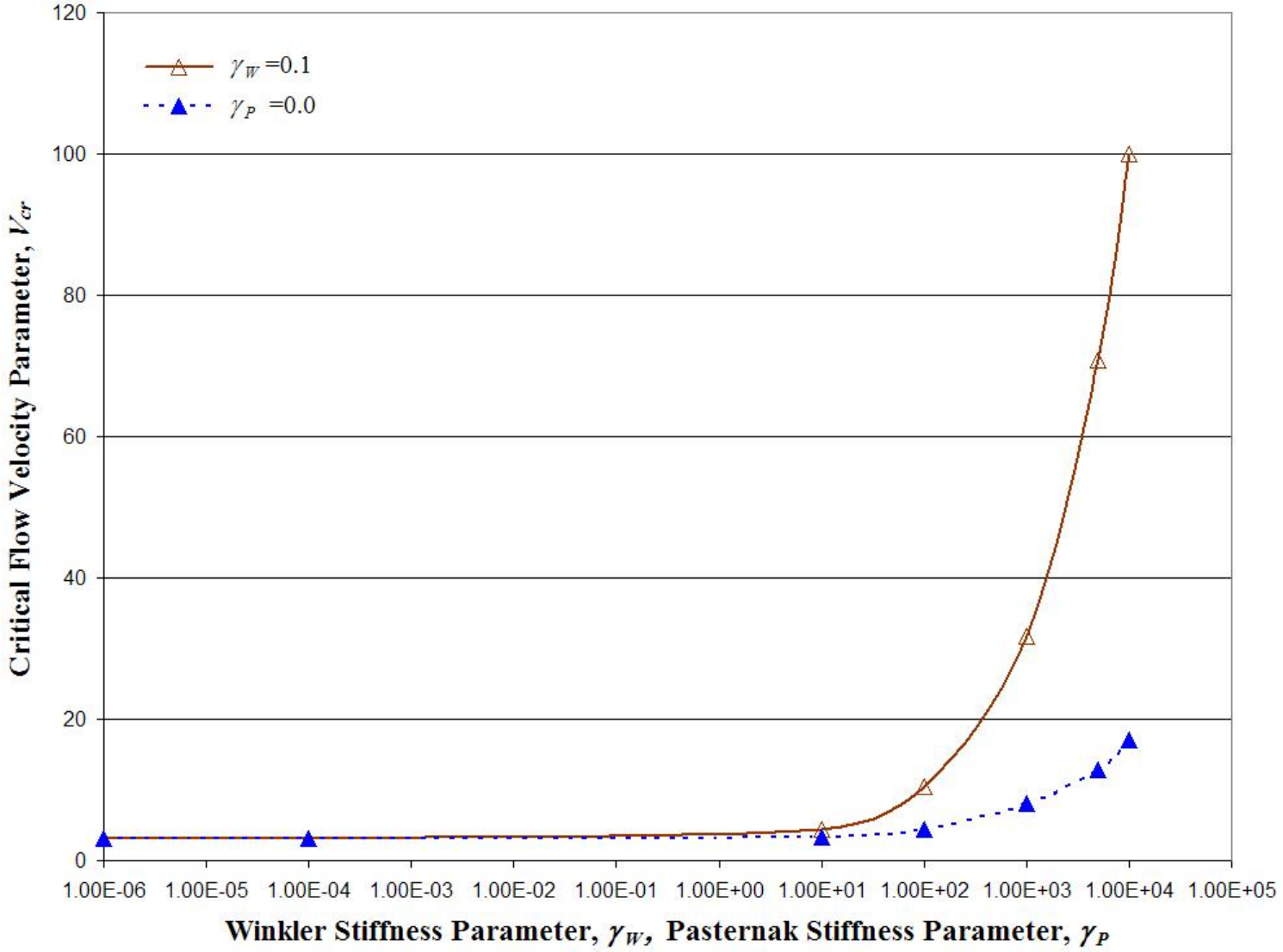

Figure 3.12 Comparison of the influence of the Pasternak Parameter versus the Winkler parameter on the critical flow velocity for a pinned-pinned pipe

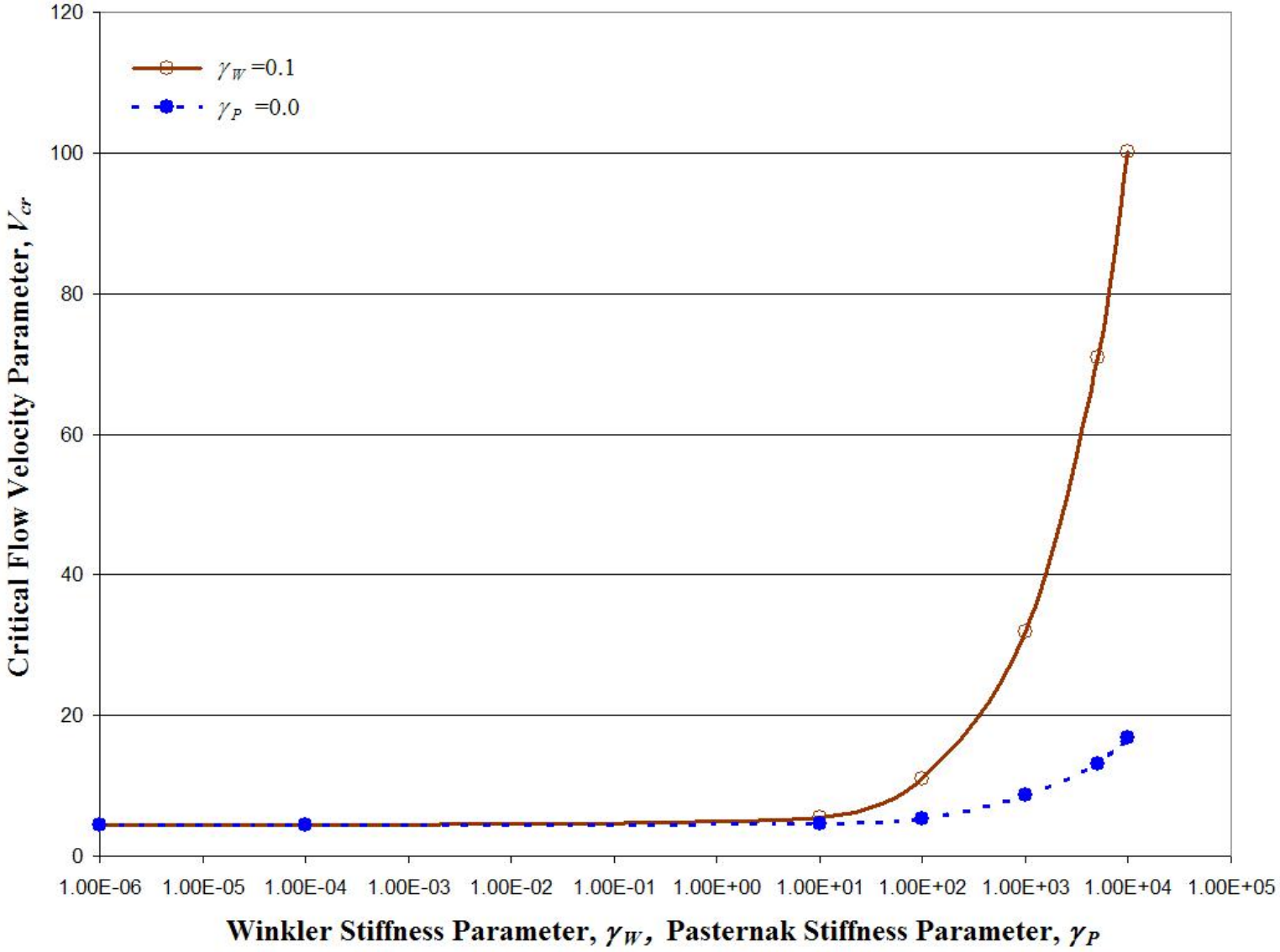

Figure 3.13 Comparison of the influence of the Pasternak Parameter versus the Winkler parameter on the critical flow velocity for a clamped-pinned pipe

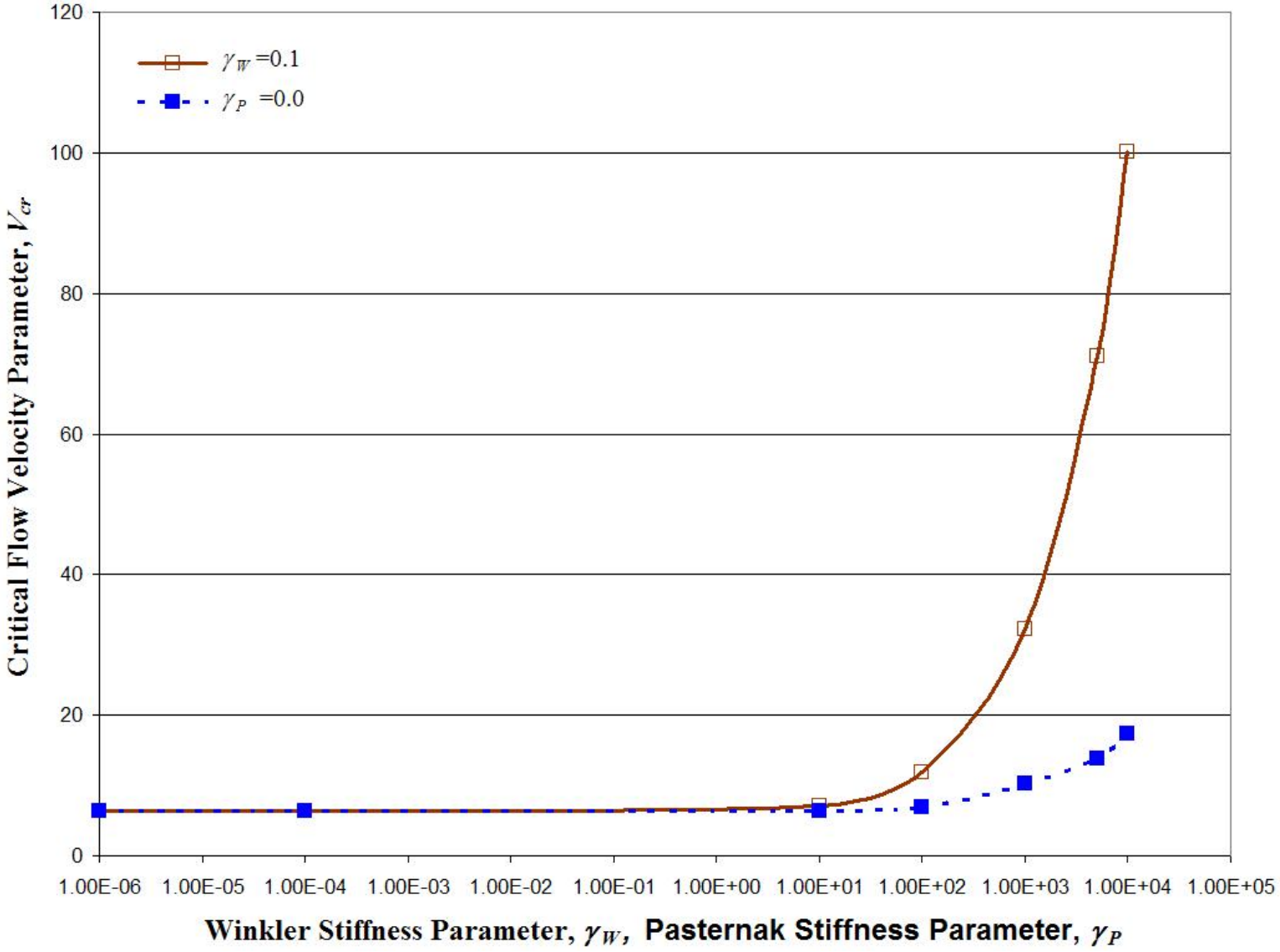

Figure 3.14 Comparison of the influence of the Pasternak Parameter versus the Winkler parameter on the critical flow velocity for a clamped-clamped pipe

The upper solid curve is for critical velocity parameter, V_{cr}, versus Pasternak stiffness parameter, γ_P, for the value of Winkler stiffness parameter, γ_W = 0.1. It is clear from the curves that the second stiffness parameter has considerable influence on the critical flow velocity from values of 10.0 onwards. Thus, the Pasternak parameter contributes more in making the fluid conveying pipe stable than the Winkler parameter.

3.6 Summary and conclusions

In this chapter, the stability of a pipe resting on both a Pasternak as well as a Winkler type elastic medium was investigated. It was explained that the pipe loses stability and buckles when the flow velocity reaches a critical value, analogous to the critical buckling load. Detailed derivations of the expressions for critical flow velocity were presented for all end conditions and for the two stiffness parameters. Comprehensive results have been presented in the form of tables and figures. The results for the stability of a fluid conveying pipe resting on a Winkler foundation were compared with those already published. It is seen that the results obtained here are in very good agreement with the earlier results, by Doaré and de Langre **[22]** and Chary **[17]**, thus validating the solution method adopted here. There is also agreement in the trend of the results with those published by previous researchers, see, for example **[89]**.

It was shown that for increasing values of the Pasternak or shear parameter, there is a sharp increase in the critical flow velocity parameter above its value of about 10.0.

The effect of the second stiffness parameter, that is the Pasternak parameter, γ_P, has been clearly brought out in the various figures. It is seen that this stiffness parameter has considerable influence on the stability of the pipe conveying fluid.

For extremely stiff Winkler type elastic medium, it is seen that there is not much change in the values of the critical velocity.

The critical velocity is the smallest for the pinned-pinned condition followed by the clamped-pinned and the clamped-clamped conditions.

In the next chapter, the natural frequencies of a fluid conveying pipe resting on a Pasternak type elastic medium are computed and detailed numerical results are presented.

Chapter 4

Natural Frequencies of Fluid Conveying Pipes Resting on Elastic Media

4.1 Introduction

In the recent years, there has been a spurt of research on problems related to dynamic behaviour of fluid conveying pipes. The renewed interest in the very practical problem of the dynamic behaviour of fluid conveying pipes was initiated by the observation of vigorous wind-induced vibrations of the Trans-Arabian Oil Pipeline. It is not known whether detailed vibration analysis was done at the design stage, prior to installation of the pipeline, and, if it was done, whether flow velocity was taken into consideration in the analysis. From the literature survey detailed in the Chapter 1, see for instance Ashley and Haviland **[1]**, it seems to be clear that the problem was recognized only after the observation of the vibrations.

It was in 1952, Housner **[2]**, developed an accurate model to describe the dynamics of the pipe conveying fluid. However, all the early researchers focused on understanding

the physics of this very important dynamical problem and contributed to the development of knowledge in formulation and solution of such problems; **[3-11]**. The early authors to consider the realistic problem of dynamics of a fluid conveying pipe resting on soil media were Stein and Tobriner **[12]**, in 1970. This was followed by Lottati and Kornecki **[15]**, in 1986, and a number of researchers in the 1990s through early 2000s **[16-22]**. All the above researchers modeled the soil as an elastic medium using the Winkler foundation model. This was understandable because the Winkler model is the simplest of all the foundation models and a linear model at that. It is seen from the literature survey that none of the researchers have considered an elastic medium other than the Winkler model. In this thesis, a two-parameter model of the elastic medium is considered. Among all the different two-parameter models, see section 2.3, the Pasternak model has been chosen because it is considered to be the most realistic model to simulate the soil, Dutta and Roy **[67]**. This model is introduced into the governing differential equation, Equation (2.35), which is a new contribution to the existing literature.

In the previous chapter, Equation (3.2) was solved to obtain the critical flow velocities of a fluid conveying pipe resting on both Pasternak and Winkler elastic media, for three ideal boundary conditions. Comprehensive results were presented and analyzed. The critical flow velocities give an indication of the stability of the pipe. However, for a complete understanding of the dynamics of such systems, it is essential to have an idea of the natural frequencies of the system.

In this chapter, the solution of the above equation will be presented to compute the natural frequencies of the system. The critical flow velocities computed in the

previous chapter will be used as a limiting condition for obtaining the natural frequencies of the pipe conveying fluid and resting on different elastic media. Wherever possible, comparisons of the results will be made to validate the solution method. Detailed numerical results will be generated and analyzed. It was also seen in the previous chapter that the critical flow velocities were independent of the mass properties of the pipe. It will be shown here that the natural frequencies are dependent on a number of factors, including the mass ratio, critical flow velocities and stiffness parameters of the elastic media.

4.2 Solution of the Equation for natural frequencies of a fluid conveying pipe resting on a Pasternak type elastic medium

The governing partial differential equation for a pipe conveying fluid is reproduced from Equation (2.35), as Equation (4.1) below:

$$EI\frac{\partial^4 w}{\partial x^4}+M\frac{\partial^2 w}{\partial t^2}+\left(m_f U^2-k_P\right)\frac{\partial^2 w}{\partial x^2}+2m_f U\frac{\partial^2 w}{\partial x\partial t}+k_W w=0 \qquad (4.1)$$

The same solution procedure adopted in Section 3.2 is followed and the determinant equations are re-evaluated to obtain the relevant frequency equations.

4.2.1 Pinned-pinned case

We start with Equation (3.27), which is reproduced below as Equation (4.2)

$$\begin{vmatrix} \left\{ EI\left(\frac{\pi}{L}\right)^4 - (m_f U^2 - k_P)\left(\frac{\pi}{L}\right)^2 + k_W - M\omega_j^2 \right\} & \left\{ \frac{16 m_f U \omega_j}{3L} \right\} \\ \left\{ \frac{16 m_f U \omega_j}{3L} \right\} & \left\{ 16EI\left(\frac{\pi}{L}\right)^4 - 4(m_f U^2 - k_P)\left(\frac{\pi}{L}\right)^2 + k_W - M\omega_j^2 \right\} \end{vmatrix} = 0 \qquad (4.2)$$

Expanding the determinant in Equation (4.2), we have

$$\begin{aligned} &\left[M^2\right]\omega_j^4 - \\ &\left[17EIM\left(\frac{\pi}{L}\right)^4 - 5M(m_f U^2 - k_P)\left(\frac{\pi}{L}\right)^2 + 2k_W M + \frac{256}{9L^2}\left(m_f U\right)^2 \right]\omega_j^2 + \\ &\left[16\left(\frac{EI\pi^4}{L^4}\right)^2 - 20EI(m_f U^2 - k_P)\left(\frac{\pi}{L}\right)^6 + 4(m_f U^2 - k_P)^2\left(\frac{\pi}{L}\right)^4 - 5k_W(m_f U^2 - k_P)\left(\frac{\pi}{L}\right)^2 + 17k_W EI\left(\frac{\pi}{L}\right)^4 + k_W^2 \right] = 0 \end{aligned} \qquad (4.3)$$

It is standard practice to simplify equations by non-dimensionalizing them. Hence, defining the following additional non-dimensional parameters,

$$\Omega_j = \omega_j\sqrt{\frac{ML^4}{EI}} \quad ; \text{which is the frequency parameter,} \qquad (4.4)$$

and using the above equation along with other non-dimensional parameters already defined in Equation (3.29) in Equation (4.3), we obtain the non-dimensionalized frequency equation as

$$\Omega_j^4 - \left[17\pi^4 - 5\left(V^2 - \gamma_P\right)\pi^2 + 2\gamma_W + \frac{256}{9}\beta V^2\right]\Omega_j^2 + \left[\begin{array}{c} 16\pi^8 - 20\left(V^2 - \gamma_P\right)\pi^6 + 4\left(V^2 - \gamma_P\right)^2\pi^4 - \\ 5\gamma_W\left(V^2 - \gamma_P\right)\pi^2 + 17\gamma_W\pi^4 + \gamma_W^2 \end{array}\right] = 0 \tag{4.5}$$

It can be observed that Equation (4.5) above is a quadratic equation in Ω_j^2, which can be solved in the usual way to obtain the frequencies. It may be seen that the if we put Ω = 0 in the above equation, we obtain the equation for critical flow velocity, Equation (3.30).

The lowest root of the above equation is the fundamental natural frequency parameter for a pinned-pinned pipe conveying fluid resting on a Pasternak elastic medium.

4.2.2 Pinned-clamped and clamped-clamped end conditions

The governing equation has been solved for the clamped-pinned and the clamped-clamped end conditions in Section 3.2.2, for critical flow velocities only. To obtain natural frequencies for these two boundary conditions, we proceed with the following set of *N* linear algebraic equations:

$$a_r\left(\begin{array}{l}\dfrac{EI}{L^4}\lambda_r^4+\dfrac{\left(m_f U^2-k_P\right)}{L^2}\sum_{s=1}^{N}\{c_{rs}\}+\\ \\ \dfrac{2m_f Ui\omega}{L}\sum_{s=1}^{N}\{b_{rs}\}+\left(k_W-M\omega^2\right)\end{array}\right)=0\ \ ;\ r=1,2,3,....,N \qquad (4.6)$$

The above equation is the same as Equation (3.47). The variables have the same meaning as defined in Section 3.2.2. The values of the integrals b_{rs} and c_{rs} are given in Tables 3.1 and 3.2.

Inserting the non-dimensional parameters of Equations (3.29) and (4.4) in Equation (4.6) and retaining only the first two terms for analysis, we obtain the following matrix equation:

$$\left[\begin{array}{ll}\left\{\begin{array}{r}\lambda_1^4+\gamma_W-\Omega_j^2+\left(V^2-\gamma_P\right)c_{11}+\\ \\ 2i\beta^{\frac{1}{2}}\Omega_j Vb_{11}\end{array}\right\} & \left\{\left(V^2-\gamma_P\right)c_{12}+2i\beta^{\frac{1}{2}}\Omega_j Vb_{12}\right\}\\ \\ \left\{\left(V^2-\gamma_P\right)c_{21}+2i\beta^{\frac{1}{2}}\Omega_j Vb_{21}\right\} & \left\{\begin{array}{r}\lambda_2^4+\gamma_W-\Omega_j^2+\left(V^2-\gamma_P\right)c_{22}+\\ \\ 2i\beta^{\frac{1}{2}}\Omega_j Vb_{22}\end{array}\right\}\end{array}\right]\left\{\begin{array}{l}a_1\\ \\ a_2\end{array}\right\}=0 \qquad (4.7)$$

For a non-trivial solution, the determinant of the coefficient matrix in the above equation is set to zero, giving

$$\begin{vmatrix} \left\{ \lambda_1^4 + \gamma_W - \Omega_j^2 + \left(V^2 - \gamma_P\right) c_{11} + \right. & \left\{ \left(V^2 - \gamma_P\right) c_{12} + 2i\beta^{\frac{1}{2}} \Omega_j V b_{12} \right\} \\ \left. 2i\beta^{\frac{1}{2}} \Omega_j V b_{11} \right\} & \\ \left\{ \left(V^2 - \gamma_P\right) c_{21} + 2i\beta^{\frac{1}{2}} \Omega_j V b_{21} \right\} & \left\{ \lambda_2^4 + \gamma_W - \Omega_j^2 + \left(V^2 - \gamma_P\right) c_{22} + \right. \\ & \left. 2i\beta^{\frac{1}{2}} \Omega_j V b_{22} \right\} \end{vmatrix} = 0 \qquad (4.8)$$

Expanding the determinant in Equation (4.8), we have for the clamped-pinned boundary condition,

$$\Omega_j^4 - \Omega_j^2 \left[\lambda_1^4 + \lambda_2^4 + 2\gamma_W + \left(V^2 - \gamma_P\right) c_{11} + \left(V^2 - \gamma_P\right) c_{22} - 4\beta V^2 b_{12} b_{21} \right] +$$

$$\left[\lambda_1^4 \lambda_2^4 + \lambda_1^4 \left(V^2 - \gamma_P\right) c_{22} + \lambda_2^4 \left(V^2 - \gamma_P\right) c_{11} + \gamma_W \left(V^2 - \gamma_P\right) c_{11} + \gamma_W \left(V^2 - \gamma_P\right) c_{22} + \left(V^2 - \gamma_P\right)^2 c_{11} c_{22} - \left(V^2 - \gamma_P\right)^2 c_{12} c_{21} + \gamma_W \left(\lambda_1^4 + \lambda_2^4\right) + \gamma_W^2 \right] = 0 \qquad (4.9)$$

Equation (4.9) can be easily solved for the natural frequencies. The lowest root of the equation gives the fundamental frequency for the clamped-pinned pipe conveying fluid and resting on a Pasternak type elastic medium.

For the clamped-clamped case, we find that the integrals c_{rs}, for $r \neq s$, equal to zero. After appropriately evaluating the integrals b_{rs} and c_{rs}, for $r,s = 1,2$, we have:

$$\Omega_j^4 - \Omega_j^2 \begin{bmatrix} \lambda_1^4 + \lambda_2^4 + 2\gamma_W + \left(V^2 - \gamma_P\right) c_{11} + \\ \\ \left(V^2 - \gamma_P\right) c_{22} - 4\beta V^2 b_{12} b_{21} \end{bmatrix} +$$

$$\begin{bmatrix} \lambda_1^4 \lambda_2^4 + \lambda_1^4 \left(V^2 - \gamma_P\right) c_{22} + \lambda_2^4 \left(V^2 - \gamma_P\right) c_{11} + \\ \\ \gamma_W \left(V^2 - \gamma_P\right) c_{11} + \gamma_W \left(V^2 - \gamma_P\right) c_{22} + \left(V^2 - \gamma_P\right)^2 c_{11} c_{22} + \\ \\ \gamma_W \left(\lambda_1^4 + \lambda_2^4\right) + \gamma_W^2 \end{bmatrix} = 0 \qquad (4.10)$$

Similar to the previous case, the lowest root of the above equation gives the fundamental natural frequency of a clamped-clamped pipe conveying fluid and resting on a Pasternak type elastic medium.

4.3 Numerical Results and Discussion

Since only two terms have been considered in evaluating the solution for all the three cases, the results for higher values of the stiffness parameters may not be accurate. However, the results are considered to be sufficiently accurate for engineering purposes. This section presents detailed numerical results for pipes in the form of tables and graphs for all the three ideal boundary conditions. Comparison of the results obtained here with those published by earlier researchers is done for the Winkler type elastic medium, wherever possible. This will also serve to validate the method of formulation and solution used in this thesis. It may be mentioned that the analysis of pipes conveying fluid in combination with Pasternak elastic medium is a new contribution and hence comparison is not possible.

We solve Equations (4.5), (4.9) and (4.10) for Ω_j, to obtain the natural frequencies for the three boundary conditions. The lowest root of the equation is the fundamental frequency parameter. The method adopted for computing the natural frequencies is the following:

a) The critical flow velocity parameter, V_{cr}, is first calculated according to the procedure given in Chapter 3.

b) The critical flow velocity parameter is then equally divided into 30 parts.

c) The natural frequency parameters, Ω_j, are then computed for each part of the critical flow velocity parameter, successively incremented by the one-thirtieth part, starting with a value of zero, which is the no-flow condition.

d) This computation is continued in a loop until the thirtieth part, which corresponds to the actual critical flow velocity parameter is reached.

e) The computation is carried out for each value of the velocity parameter, V, by keeping values of the mass ratio parameter, β, the Winkler stiffness parameter, γ_W, and the Pasternak stiffness parameter, γ_P, constant for each loop of the velocity parameter from zero to its critical value.

f) The values of the Pasternak stiffness parameter are then varied for each successive loop. Once the variation of the above parameter is completed, the Winkler stiffness parameter and the mass ratio parameter are varied next, in that order.

g) This procedure gives clear indication of the variation of the frequency with critical flow velocity, as will be shown in graphs later.

Tremendous amount of numerical data has been generated, for the Winkler and Pasternak stiffness parameters varying from zero to 1E+06 and mass ratio parameter varying from 0.12 to 0.5. However, only a selection of results is presented here in tables, for the sake of brevity. Table 4.1 shows the numerical results obtained for three values of the mass ratio parameter, β, for the pinned-pinned boundary condition. The table contains values of the fundamental frequency parameter for varying values of both the stiffness parameters, from 1E-02 to 1E+04. It can be observed from the data in the table that the fundamental frequency parameter, Ω_1, decreases with increasing mass ratio, β, but increases with increasing values of both the stiffness parameters. The decrease in the frequency for increasing values of the mass ratio parameter is more pronounced for higher values of the Pasternak stiffness parameter.

In a similar fashion, Tables 4.2 and 4.3 tabulate the values of the frequency parameter for a fluid conveying pipe resting on Pasternak type elastic medium, for the clamped-pinned and the clamped-clamped end conditions. In these cases too, the trend and the observations are similar to that of the pinned-pinned case. These results can be better comprehended visually in the figures. Fig. 4.1 shows the variation of the fundamental frequency parameter, Ω_1, with flow velocity parameter, V, for different values of the Pasternak stiffness parameter, γ_P, for the Winkler stiffness parameter, γ_W =0.02.

Table 4.1 Pinned-pinned Pipe: Values of fundamental frequency parameter, Ω_1, for different values of the mass ratio, β, and varying values of flow velocity parameter, V, Winkler stiffness parameter, γ_W, and Pasternak stiffness parameter, γ_P.

			Ω_1		
γ_W	γ_P	V	β=0.12	β=0.3	β=0.5
2.00E-02	2.00E-02	0.10484	9.87499	9.8748	9.87459
		0.94353	9.41554	9.40067	9.38423
		1.99189	7.60819	7.55199	7.49106
		3.1451	0	0	0
	2.00E+01	0.18218	17.1603	17.1596	17.1588
		1.63965	16.3416	16.2853	16.2235
		3.46148	13.131	12.9072	12.6729
		5.46549	0	0	0
	5.00E+01	0.25792	24.2942	24.2928	24.2912
		2.3213	23.1128	23.0003	22.8776
		4.90053	18.4773	18.013	17.5421
		7.73768	0	0	0
	1.00E+03	1.05928	99.7734	99.7642	99.7539
		9.53354	94.722	93.9717	93.1665
		20.1264	74.6552	71.3297	68.2218
		31.7785	0	0	0
	5.00E+03	2.35935	222.226	222.204	222.181
		21.2341	210.937	209.212	207.363
		44.8276	166.009	158.323	151.195
		70.7805	0	0	0
	1.00E+04	3.33498	314.12	314.089	314.056
		30.0148	298.155	295.707	293.084
		63.3646	234.606	223.69	213.577
		100.049	0	0	0

Table 4.1 Continued

			Ω_1		
γ_W	γ_P	V	β=0.12	β=0.3	β=0.5
5.00E+01	2.00E-02	0.12891	12.1424	12.142	12.1416
		1.16018	11.5711	11.5432	11.5126
		2.44926	9.32812	9.2206	9.10573
		3.86726	0	0	0
	2.00E+01	0.19702	18.5579	18.557	18.556
		1.77319	17.6653	17.5938	17.5156
		3.74341	14.1655	13.8767	13.5783
		5.91064	0	0	0
	5.00E+01	0.26861	25.3007	25.2991	25.2973
		2.41748	24.0633	23.9359	23.7973
		5.10357	19.2046	18.6731	18.1396
		8.05827	0	0	0
	1.00E+03	1.06194	100.023	100.014	100.004
		9.55742	94.9564	94.2003	93.3891
		20.1768	74.8226	71.4686	68.3378
		31.8581	0	0	0
	5.00E+03	2.36054	222.338	222.317	222.293
		21.2449	211.042	209.314	207.463
		44.8503	166.084	158.385	151.246
		70.8162	0	0	0
	1.00E+04	3.33582	314.199	314.169	314.135
		30.0224	298.23	295.78	293.155
		63.3806	234.658	223.734	213.613
		100.075	0	0	0

Table 4.1 Continued

			Ω_1		
γ_W	γ_P	V	β=0.12	β=0.3	β=0.5
1.00E+03	2.00E-02	0.26839	33.1166	33.1124	33.1078
		2.41549	32.006	31.6607	31.3012
		5.09936	27.4743	25.8663	24.5328
		8.05163	0	0	0
	2.00E+01	0.30697	35.9676	35.9634	35.9587
		2.76275	34.6768	34.3277	33.9609
		5.83247	29.4967	27.8541	26.4524
		9.20916	0	0	0
	5.00E+01	0.35716	39.8672	39.8628	39.8579
		3.21446	38.3326	37.9676	37.5817
		6.78609	32.2323	30.5153	29.0157
		10.7149	0	0	0
	1.00E+03	1.08771	104.661	104.651	104.639
		9.78942	99.5332	98.7004	97.8093
		20.6666	79.1727	75.418	71.9622
		32.6314	0	0	0
	5.00E+03	2.37225	224.463	224.441	224.417
		21.3502	213.14	211.378	209.49
		45.0727	168.088	160.205	152.917
		71.1675	0	0	0
	1.00E+04	3.34412	315.706	315.676	315.642
		30.0971	299.718	297.243	294.592
		63.5382	236.081	225.026	214.799
		100.324	0	0	0

Table 4.1 Continued

			Ω_1		
γ_W	γ_P	V	β=0.12	β=0.3	β=0.5
1.00E+04	2.00E-02	0.57038	100.433	100.376	100.315
		5.13343	95.9508	93.4658	91.5107
		10.8373	77.9301	73.4581	69.9854
		17.1114	0	0	0
	2.00E+01	0.58952	101.417	101.373	101.325
		5.30569	97.4354	95.0399	93.0957
		11.2009	79.8521	75.0556	71.3976
		17.6856	0	0	0
	5.00E+01	0.61715	102.871	102.837	102.799
		5.55431	99.3116	97.0926	95.2014
		11.7258	82.4384	77.2285	73.332
		18.5144	0	0	0
	1.00E+03	1.19851	141.243	141.227	141.208
		10.7866	136.215	134.833	133.384
		22.7717	116.004	109.509	103.982
		35.9553	0	0	0
	5.00E+03	2.42505	243.679	243.654	243.627
		21.8255	232.589	230.578	228.433
		46.076	188.706	179.478	171.093
		72.7515	0	0	0
	1.00E+04	3.38178	329.646	329.613	329.577
		30.436	313.851	311.201	308.366
		64.2538	251.221	239.2	228.177
		101.453	0	0	0

Table 4.2 Clamped-pinned Pipe: Values of fundamental frequency parameter, Ω_1, for different values of the mass ratio, β, and varying values of flow velocity parameter, V, Winkler stiffness parameter, γ_W, and Pasternak stiffness parameter, γ_P.

			Ω_1		
γ_W	γ_P	V	β=0.12	β=0.3	β=0.5
2.00E-02	2.00E-02	0.1501	15.4176	15.4171	15.4165
		1.3506	14.7028	14.6637	14.6208
		2.8514	11.8871	11.7375	11.5783
		4.5022	0	0	0
	2.00E+01	0.2115	21.5619	21.5609	21.5597
		1.9033	20.5461	20.4608	20.3674
		4.018	16.5538	16.2157	15.8661
		6.3442	0	0	0
	5.00E+01	0.2794	28.2929	28.2911	28.289
		2.5144	26.9362	26.7884	26.6277
		5.3083	21.608	21.0063	20.4022
		8.3815	0	0	0
	1.00E+03	1.0647	105.829	105.818	105.805
		9.5824	100.418	99.5151	98.5503
		20.2295	78.9546	75.0491	71.4602
		31.9413	0	0	0
	5.00E+03	2.3618	234.311	234.285	234.257
		21.2561	222.239	220.165	217.953
		44.874	174.236	165.229	157.028
		70.8537	0	0	0
	1.00E+04	3.3367	330.948	330.912	330.871
		30.0304	313.88	310.937	307.798
		63.3974	245.985	233.196	221.566
		100.101	0	0	0

Table 4.2 Continued

			Ω_1		
γ_W	γ_P	V	β=0.12	β=0.3	β=0.5
5.00E+01	2.00E-02	0.1646	16.9595	16.9588	16.9581
		1.4814	16.1716	16.1198	16.0629
		3.1273	13.0686	12.8677	12.656
		4.9378	0	0	0
	2.00E+01	0.222	22.6901	22.6888	22.6874
		1.9982	21.6194	21.5202	21.4118
		4.2183	17.4107	17.014	16.6077
		6.6605	0	0	0
	5.00E+01	0.2874	29.1618	29.1598	29.1575
		2.587	27.7618	27.6003	27.425
		5.4615	22.261	21.5991	20.9395
		8.6234	0	0	0
	1.00E+03	1.0669	106.065	106.053	106.041
		9.6017	100.641	99.7322	98.7615
		20.2703	79.123	75.1902	71.5798
		32.0057	0	0	0
	5.00E+03	2.3628	234.417	234.392	234.363
		21.2648	222.34	220.263	218.048
		44.8924	174.311	165.292	157.081
		70.8827	0	0	0
	1.00E+04	3.3374	331.024	330.987	330.947
		30.0365	313.952	311.006	307.866
		63.4104	246.038	233.241	221.604
		100.122	0	0	0

Table 4.2 Continued

			Ω_1		
γ_W	γ_P	V	β=0.12	β=0.3	β=0.5
1.00E+03	2.00E-02	0.2888	35.1681	35.1639	35.1592
		2.5995	33.8174	33.4762	33.1167
		5.4878	28.369	26.8716	25.5546
		8.665	0	0	0
	2.00E+01	0.325	38.2624	38.2579	38.2528
		2.925	36.7382	36.3705	35.9821
		6.175	30.6417	29.0102	27.571
		9.75	0	0	0
	5.00E+01	0.3728	42.4215	42.4165	42.411
		3.3549	40.6576	40.2547	39.8284
		7.0826	33.6455	31.8486	30.2565
		11.1831	0	0	0
	1.00E+03	1.0929	110.448	110.436	110.423
		9.8364	104.93	103.934	102.874
		20.7658	83.0262	78.6642	74.7163
		32.7881	0	0	0
	5.00E+03	2.3746	236.433	236.407	236.378
		21.3718	224.314	222.197	219.941
		45.1183	176.115	166.896	158.53
		71.2395	0	0	0
	1.00E+04	3.3458	332.454	332.417	332.377
		30.1124	315.353	312.378	309.209
		63.5706	247.319	234.38	222.633
		100.375	0	0	0

Table 4.2 Continued

			Ω_1		
γ_W	γ_P	V	β=0.12	β=0.3	β=0.5
1.00E+04	2.00E-02	0.564	101.134	101.088	101.038
		5.076	96.9973	94.4968	92.4501
		10.7161	79.3238	74.1909	70.3125
		16.9201	0	0	0
	2.00E+01	0.5834	102.256	102.217	102.174
		5.2502	98.4231	96.0307	94.0113
		11.0837	81.1778	75.7418	71.6871
		17.5006	0	0	0
	5.00E+01	0.6113	103.888	103.856	103.82
		5.5013	100.313	98.0833	96.1224
		11.6139	83.6568	77.8525	73.574
		18.3377	0	0	0
	1.00E+03	1.1955	145.583	145.563	145.542
		10.7594	140.121	138.536	136.88
		22.7143	118.221	111.042	104.996
		35.8646	0	0	0
	5.00E+03	2.4236	254.748	254.718	254.686
		21.812	242.819	240.433	237.9
		46.0476	195.596	184.979	175.497
		72.7067	0	0	0
	1.00E+04	3.3807	345.719	345.68	345.636
		30.4264	328.777	325.612	322.245
		64.2335	261.589	247.645	235.087
		101.421	0	0	0

Table 4.3 Clamped-clamped Pipe: Values of fundamental frequency parameter, Ω_1, for different values of the mass ratio, β, and varying values of flow velocity parameter, V, Winkler stiffness parameter, γ_W, and Pasternak stiffness parameter, γ_P.

			Ω_1		
γ_W	γ_P	V	β=0.12	β=0.3	β=0.5
2.00E-02	2.00E-02	0.2127	22.36598	22.3647	22.3634
		1.9141	21.28286	21.1858	21.0798
		4.0409	17.0507	16.6737	16.286
		6.3804	0	0	0
	2.00E+01	0.2597	27.30822	27.3064	27.3043
		2.3371	25.96617	25.819	25.6589
		4.9339	20.72421	20.1433	19.5593
		7.7903	0	0	0
	5.00E+01	0.3174	33.38195	33.3792	33.3762
		2.8569	31.71723	31.5022	31.2696
		6.0313	25.20979	24.349	23.5042
		9.5231	0	0	0
	1.00E+03	1.0753	113.0789	113.065	113.049
		9.6779	107.15242	106.017	104.813
		20.4312	83.69142	78.9758	74.7484
		32.2597	0	0	0
	5.00E+03	2.3666	248.86535	248.833	248.797
		21.2993	235.74295	233.134	230.375
		44.9653	183.65538	172.79	163.163
		70.9978	0	0	0
	1.00E+04	3.3401	351.23762	351.191	351.14
		30.061	332.70197	328.999	325.085
		63.4621	259.09877	243.67	230.022
		100.2032	0	0	0

Table 4.3 Continued

			Ω_1		
γ_W	γ_P	V	β=0.12	β=0.3	β=0.5
5.00E+01	2.00E-02	0.223	23.4554	23.4539	23.4524
		2.0074	22.3125	22.2004	22.0782
		4.2377	17.848	17.4097	16.963
		6.6912	0	0	0
	2.00E+01	0.2682	28.2073	28.2053	28.203
		2.4141	26.814	26.6516	26.4753
		5.0963	21.3709	20.7266	20.0842
		8.0468	0	0	0
	5.00E+01	0.3245	34.1214	34.1185	34.1153
		2.9202	32.4128	32.183	31.9347
		6.1649	25.7311	24.8076	23.9075
		9.7341	0	0	0
	1.00E+03	1.0774	113.299	113.285	113.269
		9.6968	107.358	106.216	105.005
		20.471	83.8329	79.088	74.8388
		32.3226	0	0	0
	5.00E+03	2.3675	248.966	248.933	248.897
		21.3079	235.836	233.224	230.462
		44.9834	183.719	172.839	163.202
		71.0264	0	0	0
	1.00E+04	3.3408	351.309	351.262	351.211
		30.0671	332.768	329.063	325.146
		63.4749	259.144	243.705	230.05
		100.224	0	0	0

Table 4.3 Continued

			Ω_1		
γ_W	γ_P	V	β=0.12	β=0.3	β=0.5
1.00E+03	2.00E-02	0.3405	38.7182	38.7128	38.7067
		3.0643	36.9121	36.4726	36.0116
		6.469	29.7678	27.894	26.281
		10.2143	0	0	0
	2.00E+01	0.3716	41.7683	41.7625	41.756
		3.3448	39.7844	39.3155	38.823
		7.0613	31.9369	29.9421	28.2176
		11.1495	0	0	0
	5.00E+01	0.4141	45.9695	45.9632	45.9561
		3.7267	43.7441	43.2338	42.6971
		7.8674	34.9391	32.774	30.8944
		12.4222	0	0	0
	1.00E+03	1.1077	117.412	117.397	117.379
		9.9694	111.291	110.038	108.715
		21.0464	86.9968	81.7578	77.1418
		33.2312	0	0	0
	5.00E+03	2.3815	250.864	250.831	250.794
		21.4333	237.652	234.988	232.174
		45.2482	185.177	174.066	164.259
		71.4445	0	0	0
	1.00E+04	3.3507	352.657	352.61	352.558
		30.1561	334.057	330.315	326.361
		63.6628	260.179	244.576	230.8
		100.52	0	0	0

Table 4.3 Continued

			Ω_1		
γ_W	γ_P	V	β=0.12	β=0.3	β=0.5
1.00E+04	2.00E-02	0.5771	102.426	102.384	102.339
		5.1942	98.3999	95.8399	93.6661
		10.9655	80.9604	74.9213	70.5053
		17.3139	0	0	0
	2.00E+01	0.5961	103.62	103.583	103.542
		5.3645	99.7392	97.287	95.1495
		11.325	82.5884	76.3184	71.7553
		17.8816	0	0	0
	5.00E+01	0.6234	105.386	105.353	105.317
		5.6105	101.617	99.3022	97.2193
		11.8444	84.7878	78.246	73.4949
		18.7016	0	0	0
	1.00E+03	1.2017	150.933	150.909	150.883
		10.8156	144.815	142.911	140.94
		22.833	120.384	112.255	105.541
		36.052	0	0	0
	5.00E+03	2.4266	268.194	268.157	268.116
		21.8398	255.119	252.153	249.033
		46.1063	203.378	190.812	179.885
		72.7994	0	0	0
	1.00E+04	3.3829	365.188	365.138	365.083
		30.4463	346.705	342.748	338.576
		64.2755	273.469	256.818	242.229
		101.488	0	0	0

This value of the Winkler parameter indicates that its contribution is negligible in these particular results. It can be clearly observed that as the Pasternak parameter increases, the frequency also increases, the increase being much higher for values of γ_P greater than 10.0. These values are for the value of the mass ratio parameter, β = 0.12. The trend for other values of the mass ratio parameter is similar.

Figs. 4.2, 4.3 and 4.4 show the effect of the mass ratio parameter on the fundamental frequencies of the fluid conveying pipe, for the pinned-pinned, clamped-pinned and the clamped-clamped conditions respectively. As observed in the tabulated values, the frequency decreases for increasing values of the mass ratio parameter, and this decrease is more pronounced for higher values of the Pasternak stiffness parameter. This trend is the same for all the boundary conditions considered here.

Since the data for all the three end conditions is now available, it would be interesting to study the influence of the boundary conditions on the frequency of a fluid conveying pipe. Fig. 4.5 indicates this influence. It can be seen that as the end conditions are changed from pinned to clamped, the frequency is increased. This result could help the designers design suitable ends for supporting the pipe depending on the requirement. The figure also shows clearly that for values of the Pasternak parameter greater that about 10.0, the frequency starts increasing exponentially.

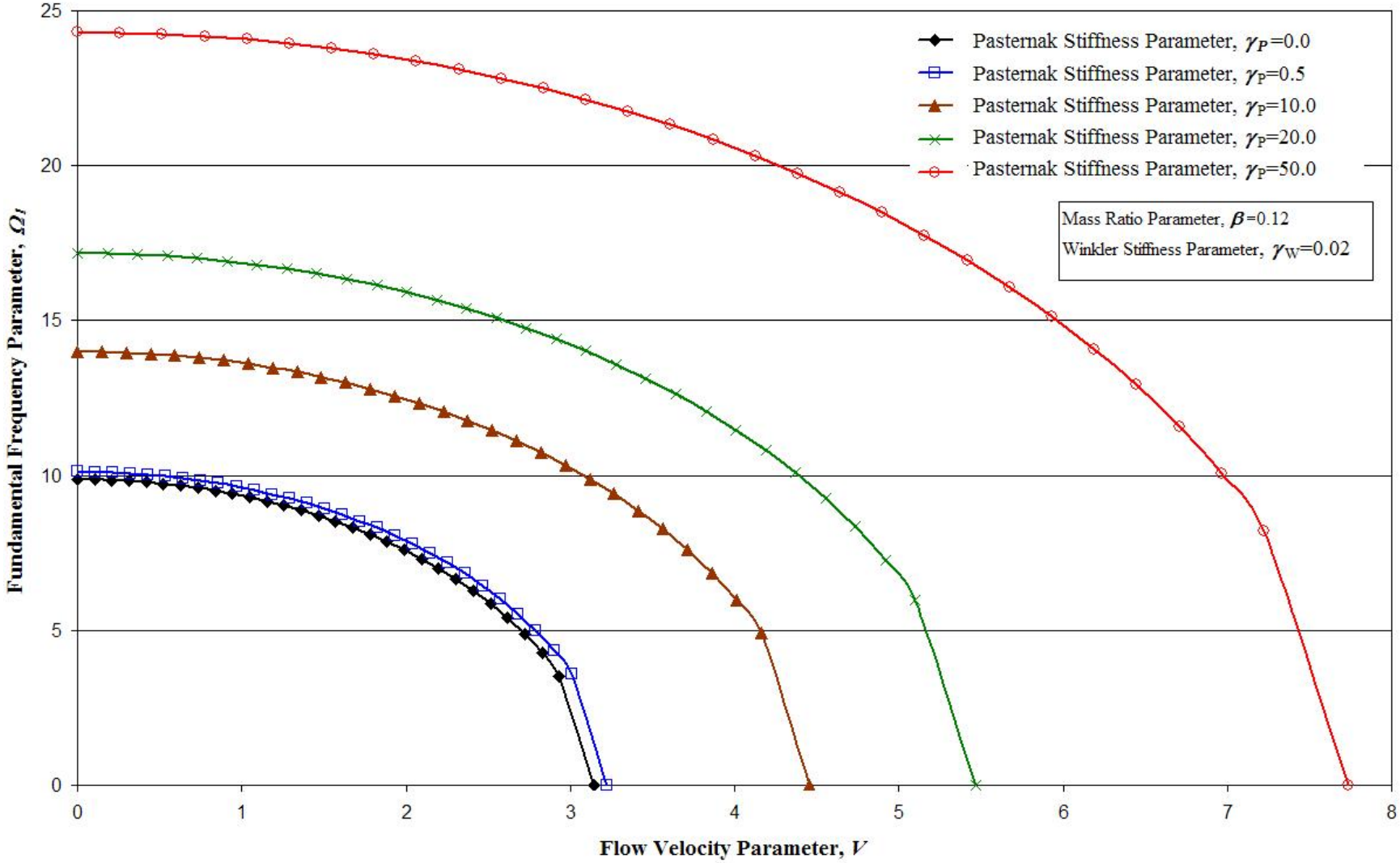

Figure 4.1 Pinned-pinned fluid conveying pipe: Non-dimensional fundamental frequency parameter, Ω_1, as a function of the flow velocity parameter, V, for different values of the Pasternak foundation modulus, for Winkler foundation parameter = 0.02 and mass ratio parameter, $\beta = 0.12$.

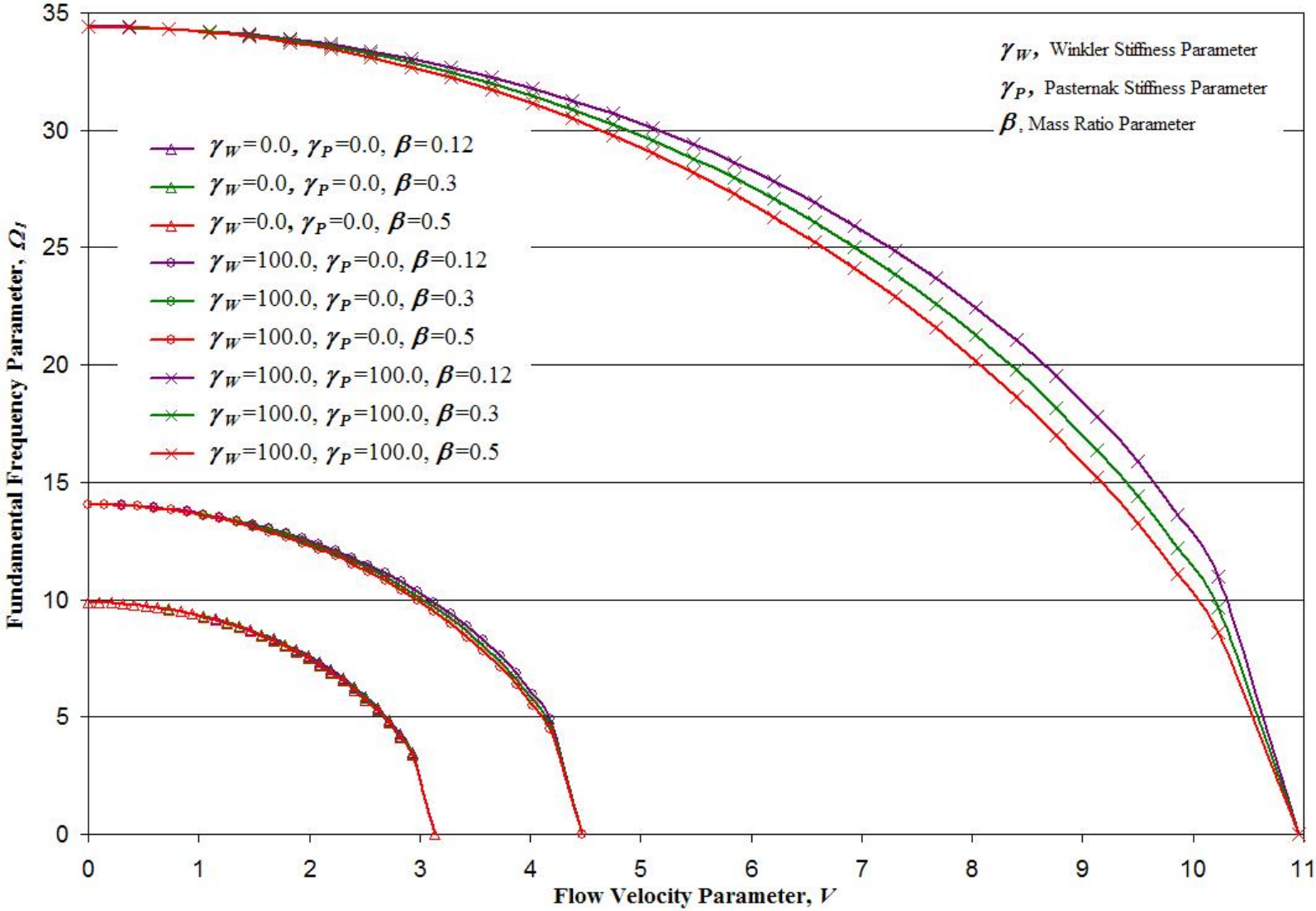

Figure 4.2 Fluid Conveying pipe: Non-dimensional fundamental frequency parameter, Ω_1, as a function of the flow velocity parameter, V, for no-foundation, Winkler foundation and Pasternak foundation, for different mass ratio parameters, β, for a pinned-pinned end condition.

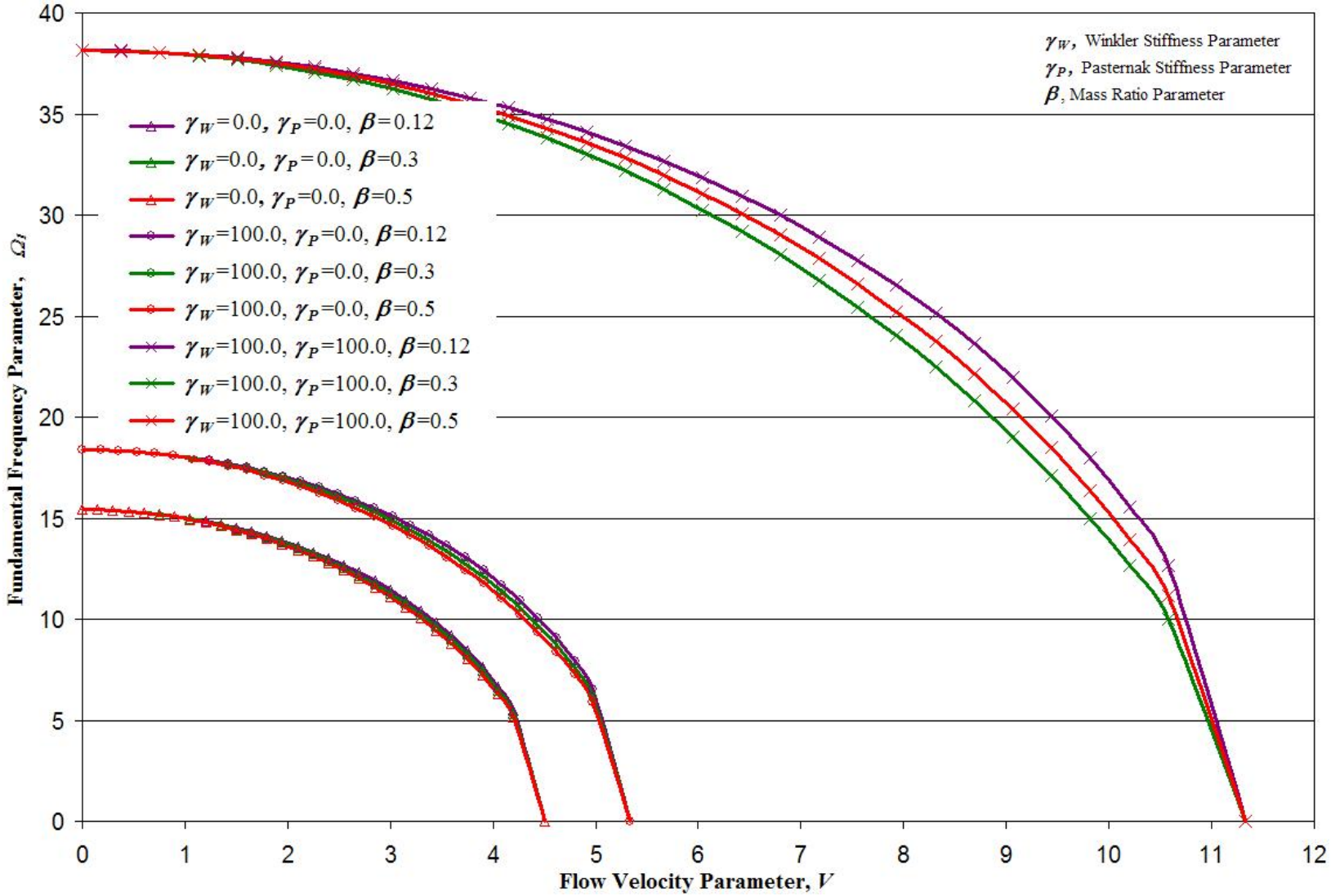

Figure 4.3 Fluid Conveying pipe: Non-dimensional fundamental frequency parameter, Ω_1, as a function of the flow velocity parameter, V, for no-foundation, Winkler foundation and Pasternak foundation, for different mass ratio parameters, β, for a pinned-clamped end condition.

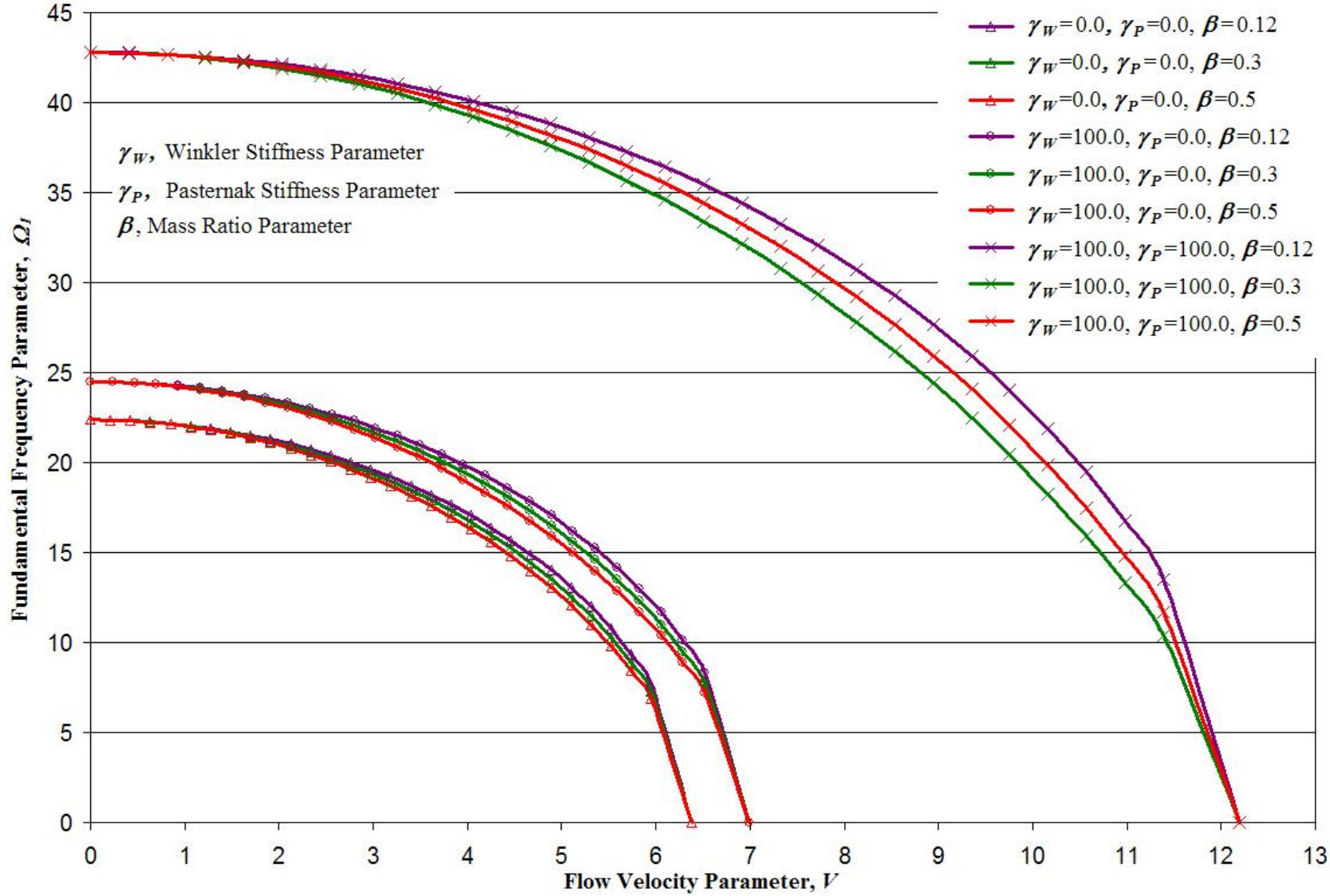

Figure 4.4 Fluid Conveying pipe: Non-dimensional fundamental frequency parameter, Ω_1, as a function of the flow velocity parameter, V, for no-foundation, Winkler foundation and Pasternak foundation, for different mass ratio parameters, β, for a clamped-clamped end condition.

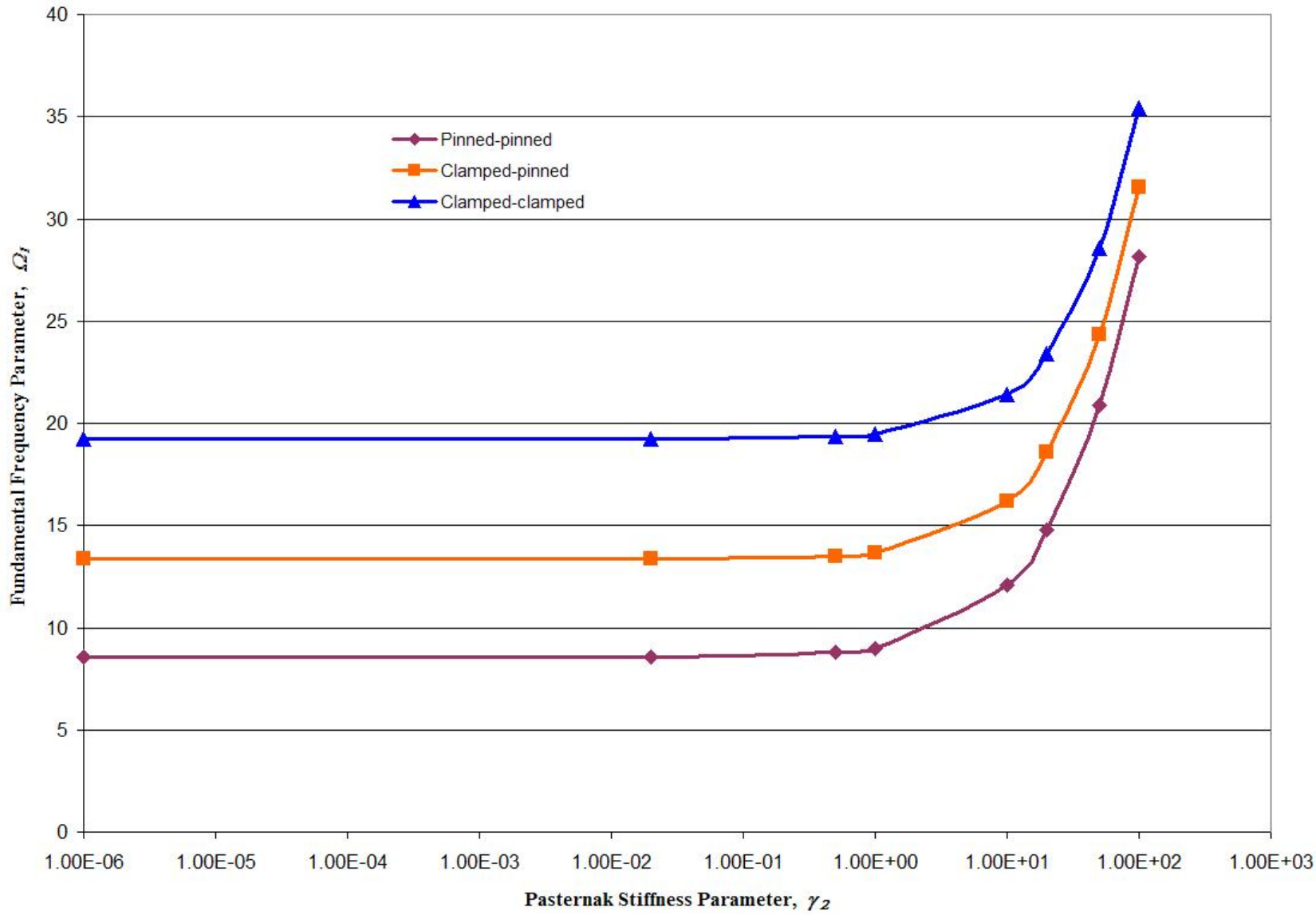

Figure 4.5 Comparison of the effects of the three boundary conditions on the non-dimensional fundamental frequency parameter, Ω_1, for Winkler stiffness parameter, $\gamma_W = 1.0$ and the mass ratio parameter, $\beta = 0.12$, for a fluid conveying pipe.

4.3.1 Comparison of results

A lot of research has been carried out over the years on the dynamic behaviour of fluid conveying pipes, as elaborated in Chapter 1. As mentioned, most of the research is either on pipes without any sort of foundation of on pipes resting on Winkler foundation; see for instance references **[5, 11, 12, 15, 17]**. At this stage, it would be useful to compare the results obtained here with those published by earlier researchers. The formulation adopted in this thesis very easily lends itself to a lot of manipulation of the terms, leading to the desired results. For example, when the Pasternak stiffness parameter, $\gamma_P = 0.0$, we obtain equations for a fluid conveying pipe on Winkler foundation alone. If we put the Winkler stiffness parameter, $\gamma_W = 0.0$, we have the case of a fluid conveying pipe with no foundation. Finally, when the flow velocity parameter, $V = 0.0$, we have the relations for a beam. In the following paragraphs, several cases are presented and compared with existing literature, starting with the no flow condition.

4.3.1.1 Case 1: No Flow Condition, γ_W and γ_P Varying

Here, the flow velocity parameter, $V = 0.0$ and the mass ratio parameter, β, is likewise zero. This condition constitutes a beam on elastic foundation. Tables 4.4 and 4.5 compare the values of the fundamental frequency obtained here with those obtained by Chen, et. al. **[71**], for the pinned-pinned and the clamped-clamped end conditions. From the percent variation computed, it is seen that there is very good agreement of the results. This exercise serves to validate the procedure adopted here. Some of these results have been published by Chellapilla and Simha **[72]**.

Table 4.4 Pinned-pinned beam: Values of fundamental frequency parameter, Ω_1, for different values of the Winkler stiffness parameter, γ_W, and Pasternak stiffness parameter, γ_P. **[72]**

γ_W	γ_P	$\sqrt{\Omega_1}$ **exact** (Ref. **[71]**)	$\sqrt{\Omega_1}$ **present**	%Variation
0.0	0.0	3.141	3.141	0.0
	0.01		3.149	
	0.1		3.217	
	0.5	3.476	3.476	0.0
	1.0	3.735	3.736	0.02
	2.5	4.296	4.297	0.02
10^2	0.0	3.748	3.748	0.0
	0.01		3.752	
	0.1		3.793	
	0.5	3.960	3.960	0.0
	1.0	4.143	4.143	0.0
	2.5	4.582	4.582	0.0
10^4	0.0	10.024	10.024	0.0
	0.01		10.024	
	0.1		10.026	
	0.5	10.036	10.036	0.0
	1.0	10.048	10.048	0.0
	2.5	10.083	10.084	0.009
10^6	0.0	31.621	31.623	0.006
	0.01		31.623	
	0.1		31.623	
	0.5	31.622	31.623	0.003
	1.0	31.622	31.624	0.006
	2.5	31.623	31.625	0.006

% Variation =

$$\left| \frac{\left(\sqrt{\Omega_1}_{present} - \sqrt{\Omega_1}_{exact} \right)}{\sqrt{\Omega_1}_{exact}} \times 100 \right|$$

Table 4.5 Clamped-clamped beam: Values of fundamental frequency parameter, Ω_1, for different values of the Winkler stiffness parameter, γ_W, and Pasternak stiffness parameter, γ_P. **[72]**

γ_W	γ_P	$\sqrt{\Omega_1}$ **exact** (Ref. **[71]**)	$\sqrt{\Omega_1}$ **present**	%Variation
0.0	0.0	4.730	4.730	0.0
	0.01		4.733	
	0.1		4.769	
	0.5	4.869	4.916	0.965
	1.0	4.994	5.083	1.782
	2.5	5.320	5.505	3.477
10^2	0.0	4.950	4.950	0.0
	0.01		4.953	
	0.1		4.984	
	0.5	5.071	5.114	0.847
	1.0	5.182	5.264	1.582
	2.5	5.477	5.649	3.14
10^4	0.0	10.123	10.122	0.009
	0.01		10.123	
	0.1		10.126	
	0.5	10.137	10.142	0.049
	1.0	10.152	10.162	0.098
	2.5	10.194	10.222	0.274

% Variation =

$$\left| \frac{\left(\sqrt{\Omega_1}_{present} - \sqrt{\Omega_1}_{exact} \right)}{\sqrt{\Omega_1}_{exact}} \times 100 \right|$$

4.3.1.2 Case 2: Fluid Conveying Pipes, no-foundation

Many of the earlier researchers have worked on the dynamic behaviour of fluid conveying pipes without considering any foundation. Table 4.6 details the first two frequency parameters for the three boundary conditions. There is very good agreement of the values of the fundamental frequency for the pinned-pinned and the clamped-clamped conditions with those published by Païdoussis and Issid **[5]**.

4.3.1.3 Case 3: Fluid conveying pipes on Elastic foundations

Finally, results will be presented for the vibrations of a fluid conveying pipe resting on both Winkler and Pasternak foundations. Data published earlier is available for pipes on Winkler foundation, see for instance Chary **[17]**, Chary et. al. **[18]**. The present results for Winkler foundation alone agree very well with those of the above references, mainly because the method followed here is an extension of the work done by Chary **[17]**. The results for fluid conveying pipes on Pasternak foundation are however new. Figs. 4.2, 4.3 and 4.4 summarize the results for fluid conveying pipes without foundation and with Winkler and Pasternak foundations for the three boundary conditions respectively. It can be observed from the above figures that the fundamental frequency increases from a no-foundation condition to Winkler foundation condition to Pasternak foundation condition, in that order. Also, the effect of the Pasternak parameter is clearly visible in that, the frequency increase is quite significant, indicating that the Pasternak parameter has more influence on the dynamic characteristics of the fluid conveying pipe.

Table 4.6 Fluid conveying pipes without foundation: Values of the first two frequency parameters, Ω_1, for different values of the mass ratio parameter, β and different end conditions. **[72]**

V	$\beta = 0.1$		$\beta = 0.3$		$\beta = 0.5$	
	Ω_1	Ω_2	Ω_1	Ω_2	Ω_1	Ω_2
Pinned - Pinned End Condition						
0	9.869	39.478	9.869	39.478	9.869	39.478
0.3	9.823	39.436	9.821	39.443	9.820	39.450
0.5	9.741	39.362	9.736	39.382	9.731	39.401
1	9.346	39.013	9.328	39.091	9.310	39.168
2	7.579	37.583	7.516	37.897	7.455	38.208
3	2.898	35.057	2.839	35.784	2.784	36.497
3.141	0.0	34.597	0.0	35.399	0.0	36.183
Pinned - clamped End Condition						
0	15.418	49.964	15.418	49.964	15.418	49.964
0.3	15.383	49.929	15.381	49.936	15.379	49.944
0.5	15.321	49.867	15.315	49.887	15.309	49.907
1	15.027	49.573	15.003	49.653	14.979	49.732
2	13.793	48.380	13.702	48.702	13.612	49.021
3	11.454	46.321	11.275	47.056	11.105	47.778
4	7.017	43.265	6.806	44.606	6.614	45.904
4.499	0.0	41.294	0.0	43.019	0.0	44.678
Clamped - clamped End Condition						
0	22.373	61.672	22.373	61.672	22.373	61.672
0.5	22.300	61.589	22.293	61.610	22.285	61.631
1	22.081	61.340	22.051	61.423	22.021	61.507
2	21.185	60.330	21.067	60.666	20.952	61.000
4	17.207	56.087	16.793	57.470	16.410	58.809
5	13.588	52.652	13.040	54.866	12.557	56.974
6	7.317	48.069	6.847	51.371	6.459	54.459
6.378	0.0	45.952	0.0	49.751	0.0	53.279

Another noticeable point from the above three figures is that the fundamental frequency depends on the end conditions, the lowest being for the pinned-pinned ends and the highest for the clamped-clamped ends, as seen in Fig. 4.5. Also, the effect of the mass ratio parameter on the fundamental frequency is more pronounced as the end conditions change from pinned-pinned to clamped-clamped. The next section summarizes the results obtained in this chapter.

4.4 Summary and conclusions

In this chapter, comprehensive results were presented for the dynamic behaviour of fluid conveying pipes resting on different elastic media. The equations of motion for the pinned-pinned case were solved by utilizing Fourier series expansion and those of the other two end conditions were solved by using the Galerkin method. In both the solution methods, the number of terms were restricted to two, which has proven to be accurate enough for engineering purposes.

Many of the earlier researchers have modeled a Winkler type elastic medium in their formulations. In this thesis, the Pasternak elastic medium has been considered for the first time, which is a more realistic model of the supporting medium, as agreed by many researchers. The results have been comprehensively presented in the form of tables and figures.

Since the analysis of a fluid conveying pipe resting on a Pasternak elastic medium is a new contribution to the literature, there are no means to directly compare the results obtained here. However, comparison of the results for the no-flow condition, representing a beam on Pasternak foundation has been made, and good agreement is

found with results published earlier **[71]**. This fact lends to validating the mathematical formulation as well as the solution procedure. For the no-foundation condition also, the results are in good agreement with those of Païdoussis and Issid **[5]**. As far as the results for the fluid conveying pipe on a Winkler foundation and also for the no-foundation case, are concerned, lot of previously published data is available which has been compared and found to be in excellent agreement as shown in the tables presented in this chapter.

The following major conclusions can be drawn from the analysis and the data obtained in this chapter:

- The fundamental frequency parameter, Ω_1, decreases with increasing mass ratio, β, but increases with increasing values of both the stiffness parameters.

- For higher values of the Pasternak parameter, this decrease is more pronounced as the mass ratio parameter is increased.

- For values of γ_P greater than 10.0, the frequency increases quite appreciably compared to lower values of the parameter.

- End conditions also have an influence on the frequencies, with the clamped-clamped boundary condition providing the highest value of the frequency for the same conditions of the stiffness parameters.

- From the data and the discussions presented, it is concluded that the Pasternak stiffness parameter plays a significant role in enhancing the fundamental frequency of the fluid conveying pipe.

- It is also observed that the fundamental frequency increases from a no-foundation condition to Winkler foundation condition to Pasternak foundation condition, in that order, indicating that the supporting media tends to stabilize the system.

In the course of the work in this thesis, it was discovered that very similar equations govern the dynamics of fluid conveying carbon nanotubes. Hence it was felt that this work should include a treatment of the dynamic behaviour of fluid conveying carbon nanotubes embedded in a Pasternak type elastic medium. This again is a new contribution to the field. The next two chapters discuss this exciting new field of research.

Chapter 5

Fluid Conveying Carbon Nanotubes – Mathematical Formulation

5.1 Introduction to carbon nanotubes

The physical concepts developed for fluid conveying pipes are equally applicable to carbon nanotubes conveying fluid. However, because of the nanoscale lengths involved, the above equations have to be modified to include their effects as well. This chapter looks at the application of the methods to the analysis of carbon nanotubes conveying fluid, not only including the effects of a two-parameter elastic support media, but also the effects of small length scales involved in carbon nanotubes.

Before we develop the equations for carbon nanotubes conveying fluid, it would be useful to understand the nature of carbon nanotubes. Carbon nanotubes were first discovered by Iijima in 1991 **[25]**, as reported in the path breaking paper in *Nature*, in which he called them "Helical microtubules of graphitic carbon". Carbon is intuitively

a well recognized element, abundantly available in nature in either pure form or as compounds of other elements. The most popular allotropic forms of carbon are graphite and diamond. In graphitic structure, each carbon atom forms strong in-plane bonds with its three nearest neighbours and intra-plane bonds are relatively weak. In a diamond structure, each carbon atom is bonded to its four nearest neighbours, in a tetrahedral form. This difference in the structure imparts such widely different physical properties of these two materials. While graphite is a soft material, diamond is the hardest known material. Fullerenes and carbon nanotubes are other allotropic forms of carbon.

A single layer of graphite, with a honeycomb crystal lattice of carbon atoms, is called graphene. This is shown in Fig. 5.1. When this graphene sheet is appropriately rolled into a cylinder, it forms a carbon nanotube. There are three ways this sheet can be rolled into a tube. To understand this, definition of a few terms are necessary. Referring to Fig. 5.1, we choose an atom of carbon in the lattice and label it as (0,0). A line joining all atoms labeled (0,0), (1,0), (2,0), (3,0) etc., in the figure is the zig-zag direction line. Similarly, a line joining the atoms labeled (0,0), (1,1), (2,2), (3,3) etc., is the armchair direction line. A vector connecting the atom (0,0) and another atom, say, (7,4), is called the chiral vector, C_h. The angle between the chiral vector and the zig-zag direction line is called the chiral angle θ, and the unit vectors in two directions are denoted by a_1 and a_2.

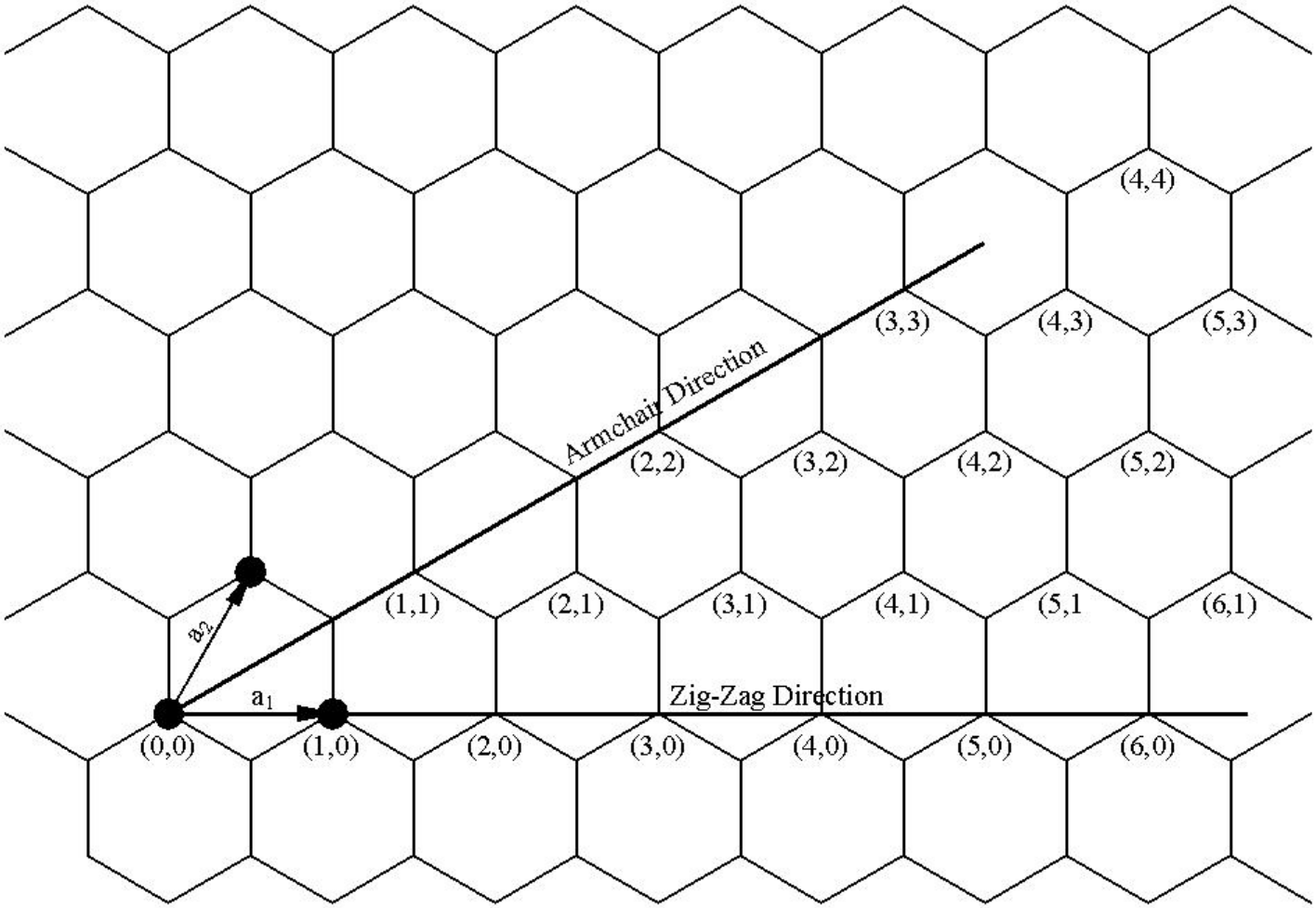

Figure 5.1 Graphene structure

The first way a graphene sheet can be rolled is along the zig-zag direction line. Thus, a (10,0) CNT is formed by rolling the sheet such that the (0,0) and the (10,0) atoms are superimposed after rolling. This type of CNT is known as a zig-zag CNT. A second way the graphene sheet can be rolled is along the armchair direction, so that the atom (0,0) is superimposed on the atom labeled (10,10). This type of CNT is called an armchair CNT. The final way the graphene sheet can be rolled into a tube is along any direction with a chiral angle $0° < \theta < 30°$. Thus a (7,4) CNT, called a chiral CNT, is formed when the atom (7,4) is superimposed on the atom (0,0). In general, a (n,m) CNT is a zig-zag one when m=0, an armchair one when n=m and a chiral CNT when $n \neq m$ and $0° < \theta < 30°$, see for instance Desselhaus, et. al. **[27]**, and Harris, **[28]**. The properties of each type vary vastly. The different types of carbon nanotubes are shown in Fig. 5.2, Fig. 5.3 and Fig. 5.4. The Fig. 5.2 has been taken from a very interesting website of Maruyama, 2010 **[29]**. There are different techniques to synthesize carbon nanotubes including arc discharge, laser ablation and chemical vapour deposition. These methods produce essentially multi-walled carbon nanotubes. The single-walled carbon nanotube was discovered in 1993 by Iijima again. Among the three methods mentioned above, the laser ablation method of synthesis gives a high yield of single-walled carbon nanotubes, at the same time, it is more expensive. Chemical vapour deposition is the process used to produce CNTs commercially. In this thesis, attention is only on the behaviour of single-walled carbon nanotubes.

A single-walled carbon nanotube has an average diameter ranging from 1.2-1.4 nm. The average Young's Modulus is 1.0 TPa and the average tensile strength is ~30.0 GPa.

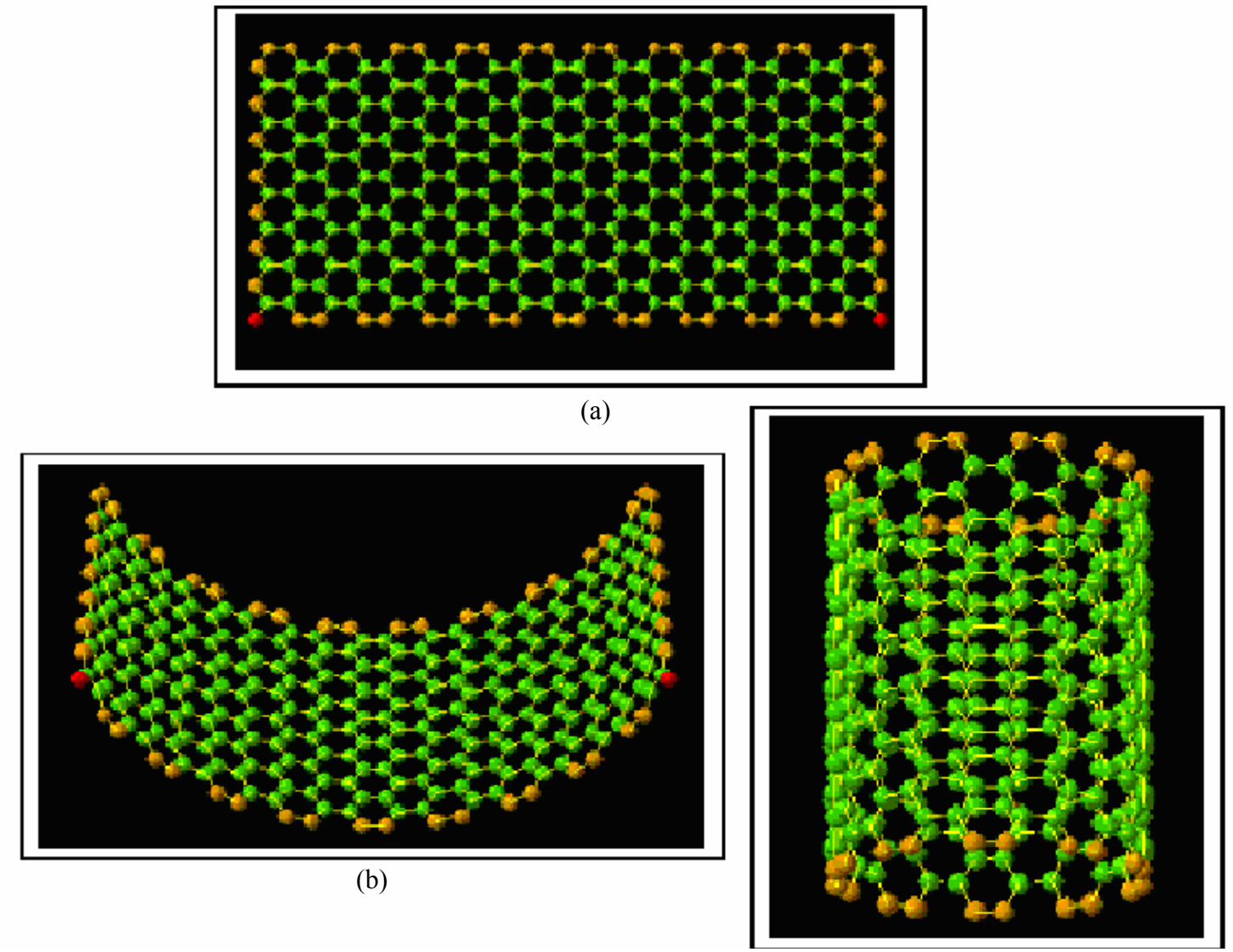

Figure 5.2. (a) Grahpene sheet, (b) Rolling of the graphene sheet, (c) A (10,10) armchair nanotube, **[29]**

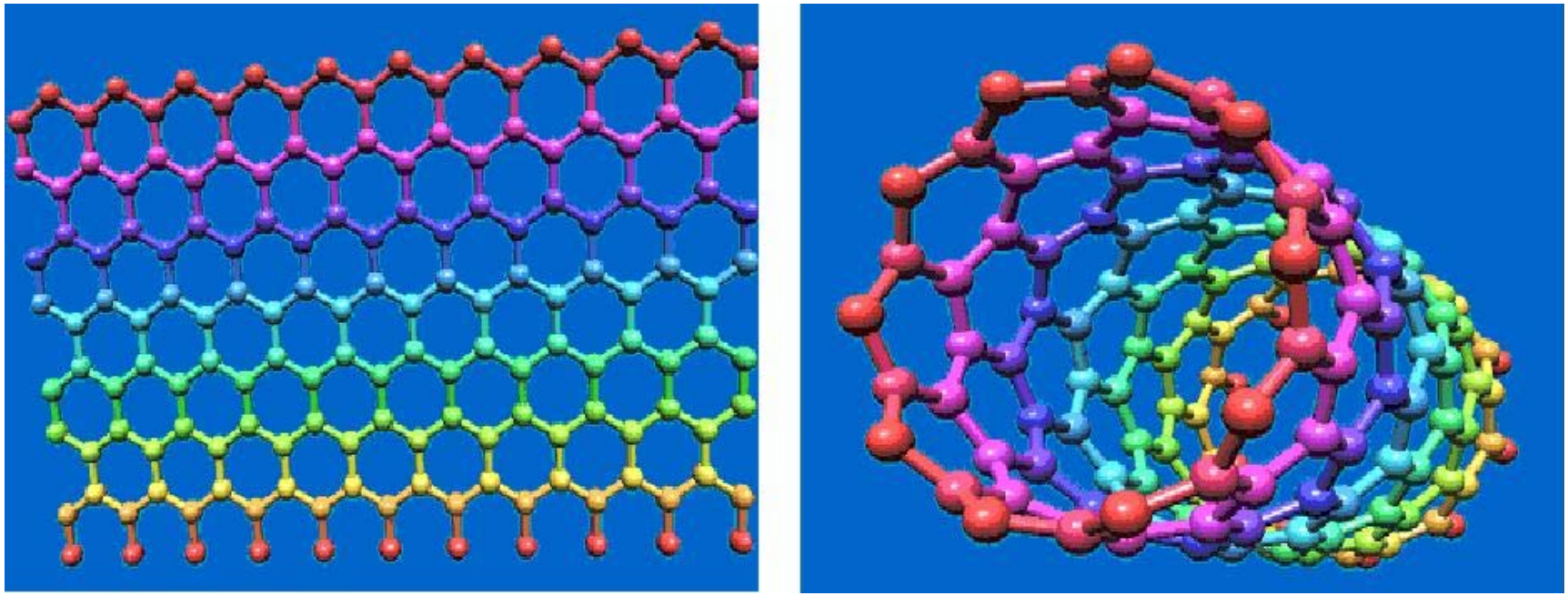

(a) (b)

Figure 5.3. (a) Grahpene sheet, (b) A (10,0) zig-zag nanotube

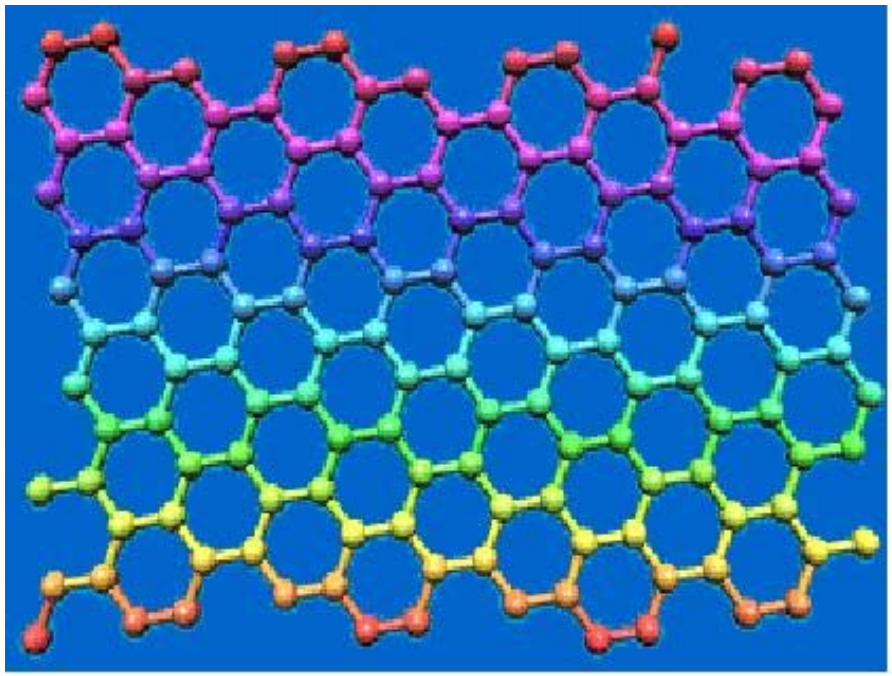

(a)

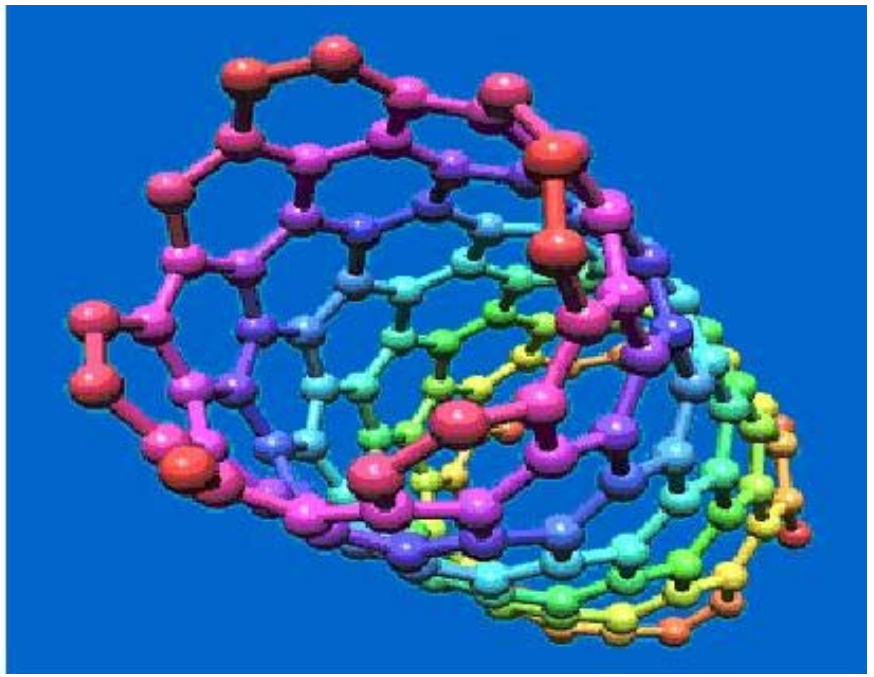

(b)

Figure 5.4. (a) Grahpene sheet, (b) A (7,4) chiral nanotube

They have low densities, in the range of 1.4-1.6 g/cm^3 and hence have a remarkably high specific strength. The application possibilities for CNTs are many including structural, fluid transport, energy storage, adsorbents, etc.

It is in the area of fluid transport, and more specifically vibrations of fluid conveying nanotubes, that this thesis focuses on. Earlier researchers in the field of vibrations of fluid conveying carbon nanotubes used Equation (5.1) below to model the system. It can be seen that this equation is identical to Equation (1.2).

$$EI\frac{\partial^4 w}{\partial x^4}+M\frac{\partial^2 w}{\partial t^2}+\rho A v^2\frac{\partial^2 w}{\partial x^2}+2\rho A v\frac{\partial^2 w}{\partial x\partial t}=0 \tag{5.1}$$

As the research in the mechanics of carbon nanostructures gained momentum, many of the researchers felt that the classical continuum mechanics model of the Euler-Bernoulli hypothesis would not accurately model the carbon nanotube, because of the small length scales involved. The above equation was later refined by researchers to take into account the extremely small length scales involved in carbon nanotubes. The non-local continuum mechanics approach was utilized and the governing equation was modified to Equation (5.2) below.

$$EI\frac{\partial^4 w}{\partial x^4}+\rho A v^2\frac{\partial^2 w}{\partial x^2}+2\rho A v\frac{\partial^2 w}{\partial x\partial t}+\frac{\partial^2}{\partial t^2}\left(Mw-m_c(e_0 a)^2\frac{\partial^2 w}{\partial x^2}\right)=0 \tag{5.2}$$

It is seen from the above equation that the last term includes parameters related to the non-local continuum mechanics model. It was felt during the course of the work on fluid conveying pipes that since similar equations are used to describe the dynamic

behaviour of fluid conveying carbon nanotubes; the analysis of such systems was taken up. This chapter develops the mathematical formulation of the complete problem of carbon nanotubes conveying fluid and embedded in an elastic medium, from which specific cases of pipes conveying fluid can be derived.

5.2 Fluid conveying carbon nanotubes

As noted earlier, since the carbon nanotubes were discovered in 1991 by Iijima **[25]** and again when he and Ichihashi **[26],** discovered the single-walled carbon nanotube in 1993, there has been a flurry of activity in the research arena on various aspects of carbon nanotubes, especially in the basic sciences areas of physics and chemistry. However, to the best of the knowledge of the author, the first study on the dynamics of fluid conveying carbon nanotubes was by Yoon et. al. **[30]**, as recently as in 2005. They applied the standard equations of motion developed for a pipe conveying fluid and also considered the carbon nanotube to be embedded in an elastic medium akin to a Winkler foundation. As for pipes, they concluded that the internal flowing fluid has an influence on the frequencies of the carbon nanotube and that the surrounding elastic medium can reduce the effect of the flowing fluid. Yoon et. al. **[31]**, extended their study to a cantilever CNT conveying fluid, in 2006 and concluded that the internal flowing fluid has a substantial effect on the vibrational frequencies and the decaying rate of amplitude. Also, they opined that the critical flow velocity for flutter instability of the cantilever CNTs may sometimes fall within the range of practical importance. They have considered the Winkler type surrounding elastic medium and have carried out the formulation based on the continuum mechanics theory. Slisik **[32]**, who worked for his M. S. thesis at the University of Akron in 2006, applied the

equations developed by Païdoussis and Issid **[5]** to analyze the dynamic behaviour of single-walled carbon nanotubes conveying fluid. He also developed equations for analysis of double-walled CNTs conveying fluid considering the van der Waals interaction forces between the two walls. He then went on to calculate the response of these nanotubes.

In 2007, Reddy et. al. **[33]**, studied the vibrations of a fluid conveying SWCNT. They have also used the equations developed for pipes in their study. However, apart from critical flow velocity, their main focus was calculate the variation of different forces like the stiffness force, Coriolis force, centrifugal force and inertial force with flow velocity. The main idea was to apply this concept of variation of forces to measure flow in the carbon nanotube by means of a Coriolis mass flow meter. Wang, et. al. **[102]**, in 2008, studied the effect of thermal loading on the dynamic behaviour of a fluid conveying carbon nanotube. They concluded that the temperature change has a significant effect on the stability of a carbon nanotube. In 2008, Wang and Ni **[103]**, reanalyzed the problem of the dynamics of a fluid conveying carbon nanotube using the differential quadrature method for obtaining the solution. Again in 2008, Wang, et. al. **[104]**, studied the buckling behaviour of a double-walled carbon nanotube conveying fluid, by considering the inter-tube radial displacements. Wang and Ni **[105]**, in 2009 concluded from their analysis that the viscosity of the flowing fluid does not have any effect on the vibrations of a carbon nanotube. Yan et. al. **[38]**, 2009, studied the dynamics of fluid conveying triple-walled carbon nanotubes. The van der Waals interactions between the three sets of nanotube walls have been taken into account in their study. However, they used the regular macro-mechanics theory to derive the governing equations of motion. Galerkin approach was used to find

numerical solution of the equations and critical flow velocities were determined. Their results show that the van der Waals forces between the walls of the nanotube enhance the stability of the system. Recently, in 2010, Ghavanloo et. al. **[106]**, used the finite element method to determine the frequencies of a fluid conveying carbon nanotube. They also considered the supporting elastic medium to be a viscoelastic Winkler medium. All the above studies did not take into account the nano-scale effects.

Lee and Chang **[34]**, in 2008, were the first to apply non-local continuum mechanics theory to analyze the vibration behaviour of a fluid conveying carbon nanotube. The non-local model they used takes into consideration the nano-scale effects in the analysis. They found that the non-local parameter characterizing the nano-scale effect significantly influenced the mode shapes of the carbon nanotube. Wang **[107]**, in 2009 analyzed the vibrations of a double-walled carbon nanotube conveying fluid using the non-local theory and considering the interaction between the tubes of the CNT. He discussed the effects of the non-local parameter on the frequencies and concluded that the non-local parameter can be neglected for computing the critical velocities. Again, in 2009, Lee and Chang **[35]**, extended their previous study to include the effects of an embedding medium modeled as a Winkler foundation. Their results showed that for lower velocities, the non-local effect significantly influenced the frequencies. Lee and Chang **[36]**, in 2009, analyzed the dynamic behaviour of short fluid conveying nanotubes based on the Timoshenko theory. In this study, however they did not model the system by the non-local theory. Also, no foundation was considered. All the above three studies were for single-walled carbon nanotubes considered to be fixed at both ends.

In 2009, Lee and Chang **[37]**, applied the non-local continuum theory to study the vibration behaviour of a double-walled fluid-conveying carbon nanotube. In their analysis, they also considered the intra-wall interaction by using the van der Waals criteria. They found that the first three frequencies of a DWCNT conveying fluid are lower that those of SWCNTs.

As far as the new field of carbon nanotubes conveying fluid is concerned, considering that the first paper appeared only in 2005, as seen from the survey above, many researchers are just beginning to contribute to the knowledge. In this field, the elastic medium is taken into consideration by only a few researchers but even they have considered only the Winkler model.

5.3 Review of the non-local continuum mechanics theory of nanobeams

Research in the dynamics of carbon nanostructures, including nanobeams, nanotubes and nanoplates started in the early years of this millennium. Earlier researchers in the field of analysis of vibrations of carbon nanotubes with or without fluid flowing within have traditionally used the continuum mechanics models based on either the Euler-Bernoulli theory of the Timoshenko theory of beams.

Yoon et. al. **[50]** described a method to analyze the vibrations of a carbon nanotube embedded in an elastic medium by means of the classical Euler-Bernoulli model. They even modeled a multi-wall carbon nanotube and the interactions between the walls. However, no fluid flow within the tube was considered in their analysis. This was followed by many other researchers extending the analysis to single-walled carbon nanotubes conveying fluid (see for example **[30-33]**), triple-walled carbon

nanotubes conveying fluid, Yan et. al. [**38]**, all using the Euler-Bernoulli hypothesis, and Chang and Lee **[36]**, using the Timoshenko beam theory.

The applicability of classical continuum models to the analysis of systems like carbon nanotubes, with associated nanometer length scales, has however been called to question by many researchers. Models based on the atomistic theory and molecular dynamics have been used but suffer the problem of being difficult to formulate accurately and certainly very difficult to solve, being computationally very intensive. Hence, a simple model which takes into account these deficiencies was proposed to be used.

The model in question is the non-local continuum mechanics model, proposed by Eringen **[51]**, in 1972 and Eringen and Edelen **[52]**, in 1972 again. Both these references are cited from Peddieson et. al. **[53]**. Since then, lot of effort went into formulating the equations based on the theory to nanobeams, nanostructures, dispersion of elastic waves, fracture mechanics, dislocation mechanics and so on, see the papers **[54-58], (**cited from **[53]**). Wang and Varadan **[95]**, in 2006, adopted a non-local continuum mechanics approach to formulate the governing equations for studying the dynamics of both a single-walled and a double-walled carbon nanotube. A study on the effect of nano length scales on the dynamic properties of nanobeams was undertaken by Lu, et. al. **[96]**, in 2006. Wang, et. Al. **[97]**, in 2007 studied the vibrations of a Timoshenko beam using the non-local elasticity model. Gibson, et. al. [**98]**, in 2007, published a review paper on the vibrations of carbon nanotubes. They have discussed both continuum based models and atomistic models. In 2007, Wang and Liew **[99]**, applied non-local continuum mechanics theory to static analysis of

nano-structures. Reddy and Pang **[62]**, in 2008, have given comprehensive treatment of the application of the non-local continuum mechanics theory to the analysis of nanobeams. They have discussed the bending, buckling and free vibration solutions considering both the Euler-Bernoulli and the Timoshenko beam models, for a variety of boundary conditions.

Recently in 2010, Lee, et. al. **[101]**, have used a non-local formulation to analyze the vibrations of a cantilever carbon nanotube with an attached mass. They have determined the frequency shift with the attached mass and tried to apply the results of the analysis to the development of a mass sensor. Very recently, in 2011, Ansari, et. al. **[90]**, have considered vibrations of a nanobeams embedded in a Pasternak type elastic medium. They have used a sixth-order compact finite difference method for the analysis considering nanoscale effects also. However, their analysis is only for beams.

Many of the studies cover only either the cantilever or the clamped-clamped type of carbon nanotubes conveying fluid. However, there has been good progress in the formulation of the equations of motion by including the non-local continuum mechanics model to account for the nano-scale effects. All the above studies were aimed at understanding the nanomechanics of nano-structures and did not consider fluid flow. These studies served as a basis for applying the non-local continuum mechanics model to fluid conveying carbon nanotubes.

In the following sections, the theory of non-local elasticity will be briefly discussed and applied to analyze the vibrations of a fluid conveying carbon nanotube.

5.3.1 Equations of non-local elasticity

As is well known, the classical elasticity models ("local models") determine the stress state at a given point by considering the strain state at the same point. However, in the non-local elasticity model, the strain rates at all the points in the body are regarded as contributing to the stress state at a given point. This formulation considers the interatomic and intermolecular forces present within a finite range. Also, while the constitutive equation of classical continuum mechanics is an algebraic relation between the stress tensor and the strain tensor at the same given point, the stress tensor at a point in non-local continuum mechanics is related to the strain tensors of all the points in the body in a weighted average sense, resulting in spatial integral equations.

The basic theory of non-local continuum mechanics is briefly given here without going into the details. As an introduction, for a homogeneous and isotropic elastic solid, the linear equations of non-local elasticity are given by

$$\sigma_{kl,l} + \rho\left(f_l - \frac{\partial^2 u_l}{\partial t^2} \right) = 0 \tag{5.3}$$

$$\sigma_{kl}(x) = \int_V \alpha\left(|x - x'|, \chi \right) \tau_{kl}(x') dV(x') \tag{5.4}$$

$$\tau_{kl}(x') = \lambda \varepsilon_{mm}(x') \delta_{kl} + 2\mu \varepsilon_{kl}(x') \tag{5.5}$$

$$\varepsilon_{kl}(x') = \frac{1}{2}\left(\frac{\partial u_k(x')}{\partial x_l'} + \frac{\partial u_l(x')}{\partial x_k'} \right) \tag{5.6}$$

where, σ_{kl} is the non-local stress tensor, ρ is the mass density of the body, f_l is the body force per unit volume, u_l is the displacement vector at a point x in the body, $\tau_{kl}(x')$ is the local (classical) stress tensor at any point x' in the body, $\varepsilon_{kl}(x')$ is the strain tensor at any point x' in the body, t is the time, V is the volume, λ and μ are Lame's constants, $|x-x'|$ is the distance in the Eucledian norm, $\alpha\left(|x-x'|,\chi\right)$ is a kernel function which represents the non-local modulus and χ is a material constant that depends on internal and external characteristic lengths such as lattice spacing and wave length, respectively.

As discussed by Eringen, **[56, 59]**, the constant χ is taken as e_0a/l, where e_0 is a material constant which is appropriately taken to match the model with reliable results of experiments, a is the internal characteristic length like the lattice parameter or C-C bond length and l is the external characteristic length like wave length or crack length. The integro-partial differential equation (5.3) can be reduced to a partial differential equation by appropriately choosing kernel function to take on a Green's function of a linear differential operator. Consequently, the non-local constitutive relations can be written as

$$\left[1-(e_0a)^2\nabla^2\right]\sigma_{kl}=\tau_{kl} \tag{5.7}$$

The theory of non-local continuum mechanics itself is out of the scope of the present Thesis and hence only a brief introduction has been given above for the sake of completeness. Moreover, a number of researchers have adopted the final constitutive

equation, Equation (5.7), resulting from the application of the non-local model as the starting point for further analysis, and this approach is followed here also.

More detailed explanation of the derivations is given by Eringen himself **[56]**, Lu et. al **[60]**, Civalek and Demir **[61]** and Reddy and Pang **[62]**.

5.3.2 Non-local transverse vibrations of a carbon nanotube

For a one-dimensional structure like a carbon nanotube, the non-local constitutive equation, Equation (5.7), can be written as

$$\sigma_{xx} - (e_0 a)^2 \frac{\partial^2 \sigma_{xx}}{\partial x^2} = E\varepsilon_{xx} \tag{5.8}$$

where, σ_{xx} is the axial stress, ε_{xx} is the axial strain of the carbon nanotube and E is the modulus of elasticity for the carbon nanotube. Referring to Fig. 2.1, in which the pipe depicted therein may be thought of as a carbon nanotube of length L, the equilibrium equation according to Euler-Bernoulli hypothesis is

$$\frac{\partial^2 M_b}{\partial x^2} = -m_c \frac{\partial^2 w}{\partial t^2} \tag{5.9}$$

where, m_c is the mass of the carbon nanotube per unit length.

According to the same theory, the strain displacement relationship and the moment are given by

$$\varepsilon_{xx} = z\frac{\partial^2 w}{\partial x^2} \quad \text{and}$$

$$M_b(x,t) = \int_A z\sigma_{xx} dA \tag{5.10}$$

where, z is the distance of the fibre under consideration from the neutral axis. Equation (5.8) is now multiplied on both sides by z and integrated over the cross-sectional area of the carbon nanotube, to give

$$\int_A z\sigma_{xx} dA - (e_0 a)^2 \int_A z\frac{\partial^2 \sigma_{xx}}{\partial x^2} dA - \int_A zE\varepsilon_{xx} dA = 0 \tag{5.11}$$

Substituting Equation (5.10) into Equation (5.11), we have

$$M_b - (e_0 a)^2 \frac{\partial^2 M_b}{\partial x^2} - EI\frac{\partial^2 w}{\partial x^2} = 0 \tag{5.12}$$

where, $\int_A z^2 dA = I$. Differentiating Equation (5.12) with respect to x, twice, we obtain

$$\frac{\partial^2 M_b}{\partial x^2} - (e_0 a)^2 \frac{\partial^4 M_b}{\partial x^4} - EI\frac{\partial^4 w}{\partial x^4} = 0 \tag{5.13}$$

which can be written as

$$\frac{\partial^2 M_b}{\partial x^2} - (e_0 a)^2 \frac{\partial^2}{\partial x^2}\left(\frac{\partial^2 M_b}{\partial x^2}\right) - EI\frac{\partial^4 w}{\partial x^4} = 0 \tag{5.14}$$

Substituting Equation (5.9) into Equation (5.14), we have

$$EI\frac{\partial^4 w}{\partial x^4} + m_c\frac{\partial^2 w}{\partial t^2} - m_c(e_0 a)^2\frac{\partial^4 w}{\partial x^2 \partial t^2} = 0 \qquad (5.15)$$

This is the non-local governing differential equation for a bare carbon nanotube for analyzing its transverse vibrations. The above model has been utilized by many researchers for the analysis of nano-structures either considered as beams or considered as fluid conveying tubes; see for example Lee and Chang **[34, 35, 37]**, Zhang, et. al. **[100]**, Wang, **[107]**, Lee, et. al. **[101]**. In this thesis also, the above model considering the small scale effects is utilized to derive the governing equations for a carbon nanotube conveying fluid and embedded in a Pasternak type elastic medium.

5.4 Transverse vibrations of a fluid conveying carbon nanotube embedded in a Pasternak type elastic medium

A number of research papers have been published studying the transverse vibrations of carbon nanotubes conveying fluid. Before going on to derive the equations, it would be interesting to follow the development of the models for these systems.

Equation (5.15) above is the fundamental equation of motion for the transverse vibrations of a carbon nanotube. In this section, a comprehensive equation of motion will be developed for a carbon nanotube conveying fluid, considering small length scale effects and embedded in a Pasternak type elastic medium. The derivation essentially follows the method adopted for a pipe conveying fluid, see section 2.6.1, and hence the details will not be repeated here. However, this section focuses on the introduction of the nano-scale effects into the governing differential equation. Fig. 5.5

schematically shows a carbon nanotube conveying fluid embedded in an elastic medium. Fig. 5.6 shows a carbon nanotube conveying fluid and embedded in a Pasternak elastic medium. The system in the figure consists of a carbon nanotube of length L supported at both the ends in some way, flexural rigidity EI, mass per unit length m_c, conveying an incompressible fluid of mass m_f with a uniform flow velocity of U in the x-direction.

The area of cross-section of the carbon nanotube through which the fluid flows is A. All other symbols have already been defined in the course of the formulation for pipes.

We start with the equation already derived for a pipe conveying fluid resting on a Pasternak type elastic medium, Equation (2.35), which is reproduced as Equation (5.16) below:

$$EI\frac{\partial^4 w}{\partial x^4}+M\frac{\partial^2 w}{\partial t^2}+\left(m_f U^2-k_P\right)\frac{\partial^2 w}{\partial x^2}+2m_f U\frac{\partial^2 w}{\partial x\partial t}+k_W w=0 \qquad (5.16)$$

The above equation has not considered the effect of nanoscale dimensions of the carbon nanotube. This can be easily accounted for by comparing Equation (5.16) to Equation (5.15), which has been derived using the non-local continuum mechanics approach. Thus, the above equation gets modified to

$$\begin{aligned} EI\frac{\partial^4 w}{\partial x^4}+M\frac{\partial^2 w}{\partial t^2}+\left(m_f U^2-k_P\right)\frac{\partial^2 w}{\partial x^2}+2m_f U\frac{\partial^2 w}{\partial x\partial t} \\ +k_W w-m_c(e_0 a)^2\frac{\partial^4 w}{\partial x^2\partial t^2}=0 \end{aligned} \qquad (5.17)$$

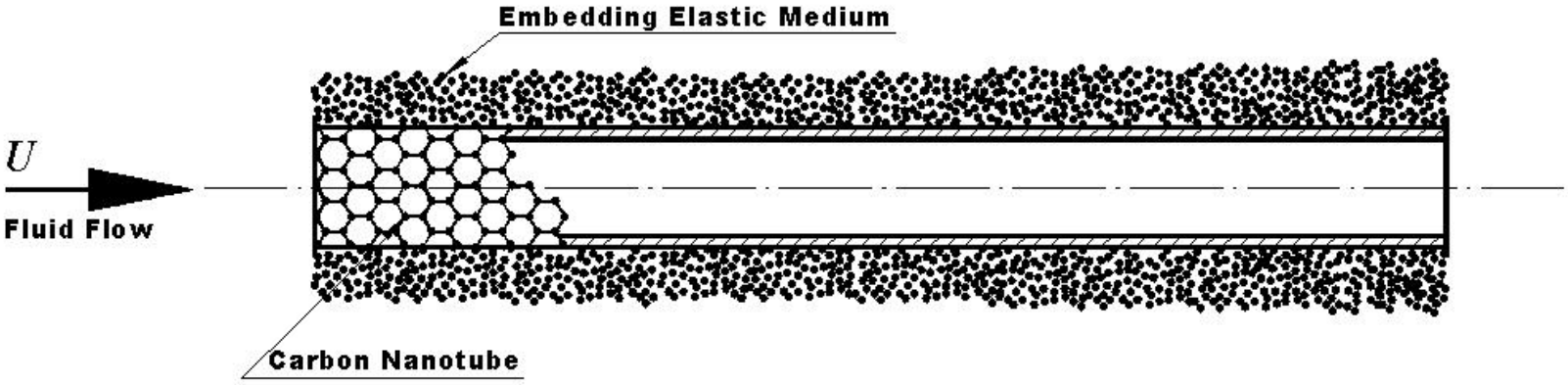

Figure 5.5 Schematic representation of a carbon nanotube embedded in an elastic medium

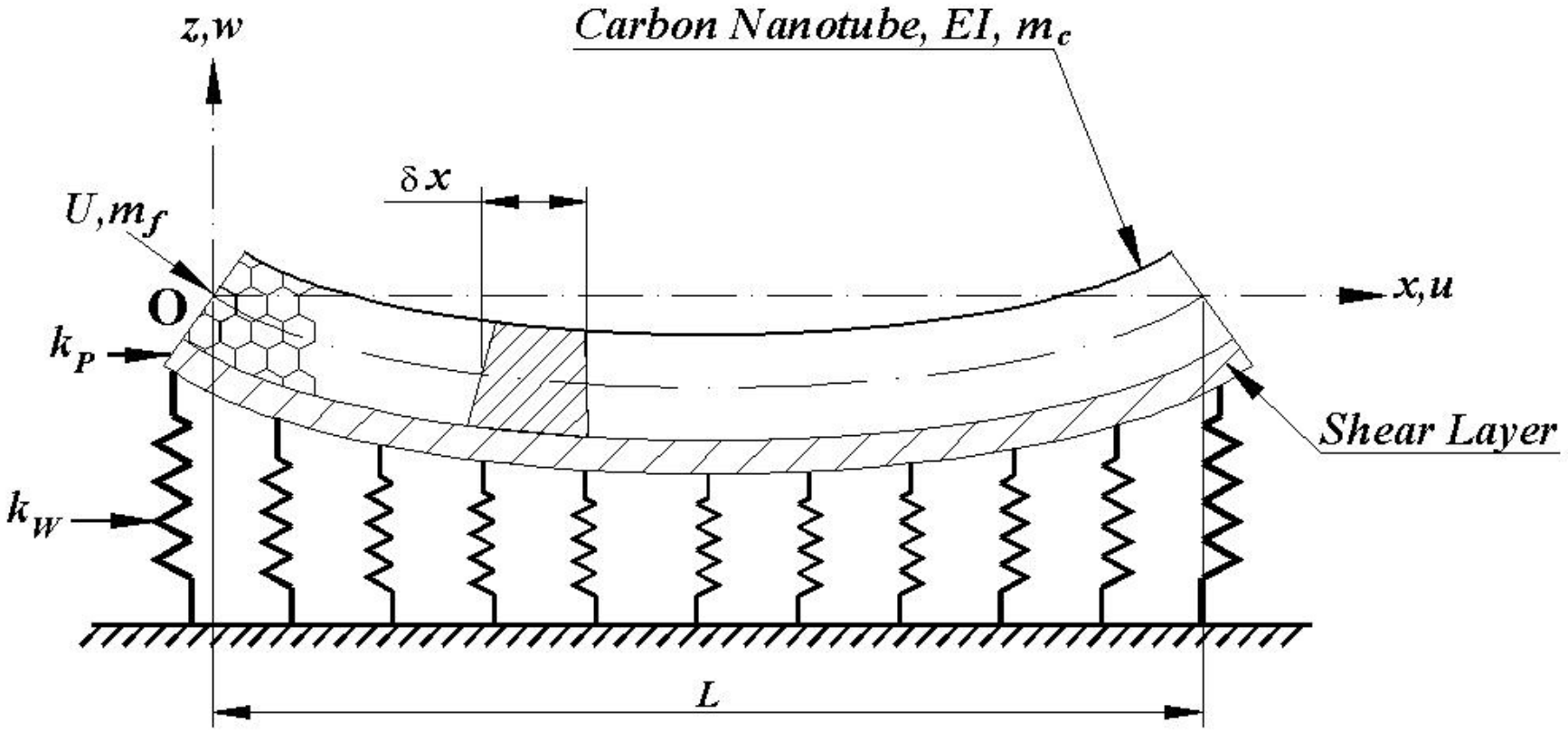

Figure 5.6 Model of a Carbon Nanotube Conveying Fluid and Embedded in a Pasternak Type Elastic Medium

In the above equation, M is the total mass per unit length of carbon nanotube (m_c) plus fluid (m_f). The last term of the Equation (5.17) considers the nanoscale length effects in the governing equation of motion of a carbon nanotube conveying fluid. As indicated in the literature survey, Lee and Chang [34], in 2008, were the first to use the non-local model to formulate the governing equations. The above equation has been derived by many other researchers as well, however, none of the above researchers considered the Pasternak type of embedding medium for the carbon nanotube.

This is accounted for in the above equation by the third term, which is an original contribution of this work. Equation (5.17) is the final governing differential equation of motion of a fluid conveying carbon nanotube embedded in a Pasternak type elastic medium.

5.5 Summary

In this chapter, an introduction to carbon nanotubes was given and a fairly detailed literature survey was presented on the development of the theories for the analysis of nano-structures and carbon nanotubes conveying fluid. It was shown that the equations governing the dynamics of these systems are similar to those of the pipe. However, to accurately model the nanoscale lengths involved in carbon nanotubes, the theory of non-local continuum mechanics, developed by Eringen, was applied and modified equations of motion were developed. Except for the last term in Equation (5.17), the derivation of all other terms follows the method discussed in Chapter 2.

In the next chapter, Equation (5.17) will be solved for the three ideal boundary conditions of pinned-pinned, clamped-pinned and clamped-clamped, and detailed numerical results presented for carbon nanotubes conveying fluid embedded inelastic media.

Chapter 6

Natural Frequencies of Fluid Conveying Carbon Nanotubes Embedded in Elastic Media

6.1 Introduction

The research on behaviour of carbon nanotubes is fairly recent and initially, many researchers applied the same equations developed for a pipe to the analysis of nanotubes, see for example, Yoon, et. al. **[30, 31]**, Slisik **[32]** and Reddy et. al **[33]**. However, it has acquired momentum with researchers applying the non-local continuum mechanics theory to develop the mathematical model, see for instance Lee and Chang, **[34-37]**. The genesis of research in carbon nanotubes conveying fluid lies in the vast progress made in understanding the theory of fluid conveying pipes over the years. This topic has been dealt with in detail in the earlier chapters of this thesis.

In this chapter, the solution of Equation (5.17) derived in the previous chapter will be presented for the three ideal boundary conditions. The analysis takes the effects of

nano length scales into account by utilizing Eringen's non-local continuum mechanics theory **[59]**.

6.2 Solution of the equation for natural frequencies of a fluid conveying carbon nanotube embedded in a Pasternak type elastic medium

The governing partial differential equation for a carbon nanotube conveying fluid and embedded in a Pasternak type elastic medium is reproduced below

$$EI\frac{\partial^4 w}{\partial x^4}+M\frac{\partial^2 w}{\partial t^2}+\left(m_f U^2-k_P\right)\frac{\partial^2 w}{\partial x^2}+2m_f U\frac{\partial^2 w}{\partial x\partial t} + k_W w-m_c(e_0 a)^2\frac{\partial^4 w}{\partial x^2\partial t^2}=0 \tag{6.1}$$

We follow the same solution methodology adopted in Chapters 3 and 4 to solve the above equation. The solution method for the pinned-pinned carbon nanotube is the Fourier series method, while for the clamped-pinned and the clamped-clamped boundary conditions, the Galerkin procedure, with assumed beam eigen functions, is followed. This will be the first time that these methods have been applied to carbon nanotubes. In the following sections, the solution of the above equation is pursued for the three ideal boundary conditions.

6.2.1 Pinned-pinned end conditions

The solution of the above equation is considered the same as Equation (3.7), reproduced below for the sake of clarity as Equation (6.2).

$$w_j(x,t) = \sum_{n=1,3,5,\ldots} a_n \sin\left(\frac{n\pi x}{L}\right)\sin\omega_j t + \sum_{n=2,4,6,\ldots} a_n \sin\left(\frac{n\pi x}{L}\right)\cos\omega_j t; \quad j = 1,2,3,\ldots \tag{6.2}$$

The symbols have the same meaning as in Equation (3.7). Differentiating the above equation according to the order of differentiation in the governing equation, Equation (6.1), we need one extra equation for the last term in the above equation in addition to Equations (3.8) to (3.11). This is given below:

$$\frac{\partial^4 w_j}{\partial x^2 \partial t^2} = a_1 \frac{\pi^2}{L^2}\omega_j^2 \sin\left(\frac{\pi x}{L}\right)\sin\omega_j t + a_2 \frac{4\pi^2}{L^2}\omega_j^2 \sin\left(\frac{2\pi x}{L}\right)\cos\omega_j t + a_3 \frac{9\pi^2}{L^2}\omega_j^2 \sin\left(\frac{3\pi x}{L}\right)\sin\omega_j t + a_4 \frac{16\pi^2}{L^2}\omega_j^2 \sin\left(\frac{4\pi x}{L}\right)\cos\omega_j t \tag{6.3}$$

Substituting Equations (3.8) to (3.11) and Equation (6.3) in the equation of motion, Equation (6.1), and following the same procedure as explained in section 3.2.1, we obtain the following two equations containing the coefficients of $\sin\omega_j t$ and $\cos\omega_j t$.

The equation with $\sin\omega_j t$ is given below:

$$\left\{\begin{array}{l} EI\dfrac{\pi^4}{L^4}\left[a_1\sin\dfrac{\pi x}{L}+81a_3\sin\dfrac{3\pi x}{L}\right] \\ -\dfrac{\pi^2}{L^2}(m_f U^2-k_P)\left[a_1\sin\dfrac{\pi x}{L}+9a_3\sin\dfrac{3\pi x}{L}\right]+ \\ \dfrac{\pi}{L}(2m_f U)\omega_j\left[\begin{array}{l} -2a_2\left(\dfrac{-4}{3\pi}\sin\dfrac{\pi x}{L}+\dfrac{12}{5\pi}\sin\dfrac{3\pi x}{L}\right) \\ -4a_4\left(\dfrac{-4}{15\pi}\sin\dfrac{\pi x}{L}-\dfrac{12}{7\pi}\sin\dfrac{3\pi x}{L}\right)\end{array}\right]+ \\ k_W\left[\begin{array}{l} a_1\sin\dfrac{\pi x}{L} \\ +a_3\sin\dfrac{3\pi x}{L}\end{array}\right]-m_c\left(e_0 a\right)^2\dfrac{\pi^2}{L^2}\omega_j^2\left[\begin{array}{l} a_1\sin\dfrac{\pi x}{L} \\ +9a_3\sin\dfrac{3\pi x}{L}\end{array}\right]- \\ M\omega_j^2\left[a_1\sin\dfrac{\pi x}{L}+a_3\sin\dfrac{3\pi x}{L}\right]\end{array}\right\}\sin\omega_j t=0 \tag{6.4}$$

and the equation containing the coefficients of $\cos\omega_j t$ is:

$$\left\{\begin{array}{l} EI\dfrac{\pi^4}{L^4}\left[16a_2\sin\dfrac{2\pi x}{L}+256a_4\sin\dfrac{4\pi x}{L}\right] \\ -\dfrac{\pi^2}{L^2}(m_fU^2-k_P)\left[4a_2\sin\dfrac{2\pi x}{L}+16a_4\sin\dfrac{4\pi x}{L}\right]+ \\ \dfrac{\pi}{L}(2m_fU)\omega_j\left[\begin{array}{l} a_1\left(\dfrac{8}{3\pi}\sin\dfrac{2\pi x}{L}+\dfrac{16}{15\pi}\sin\dfrac{4\pi x}{L}\right) \\ +3a_3\left(\dfrac{-8}{5\pi}\sin\dfrac{2\pi x}{L}-\dfrac{16}{7\pi}\sin\dfrac{4\pi x}{L}\right)\end{array}\right]+ \\ k_W\left[a_2\sin\dfrac{2\pi x}{L}+a_4\sin\dfrac{4\pi x}{L}\right] \\ -m_c\left(e_0a\right)^2\dfrac{\pi^2}{L^2}\omega_j^2\left[4a_2\sin\dfrac{2\pi x}{L}+16a_4\sin\dfrac{4\pi x}{L}\right]- \\ M\omega_j^2\left[a_2\sin\dfrac{2\pi x}{L}+a_4\sin\dfrac{4\pi x}{L}\right] \end{array}\right\}\cos\omega_j t=0 \qquad (6.5)$$

Following the steps indicated in Section 3.2.1, we obtain the following two systems of equation

$$a_n\left\{EI\left(\frac{n\pi}{L}\right)^4-(m_fU^2-k_P)\left(\frac{n\pi}{L}\right)^2+k_W-m_c\left(e_0a\right)^2\omega_j^2\left(\frac{n\pi}{L}\right)^2-M\omega_j^2\right\}$$

$$=-\frac{8m_fU\omega_j}{L}\sum_{r=2,4,6,\ldots}a_r\frac{rn}{\left[r^2-n^2\right]}\ ;\ n=1,3,5,\ldots \qquad (6.6)$$

and

$$a_n\left\{EI\left(\frac{n\pi}{L}\right)^4-(m_fU^2-k_P)\left(\frac{n\pi}{L}\right)^2+k_W-m_c\left(e_0a\right)^2\omega_j^2\left(\frac{n\pi}{L}\right)^2-M\omega_j^2\right\}$$
$$=+\frac{8m_fU\omega_j}{L}\sum_{r=1,3,5,\ldots}a_r\frac{rn}{\left[r^2-n^2\right]}\ ;\ n=2,4,6,\ldots \tag{6.7}$$

Expressing the above equations in a matrix form,

$$\left[\mathbf{K}-\omega_j^2\mathbf{MI}\right]\{\mathbf{a}\}=\mathbf{0} \tag{6.8}$$

where, **K** is the stiffness matrix, **M** is the mass matrix and **I** is the identity matrix. The elements of the stiffness matrix have been elaborated earlier in Equation (3.25). Setting the determinant of the above equation to zero and retaining only the first two terms, as explained previously, we obtain,

$$\begin{vmatrix}\left\{EI\left(\frac{\pi}{L}\right)^4-(m_fU^2-k_P)\left(\frac{\pi}{L}\right)^2\right. & \left\{\frac{16m_fU\omega_j}{3L}\right\} \\ \left.+k_W-m_c\left(e_0a\right)^2\omega_j^2\left(\frac{\pi}{L}\right)^2-M\omega_j^2\right\} & \\ \left\{\frac{16m_fU\omega_j}{3L}\right\} & \left\{16EI\left(\frac{\pi}{L}\right)^4-4(m_fU^2-k_P)\left(\frac{\pi}{L}\right)^2\right. \\ & \left.+k_W-4m_c\left(e_0a\right)^2\omega_j^2\left(\frac{\pi}{L}\right)^2-M\omega_j^2\right\}\end{vmatrix}=0 \tag{6.9}$$

Expanding the determinant in the above equation, we obtain,

$$\left[M^2 + 5Mm_c\left(e_0 a\right)^2\left(\frac{\pi}{L}\right)^2 + 4m_c^2\left(e_0 a\right)^4\left(\frac{\pi}{L}\right)^4 \right]\omega_j^4 -$$

$$\left[\begin{array}{l} 20EIm_c\left(e_0 a\right)^2\left(\frac{\pi}{L}\right)^6 + 17EIM\left(\frac{\pi}{L}\right)^4 - \\ \\ 8(m_f U^2 - k_P)m_c\left(e_0 a\right)^2\left(\frac{\pi}{L}\right)^4 - \\ \\ 5M(m_f U^2 - k_P)\left(\frac{\pi}{L}\right)^2 + 5k_W m_c\left(e_0 a\right)^2\left(\frac{\pi}{L}\right)^2 \\ \\ +2k_W M + \frac{256}{9L^2}\left(m_f U\right)^2 \end{array}\right]\omega_j^2 +$$

$$\left[\begin{array}{l} 16\left(\frac{EI\pi^4}{L^4}\right)^2 - 20EI(m_f U^2 - k_P)\left(\frac{\pi}{L}\right)^6 + \\ \\ 4(m_f U^2 - k_P)^2\left(\frac{\pi}{L}\right)^4 - 5k_W(m_f U^2 - k_P)\left(\frac{\pi}{L}\right)^2 + \\ \\ 17k_W EI\left(\frac{\pi}{L}\right)^4 + k_W^2 \end{array}\right] = 0 \qquad (6.10)$$

The above equation is similar to that obtained for a pipe conveying fluid, with the exception that it has a number of non-local terms embedded.

We now define another non-dimensional parameter for the non-local variables as,

$$e_n = \frac{e_0 a}{L} \quad \text{; which is the non-local parameter,} \qquad (6.11)$$

and using the previously defined non-dimensional parameters in Equations (3.29) and (4.4) along with Equation (6.11) in Equation (6.10), we obtain,

$$\Omega_j^4 - \frac{\left[\begin{array}{l}\left(1-\beta\right)e_n^2\pi^2\left\{20\pi^4 - 8\left(V^2-\gamma_P\right)\pi^2 + 5\gamma_W\right\} + \\ \\ 17\pi^4 - 5\left(V^2-\gamma_P\right)\pi^2 + 2\gamma_W + \frac{256}{9}\beta V^2\end{array}\right]}{\left[\left(1-\beta\right)e_n^2\pi^2\left\{5+4\left(1-\beta\right)e_n^2\pi^2\right\}+1\right]}\Omega_j^2 + \frac{\left[\begin{array}{l}16\pi^8 - 20\left(V^2-\gamma_P\right)\pi^6 + 4\left(V^2-\gamma_P\right)^2\pi^4 - \\ \\ 5\gamma_W\left(V^2-\gamma_P\right)\pi^2 + 17\gamma_W\pi^4 + \gamma_W^2\end{array}\right]}{\left[\left(1-\beta\right)e_n^2\pi^2\left\{5+4\left(1-\beta\right)e_n^2\pi^2\right\}+1\right]} = 0 \tag{6.12}$$

The above equation is the non-dimensional frequency equation for a fluid conveying carbon nanotube embedded in a Pasternak type elastic medium, with pinned-pinned end conditions and considering non-local effects also. It is seen that the above equation is quadratic in Ω_j^2, which can be solved in the standard way to obtain values of Ω_j, as its roots. The lowest root of the equation gives the fundamental frequency parameter that we seek.

6.2.2 Clamped-pinned and clamped-clamped end conditions

We seek a solution to Equation (6.1) in the form

$$w(x,t) = \Re\left[\varphi(x)e^{i\omega t}\right] \tag{6.13}$$

Substituting the above equation in the governing differential equation, we obtain

$$EI\frac{\partial^4\varphi(x)}{\partial x^4}-M\omega^2\varphi(x)+\left(m_fU^2-k_P\right)\frac{\partial^2\varphi(x)}{\partial x^2}+2m_fUi\omega\frac{\partial\varphi(x)}{\partial x} + k_W\varphi(x)+m_c(e_0a)^2\omega^2\frac{\partial^2\varphi(x)}{\partial x^2}=0 \tag{6.14}$$

Following the procedure detailed in Section 3.2.2, substitution of the beam eigen functions $\psi_r(\xi)$ in Equation (3.40) will result in the following equation.

$$\int_0^1 \mathrm{L}\left(\sum_{r=1}^{N}a_r\psi_r(\xi)\right)\psi_s(\xi)d\xi=\sum_{r=1}^{N}a_r\left(\begin{array}{l}\frac{EI}{L^4}\lambda_r^4\sum_{s=1}^{N}\left\{\int_0^1\psi_r\psi_s d\xi\right\}+\\ \frac{\left(m_fU^2-k_P\right)}{L^2}\sum_{s=1}^{N}\left\{\int_0^1\frac{\partial^2\psi_r}{\partial\xi^2}\psi_s d\xi\right\}+\\ \frac{2m_fUi\omega}{L}\sum_{s=1}^{N}\left\{\int_0^1\frac{\partial\psi_r}{\partial\xi}\psi_s d\xi\right\}+\\ \left(k_W-M\omega^2\right)\sum_{s=1}^{N}\left\{\int_0^1\psi_r\psi_s d\xi\right\}\end{array}\right)=0 \tag{6.15}$$

Using the orthagonality relations of the eigenfunctions, we obtain the following set if algebraic equations,

$$a_r\left(\begin{array}{l}\dfrac{EI}{L^4}\lambda_r^4+\dfrac{\left(m_f U^2-k_P\right)}{L^2}\sum_{s=1}^{N}\{c_{rs}\}+\\ \dfrac{2m_f Ui\omega}{L}\sum_{s=1}^{N}\{b_{rs}\}+\ \dfrac{m_c(e_0a)^2\omega^2}{L^2}\sum_{s=1}^{N}\{c_{rs}\}+\\ \left(k_W-M\omega^2\right)\end{array}\right)=0\ \ ;\ r=1,2,3,....,N \qquad (6.16)$$

where the constants b_{rs} and c_{rs} are given in Tables 3.1 and 3.2. Non-dimensionalizing the above equation using the non-dimensional parameters defined earlier, and retaining only the first two terms for analysis, we obtain the following matrix equation:

$$\left[\begin{array}{ll}\left\{\begin{array}{l}\lambda_1^4+\gamma_W-\Omega_j^2+\left(V^2-\gamma_P\right)c_{11}+\\ 2i\beta^{\frac{1}{2}}\Omega_j Vb_{11}+\left(1-\beta\right)e_n^2\Omega_j^2c_{11}\end{array}\right\} & \left\{\begin{array}{l}\left(V^2-\gamma_P\right)c_{12}+2i\beta^{\frac{1}{2}}\Omega_j Vb_{12}\\ +\left(1-\beta\right)e_n^2\Omega_j^2c_{12}\end{array}\right\}\\ \left\{\begin{array}{l}\left(V^2-\gamma_P\right)c_{21}+2i\beta^{\frac{1}{2}}\Omega_j Vb_{21}\\ +\left(1-\beta\right)e_n^2\Omega_j^2c_{21}\end{array}\right\} & \left\{\begin{array}{l}\lambda_2^4+\gamma_W-\Omega_j^2+\left(V^2-\gamma_P\right)c_{22}+\\ 2i\beta^{\frac{1}{2}}\Omega_j Vb_{22}+\left(1-\beta\right)e_n^2\Omega_j^2c_{22}\end{array}\right\}\end{array}\right]\left\{\begin{array}{l}a_1\\ a_2\end{array}\right\}=0 \qquad (6.17)$$

Setting the determinant of the coefficient matrix in the above equation to zero, giving

$$\begin{vmatrix} \left\{ \begin{array}{l} \lambda_1^4 + \gamma_W - \Omega_j^2 + \left(V^2 - \gamma_P\right) c_{11} + \\ \\ 2i\beta^{\frac{1}{2}} \Omega_j V b_{11} + \left(1-\beta\right) e_n^2 \Omega_j^2 c_{11} \end{array} \right\} & \left\{ \begin{array}{l} \left(V^2 - \gamma_P\right) c_{12} + 2i\beta^{\frac{1}{2}} \Omega_j V b_{12} \\ \\ + \left(1-\beta\right) e_n^2 \Omega_j^2 c_{12} \end{array} \right\} \\ \left\{ \begin{array}{l} \left(V^2 - \gamma_P\right) c_{21} + 2i\beta^{\frac{1}{2}} \Omega_j V b_{21} \\ \\ + \left(1-\beta\right) e_n^2 \Omega_j^2 c_{21} \end{array} \right\} & \left\{ \begin{array}{l} \lambda_2^4 + \gamma_W - \Omega_j^2 + \left(V^2 - \gamma_P\right) c_{22} + \\ \\ 2i\beta^{\frac{1}{2}} \Omega_j V b_{22} + \left(1-\beta\right) e_n^2 \Omega_j^2 c_{22} \end{array} \right\} \end{vmatrix} = 0 \qquad (6.18)$$

Expanding the determinant in Equation (6.18), we have for the clamped-pinned boundary condition,

$$\Omega_j^4 \left[1 - \left(1-\beta\right) e_n^2 c_{11} - \left(1-\beta\right) e_n^2 c_{22} + \left(1-\beta\right)^2 e_n^4 c_{11} c_{22} - \left(1-\beta\right)^2 e_n^4 c_{12} c_{21} \right] +$$

$$\Omega_j^2 \left[\begin{array}{l} \lambda_1^4 \left(1-\beta\right) e_n^2 c_{22} + \lambda_2^4 \left(1-\beta\right) e_n^2 c_{11} - \lambda_1^4 - \lambda_2^4 - 2\gamma_W + \\ \\ \gamma_W \left(1-\beta\right) e_n^2 c_{11} + \gamma_W \left(1-\beta\right) e_n^2 c_{22} - \left(V^2 - \gamma_P\right) c_{11} - \\ \\ \left(V^2 - \gamma_P\right) c_{22} + 2\left(V^2 - \gamma_P\right)\left(1-\beta\right) e_n^2 c_{11} c_{22} - \\ \\ 2\left(V^2 - \gamma_P\right)\left(1-\beta\right) e_n^2 c_{12} c_{21} + 4\beta V^2 b_{12} b_{21} \end{array} \right] +$$

$$\left[\begin{array}{l} \lambda_1^4 \lambda_2^4 + \lambda_1^4 \left(V^2 - \gamma_P\right) c_{22} + \lambda_2^4 \left(V^2 - \gamma_P\right) c_{11} + \\ \\ \gamma_W \left(V^2 - \gamma_P\right) c_{11} + \gamma_W \left(V^2 - \gamma_P\right) c_{22} + \left(V^2 - \gamma_P\right)^2 c_{11} c_{22} - \\ \\ \left(V^2 - \gamma_P\right)^2 c_{12} c_{21} + \gamma_W \left(\lambda_1^4 + \lambda_2^4\right) + \gamma_W^2 \end{array} \right] = 0 \qquad (6.19)$$

The lowest root of the above equation gives the fundamental frequency for the clamped-pinned carbon nanotube conveying fluid and embedded in a Pasternak type elastic medium.

For the clamped-clamped end conditions, we evaluate the integrals b_{rs} and c_{rs}, for r,s = 1,2, and after substitution, we have:

$$\Omega_j^4\left[1-(1-\beta)e_n^2c_{11}-(1-\beta)e_n^2c_{22}+(1-\beta)^2e_n^4c_{11}c_{22}\right]+$$

$$\Omega_j^2\left[\begin{array}{l}\lambda_1^4(1-\beta)e_n^2c_{22}+\lambda_2^4(1-\beta)e_n^2c_{11}-\lambda_1^4-\lambda_2^4-2\gamma_W+\\ \gamma_W(1-\beta)e_n^2c_{11}+\gamma_W(1-\beta)e_n^2c_{22}-(V^2-\gamma_P)c_{11}-\\ (V^2-\gamma_P)c_{22}+2(V^2-\gamma_P)(1-\beta)e_n^2c_{11}c_{22}+4\beta V^2b_{12}b_{21}\end{array}\right]+$$

$$\left[\begin{array}{l}\lambda_1^4\lambda_2^4+\lambda_1^4(V^2-\gamma_P)c_{22}+\lambda_2^4(V^2-\gamma_P)c_{11}+\\ \gamma_W(V^2-\gamma_P)c_{11}+\gamma_W(V^2-\gamma_P)c_{22}+(V^2-\gamma_P)^2c_{11}c_{22}+\\ \gamma_W(\lambda_1^4+\lambda_2^4)+\gamma_W^2\end{array}\right]=0 \qquad (6.20)$$

Again, the lowest root of the above equation gives the fundamental natural frequency of a clamped-clamped carbon nanotube conveying fluid and embedded in a Pasternak type elastic medium.

6.3 Numerical Results and Discussion

This section presents detailed numerical results for carbon nanotubes and pipes in the form of tables and graphs for all the three ideal boundary conditions. Comparison of the results obtained here with those published by earlier researchers is done for the Winkler type elastic medium, for the clamped-clamped boundary condition, and hence, these results are presented first. For the other two boundary conditions, no earlier published results are available to the best of the author's knowledge. It may be mentioned that the analysis of carbon nanotubes conveying fluid embedded in a Pasternak elastic medium is a new contribution and hence comparison is not possible.

6.3.1 CNT: Clamped-clamped End condition

We solve Equation (6.20) for Ω_j, to obtain the natural frequencies for the clamped-clamped case. The lowest root of the equation is the fundamental frequency parameter. The method adopted for computing the natural frequencies is the same as elaborated in Section 4.3.

The results are presented in a similar fashion as pipes conveying fluid, in Chapter 4, to enable quick comparisons. Tables 6.1, 6.2 and 6.3 show the numerical results obtained for three values of the mass ratio parameter, β, respectively. Each table contains values of the fundamental frequency parameter for different values of the non-local parameter, e_n, for varying values of both the stiffness parameters, from 1E-02 to 5E+01. These values have been chosen because the polymer matrix or the human tissues in which the carbon nanotubes are embedded are not expected to have higher

stiffness values. Moreover, results are available in the literature for a Winkler type elastic medium for these values, making comparisons useful. From the data obtained, the following trend is observed for the clamped-clamped boundary condition:

- The fundamental frequency decreases for increasing values of the non-local parameter.

- The fundamental frequency decreases for increasing values of the mass ratio parameter.

- The fundamental frequency increases for increasing values of both the stiffness parameters.

The behaviour can be more readily seen in Figs. 6.1 through 6.6. In Figs. 6.1 and 6.2, the dynamic behaviour of the carbon nanotube is shown graphically. It can be seen that higher values of the non-local parameter, e_n, have the influence of decreasing the fundamental frequency of the system. Also, it can be seen that the Pasternak stiffness parameter, γ_P, increases the fundamental frequency of the carbon nanotube. The trend shown is for particular values of the Winkler stiffness parameter, γ_W, and the mass ratio parameter, β. Even for other values of these two parameters, the trend is the same.

Fig. 6.3 shows the effect of varying only the Winkler stiffness parameter on the fundamental frequency parameter, all other parameters being maintained constant. It can be seen that higher the value of the Winkler parameter, higher is the fundamental frequency.

Table 6.1 Clamped-clamped carbon nanotube: Values of fundamental frequency parameter, Ω_1, for different values of the non-local parameter, e_n, and varying values of flow velocity parameter, V, Winkler stiffness parameter, γ_W, and Pasternak stiffness parameter, γ_P, for the value of the mass ratio, $\beta = 0.12$.

$e_n \rightarrow$		0.05		0.1	
γ_W	γ_P	V	Ω_1	V	Ω_1
2.00E-02	2.00E-02	0.2127	22.0693	0.2127	21.2455
		1.9141	21.0016	1.9141	20.2205
		4.0409	16.8294	4.0409	16.2142
		6.3804	0	6.3804	0
	2.00E+01	0.2597	26.946	0.2597	25.9402
		2.3371	25.6231	2.3371	24.6703
		4.9339	20.456	4.9339	19.7106
		7.7903	0	7.7903	0
	5.00E+01	0.3174	32.9392	0.3174	31.7096
		2.8569	31.2981	2.8569	30.1342
		6.0313	24.8841	6.0313	23.9789
		9.5231	0	9.5231	0

Table 6.1 Continued

$e_n \rightarrow$		0.05		0.1	
γ_W	γ_P	V	Ω_1	V	Ω_1
2.00E+01	2.00E-02	0.2169	22.5052	0.2169	21.6651
		1.9519	21.4137	1.9519	20.6173
		4.1207	17.1493	4.1207	16.5228
		6.5064	0	6.5064	0
	2.00E+01	0.2631	27.3041	0.2631	26.2849
		2.3682	25.9609	2.3682	24.9955
		4.9995	20.7143	4.9995	19.9597
		7.8939	0	7.8939	0
	5.00E+01	0.3203	33.2328	0.3203	31.9923
		2.8824	31.5744	2.8824	30.4001
		6.0851	25.0916	6.0851	24.1789
		9.608	0	9.608	0
5.00E+01	2.00E-02	0.223	23.1443	0.223	22.2803
		2.0074	22.0176	2.0074	21.1988
		4.2377	17.6167	4.2377	16.9737
		6.6912	0	6.6912	0
	2.00E+01	0.2682	27.8332	0.2682	26.7943
		2.4141	26.4597	2.4141	25.4758
		5.0963	21.0945	5.0963	20.3264
		8.0468	0	8.0468	0
	5.00E+01	0.3245	33.6688	0.3245	32.412
		2.9202	31.9845	2.9202	30.7949
		6.1649	25.3987	6.1649	24.475
		9.7341	0	9.7341	0

Table 6.2 Clamped-clamped carbon nanotube: Values of fundamental frequency parameter, Ω_1, for different values of the non-local parameter, e_n, and varying values of flow velocity parameter, V, Winkler stiffness parameter, γ_W, and Pasternak stiffness parameter, γ_P, for the value of the mass ratio, $\beta = 0.3$.

$e_n \rightarrow$		0.05		0.1	
γ_W	γ_P	V	Ω_1	V	Ω_1
2.00E-02	2.00E-02	0.2127	22.1278	0.2127	21.4599
		1.9141	20.9635	1.9141	20.3363
		4.0409	16.5063	4.0409	16.0332
		6.3804	0	6.3804	0
	2.00E+01	0.2597	27.0171	0.2597	26.2016
		2.3371	25.5481	2.3371	24.7842
		4.9339	19.9426	4.9339	19.3753
		7.7903	0	7.7903	0
	5.00E+01	0.3174	33.0257	0.3174	32.0287
		2.8569	31.1716	2.8569	30.2395
		6.0313	24.1074	6.0313	23.425
		9.5231	0	9.5231	0

Table 6.2 Continued

$e_n \rightarrow$		0.05		0.1	
γ_W	γ_P	V	Ω_1	V	Ω_1
2.00E+01	2.00E-02	0.2169	22.5648	0.2169	21.8837
		1.9519	21.3709	1.9519	20.7316
		4.1207	16.8034	4.1207	16.3225
		6.5064	0	6.5064	0
	2.00E+01	0.2631	27.3761	0.2631	26.5498
		2.3682	25.8809	2.3682	25.107
		4.9995	20.1769	4.9995	19.6035
		7.8939	0	7.8939	0
	5.00E+01	0.3203	33.32	0.3203	32.3142
		2.8824	31.4428	2.8824	30.5025
		6.0851	24.291	6.0851	23.6036
		9.608	0	9.608	0
5.00E+01	2.00E-02	0.223	23.2055	0.223	22.505
		2.0074	21.9674	2.0074	21.3104
		4.2377	17.2354	4.2377	16.7432
		6.6912	0	6.6912	0
	2.00E+01	0.2682	27.9065	0.2682	27.0641
		2.4141	26.372	2.4141	25.5835
		5.0963	20.5205	5.0963	19.938
		8.0468	0	8.0468	0
	5.00E+01	0.3245	33.7571	0.3245	32.7381
		2.9202	31.8452	2.9202	30.8928
		6.1649	24.5616	6.1649	23.8669
		9.7341	0	9.7341	0

Table 6.3 Clamped-clamped carbon nanotube: Values of fundamental frequency parameter, Ω_1, for different values of the non-local parameter, e_n, and varying values of flow velocity parameter, V, Winkler stiffness parameter, γ_W, and Pasternak stiffness parameter, γ_P, for the value of the mass ratio, $\beta = 0.5$.

$e_n \rightarrow$		0.05		0.1	
γ_W	γ_P	V	Ω_1	V	Ω_1
2.00E-02	2.00E-02	0.2127	22.1934	0.2127	21.7059
		1.9141	20.9221	1.9141	20.4693
		4.0409	16.1726	4.0409	15.8465
		6.3804	0	6.3804	0
	2.00E+01	0.2597	27.0968	0.2597	26.5015
		2.3371	25.467	2.3371	24.9164
		4.9339	19.4248	4.9339	19.0379
		7.7903	0	7.7903	0
	5.00E+01	0.3174	33.1226	0.3174	32.3949
		2.8569	31.0357	2.8569	30.3646
		6.0313	23.3438	6.0313	22.8827
		9.5231	0	9.5231	0

Table 6.3 Continued

$e_n \rightarrow$		0.05		0.1	
γ_W	γ_P	V	Ω_1	V	Ω_1
2.00E+01	2.00E-02	0.2169	22.6316	0.2169	22.1345
		1.9519	21.3244	1.9519	20.863
		4.1207	16.4475	4.1207	16.1167
		6.5064	0	6.5064	0
	2.00E+01	0.2631	27.4568	0.2631	26.8536
		2.3682	25.7944	2.3682	25.2368
		4.9995	19.6369	4.9995	19.2463
		7.8939	0	7.8939	0
	5.00E+01	0.3203	33.4177	0.3203	32.6836
		2.8824	31.3015	2.8824	30.6246
		6.0851	23.5061	6.0851	23.0421
		9.608	0	9.608	0
5.00E+01	2.00E-02	0.223	23.2741	0.223	22.7628
		2.0074	21.913	2.0074	21.4391
		4.2377	16.8455	4.2377	16.5078
		6.6912	0	6.6912	0
	2.00E+01	0.2682	27.9887	0.2682	27.3738
		2.4141	26.2773	2.4141	25.7092
		5.0963	19.9466	5.0963	19.5506
		8.0468	0	8.0468	0
	5.00E+01	0.3245	33.856	0.3245	33.1122
		2.9202	31.6958	2.9202	31.0103
		6.1649	23.7446	6.1649	23.2763
		9.7341	0	9.7341	0

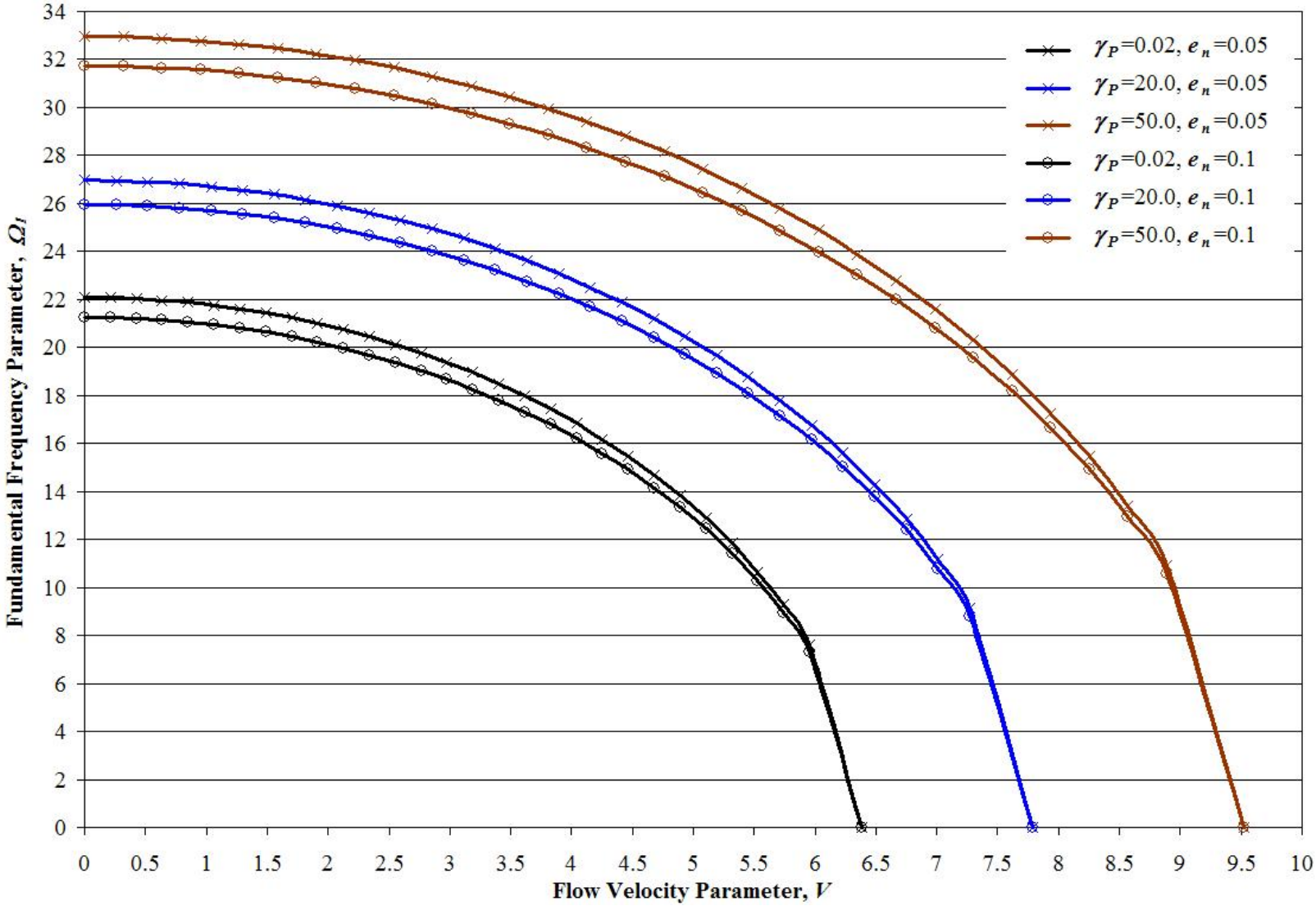

Figure 6.1 Clamped-clamped carbon nanotube: Variation of non-dimensional fundamental frequency parameter, Ω_1, with flow velocity parameter, V, for different values of the non-local parameter, e_n, and Pasternak stiffness parameter, γ_P, for the value of Winkler stiffness parameter, $\gamma_W = 0.02$, and mass ratio parameter, $\beta = 0.12$.

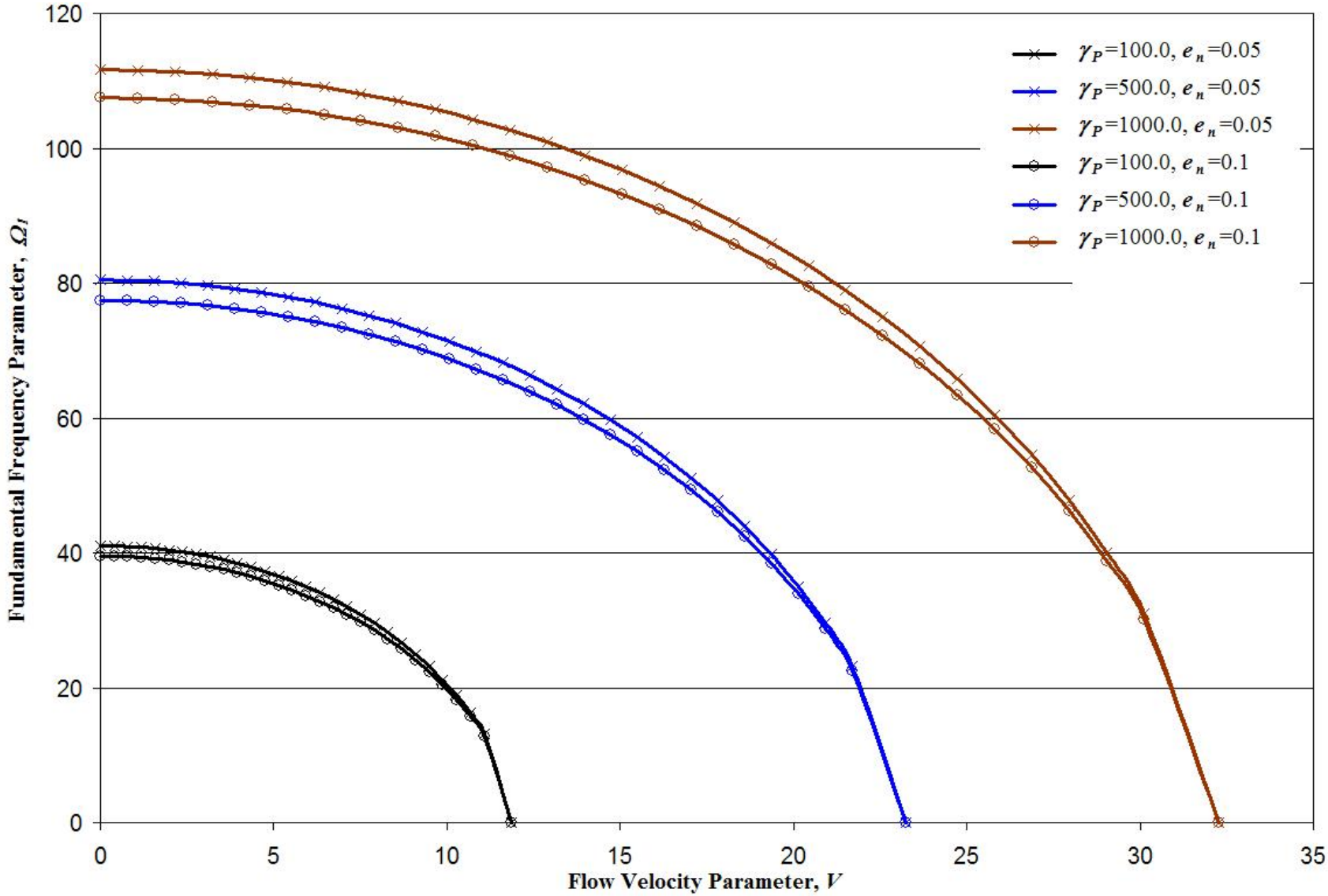

Figure 6.2 Clamped-clamped carbon nanotube: Variation of non-dimensional fundamental frequency parameter, Ω_1, with flow velocity parameter, V, for different values of the non-local parameter, e_n, and Pasternak stiffness parameter, γ_P, for the value of Winkler stiffness parameter, $\gamma_W = 0.02$, and mass ratio parameter, $\beta = 0.12$.

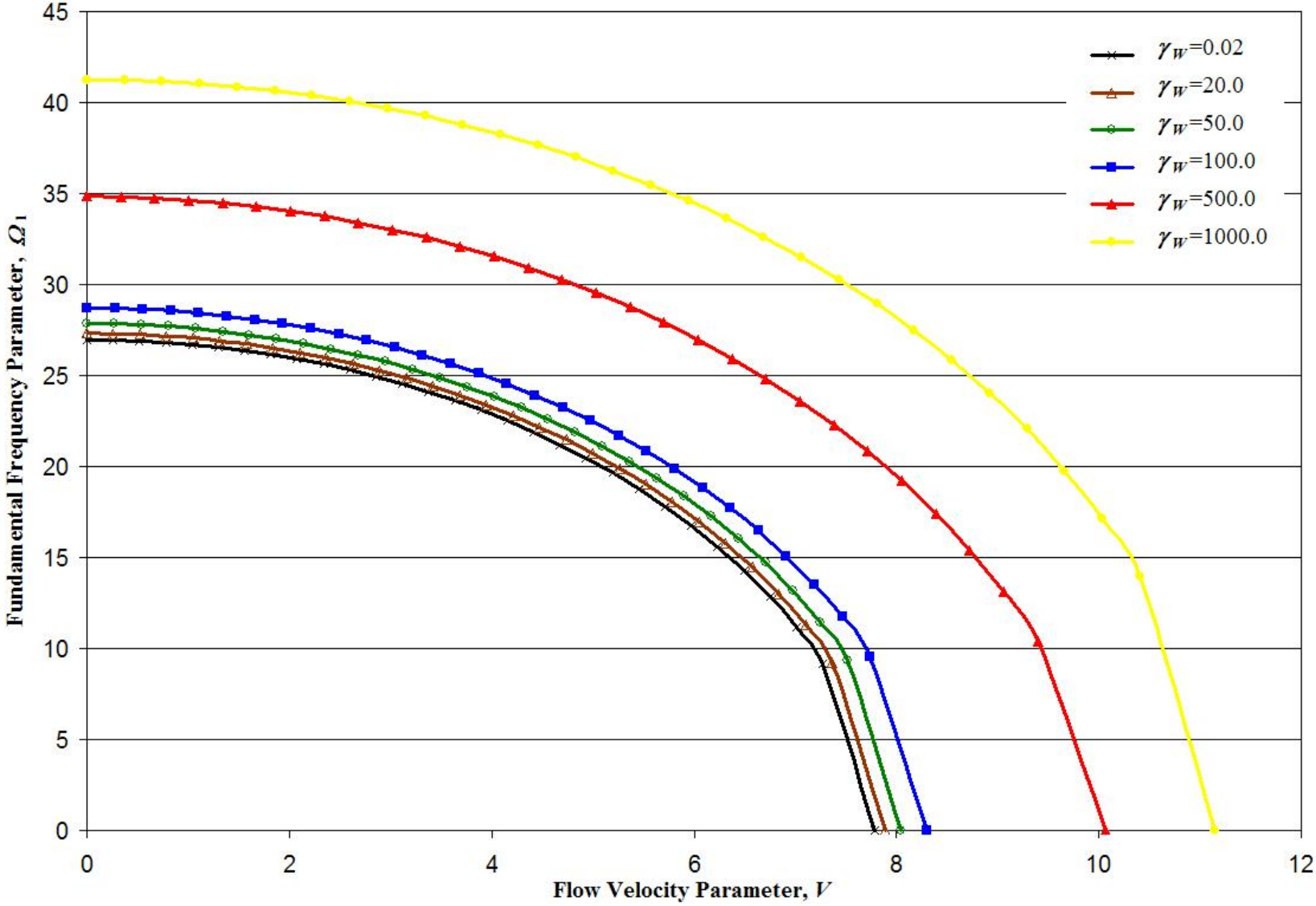

Figure 6.3 Clamped-clamped carbon nanotube: Variation of non-dimensional fundamental frequency parameter, Ω_1, with flow velocity parameter, V, for different values of the Winkler stiffness parameter, γ_W, and for the non-local parameter, e_n = 0.05, and Pasternak stiffness parameter, γ_P = 20.0, and mass ratio parameter, β = 0.12.

In Fig. 6.4, the mass ratio parameter has also been varied along with the Winkler parameter. It is shown that higher mass ratios tend to lower the fundamental frequencies, although, at the critical velocity, the frequency is zero irrespective of the mass ratio.

Fig. 6.5 plots the variation of the fundamental frequency parameter with the velocity parameter for varying values of the Pasternak stiffness parameter. It can be observed that the Pasternak parameter has a significant effect on the fundamental frequencies. Also shown in the figure is the effect of mass ratio parameter on the frequencies. A comparison of the effects of the Winkler stiffness parameter and the Pasternak stiffness parameter on the fundamental frequencies is shown in Fig. 6.6. It is clear from the curves that the Pasternak parameter has a much greater influence on the frequencies of a carbon nanotube than the Winkler parameter. The results shown in Figs. 6.3 to 6.6 are for the value of the non-local parameter e_n = 0.05. The trend is the same for other values of the non-local parameter.

It may be mentioned that results on the dynamic behaviour of carbon nanotubes has been reported earlier, see for example, Lee and Chang **[34, 35]**. Their results for the behaviour of carbon nanotubes embedded in a Winkler type elastic medium can be compared with the results obtained here. Fig. 6.7 shows the variation of the fundamental frequency parameter, Ω_1, with the velocity parameter, V, for three different values of the non-local parameter, e_n, with γ_W = 0.02, β = 0.12, and the Pasternak stiffness parameter, γ_P = 0. It can be seen that there is an exact match of the curves shown herein with those in Fig. 2. of reference **[35]**.

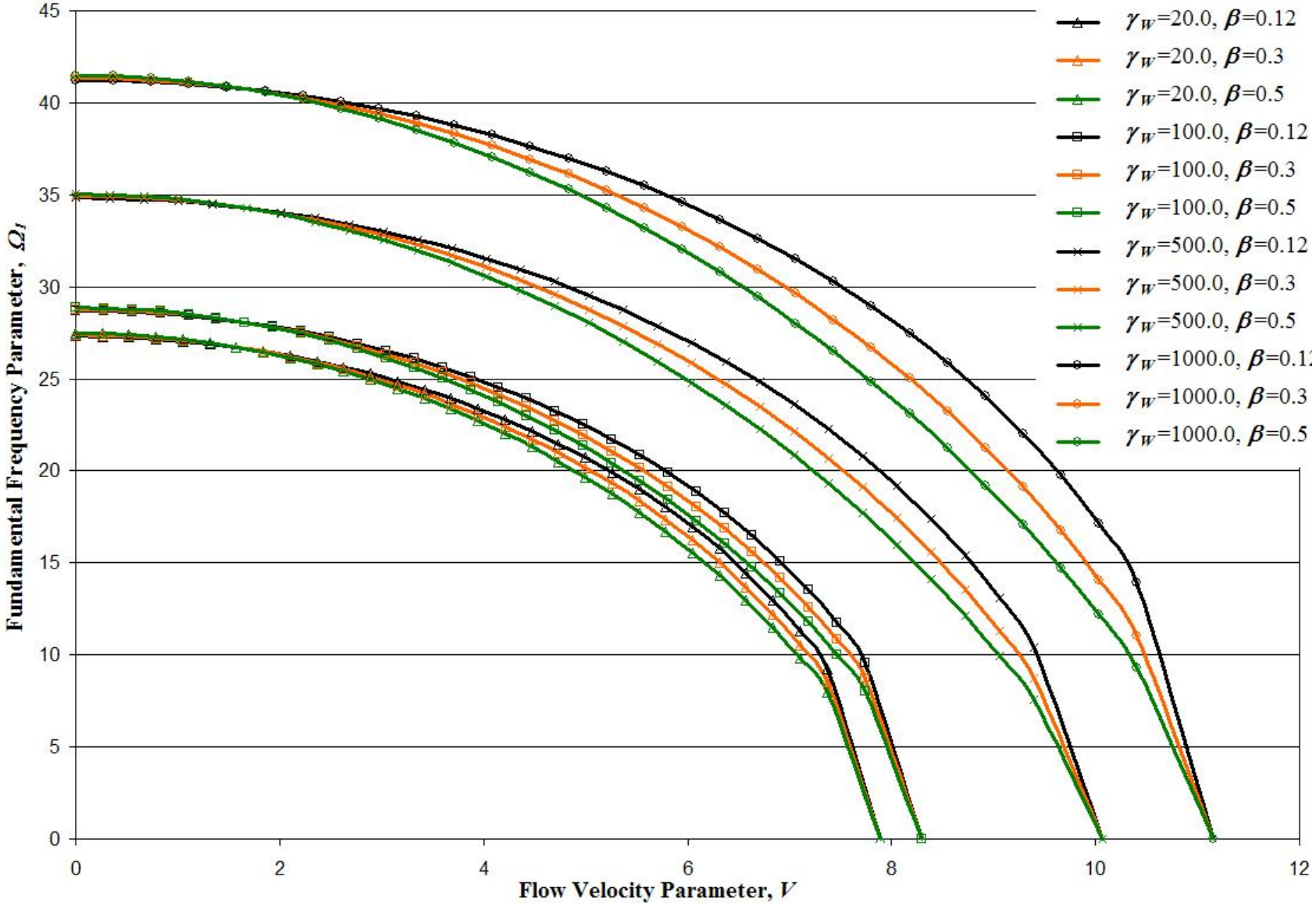

Figure 6.4 Clamped-clamped carbon nanotube: Variation of non-dimensional fundamental frequency parameter, Ω_1, with flow velocity parameter, V, for different values of the Winkler stiffness parameter, γ_W, and mass ratio parameter, β, and for the non-local parameter, e_n = 0.05, and Pasternak stiffness parameter, γ_P = 20.0.

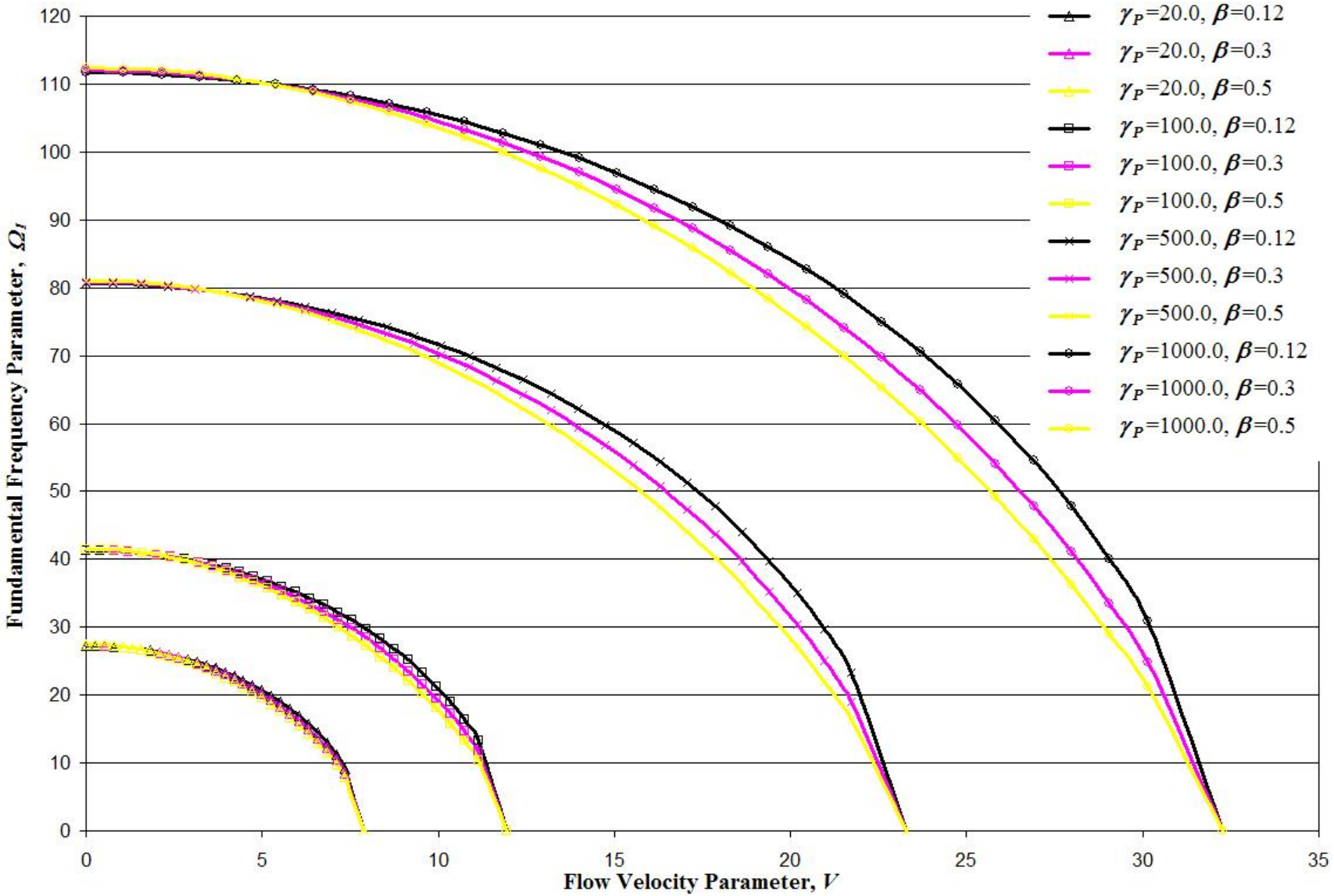

Figure 6.5 Clamped-clamped carbon nanotube: Variation of non-dimensional fundamental frequency parameter, Ω_1, with flow velocity parameter, V, for different values of the Pasternak stiffness parameter, γ_P, and mass ratio parameter, β, and for the non-local parameter, e_n = 0.05, and Winkler stiffness parameter, γ_W = 20.0.

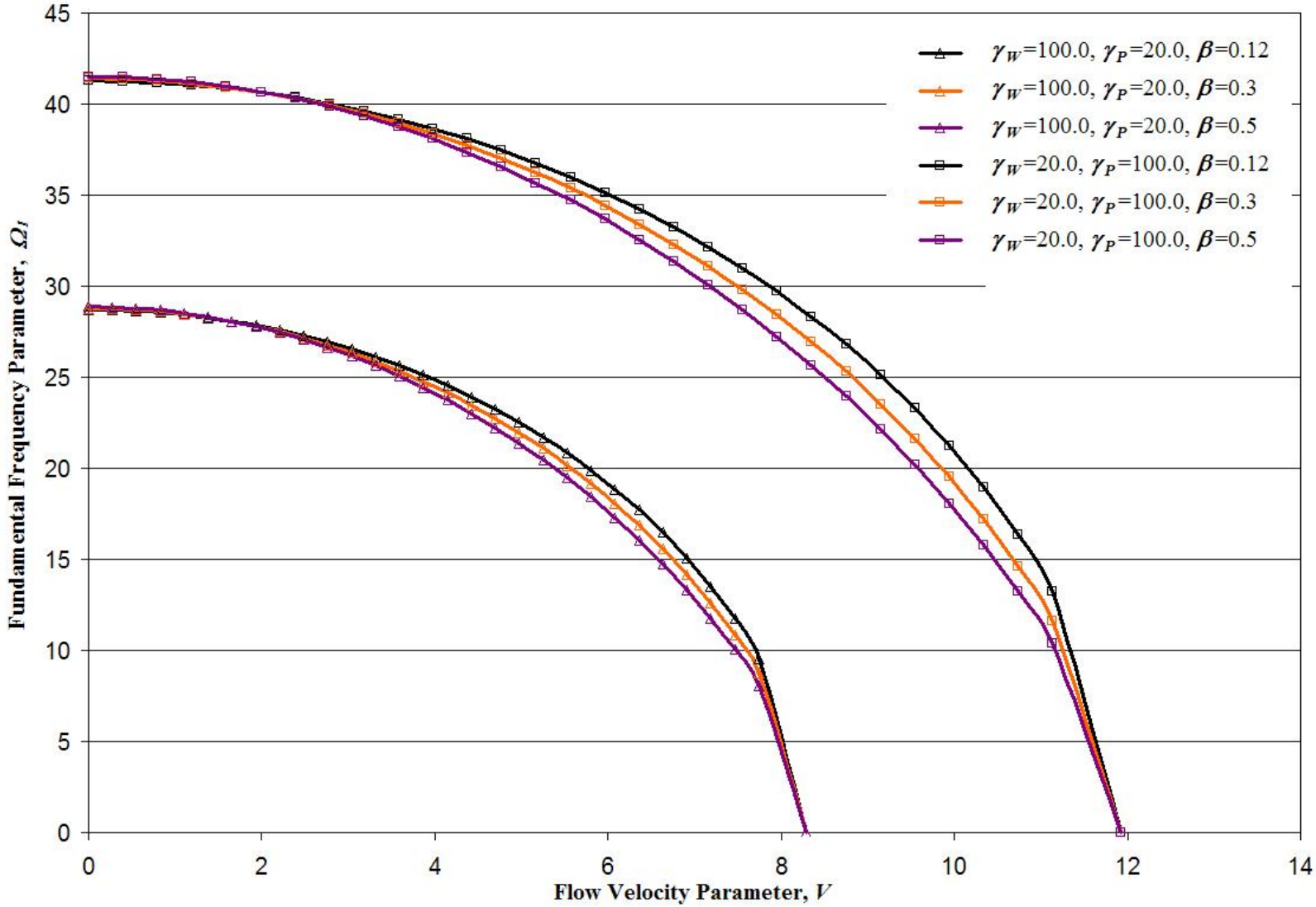

Figure 6.6 Clamped-clamped carbon nanotube: Comparison of the effects of the Winkler stiffness parameter, γ_W, and Pasternak stiffness parameter, γ_P, on the non-dimensional fundamental frequency parameter, Ω_1, for different values of the mass ratio parameter, β and for non-local parameter, $e_n = 0.05$.

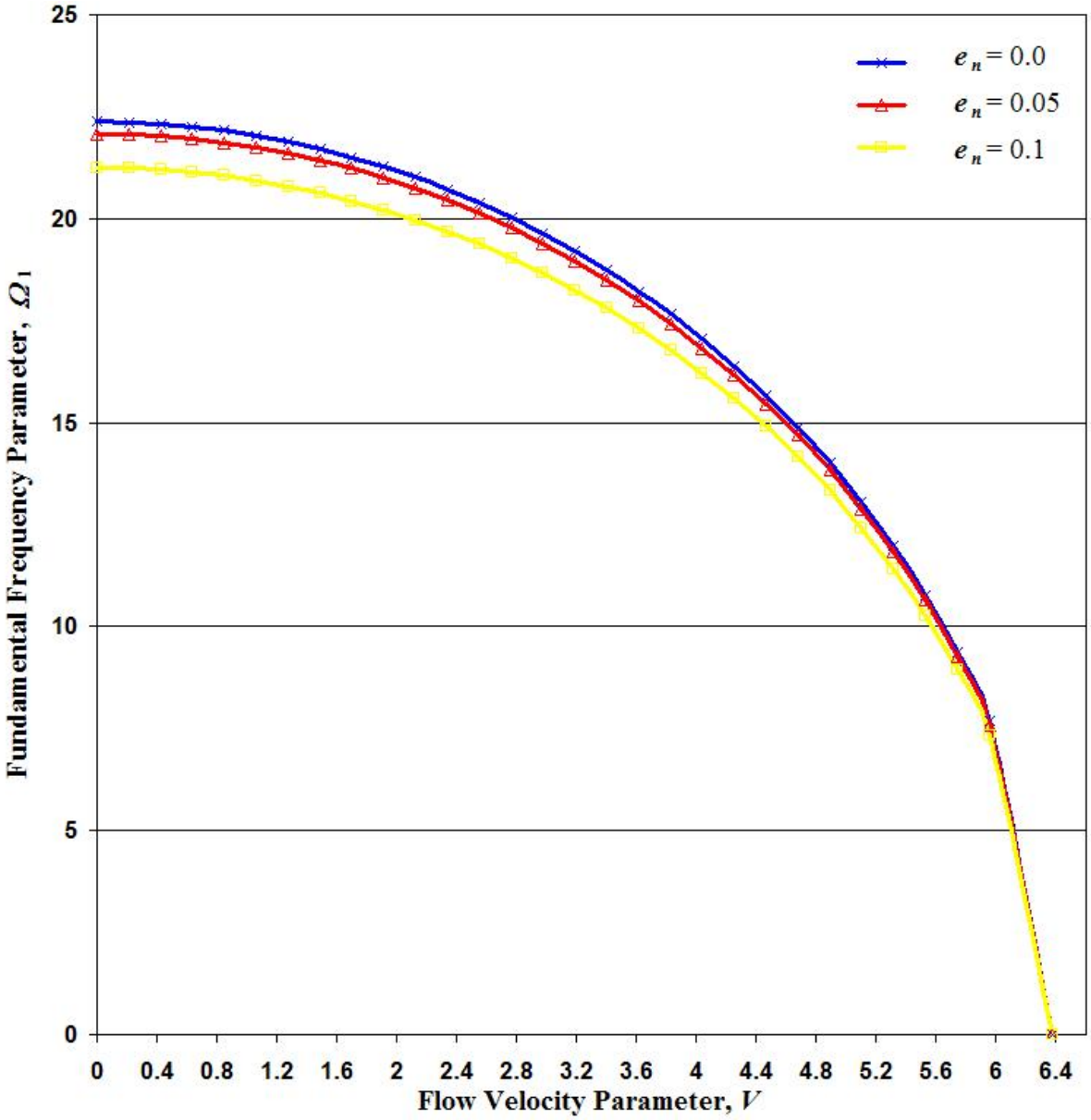

Figure 6.7 Clamped-clamped carbon nanotube: Non-dimensional fundamental frequency parameter, Ω_1, as a function of non-dimensional flow velocity parameter, V, for different non-local parameters, e_n , for the Winkler stiffness parameter, γ_W =0.02, the Pasternak stiffness parameter, γ_P = 0.0 and the mass ratio parameter, β =0.12. These curves match exactly with Fig. 2 of reference **[35]**.

Similarly, Fig. 6.8 shows the variation of Ω_1, with V for different values of γ_W, with e_n = 0.05 and β = 0.12. It is again seen that there is an exact match of the curves with those in Fig. 5 of reference **[35]**. This serves to validate the solution procedure adopted here. The Pasternak model of the embedding medium was not considered in their analysis.

6.3.2 CNT: Pinned-pinned End condition

Equation (6.12) is solved for Ω_j, to obtain the natural frequencies for the pinned-pinned case. The organization of data and figures is kept similar to that of the clamped-clamped end condition presented in the previous section to facilitate easy comparison of the differences in the results.

Tables 6.4, 6.5 and 6.6 present the numerical results for different values of the stiffness parameters and the non-local parameter, for three values of mass ratio, respectively. The data here too is restricted to values of the stiffness parameters between 0.02 and 50.0. Similar conclusions can be drawn as for the clamped-clamped case, except that the fundamental frequencies are significantly lower for the pinned-pinned boundary condition.

More comprehensive selection of data is made use of to develop the curves shown in Figures 6.9 to 6.14. It can be seen that the trend is similar to the clamped-clamped case, although the actual values are different.

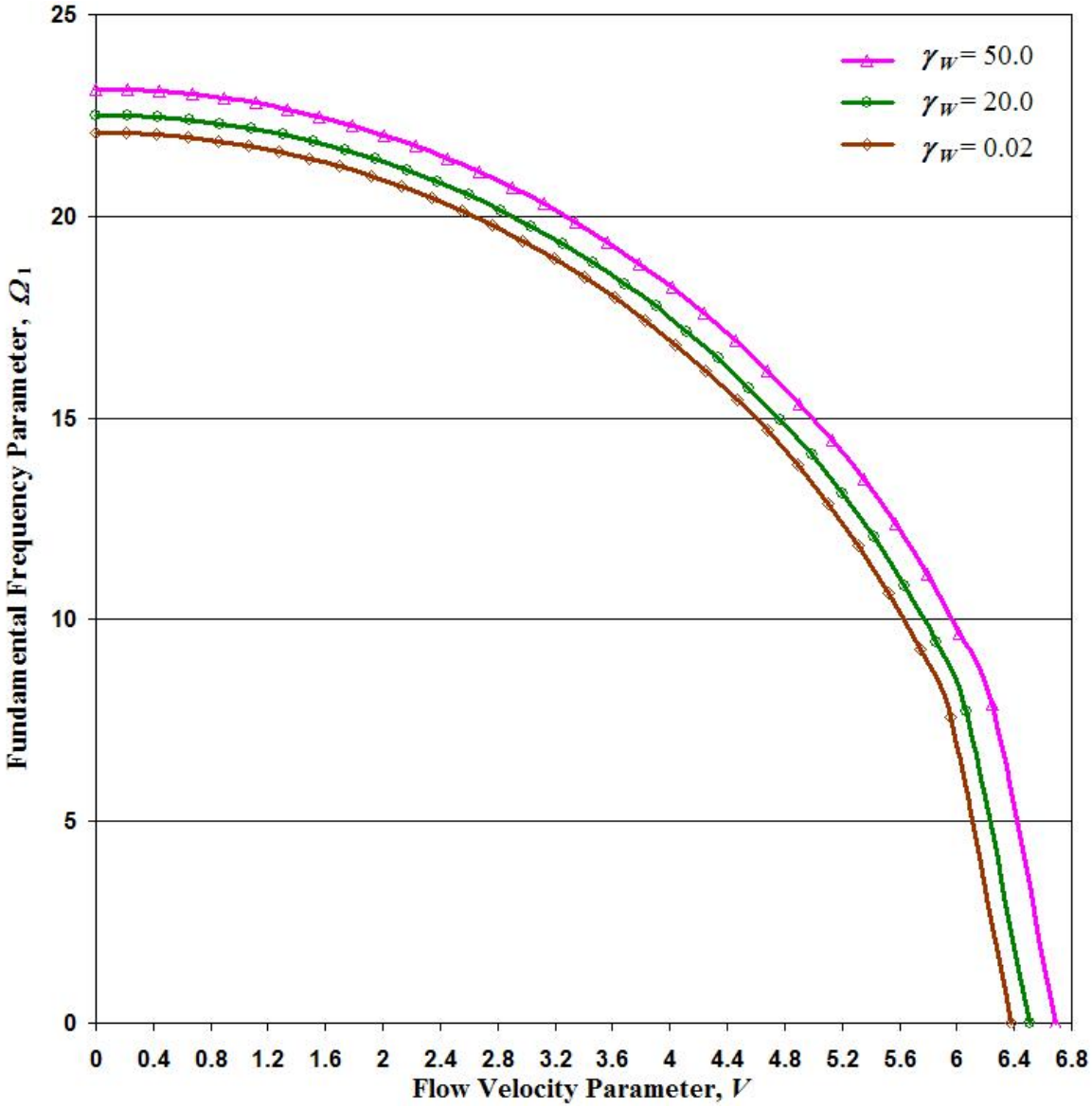

Figure 6.8 Clamped-clamped carbon nanotube: Non-dimensional fundamental frequency parameter, Ω_1, as a function of non-dimensional flow velocity parameter, V, for different Winkler stiffness parameter, γ_W, with the non-local parameters, e_n = 0.05, the Pasternak stiffness parameter, γ_P = 0.0 and the mass ratio parameter, β =0.12. These curves match exactly with Fig. 5 of reference **[35]**.

Table 6.4 Pinned-pinned carbon nanotube: Values of fundamental frequency parameter, Ω_1, for different values of the non-local parameter, e_n, and varying values of flow velocity parameter, V, Winkler stiffness parameter, γ_W, and Pasternak stiffness parameter, γ_P, for the value of the mass ratio, $\beta = 0.12$.

$e_n \rightarrow$		0.05		0.1	
γ_W	γ_P	V	Ω_1	V	Ω_1
2.00E-02	2.00E-02	0.1048	9.7695	0.1048	9.47222
		0.9435	9.31513	0.9435	9.03213
		1.9919	7.52761	1.9919	7.30042
		3.1451	0	3.1451	0
	2.00E+01	0.1822	16.97703	0.1822	16.46043
		1.6396	16.16746	1.6396	15.6768
		3.4615	12.993	3.4615	12.60384
		5.4655	0	5.4655	0
	5.00E+01	0.2579	24.03466	0.2579	23.3033
		2.3213	22.86655	2.3213	22.17264
		4.9005	18.28368	4.9005	17.73769
		7.7377	0	7.7377	0

Table 6.4 Continued

$e_n \rightarrow$		0.05		0.1	
γ_W	γ_P	V	Ω_1	V	Ω_1
2.00E+01	2.00E-02	0.1151	10.72268	0.1151	10.39639
		1.0356	10.22177	1.0356	9.91131
		2.1862	8.2529	2.1862	8.00421
		3.452	0	3.452	0
	2.00E+01	0.1883	17.54283	0.1883	17.00902
		1.6943	16.70359	1.6943	16.19669
		3.5768	13.41316	3.5768	13.01169
		5.6477	0	5.6477	0
	5.00E+01	0.2622	24.43758	0.2622	23.69397
		2.3602	23.24718	2.3602	22.5417
		4.9827	18.57565	4.9827	18.02101
		7.8674	0	7.8674	0
5.00E+01	2.00E-02	0.1289	12.01264	0.1289	11.64711
		1.1602	11.44773	1.1602	11.10015
		2.4493	9.2297	2.4493	8.95219
		3.8673	0	3.8673	0
	2.00E+01	0.197	18.35966	0.197	17.80099
		1.7732	17.47709	1.7732	16.94675
		3.7434	14.01682	3.7434	13.59768
		5.9106	0	5.9106	0
	5.00E+01	0.2686	25.03039	0.2686	24.26874
		2.4175	23.80694	2.4175	23.08442
		5.1036	19.00337	5.1036	18.43601
		8.0583	0	8.0583	0

Table 6.5 Pinned-pinned carbon nanotube: Values of fundamental frequency parameter, Ω_1, for different values of the non-local parameter, e_n, and varying values of flow velocity parameter, V, Winkler stiffness parameter, γ_W, and Pasternak stiffness parameter, γ_P, for the value of the mass ratio, $\beta = 0.3$.

$e_n \rightarrow$		0.05		0.1	
γ_W	γ_P	V	Ω_1	V	Ω_1
2.00E-02	2.00E-02	0.1048	9.79062	0.1048	9.55042
		0.9435	9.32086	0.9435	9.09312
		1.9919	7.48896	1.9919	7.30899
		3.1451	0	3.1451	0
	2.00E+01	0.1822	17.01335	0.1822	16.59597
		1.6396	16.14735	1.6396	15.75384
		3.4615	12.80148	3.4615	12.49952
		5.4655	0	5.4655	0
	5.00E+01	0.2579	24.08568	0.2579	23.49479
		2.3213	22.80552	2.3213	22.24987
		4.9005	17.86653	4.9005	17.4483
		7.7377	0	7.7377	0

Table 6.5 Continued

$e_n \rightarrow$		0.05		0.1	
γ_W	γ_P	V	Ω_1	V	Ω_1
2.00E+01	2.00E-02	0.1151	10.74581	0.1151	10.48218
		1.0356	10.22472	1.0356	9.97506
		2.1862	8.19723	2.1862	8.00099
		3.452	0	3.452	0
	2.00E+01	0.1883	17.58031	0.1883	17.14902
		1.6943	16.67882	1.6943	16.27241
		3.5768	13.1978	3.5768	12.88704
		5.6477	0	5.6477	0
	5.00E+01	0.2622	24.48941	0.2622	23.88862
		2.3602	23.18116	2.3602	22.61631
		4.9827	18.13307	4.9827	17.70878
		7.8674	0	7.8674	0
5.00E+01	2.00E-02	0.1289	12.03849	0.1289	11.74315
		1.1602	11.44539	1.1602	11.16615
		2.4493	9.14437	2.4493	8.92664
		3.8673	0	3.8673	0
	2.00E+01	0.197	18.39881	0.197	17.94744
		1.7732	17.44485	1.7732	17.01984
		3.7434	13.76348	3.7434	13.44015
		5.9106	0	5.9106	0
	5.00E+01	0.2686	25.0834	0.2686	24.46804
		2.4175	23.73319	2.4175	23.1548
		5.1036	18.52136	5.1036	18.08817
		8.0583	0	8.0583	0

Table 6.6 Pinned-pinned carbon nanotube: Values of fundamental frequency parameter, Ω_1, for different values of the non-local parameter, e_n, and varying values of flow velocity parameter, V, Winkler stiffness parameter, γ_W, and Pasternak stiffness parameter, γ_P, for the value of the mass ratio, $\beta = 0.5$.

$e_n \rightarrow$		0.05		0.1	
γ_W	γ_P	V	Ω_1	V	Ω_1
2.00E-02	2.00E-02	0.1048	9.81424	0.1048	9.63963
		0.9435	9.32728	0.9435	9.16246
		1.9919	7.44687	1.9919	7.31888
		3.1451	0	3.1451	0
	2.00E+01	0.1822	17.05398	0.1822	16.75057
		1.6396	16.12545	1.6396	15.84173
		3.4615	12.60041	3.4615	12.39036
		5.4655	0	5.4655	0
	5.00E+01	0.2579	24.14276	0.2579	23.71323
		2.3213	22.73938	2.3213	22.33945
		4.9005	17.44299	4.9005	17.15592
		7.7377	0	7.7377	0

Table 6.6 Continued

$e_n \rightarrow$		0.05		0.1	
γ_W	γ_P	V	Ω_1	V	Ω_1
2.00E+01	2.00E-02	0.1151	10.77169	0.1151	10.58004
		1.0356	10.22806	1.0356	10.04753
		2.1862	8.13694	2.1862	7.99796
		3.452	0	3.452	0
	2.00E+01	0.1883	17.62225	0.1883	17.30872
		1.6943	16.65184	1.6943	16.35893
		3.5768	12.97291	3.5768	12.75726
		5.6477	0	5.6477	0
	5.00E+01	0.2622	24.54739	0.2622	24.11066
		2.3602	23.10968	2.3602	22.70319
		4.9827	17.68564	4.9827	17.39482
		7.8674	0	7.8674	0
5.00E+01	2.00E-02	0.1289	12.06741	0.1289	11.85271
		1.1602	11.44289	1.1602	11.24118
		2.4493	9.05284	2.4493	8.89958
		3.8673	0	3.8673	0
	2.00E+01	0.197	18.44261	0.197	18.11449
		1.7732	17.40977	1.7732	17.1036
		3.7434	13.50112	3.7434	13.27754
		5.9106	0	5.9106	0
	5.00E+01	0.2686	25.14271	0.2686	24.69539
		2.4175	23.65346	2.4175	23.2373
		5.1036	18.03727	5.1036	17.74095
		8.0583	0	8.0583	0

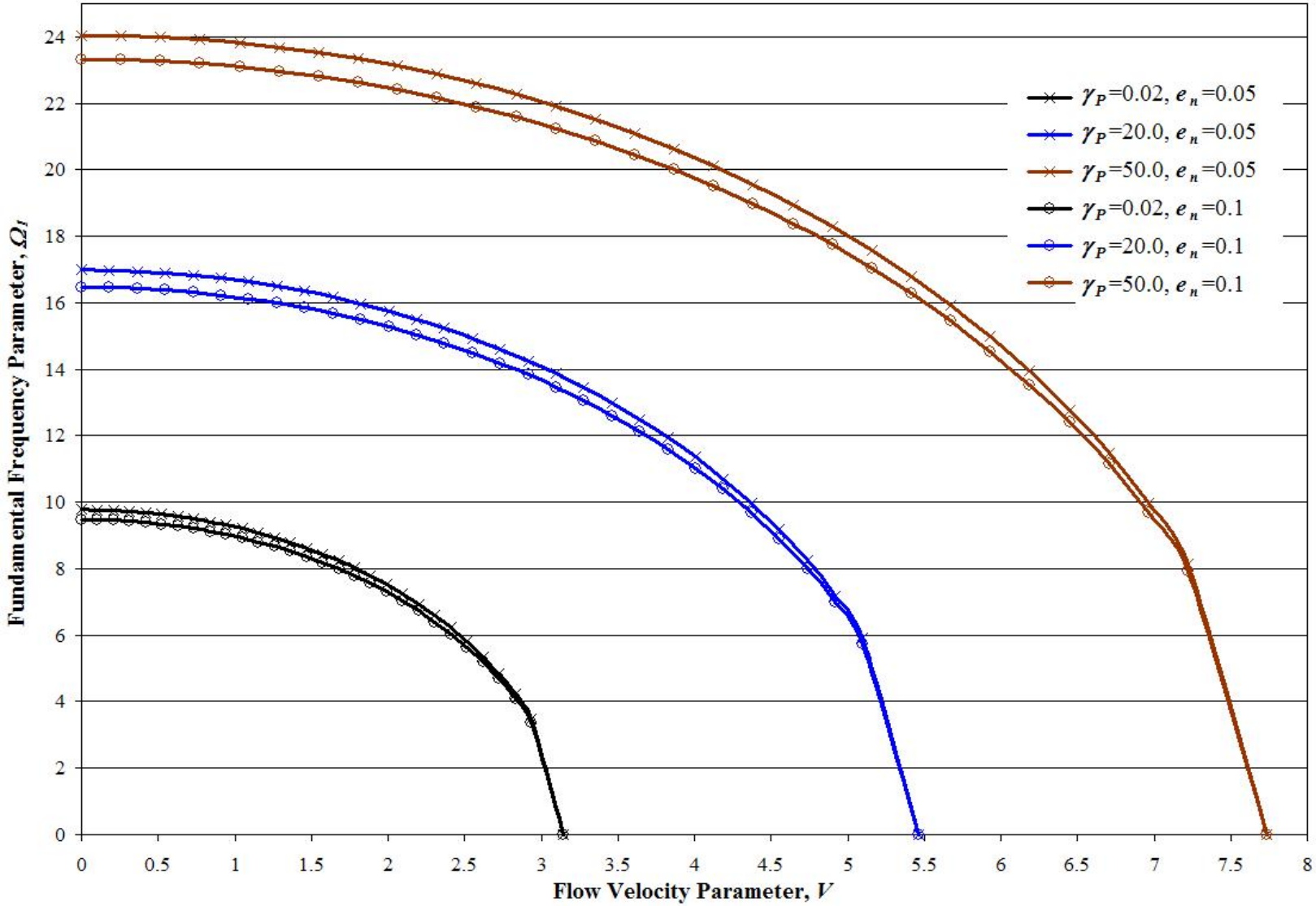

Figure 6.9 Pinned-pinned carbon nanotube: Variation of non-dimensional fundamental frequency parameter, Ω_1, with flow velocity parameter, V, for different values of the non-local parameter, e_n, and Pasternak stiffness parameter, γ_P, for the value of Winkler stiffness parameter, $\gamma_W = 0.02$, and mass ratio parameter, $\beta = 0.12$.

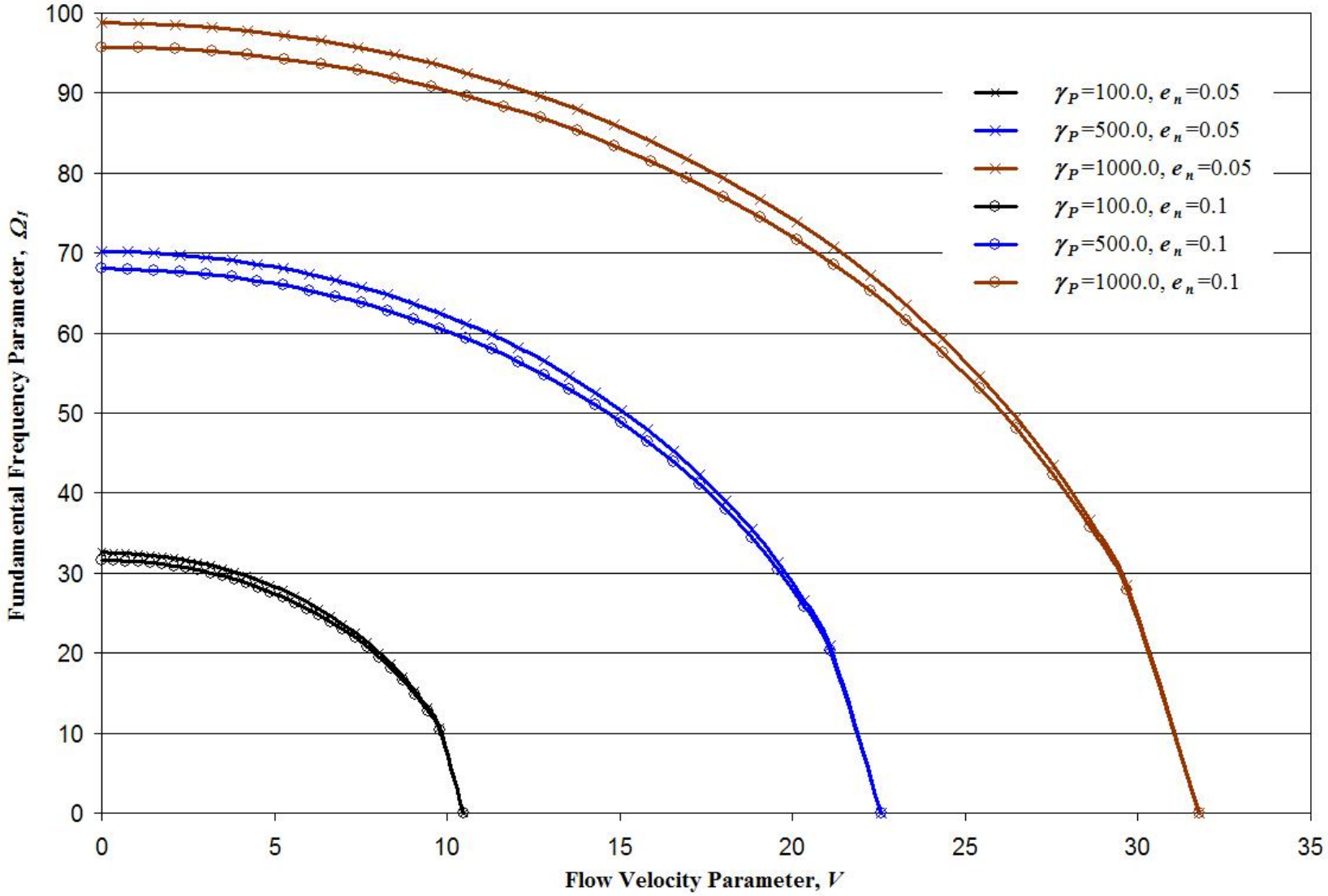

Figure 6.10 Pinned-pinned carbon nanotube: Variation of non-dimensional fundamental frequency parameter, Ω_1, with flow velocity parameter, V, for different values of the non-local parameter, e_n, and Pasternak stiffness parameter, γ_P, for the value of Winkler stiffness parameter, $\gamma_W = 0.02$, and mass ratio parameter, $\beta = 0.12$.

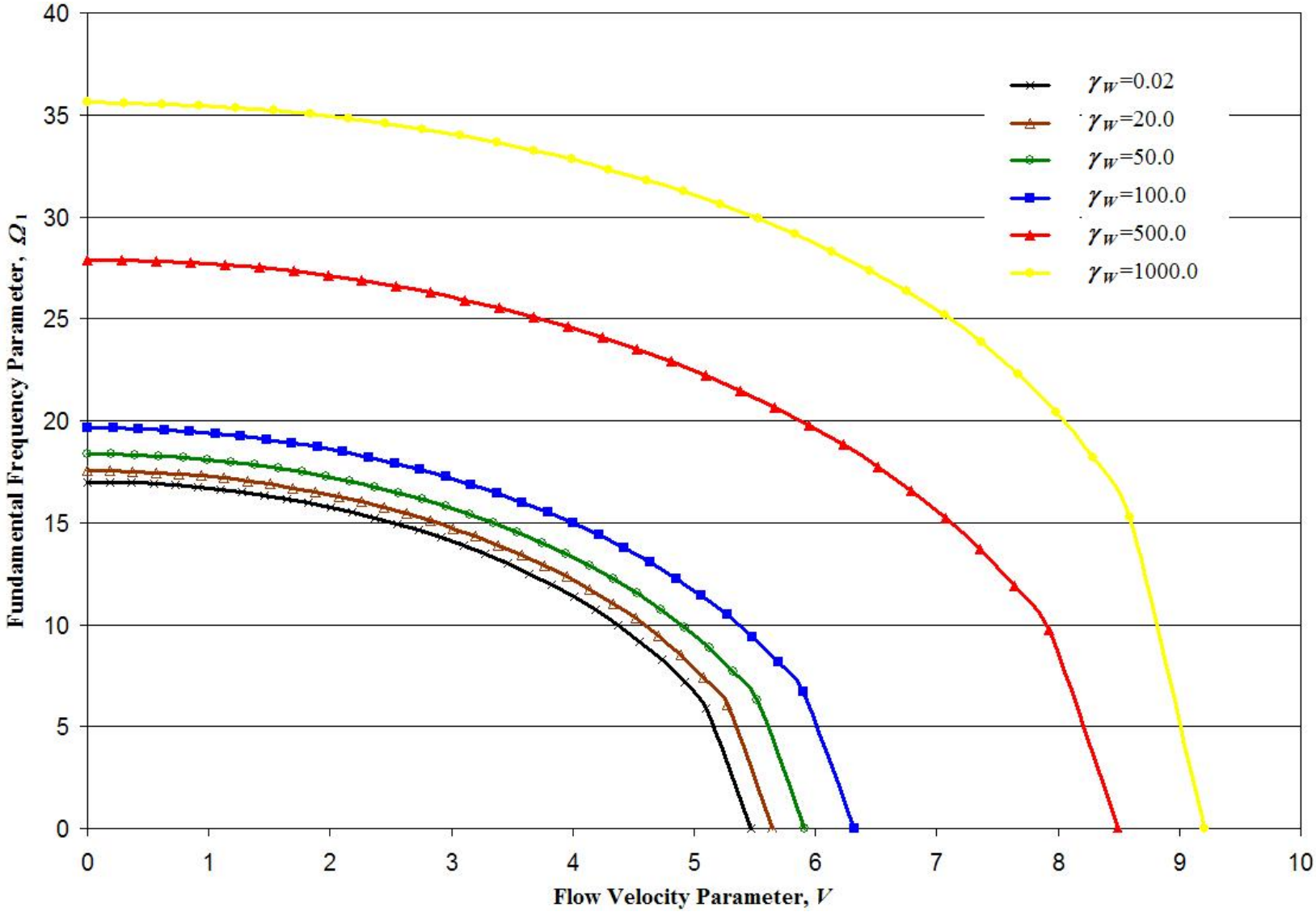

Figure 6.11 Pinned-pinned carbon nanotube: Variation of non-dimensional fundamental frequency parameter, Ω_1, with flow velocity parameter, V, for different values of the Winkler stiffness parameter, γ_W, and for the non-local parameter, e_n = 0.05, and Pasternak stiffness parameter, γ_P = 20.0, and mass ratio parameter, β = 0.12.

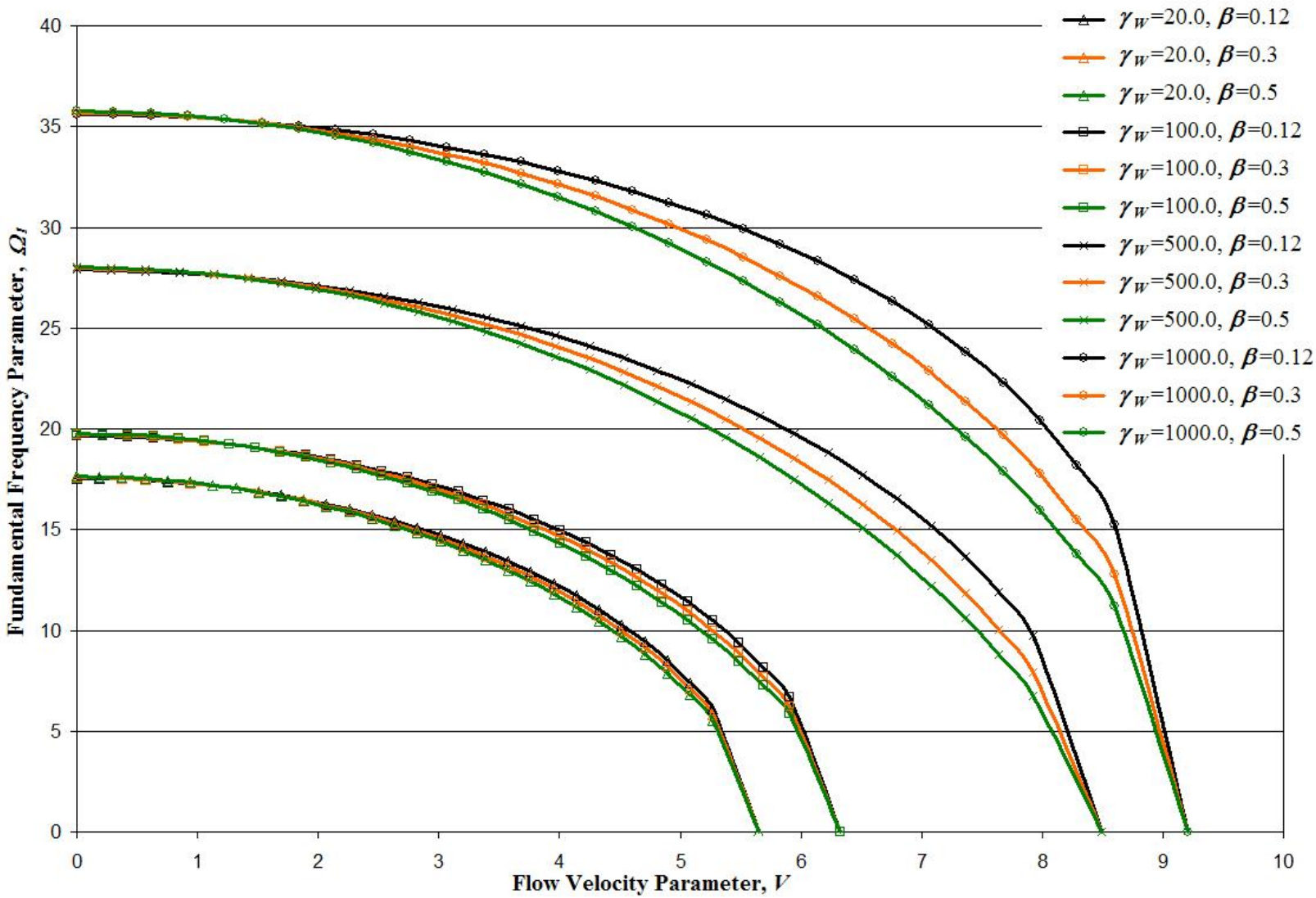

Figure 6.12 Pinned-pinned carbon nanotube: Variation of non-dimensional fundamental frequency parameter, Ω_1, with flow velocity parameter, V, for different values of the Winkler stiffness parameter, γ_W, and mass ratio parameter, β, and for the non-local parameter, e_n = 0.05, and Pasternak stiffness parameter, γ_P = 20.0.

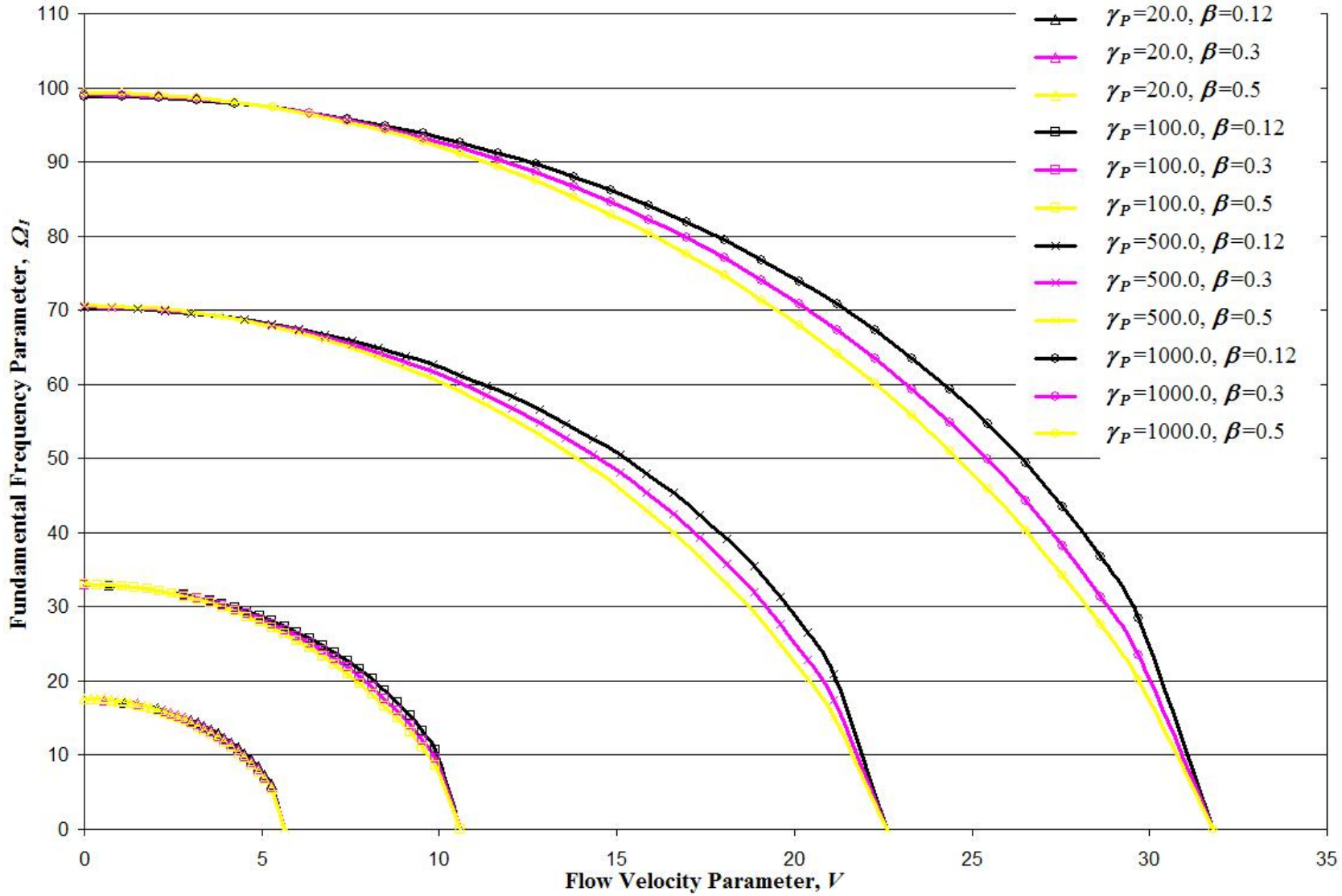

Figure 6.13 Pinned-pinned carbon nanotube: Variation of non-dimensional fundamental frequency parameter, Ω_1, with flow velocity parameter, V, for different values of the Pasternak stiffness parameter, γ_P, and mass ratio parameter, β, and for the non-local parameter, e_n = 0.05, and Winkler stiffness parameter, γ_W = 20.0.

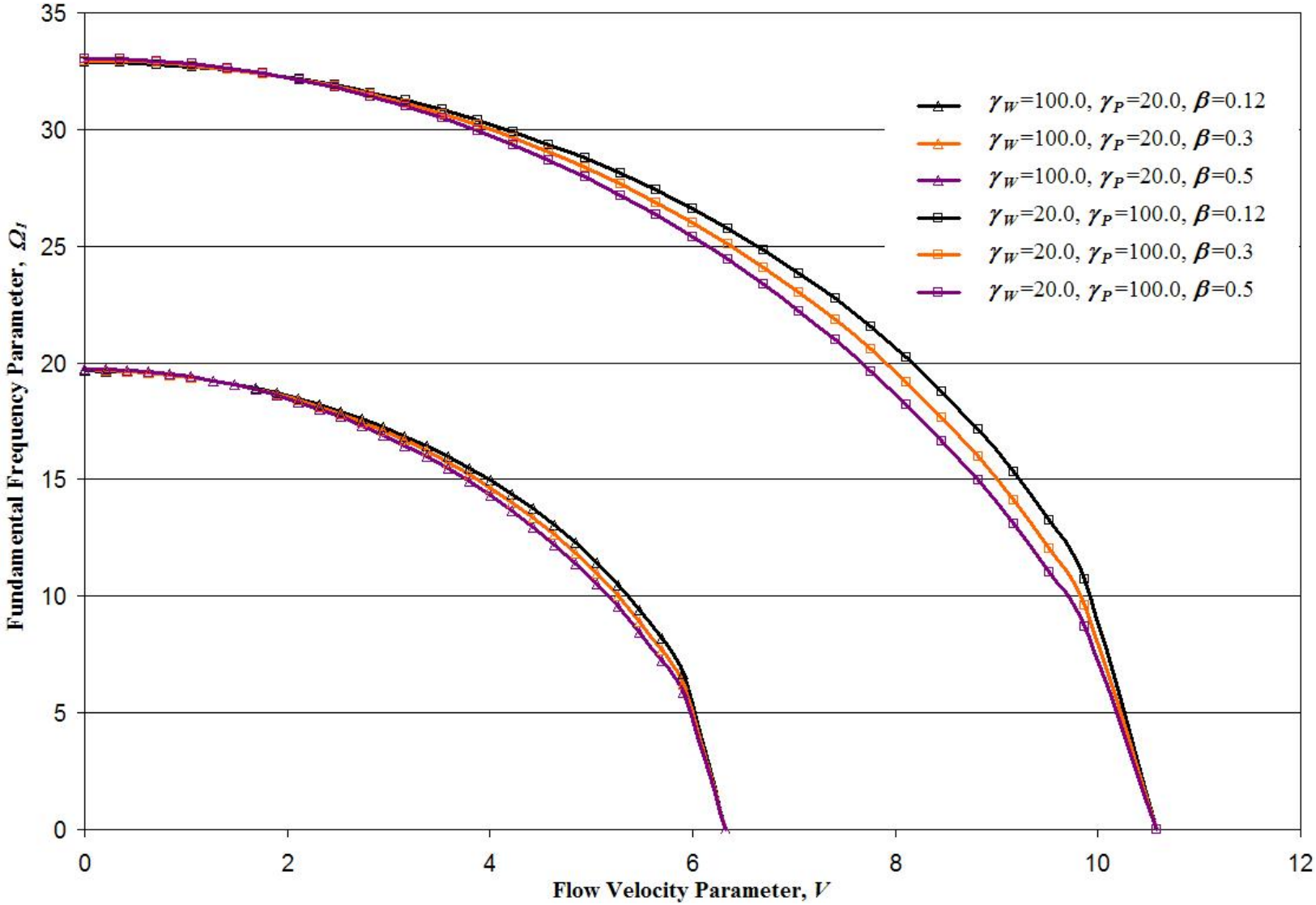

Figure 6.14 Pinned-pinned carbon nanotube: Comparison of the effects of the Winkler stiffness parameter, γ_W, and Pasternak stiffness parameter, γ_P, on the non-dimensional fundamental frequency parameter, Ω_1, for different values of the mass ratio parameter, β and for non-local parameter, e_n = 0.05.

Although some work has been reported in the literature on the dynamics of simply supported single-walled carbon nanotubes conveying fluid embedded in a Winkler medium by Yoon et. al., **[30]**, comparison of the results is difficult because they have not used non-local continuum mechanics formulation and also have not non-dimensionalized the parameters of interest. However, from the plots of their results, it can be observed that the trend is the same.

6.3.3 CNT: Pinned-clamped Boundary condition

Solving Equation (6.19) for Ω_j, we obtain the natural frequencies for the pinned-clamped boundary condition. The method followed for generating the numerical results is identical to that used for the clamped-clamped case. Numerical results are once again obtained for three values of the mass ratio parameter, β. Tables 6.7, 6.8 and 6.9 show the tabulated results for the above values respectively. The pattern of the tables and subsequent curves has been kept the same as for the pinned-pinned case for easy comparison. A similar trend is observed from the data obtained for different values of the non-local parameter, the mass ratio parameter and the stiffness parameters.

The introduction of a clamped condition at one of the ends of the carbon nanotube makes it behave more stiffly, as seen from the values of both the critical velocities as well as the fundamental frequencies. The behaviour can be more readily seen in Figs. 6.15 through 6.20. Increase in the values of the non-local parameter, e_n, tends to decrease the fundamental frequency slightly and increase in the mass ratio parameter, β, increases the fundamental frequency slightly. The values of the fundamental

Table 6.7 Pinned-clamped carbon nanotube: Values of fundamental frequency parameter, Ω_1, for different values of the non-local parameter, e_n, and varying values of flow velocity parameter, V, Winkler stiffness parameter, γ_W, and Pasternak stiffness parameter, γ_P, for the value of the mass ratio, $\beta = 0.12$.

$e_n \rightarrow$		0.05		0.1	
γ_W	γ_P	V	Ω_1	V	Ω_1
2.00E-02	2.00E-02	0.1501	15.2259	0.1501	14.6904
		1.3506	14.52	1.3506	14.0093
		2.8514	11.7394	2.8514	11.3269
		4.5022	0	4.5022	0
	2.00E+01	0.2115	21.299	0.2115	20.5636
		1.9033	20.2958	1.9033	19.5954
		4.018	16.3529	4.018	15.7911
		6.3442	0	6.3442	0
	5.00E+01	0.2794	27.9526	0.2794	26.9999
		2.5144	26.6125	2.5144	25.7066
		5.3083	21.3505	5.3083	20.6298
		8.3815	0	8.3815	0

Table 6.7 Continued

$e_n \rightarrow$		0.05		0.1	
γ_W	γ_P	V	Ω_1	V	Ω_1
2.00E+01	2.00E-02	0.1561	15.8522	0.1561	15.2946
		1.4046	15.1165	1.4046	14.5848
		2.9653	12.2192	2.9653	11.7897
		4.6821	0	4.6821	0
	2.00E+01	0.2158	21.7514	0.2158	21.0003
		1.9419	20.726	1.9419	20.0108
		4.0997	16.6963	4.0997	16.1225
		6.4731	0	6.4731	0
	5.00E+01	0.2826	28.2989	0.2826	27.3344
		2.5438	26.9415	2.5438	26.0242
		5.3703	21.6105	5.3703	20.8808
		8.4795	0	8.4795	0
5.00E+01	2.00E-02	0.1646	16.7486	0.1646	16.1594
		1.4814	15.9705	1.4814	15.4085
		3.1273	12.906	3.1273	12.4519
		4.9378	0	4.9378	0
	2.00E+01	0.222	22.4134	0.222	21.6394
		1.9982	21.3559	1.9982	20.6187
		4.2183	17.1993	4.2183	16.6077
		6.6605	0	6.6605	0
	5.00E+01	0.2874	28.811	0.2874	27.829
		2.587	27.4281	2.587	26.4941
		5.4615	21.9955	5.4615	21.2523
		8.6234	0	8.6234	0

Table 6.8 Pinned-clamped carbon nanotube: Values of fundamental frequency parameter, Ω_1, for different values of the non-local parameter, e_n, and varying values of flow velocity parameter, V, Winkler stiffness parameter, γ_W, and Pasternak stiffness parameter, γ_P, for the value of the mass ratio, $\beta = 0.3$.

$e_n \rightarrow$		0.05		0.1	
γ_W	γ_P	V	Ω_1	V	Ω_1
2.00E-02	2.00E-02	0.1501	15.2641	0.1501	14.8305
		1.3506	14.5187	1.3506	14.1079
		2.8514	11.6234	2.8514	11.3
		4.5022	0	4.5022	0
	2.00E+01	0.2115	21.351	0.2115	20.7557
		1.9033	20.2626	1.9033	19.7007
		4.018	16.0629	4.018	15.6295
		6.3442	0	6.3442	0
	5.00E+01	0.2794	28.0194	0.2794	27.2484
		2.5144	26.5327	2.5144	25.8069
		5.3083	20.8128	5.3083	20.2634
		8.3815	0	8.3815	0

Table 6.8 Continued

$e_n \rightarrow$		0.05		0.1	
γ_W	γ_P	V	Ω_1	V	Ω_1
2.00E+01	2.00E-02	0.1561	15.8919	0.1561	15.4404
		1.4046	15.1119	1.4046	14.6843
		2.9653	12.085	2.9653	11.749
		4.6821	0	4.6821	0
	2.00E+01	0.2158	21.8044	0.2158	21.1965
		1.9419	20.6886	1.9419	20.1148
		4.0997	16.3846	4.0997	15.9426
		6.4731	0	6.4731	0
	5.00E+01	0.2826	28.3665	0.2826	27.5859
		2.5438	26.857	2.5438	26.1223
		5.3703	21.0499	5.3703	20.4941
		8.4795	0	8.4795	0
5.00E+01	2.00E-02	0.1646	16.7905	0.1646	16.3134
		1.4814	15.9604	1.4814	15.5087
		3.1273	12.7428	3.1273	12.3889
		4.9378	0	4.9378	0
	2.00E+01	0.222	22.468	0.222	21.8415
		1.9982	21.3118	1.9982	20.7206
		4.2183	16.8539	4.2183	16.3994
		6.6605	0	6.6605	0
	5.00E+01	0.2874	28.8797	0.2874	28.0851
		2.587	27.3367	2.587	26.5887
		5.4615	21.4	5.4615	20.8348
		8.6234	0	8.6234	0

Table 6.9 Pinned-clamped carbon nanotube: Values of fundamental frequency parameter, Ω_1, for different values of the non-local parameter, e_n, and varying values of flow velocity parameter, V, Winkler stiffness parameter, γ_W, and Pasternak stiffness parameter, γ_P, for the value of the mass ratio, $\beta = 0.5$.

$e_n \rightarrow$		0.05		0.1	
γ_W	γ_P	V	Ω_1	V	Ω_1
2.00E-02	2.00E-02	0.1501	15.3068	0.1501	14.9908
		1.3506	14.5175	1.3506	14.2202
		2.8514	11.4993	2.8514	11.2718
		4.5022	0	4.5022	0
	2.00E+01	0.2115	21.4092	0.2115	20.9756
		1.9033	20.2267	1.9033	19.8213
		4.018	15.7622	4.018	15.4623
		6.3442	0	6.3442	0
	5.00E+01	0.2794	28.0942	0.2794	27.5327
		2.5144	26.4464	2.5144	25.9237
		5.3083	20.2721	5.3083	19.8966
		8.3815	0	8.3815	0

Table 6.9 Continued

$e_n \rightarrow$		0.05		0.1	
γ_W	γ_P	V	Ω_1	V	Ω_1
2.00E+01	2.00E-02	0.1561	15.9363	0.1561	15.6073
		1.4046	15.1071	1.4046	14.7978
		2.9653	11.9421	2.9653	11.7064
		4.6821	0	4.6821	0
	2.00E+01	0.2158	21.8637	0.2158	21.4209
		1.9419	20.648	1.9419	20.2341
		4.0997	16.0626	4.0997	15.7573
		6.4731	0	6.4731	0
	5.00E+01	0.2826	28.4421	0.2826	27.8737
		2.5438	26.7659	2.5438	26.2368
		5.3703	20.488	5.3703	20.1086
		8.4795	0	8.4795	0
5.00E+01	2.00E-02	0.1646	16.8374	0.1646	16.4898
		1.4814	15.9495	1.4814	15.6231
		3.1273	12.5702	3.1273	12.3228
		4.9378	0	4.9378	0
	2.00E+01	0.222	22.529	0.222	22.0727
		1.9982	21.2639	1.9982	20.8377
		4.2183	16.4992	4.2183	16.1861
		6.6605	0	6.6605	0
	5.00E+01	0.2874	28.9567	0.2874	28.378
		2.587	27.2381	2.587	26.6996
		5.4615	20.806	5.4615	20.4208
		8.6234	0	8.6234	0

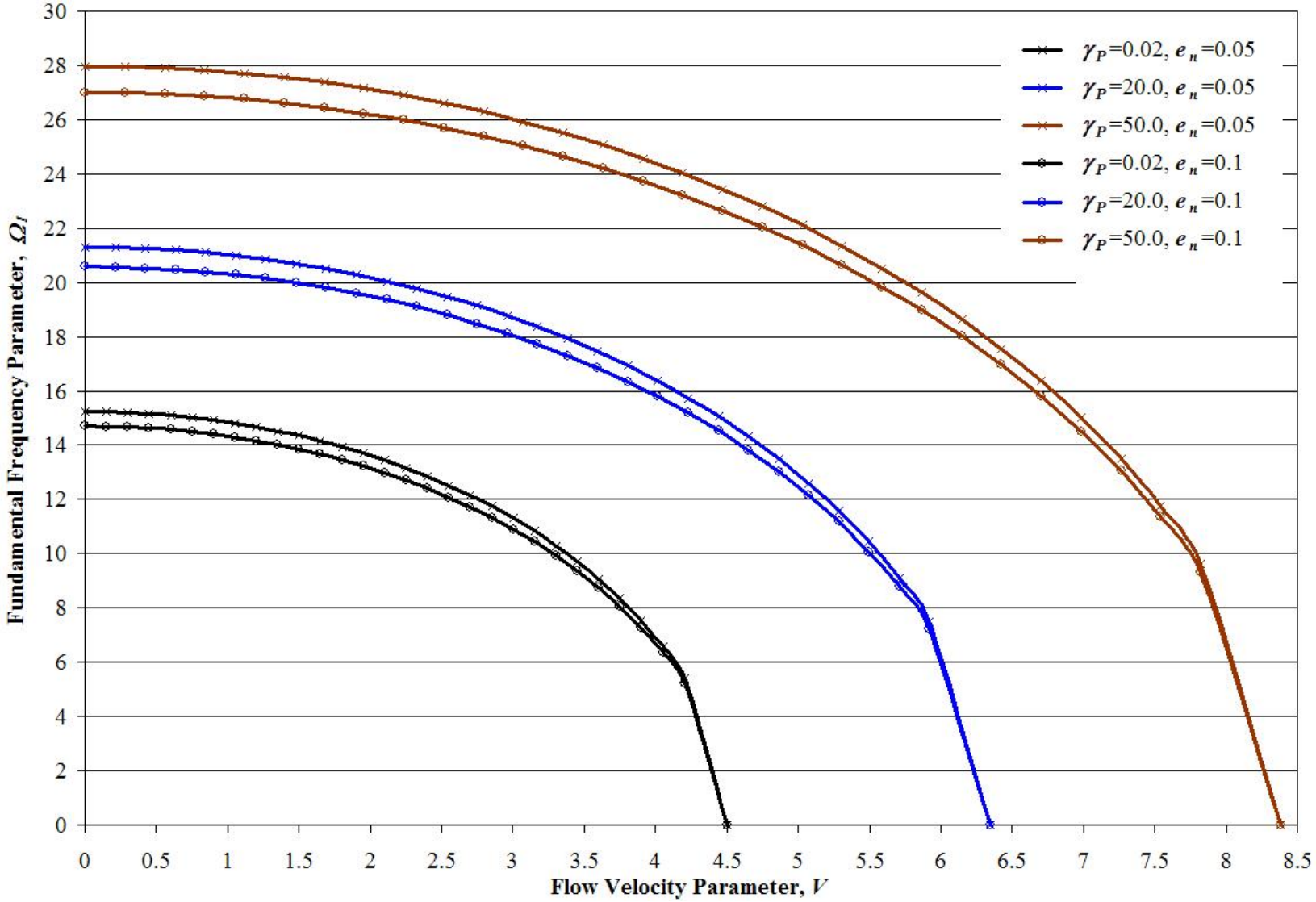

Figure 6.15 Pinned-clamped carbon nanotube: Variation of non-dimensional fundamental frequency parameter, Ω_1, with flow velocity parameter, V, for different values of the non-local parameter, e_n, and Pasternak stiffness parameter, γ_P, for the value of Winkler stiffness parameter, $\gamma_W = 0.02$, and mass ratio parameter, $\beta = 0.12$.

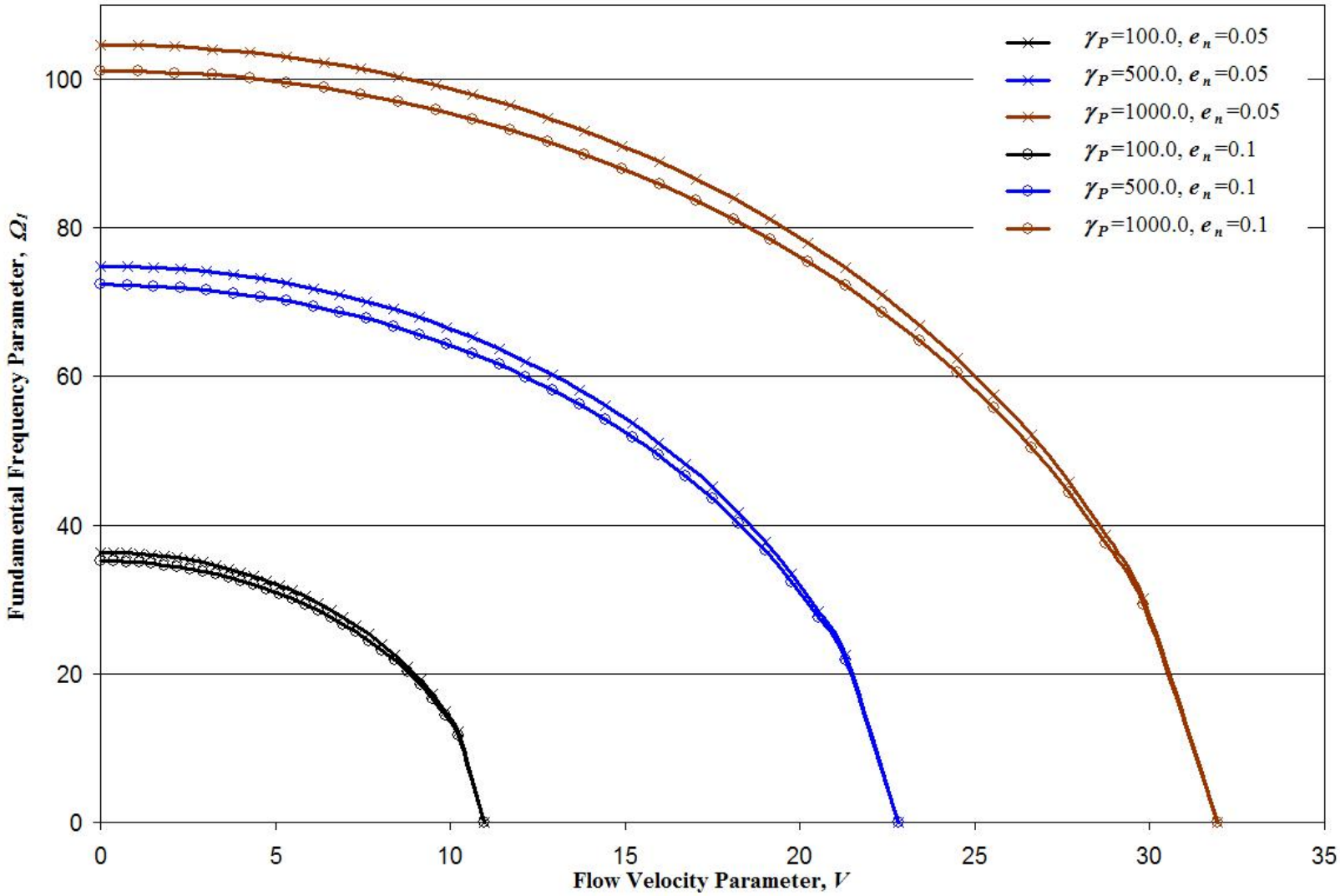

Figure 6.16 Pinned-clamped carbon nanotube: Variation of non-dimensional fundamental frequency parameter, Ω_1, with flow velocity parameter, V, for different values of the Winkler stiffness parameter, γ_W, and for the non-local parameter, e_n = 0.05, and Pasternak stiffness parameter, γ_P = 20.0, and mass ratio parameter, β = 0.12.

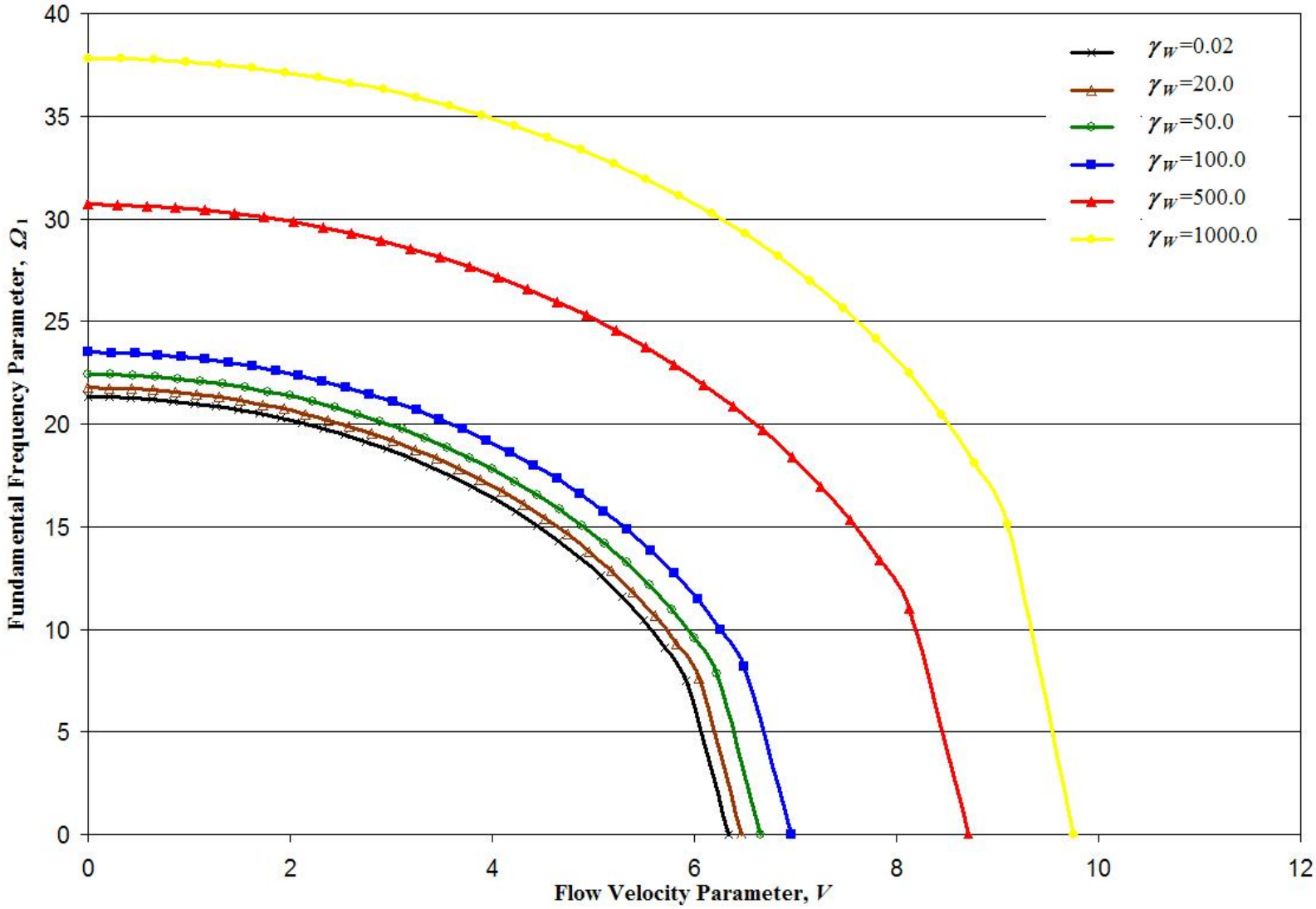

Figure 6.17 Pinned-clamped carbon nanotube: Variation of non-dimensional fundamental frequency parameter, Ω_1, with flow velocity parameter, V, for different values of the Winkler stiffness parameter, γ_W, and mass ratio parameter, β, and for the non-local parameter, e_n = 0.05, and Pasternak stiffness parameter, γ_P = 20.0.

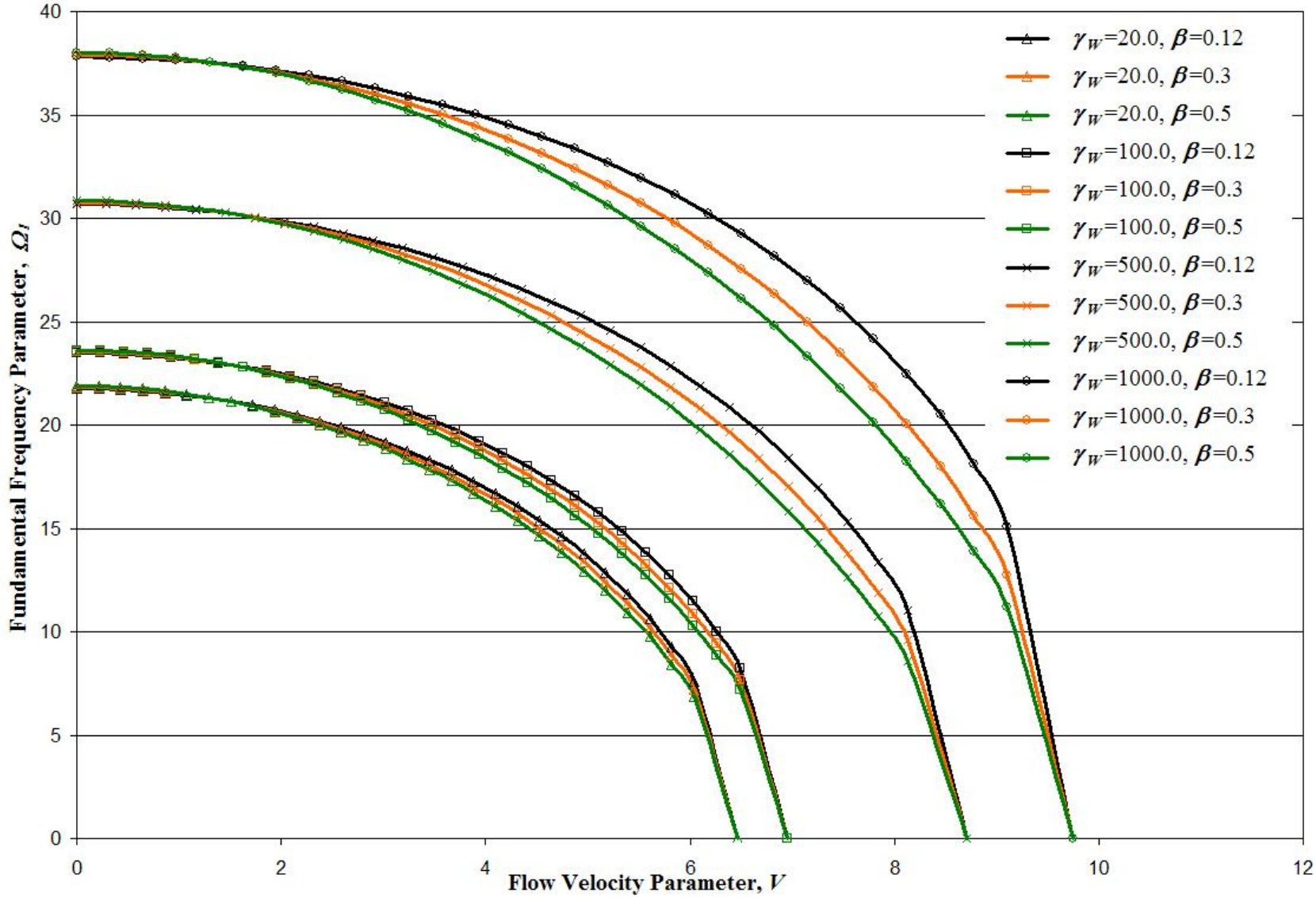

Figure 6.18 Pinned-clamped carbon nanotube: Variation of non-dimensional fundamental frequency parameter, Ω_1, with flow velocity parameter, V, for different values of the Pasternak stiffness parameter, γ_P, and mass ratio parameter, β, and for the non-local parameter, e_n = 0.05, and Winkler stiffness parameter, γ_W = 20.0.

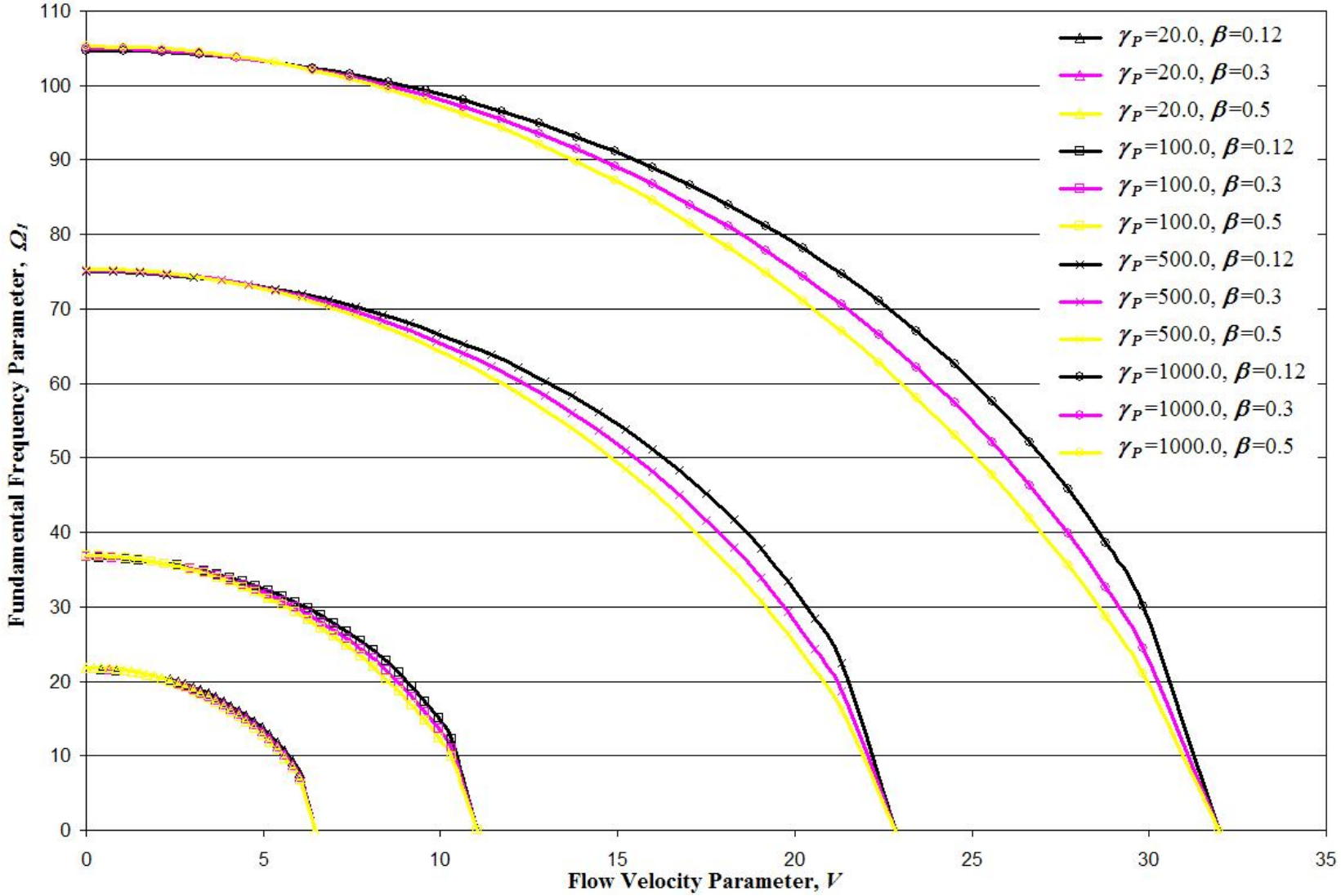

Figure 6.19 Pinned-clamped carbon nanotube: Comparison of the effects of the Winkler stiffness parameter, γ_W, and Pasternak stiffness parameter, γ_P, on the non-dimensional fundamental frequency parameter, Ω_1, for different values of the mass ratio parameter, β and for non-local parameter, e_n = 0.05.

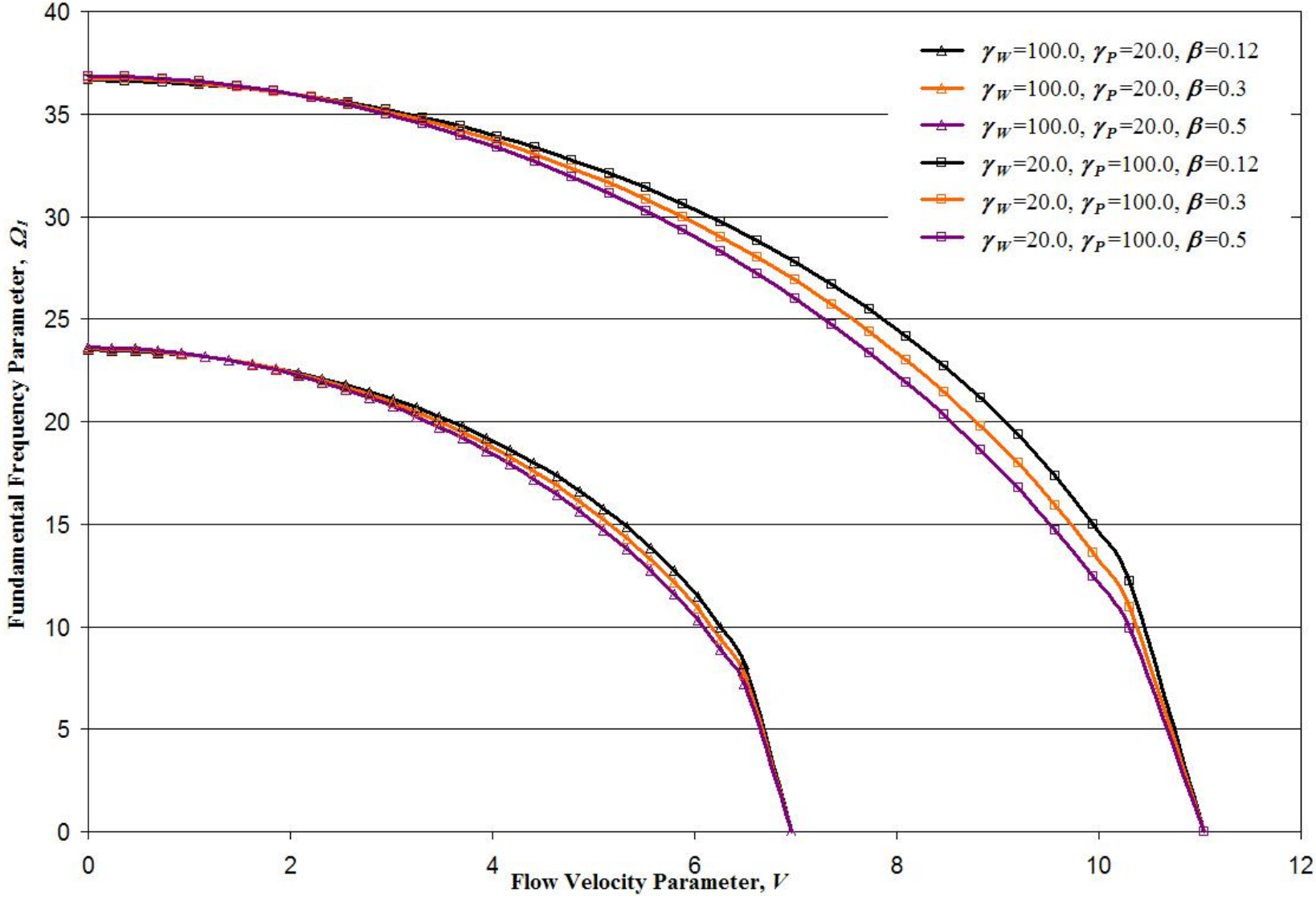

Figure 6.20 Pinned-clamped carbon nanotube: Comparison of the effects of the Winkler stiffness parameter, γ_W, and Pasternak stiffness parameter, γ_P, on the non-dimensional fundamental frequency parameter, Ω_1, for different values of the mass ratio parameter, β and for non-local parameter, e_n = 0.05.

frequency fall in between those for pinned-pinned and the clamped-clamped cases. Now that comprehensive results are available for all three boundary conditions, it would be useful to analyze their relative influence on the dynamics of carbon nanotubes. Fig. 6.21 plots the fundamental frequency parameter as a function of the velocity parameter for all three boundary conditions for the same values of the stiffness parameters, mass ratio parameters and the non-local parameters. It can be seen that as clamping conditions are introduced, the fundamental frequency increases. This result could be used to properly design the supports for the given conditions.

6.4 Summary and conclusions

In this chapter, comprehensive results were presented for the dynamic behaviour of fluid conveying carbon nanotubes embedded in elastic media. The results are obtained considering the nano length scales involved in the analysis of such nanostructures. The effect of the non-local parameter has been clearly brought out. The major conclusions from the analysis of fluid conveying carbon nanotubes embedded in a Pasternak type elastic medium may be summarized as below:

- The fundamental frequency decreases for increasing values of the non-local parameter, indicating that the non-local formulation definitely has its effect on the dynamics of the system. The fundamental frequency also decreases for increasing values of the mass ratio parameter, as is the case with pipes.

- The effect of both the stiffness parameters on the fundamental frequency was clearly brought out. It is seen that it increases for increasing values of both the stiffness parameters. Moreover, it has been shown that the Pasternak parameter

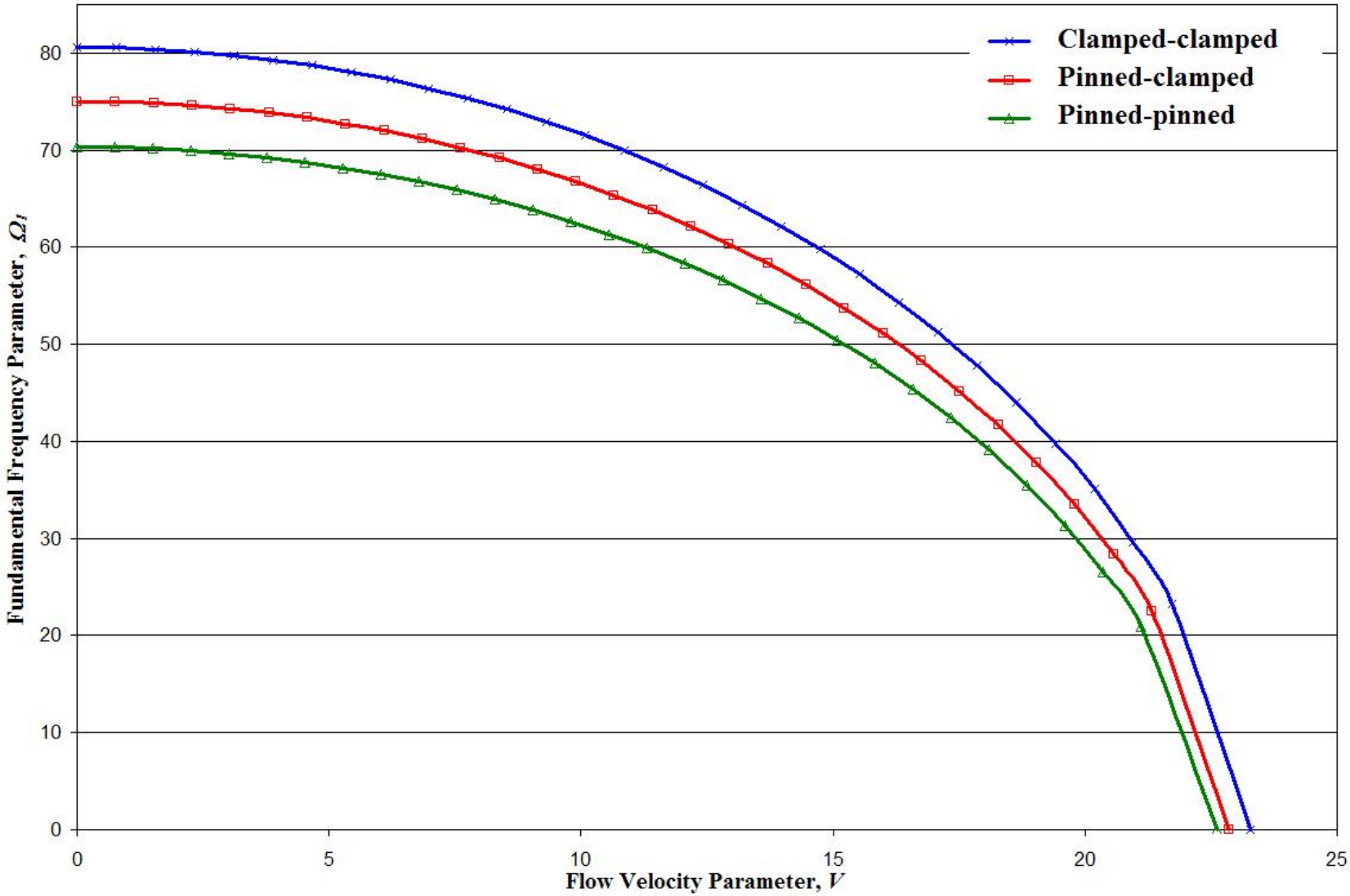

Figure 6.21 Carbon nanotube: Comparison of the effects of the three boundary conditions on the non-dimensional fundamental frequency parameter, Ω_1, for Winkler stiffness parameter, γ_W = 20.0, Pasternak stiffness parameter, γ_P = 500.0, the mass ratio parameter, β = 0.12 and for non-local parameter, e_n = 0.05.

has a more significant role in increasing the fundamental frequency of the nanotube.

- The results for a carbon nanotube embedded in a Winkler type elastic medium show very good agreement with the results published by Lee and Chang **[34, 35]**, thus validating the formulation and the solution method employed here.

- It is also seen that the end conditions effect the dynamic properties of the carbon nanotube. As for pipes, the fundamental frequency increases as clamping conditions are introduced at both the ends.

- It may be mentioned that the results presented in this chapter are new and as yet unpublished. The main contribution of the previous two chapters has been the formulation of the dynamical problem considering a Pasternak type embedding medium and also including the non-local continuum mechanics model.

The next chapter gives major conclusions of the research work done in this thesis and also suggests scope for further work in this area.

Chapter 7

Conclusions and Recommendations

This chapter summarizes the entire work done in this thesis and gives a bird's eye view of the major conclusions of the analysis. Finally, the chapter ends with recommendations for future research on this *"Model Dynamical Problem"*.

The first chapter introduces the reader to the subject under investigation. A fairly comprehensive literature survey is presented with references most relevant to the present research being included in the list of references. It also details how the thesis is organized for quick cross reference.

In the second chapter, the mathematical formulation is developed for the dynamical problem of a fluid conveying pipe resting on a Pasternak elastic medium, in a fairly detailed manner. Various models of the supporting media are discussed and the Pasternak model is chosen for analysis because it is the closest to the real soil medium. The governing partial differential equation to describe the motion of the pipe has been derived for the first time including the Pasternak stiffness modulus.

The third chapter discusses in detail the methods of solution adopted to solve the governing equation for different boundary conditions. The focus in this chapter is on the stability aspects of the pipe conveying fluid. The Critical flow velocity, which determines the stability regime of the system, is computed. The Fourier series approach has been adopted for solving the equation for the pipe with pinned-pinned ends, whereas, the Galerkin method, in which the trial functions are the actual mode shapes of a bare beam, is utilized to obtain the solution for the clamped-pinned and the clamped-clamped end conditions of the pipe. Comprehensive results have been presented in the form of tables and graphs and comparisons made.

In the fourth chapter, results are obtained for the natural frequencies of the system, for the above three boundary conditions. Again, comprehensive results are presented for all relevant variations in the different parameters of the system. Comparisons of the results obtained with those obtained by earlier researchers have been made and were found to be in very good agreement. The results of both critical velocities and the natural frequencies of pipes conveying fluid and resting on Pasternak foundation are new and have been published by the author (see **[68, 72]**).

The fifth chapter can be considered an extension of the matter presented in earlier chapters to the analysis of carbon nanotubes conveying fluid. This exciting new application of the established equations for pipes is a relatively new phenomenon and has started around 2005, **[30]**. However further refinement of the governing equations were considered necessary for taking into account the nanoscale lengths involved. Thus, the governing equations were refined by using Eringen's non-local continuum mechanics theory (see, **56, 57, 59}**), which includes the contributions of the strains

induced in the material in a region around a point at which the stress is desired. With the application of this theory, there has been a spurt of research on carbon nanotubes conveying fluid. In this chapter, the non-local theory is used and, the governing equation of a carbon nanotube conveying fluid and embedded in a Pasternak type elastic medium, has been derived for the first time.

The sixth chapter details how the equation of motion derived in Chapter 5 can be solved for the natural frequencies of the system, considering the three ideal boundary conditions discussed earlier. The solution method is identical to that followed for pipes, with the only difference being the inclusion of several terms containing the non-local parameter in the equations. Again comprehensive results are presented in tables and graphs and comparisons made. These results are as yet unpublished.

The major conclusions of this research work are summarized in the next section.

7.1 Conclusions

The following are the conclusions drawn from the results generated for the various conditions described in the text:

- There exists a critical velocity at which the fundamental frequency becomes zero, leading to the buckling of the pipe.

- Critical velocities are different for different end conditions, with the lowest being for the pinned-pinned condition and the highest being for the clamped-clamped condition, all other conditions being the same.

- However, for extremely stiff Winkler elastic media, for γ_W greater than say, 500000.0, the trend is reversed, with the pinned-pinned pipe having higher critical flow velocity that the clamped-clamped end.

- Critical velocities also depend on the stiffness parameters, with their values showing an increase for increasing values of the stiffness.

- Both the Winkler as well as the Pasternak stiffness parameters tends to stabilize the pipe and carbon nanotube conveying fluid.

- The fundamental frequency of the system decreases with increasing fluid velocity.

- There is however an increase in the value of the fundamental frequency for increasing values of the stiffness parameters.

- The influence of the Pasternak parameter on the stability as well as the natural frequency is greater as compared to the Winkler parameter. It is hoped that this new information will be further validated by future researchers.

- The mass ratio also has an influence on the fundamental frequency. The fundamental frequency parameter, Ω_1, decreases with increasing mass ratio, β, and this decrease is more pronounced for higher values of the Pasternak stiffness parameter, γ_P.

- The results obtained here for both critical flow velocities as well as fundamental frequencies have been compared with existing literature, wherever possible, and have been found to be in very good agreement.

- For increasing values of the non-local parameter, the fundamental frequency of a carbon nanotube conveying fluid decreases.

- All other conclusions for the carbon nanotubes, regarding the effect of the stiffness parameters and the mass ratio parameters are similar to those for pipes.

- Results compare excellently for a clamped-clamped carbon nanotube conveying fluid embedded in a Winkler elastic medium. For other end conditions and for the Pasternak elastic medium, the results obtained here are new and hence no comparisons are possible.

In the next section, recommendations for future work are briefly enumerated.

7.2 Recommendations for future work

7.2.1 Pipes conveying fluid

In this work, only three ideal boundary conditions have been considered. The real end conditions are however rarely ideal. Hence, the analysis could be performed by considering elastically restrained end conditions, simulating the real ends in a better way.

The elastic medium considered here is a continuous elastic support with constant modulus. A more generalized elastic medium could be modeled and incorporated into the governing equation, which can vary in stiffness along the length of the pipe. Partial elastic foundations can also be considered for analysis of fluid conveying pipes.

The effects of pressure, temperature, viscosity of the fluid, pulsating flow field, change of cross-sectional area of the pipe and axial load, all provide interesting problems for future work.

The area of curved pipes conveying fluid is also another interesting area that can be pursued. Non-linear aspects of the problem have not been touched upon at all in this work. Material and geometric non-linearity of the pipe and the elastic media can be investigated.

Even non-metallic piping systems, additional masses in the span as well as intermediate supports can also be another topic for research.

The present commercial finite element software are not suited to handle this problem of either pipes or carbon nanotubes conveying fluid. Finite element modeling of the above problem is another good area for further research.

7.2.2 Carbon nanotubes conveying fluid

The formulation method followed here is the basic and popular non-local continuum mechanics model first developed by Eringen and applied by many researchers to

carbon nanotubes conveying fluid. In the very recent literature, there have been suggested improvements in the formulation of the problem using non-local theory, (see for example, Wang, **[91, 92]** and Li, et. al. **[93]**).

The analysis of buckling of carbon nanotubes also can be addressed using the modified theory.

It is hoped that the matter presented in this thesis will turn out to be a starting point for much further work in the future in this exciting field.

REFERENCES

1. ASHLEY, H. & HAVILAND, G., 1950, "Bending Vibrations of a Pipe Line Containing Flowing Fluid", *Transactions of the ASME, Journal of Applied Mechanics,* **17**, 229-232.

2. HOUSNER, G. W., 1952, "Bending Vibrations of a Pipe Line Containing Flowing Fluid", *Transactions of the ASME, Journal of Applied Mechanics*, **19**, 205-208.

3. THURMAN, A. L. & MOTE, C. D. Jr., 1969, "Nonlinear Oscillation of a Cylinder Containing a Flowing Fluid", *Journal of Engineering for Industry, Transactions of ASME,* November, 1147-1155.

4. CHEN, S. S., 1971, "Dynamic Stability of Tube Conveying Fluid", *Journal of the Engineering Mechanics Division, ASCE*, **97**, 1469-1485.

5. PAÏDOUSSIS M. P. & ISSID, N. T., 1974, "Dynamic Stability of Pipes Conveying Fluid", *Journal of Sound and Vibration*, **33**, 267-294.

6. LEE, U., PAK, C. H. & HONG, S. C., 1995, "The Dynamics of a Piping System with Internal Unsteady Flow", *Journal of Sound and Vibration*, **180**(2), 297-311.

7. PAÏDOUSSIS, M. P. & LAITHIER, B. E., 1976, "Dynamics of Timoshenko Beams Conveying Fluid", *Journal of Mechanical Engineering Science*, **18**, 210-220.

8. LONG, R. H. JR., 1955, “Experimental and Theoretical Study of Transverse Vibration of a Tube Containing Flowing Fluid”, *Transactions of the ASME, Journal of Applied Mechanics,* **22**, 65-68.

9. GREGORY R.W. & PAÏDOUSSIS M. P., 1966, “Unstable Oscillations of Tubular Cantilevers Conveying Fluid I. Theory“, *Proceedings of the Royal Society (London),* A **293**, 512-527.

10. PAÏDOUSSIS M. P., 1970, “Dynamics of Tubular Cantilevers Conveying Fluid”, *Journal of Mechanical Engineering Science*, **12**(2), 85-103.

11. NAGULESWARAN, S. & WILLIAMS, C. J. H., 1968, “Lateral Vibrations of a Pipe Conveying a Fluid”, *Journal of Mechanical Engineering Science,* **10**, 228-238.

12. STEIN R. A. & TOBRINER, M. W., 1970, “Vibration of Pipes Containing Flowing Fluids”, *Transactions of the ASME, Journal of Applied Mechanics,* **37**, 906-916.

13. KOHLI, A. K. & NAKRA, B. C., 1984, “Vibration Analysis of Straight and Curved Tubes Conveying Fluid by Means of Straight Beam Finite Elements”, *Journal of Sound and Vibration,* **93**, 307-311.

14. PRAMILA, A, LAUKANNEN, J & LIUKONNEN, S., 1991, “Dynamics and Stability of Short Fluid Conveying Timoshenko Element Pipes”, *Journal of Sound and Vibration,* **144**(3), 421-425.

15. LOTTATI, I, & KORNECKI, A., 1986, "The Effect of an Elastic Foundation and of Dissipative Forces on the Stability of Fluid Conveying Pipes", *Journal of Sound and Vibration,* **109**, 327-338.

16. DERMENDJIAN-IVANOVA D. S., 1992, "Critical Flow Velocities of a Simply Supported Pipeline on Elastic Foundations", *Journal of Sound and Vibration,* **157**(2), 370-374.

17. CHARY, S. R., 1993, "Vibration of Pipes Resting on Soil Medium", *M. S. Thesis, Department of Civil Engineering*, Indian Institute of Science, India.

18. CHARY, S. R., RAO, C. K. & Iyengar, R. N., 1993, "Vibrations of Fluid Conveying Pipes Resting on Winkler Foundation", *Proceedings of the 8th National Convention of Aerospace Engineers, Institution of Engineers (India),* 266-287.

19. DJONDJOROV, P., VASSILEV, V. & DZHUPANOV, V., 2001, "Dynamic Stability of Fluid Conveying Cantilevered Pipes on Elastic Foundation", *Journal of Sound and Vibration,* **247**(3), 537-546.

20. VASSILEV V. M. & DJONDJOROV, P. A., 2006, "Dynamic Stability of viscoelastic pipes on elastic foundations of variable modulus", *Journal of Sound and Vibration,* **297**, 414-419.

21. ELISHAKOFF, I & IMPOLLONIA, N., 2001, "Does a Partial Elastic Foundation increase flutter velocities of a pipe conveying fluid?", *Transactions of the ASME, Journal of Applied Mechanics,* **206**, 206-212.

22. DOARÉ, O & DE LANGRE, E., 2002, “Local and global instabilities of fluid conveying pipes on elastic foundations”, *Journal of Fluids and Structures*, **16**(1), 1-14.

23. DZHUPANOV, V., 1998, “Systematic Review on the Models of a Cantilevered Pipe Conveying Fluid and Lying on a Multi-parametric Resting Medium”, *Journal of Theoretical and Applied Mechanics*, **28**, 34-53.

24. LILKOVA-MARKOVA, S. V. & LOLOV, D. S., 2004, “Vibrations of a Pipe on Elastic Foundations”, *Sadhana*, **29**(3), 259-262.

25. IIJIMA, S., 1991, "Helical microtubules of graphitic carbon", *Nature*, **354** (6348), 56–58.

26. IIJIMA, S. & ICHIHASHI, T., 1993, "Single-shell carbon nanotubes of 1-nm diameter", *Nature*, **363** (6430), 603–605.

27. DRESSELHAUS, M. S., DRESSELHAUS, G. & EKLUND, P. C., 1996, “Science of Fullerenes and Carbon Nanotubes”, Academic Press, San Diego, CA.

28. HARRIS, P., 2010, “A Carbon Nanotube Page”, http://www.personal.reading.ac.uk/~scsharip/tubes.htm

29. MARUYAMA, S., 2010, “S. Maruyama’s Site on Nanotube Animation”, http://www.photon.t.u-tokyo.ac.jp/~maruyama/agallery/agallery.html

30. YOON, J., RU, C. Q. & MIODUCHOWSKI, A., 2005, “Vibration and instability of carbon nanotubes conveying fluid”, *Composites Science and Technology*, **65**, 1326–1336.

31. YOON, J., RU, C. Q. & MIODUCHOWSKI, A., 2006, “Flow-induced flutter instability of cantilever carbon nanotubes”, *International Journal of Solids and Structures*, **43** 3337–3349.

32. SLISIK, J. A., 2006, “Flow-induced Vibration of Carbon Nanotubes”, *M. S. Thesis*, University of Akron.

33. REDDY, C. D., LU, C., RAJENDRAN, S. & LIEW, K. M., 2007, “Free Vibration Analysis of Fluid-conveying Single-walled Carbon Nanotubes”, *Applied Physics Letters*, **90**, 133122.

34. LEE, H. L. & CHANG, W. J., 2008, “Free Transverse Vibration of the Fluid-conveying Single-walled Carbon Nanotube Using Nonlocal Elastic Theory”, *Journal of Applied Physics*, **103**, 024302.

35. LEE, H. L. & CHANG, W. J., 2009, “Vibration Analysis of a Viscous Fluid-conveying Single-walled Carbon Nanotube Embedded in an Elastic Medium”, *Physica E*, **41**, 529-532.

36. LEE, H. L. & CHANG, W. J., 2009,“Free Vibration of a Single-walled Carbon Nanotube Containing a Fluid Flow using the Timoshenko Beam Model”, *Physics Letters A*, **373**, 982-985.

37. LEE, H. L. & CHANG, W. J., 2009, "Vibration Analysis of Fluid-conveying Double-walled Carbon Nanotubes Based on Nonlocal Elastic Theory", *Journal of Physics of Condensed Matter*, **21**, 115302.

38. YAN, Y., HE, X. Q., ZHANG, L. X. & WANG, C. M., 2009, "Dynamic Behaviour of Triple-walled Carbon Nanotubes Conveying Fluid", *Journal of Sound and Vibration*, **319**, 1003-1018.

39. TIMOSHENKO, S., 1937, "Vibration Problems in Engineering", *2nd Edition*, D.Van Nostrand Company, Inc., NY.

40. PAÏDOUSSIS, M. P. & LI, G. X., 1993, "Pipes Conveying Fluid: A Model Dynamical Problem", *Journal of Fluids and Structures*, **7**, 137-204.

41. PAÏDOUSSIS, M. P, 1998, "Fluid-Structure Interactions-Slender Structures and Axial Flow, Volume 1", *Academic Press Limited*, London, UK.

42. PAÏDOUSSIS, M. P, 2004, "Fluid-Structure Interactions-Slender Structures and Axial Flow, Volume 2", *Elsevier Academic Press*, San Diego, CA.

43. WANG, L. & NI, Q., 2009, "Vibration of Slender Structures Subjected to Axial Flow or Axially Towed in Quiescent Fluid", *Advances in Acoustics and Vibrations*, Volume 2009, 1-19.

44. ALLEN, Jr. T. & DITSWORTH, R. L., 1972, "Fluid Mechanics", *McGraw-Hill Book Company*, NY.

45. KERR, A. D., 1964, “Elastic and Viscoelastic Foundation Models”, *Transactions of the ASME, Journal of Applied Mechanics,* September, 491-498.

46. KUMAR, K. L., 1986, “Engineering Mechanics”, *Tata McGraw-Hill Publishing Company Limited,* New Delhi.

47. RAGAB, A. R. and BAYOUMI, S. E., 1999, “Engineering Solid Mechanics-Fundamentals and Applications”, *CRC Press LLC,* Florida.

48. HUTTON, D. V., 1981, “Applied Mechanical Vibrations”, *McGraw-Hill Book Company,* NY.

49. RAO, S. S., 1986, “Mechanical Vibrations”, *Addison-Wesley Publishing Company,* MA.

50. YOON, J., RU, C. Q. & MIODUCHOWSKI, A., 2003, “Vibration of an Embedded Multi-wall Carbon Nanotube”, *Composites Science and Technology*, **63**, 1533–1542.

51. ERINGEN, A. C., 1972, “Nonlocal Polar Elastic Continua”, *International Journal of Engineering Science,* **10**, 1-16.

52. ERINGEN, A. C. and EDELEN, D. G., B., 1972, “On Nonlocal Elasticity”, *International Journal of Engineering Science,* **10**, 233-248.

53. PEDDIESON, J., BUCHANAN, G. R. and McNITT, R. P., 2003, “Application of Nonlocal Continuum Models to Nanotechnology”, *International Journal of Engineering Science,* **41**, 305-312.

54. ERINGEN, A. C., 1972, “Linear Theory of Nonlocal Elasticity and Dispersion of Plane Waves”, *International Journal of Engineering Science*, **10**, 425-435.

55. ERINGEN, A. C., 1972, “On Nonlocal Fluid Mechanics”, *International Journal of Engineering Science*, **10**, 561-575.

56. ERINGEN, A. C., 1983, “On Differential Equations of Nonlocal Elasticity and Solutions of Screw Dislocation and Surface Waves, *Journal of Applied Physics*, **54**, 4703–4710.

57. ERINGEN, A. C., 1992, “Vistas of Nonlocal Continuum Physics”, *International Journal of Engineering Science*, 3**0**, 1551-1565.

58. ENGELBRECHT, J. and BRAUN, M., 1998, “Nonlinear Waves in Nonlocal Media”, *Applied Mechanics Reviews*, **51**, 475-488.

59. ERINGEN, A. C., 2002, “Nonlocal Continuum Field Theories”, *Springer-Verlag*, NY.

60. LU, P., LEE, H. P. and LU, C, 2006, “Dynamic Properties of Flexural Beams Using a Nonlocal Elasticity Model”, *Journal of Applied Physics*, **99**, 073510.

61. CIVALEK, Ö. and DEMIR, Ç., 2011, “Bending Analysis of Microtubules Using Nonlocal Euler-Bernoulli Beam Theory”, *Applied Mathematical Modeling*, **35**, 2053-2067.

62. REDDY, J. N. and PANG, S. D., 2008, “Nonlocal Continuum Theories of Beams for the Analysis of Carbon Nanotubes”, *Journal of Applied Physics*, **103**, 023511.

63. TIMOSHENKO, S., 1986, "Strength of Materials, Part I", *CBS Publishers & Distributors*, New Delhi.

64. POPOV, E. P., 1991, "Mechanics of Materials", 2nd Edition, *Prentice-Hall of India Private Limited*, New Delhi.

65. ELISHAKOFF, I. and VITTORI, P., 2005, "A paradox of non-monotonicity in stability of pipes conveying fluid", *Theoretical and Applied Mechanics*, **32**, 235-282.

66. FELGAR, R. P., 1950, "Formulas for integrals containing characteristic functions of a vibrating beam", *University of Texas, Circular No. 14, Bureau of Engineering Research*, Austin, Texas.

67. DUTTA, S. C. & ROY, R., 2002, "A critical review on idealization and modelling for interaction among soil foundation-structure system", *Computers and Structures*, **80**, 1579–1594.

68. CHELLAPILLA, K. R. & SIMHA, H. S., 2007, "Critical Velocity of fluid conveying pipes resting on two-parameter foundation", *Journal of Sound and Vibration*, **302**, 387-397.

69. DOARÉ, O, 2006, Personal communication.

70. TIMOSHENKO, S. P. and GERE, J. M., 1961, "Theory of Elastic Stability", 2nd Edition, McGraw-Hill International Book Company, New Delhi.

71. CHEN, W. Q, LÜ, C. F. and BIAN, Z. G., 2004, "A mixed method for bending and free vibration of beams resting on a Pasternak elastic foundation", *Applied Mathematical Modeling*, **28**, 877-890.

72. CHELLAPILLA, K. R. & SIMHA, H. S., 2008, "Vibrations of fluid conveying pipes resting on two-parameter foundation", *The Open Acoustics Journal*, **1**, 24-33.

73. CHANG, C. O. & CHEN, K. C., 1994, "Dynamics and Stability of Pipes Conveying Fluid" *Transactions of the ASME, Journal of Pressure Vessel Technology*, **116**, pp. 57-66.

74. CHELLAPILLA, K.R., SIMHA, H. & MADABHUSHI, R., 2005, "Critical Velocities of Elastically Restrained Multi-Span Fluid Conveying Pipes Resting on Continuous Elastic Foundation", *Proceedings of the 13th International Conference on Nuclear Engineering (ICONE-13)*, Beijing, China, **Paper No. 50473**.

75. DE LANGRE, E. & OUVRARD, A. E., 1999, "Absolute and convective bending instabilities in fluid conveying pipes" *Journal of Fluids and Structures*, **13**, 663-680.

76. HILL, J. L. & DAVIS, C. G., 1974, "The Effect of Initial Forces on the Hydroelastic Vibration and Stability of Planar Curved Tubes", *Transactions of the ASME, Journal of Applied Mechanics*, **41**, 355-359.

77. LEE, S.-Y. & MOTE, C. D. Jr., 1997, "Generalized Treatment of the Energetics of Translating Continua, Part I: Strings and Second Order Tensioned Pipes", *Journal of Sound and Vibration*, **204**(5), 717-734.

78. LEE, S.-Y. & MOTE, C. D. Jr., 1997, “Generalized Treatment of the Energetics of Translating Continua, Part II: Beams and Fluid Conveying Pipes”, *Journal of Sound and Vibration*, **204**(5), 735-753.

79. PANTELIDES, C. P., 1992, “Stability of Columns on Biparametric Foundations”, *Computers and Structures*, **42**(1), 21-29.

80. SIMHA, H. & RAO, C. K., 1997, “Finite Element Analysis of Vibrations of Fluid Conveying Pipes Resting on Soil Medium”, *Proceedings of the Technical Conference on Pressure Vessels and Piping, Hyderabad, India*, 173-182.

81. SIMHA, H. & RAO, C. K., 2001, “Finite Element Analysis of Vibrations of Rotationally Restrained Fluid Conveying Pipes Resting on Soil Medium”, *Proceedings of the National Symposium on Advances in Structural Dynamics & Design*, Chennai, India, 569-578.

82. WEAVER, D. S. & UNNY, T. E., 1973, “On the Dynamic Stability of Fluid Conveying Pipes”, *Transactions of the ASME, Journal of Applied Mechanics*, **40**, 48-52.

83. WEAVER, D. S. & MYKLATUN, B., 1973, “On the Stability of Thin Pipes with an Internal Flow”, *Journal of Sound and Vibration*, **31**, 399-410.

84. IBRAHIM, R. A., 2010, “Overview of Mechanics of Pipes Conveying Fluid-Part I: Fundamental Studies”, *Transactions of the ASME, Journal of Pressure Vessel Technology*, **132**, 034001-1 to 32.

85. IBRAHIM, R. A., 2010, “Mechanics of Pipes Conveying Fluids-Part II: Applications and Fluidelastic Problems”, *Transactions of the ASME, Journal of Pressure Vessel Technology,* **133**, 024001-1 to 30.

86. OLUNLOYO, V. O. S., OYEDIRAN, A. A., ADEWALE, A., ADELAJA, A. O. and OSHEKO, C. A., 2007, “Concerning the Transverse and Longitudinal Vibrations of a Fluid Conveying Beam and the Pipe Walking Phenomenon”, *Proceedings of the 26th International Conference on Offshore Mechanics and Arctic Engineering-OMAE,* San Diego, CA, Volume 3, 285-298.

87. MOVCHAN, A. A., 1965, “On the Problem of Stability of a Pipe with Fluid Flowing Through it”, *Transactions of the ASME, Journal of Applied Mechanics*, **29**, 760-762.

88. PLAUT, R. H. and HUSEYIN, K, 1975, “Instability of Fluid Conveying Pipes Under Axial Load”, *Transactions of the ASME, Journal of Applied Mechanics*, **42**, 889-890.

89. BECKER, M., HAUGER, W. and WINZEN, W., 1978, “Exact Stability Analysis of Uniform Cantilevered Pipe Conveying Fluid or Gas”, *Arch. Mechanics*, **30**, 757-768.

90. ANSARI, R., GHOLAMIA, R., HOSSEINI, K. AND SAHMANIA, S., 2011, “A sixth-order compact finite difference method for vibrational analysis of nanobeams embedded in an elastic medium based on nonlocal beam theory”, *Mathematical and Computer Modelling,* **54,** 2577–2586.

91. WANG, L., 2009, “Vibration and instability analysis of tubular nano- and micro-beams conveying fluid using nonlocal elastic theory”, *Physica* E, **41,** 1835–1840.

92. WANG, L., 2010, “Vibration analysis of fluid-conveying nanotubes with consideration of surface effects”, *Physica* E, **43**, 437–439.

93. LI, C., LIM, C. W., YU, J. L. and ZENG, Q. C., 2011, “Analytical Solutions for Vibration of simply supported Non-local Nanobeams with an Axial Force”, *International Journal of Structural Stability and Dynamics*, **11(2)**, 257-271.

94. LEE, H. L., HSU, J. C. & CHANG, W. J., 2010, “Frequency Shift of Carbon-Nanotube-Based Mass Sensor Using Nonlocal Elasticity Theory”, *Nanoscale Research Letters*, **5,** 1774–1778.

95. WANG, Q. and VARADAN, V. K., 2006, “Vibration of Carbon Nanotubes Studied Using Non-local Continuum Mechanics”, *Smart Materials and Structures*, **15**, 659-666.

96. LU, P, LEE, H. P., LU, C. and ZHANG, P. Q., 2006, “Dynamic Properties of Flexural Beams Using a Non-local Elasticity Model”, *Journal of Applied Physics*, **99**, 073510, 1-9.

97. WANG, C. M., ZHANG, Y. Y. and HE, X. Q., 2007, “Vibration of Non-local Timoshenko Beams”, *Nanotechnology*, **18**, 105401, 1-9.

98. GIBSON, R. F., AYORINDE, E. O. and Wen, Y. F., 2007, "Vibrations of Carbon Nanotubes and their Composites: a Review", *Composites Science and Technology*, **67**, 1-28.

99. WANG, Q. and LIEW, K. M., 2007, "Application of Non-local Continuum Mechanics to Static Analysis of Micro- and Nano-structures", *Physics Letters A*, **363**, 236-242.

100. ZHANG, Y. Q., LIU, G. R. and XIE, X. Y., 2005, "Free transverse vibrations of double-walled carbon nanotubes using a theory of non-local elasticity", *Physical Review B*, **71**, 195404, 1-7.

101. LEE, H. L., HSU, J. C. and CHANG, W. J., 2010, "Frequency Shift of Carbon-Nanotube-Based Mass Sensor Using Nonlocal Elasticity Theory", *Nanoscale Research Letters*, **5**, 1774-1778.

102. WANG, L, NI, Q., LI, M. and QIAN, Q., 2008, "The Thermal Effect on Vibrations and Instability of Carbon Nanotubes Conveying Fluid", *Physica E*, **40**, 3179-3182.

103. WANG, L. and NI, Q., 2008, "On Vibration and Instability of Carbon Nanotubes Conveying Fluid", *Computational Materials Science*, **43**, 399-402.

104. WANG, L., Ni. Q. and LI, M., 2009, "Buckling Instability of Double-walled Carbon Nanotubes Conveying Fluid", *Computational Materials Science*, **44**, 821-825.

105. WANG, L. and NI, Q., 2008, “A Reappraisal of the Computational Modeling of Carbon Nanotubes Conveying Viscous Fluid”, *Mechanics Research Communications*, **38**, 833-837.

106. GHAVANLOO, E., DANESHMAND, F. and RAFFIEI, M., 2010, “Vibration and Instability of Carbon Nanotubes Conveying Fluid Resting on a Linear Viscoelastic Winkler Foundation”, *Physica E*, **42**, 2218-2224.

107. WANG, L., 2009, “Dynamical Behaviours of Double-walled Carbon Nanotubes Conveying Fluid Accounting for the Role of Small Length Scale”, *Computational Materials Science*, **45**, 584-588.